UNIVERSITY OF SOUTHAMPTON

Novel Mixed Donor *N*-Heterocyclic Carbene Complexes

Arran Alexander Dickon Tulloch

Doctor of Philosophy

Department of Chemistry

June 2002

UNIVERSITY OF SOUTHAMPTON

ABSTRACT

FACULTY OF SCIENCE

CHEMISTRY

Doctor of Philosophy

NOVEL MIXED DONOR *N*-HETEROCYCLIC CARBENE COMPLEXES

By Arran Alexander Dickon Tulloch

A series of novel imidazolium salts functionalised with nitrogen, oxygen and phosphorus donors have been synthesised. The donor functionalised salts are: (3-^{t}Bu-1-py-imid) Br; (3-Ar'-1-py-imid) Br; (3-Ar-1-py-imid) Br; (3-Ar'-1-pic-imid) Br; (3-Ar-1-pic-imid) Br; (3-Ar'-1-lu-imid) Br; (3-Ar-1-lu-imid) Br; [α,α'-(3-Ar-imid)$_2$lutidine] 2Br; [2,6-(3-Ar-imid)$_2$pyridine] 2Br; [1-(3-Ar-imid)-1-CH_2OCH_3] Br; [1,1-(3-Ar-imid)$_2CH_2$] 2Br; [1-(3-Ar-imid)-$CH_2CH_2CH_2Br$] Br; [1-(3-Ar-imid)-2-(P^{t}Bu$_2$BH$_3$)-CH_2CH_2]$_2$ SO_4; [1-(3-Ar-imid)-2-P^{t}Bu$_2$-CH_2CH_2]$_2$ SO_4; [1-(3-Ar-imid)-2-(P^{t}Bu$_2$O)-CH_2CH_2]$_2$ SO_4; (3-^{t}Bu-1-allyl-imid) Br; [1-(3-^{t}Bu-imid)-3-PPh_2-$CH_2CH_2CH_2$] Br; {3-[$(CH_3)_2$CH]-1-vinyl-imid} I and {1-{3-[$(CH_3)_2$CH]-imid}-2-PPh_2-CH_2CH_2} I; where Ar = 2,6-diisopropylphenyl, Ar' = mesityl, ^{t}Bu = *tert*butyl, imid = imidazolium, ylidene = imidazol-2-ylidene, py = 2-pyridyl, pic = α-picolyl and lu = α-lutidyl.

A series of novel silver (I) and copper (I) *N*-heterocyclic carbene complexes functionalised with nitrogen, oxygen and phosphorus donors have been synthesised. The mixed donor carbene complexes of silver and copper are: (3-^{t}Bu-1-pic-ylidene) AgBr; (3-Ar-1-py-ylidene) AgBr; (3-Ar-1-pic-ylidene) AgBr; (3-Ar-1-lu-ylidene) AgBr; (3-Ar'-1-pic-ylidene) AgBr; (3-Ar'-1-lu-ylidene) AgBr; [1-(3-Ar- ylidene)-1-CH_2OCH_3] AgCl; [1,1-(3-Ar- ylidene)$_2$-CH_2] Ag_2Cl_2; [1-(3-Ar- ylidene)-2-(P^{t}Bu$_2$BH$_3$)-CH_2CH_2] $AgSO_4$; (3-Ar'-1-pic-ylidene) CuBr; (3-Ar-1-pic-ylidene) CuBr; (3-Ar-1-py-ylidene) CuBr; (3-Ar-1-py-ylidene) $CuPF_6$·MeCN; (3-Ar-1-py-ylidene) $CuSO_3CF_3$.

A series of novel palladium carbene complexes functionalised with nitrogen and oxygen donors have been synthesised. The mixed donor carbene complexes of palladium are: (3-^{t}Bu-1-pic-ylidene) PdMeX, X = Br, $SO_3C_6H_4CH_3$, SO_3CF_3, CO_2CF_3, $CO_2C_6H_5$; (3-Ar'-1-pic-ylidene) PdMeX, X = Br, $SO_3C_6H_4CH_3$, SO_3CF_3, CO_2CF_3, $CO_2C_6H_5$; (3-Ar-1-pic-ylidene) PdMeX, X = Br, $SO_3C_6H_4CH_3$; (3-Ar-1-py-ylidene) PdMeX, X = Br, $SO_3C_6H_4CH_3$; (3-Ar-1-lu-ylidene) PdMeBr; (3-^{t}Bu-1-py-imid) $PdBr_2OAc$; [1-(3-Ar-ylidene)-1-CH_2OCH_3]$_2$ $PdCl_2$; [α,α'-(3-Ar-ylidene)$_2$lutidine] $PdCl_2$; [2,6-(3-Ar-ylidine)$_2$pyridine] $PdCl_2$; [α,α'-(3-Ar'-ylidene)$_2$lutidine] $PdCl_2$; [2,6-(3-Ar'-ylidine)$_2$pyridine] $PdCl_2$; [α,α'-(3-Ar-ylidene)$_2$ *o*-$(CH_2)_2$Ph] $PdCl_2$.

Novel mixed donor picolyl-carbene complexes of nickel, rhodium and ruthenium have been synthesised. The mixed donor carbene complexes of nickel, rhodium and ruthenium are: (3-Ar'-1-pic-ylidene) $NiBr_2$; (3-Ar'-1-pic-ylidene) RhCl(COD); (3-Ar'-1-pic-ylidene) RuCl(*p*-cymene).

A number of the palladium complexes were shown to be extremely good pre-catalysts for the Heck reaction. Subtle differences in the complexes were shown to affect their effectiveness as catalysts: for the bidentate ligands larger bite angles give higher turnover frequencies but smaller bite angles increase stability of the active catalyst, for tridentate ligands less bulky substituents enable the reaction to proceed faster but do not affect the stability of the catalyst. Turnover numbers comparable to the best-known systems were achieved with aryl iodides. The chiral palladium carbene complexes were shown to catalyse the Heck reaction at temperatures bellow that of enantiomer interconversion. These chiral complexes also catalyse the Heck reaction effectively with aryl chlorides.

Table of Contents

List of Figures

List of Tables

List of Schemes

Acknowledgements

I would like to acknowledge Ineos Acrylics and EPSRC for the financial support enabling this research to be undertaken.

I would like to offer my thanks to my supervisors Andreas A. Danopoulos, Graham Eastham and Robert P. Tooze for their continuous guidance and advice throughout my three years at Southampton. My thanks are extended to the other members of Andreas' research group, and my good friends in the Department. Lastly, I would like to thank my family, especially Lucy, for their love and support.

List of Abbreviations

Et	ethyl
Me	methyl
^{i}Pr	*iso*propyl
^{t}Bu	*tert*butyl
Ph	phenyl
mesityl	2,4,6-trimethylphenyl
R	alkyl group
Ar	aryl group
py	pyridyl
pic	picolyl
lu	lutidyl
ylidene	imidazol-2-ylidene
imid	imidazolium
COD	1,5-cyclooctadiene
THF	tetrahydrofuran
Cym	*p*-cymene
X	halogen or pseudo-halogen
NMR	Nuclear Magnetic Resonance
δ	chemical shift
ppm	parts per million
s	singlet
d	doublet
t	triplet
m	multiplet
br.	broad peak
dt	doublet of triplets
dd	doublet of doublets
Hz	hertz

Chapter 1

Introduction

Chapter 1
Introduction

1.1 Introduction

Nearly thirty-five years on from when the first complexes containing *N*-heterocyclic carbenes were independently published by Öfele[1] and Wanzlick,[2] the area continues to create an intense amount of interest within the academic and industrial community. However, the tidal wave of publications in the area has only really built up in the last ten years since Arduengo published the first structurally characterised example of a stable crystalline free carbene (*Scheme 1.1*).[3]

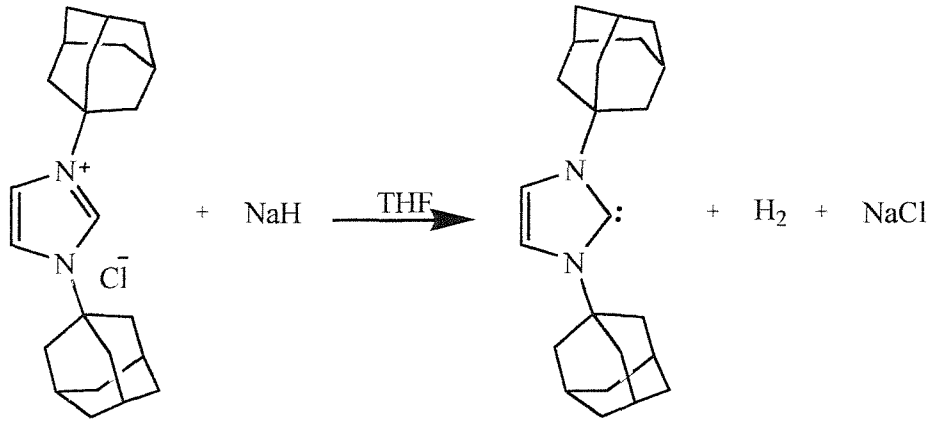

Scheme 1.1. Synthesis of the first structurally characterised free carbene reported by Arduengo *et al.*[3]

The interest in the isolation of free *N*-heterocyclic carbenes and their complexes has been fuelled by the understanding that they are very strong σ-donating ligands and are more comparable to phosphorus or nitrogen ligands than to classical carbenes.[4,5] The chemically and thermally inert metal-carbene bond and its very high dissociation energy sets them apart from other types of ligand. These properties make the ligands very suitable for use in catalysis, and *N*-heterocyclic carbene complexes have been shown to have unprecedented catalytic activity in a number of important transformations.[6] The potential for functionalising these carbenes provides vast opportunities for ligand design allowing an enormous number of steric and electronic modifications to be made, giving rise to a number of recent reviews in the area.[6,7,8,9,10,11]

1.2 Carbenes

Carbenes are neutral species featuring a divalent carbon atom with only six electrons in its valence shell and no formal charge on the carbon. The carbon in these types of two-coordinate compounds is formally in an oxidation state (II). Carbenes adopt either a near-linear configuration with *sp*-type hybridisation of the bonding orbitals or a bent configuration with sp^2-type hybridisation of the orbitals. The two non-bonding electrons can be either unpaired giving a near-linear molecule (triplet) or paired in a σ-character orbital giving a bent molecule (singlet).

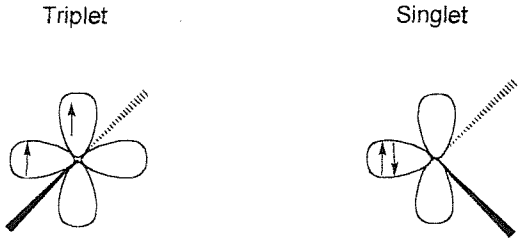

Figure 1.1. Ground state electronic configurations of singlet and triplet carbenes

Triplet carbenes are considered as di-radicals as they have two singly occupied orbitals. In contrast, singlet carbenes comprise of a filled and a vacant orbital, which give them potential for ambiphilic behaviour. The ground state multiplicity (*Figure 1.1*) is related to the relative energies of the σ- and π-character orbital and therefore greatly influenced by the substituents on the carbene carbon. σ-Electron withdrawing substituents stabilise the singlet state by increasing the *s*-type character of the σ-type sp^2 orbital of the carbene.

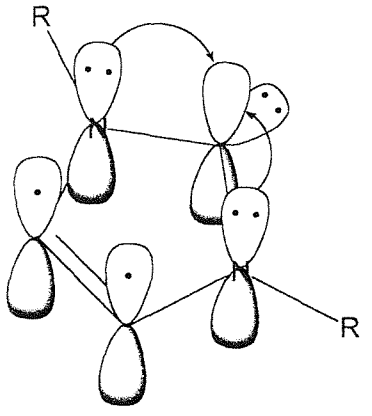

Figure 1.2. Ground state electronic configuration of unsaturated N-heterocyclic singlet carbenes, showing the donation of electrons from the substituent nitrogen atoms in to the empty *p*-orbital of the carbene.

However, the mesomeric effects of the substituents play a more significant role. Carbenes with π-electron donating substituents are singlet carbenes as the energy of the vacant *p*-orbital of the carbene is increased, forcing the singlet state. Donation of both the substituents' lone pairs results in a four-electron-three-centre π-system, which gives some multiple bond character to the carbene-substituent bond and some negative charge to the carbene carbon.

The ambiphilic nature of singlet carbenes gives them the opportunity to act as nucleophiles through the occupied σ-character sp^2 orbital or as electrophiles by using the empty π-character *p* orbital. Singlet carbenes are often restricted from acting as an electrophile as the empty π-character *p* orbital undergoes conjugation with the lone pairs on adjacent heteroatoms (*Figure 1.2*).

Formally, carbene complexes can be divided in two types, Fischer[12] (electrophilic) and Schrock[13] (nucleophilic). Fischer carbenes have heteroatom substituents and show behaviour typical of electrophiles, while Schrock carbenes, have alkyl or hydrogen substituents and show behaviour typical of nucleophiles. Carbene complexes of the Fischer type show significantly less π-bonding between the metal and the carbon atom than that for the Schrock type, as they have their HOMO (essentially non-bonding) centred on the metal and the LUMO centred on the carbon, with the reverse being the case for Schrock carbenes.

1.3 Stable carbenes

Bulky substituents stabilise all types of carbene by preventing the dimerisation to the corresponding olefin. However, triplet carbenes are very difficult to stabilise and at best can only be described as persistent rather than stable. The most stable triplet carbenes are sterically hindered diarylcarbenes, in particular polymethylated and polyhalogenated diphenyl carbenes. The most stable, isolated by Tomioka *et al.*,[14] only exists in solution for a few seconds at room temperature, but is indefinitely stable in the solid state at ambient temperatures (*Figure 1.3*).

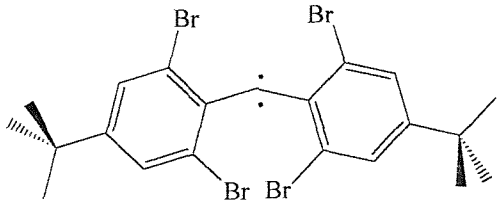

Figure 1.3. Stabilised triplet carbene, synthesised by Tomioka *et al.*[14]

However, singlet carbenes can be stabilised by a variety of different substituents and frameworks. They are stabilised both sterically by bulky substituents and electronically by the mesomeric effect of the lone pairs of the substituents as well as the inductive effect from the electronegativity of heteroatoms adjacent to the carbene. The balance of inductive and mesomeric effects is best for nitrogen substituents as they are the most effective at stabilising the carbene electronically. Most stable singlet carbenes are aminocarbenes although some stable phosphinocarbenes have been isolated. Aminocarbenes have been isolated with oxygen and sulphur co-substituents; however, diamino carbenes are the most commonly reported (*Figure 1.4*).[15]

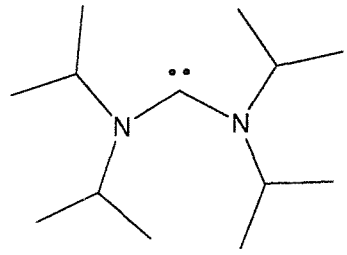

Figure 1.4. An acyclic stable singlet carbene synthesised by Alder *et al.*[16]

One of the most typical reactions of singlet carbenes is the dimerisation to form electron rich olefins. This dimerisation can be prevented by increasing the steric bulk on the substituents of the carbene. Wanzlick demonstrated the formation of a relatively stable triplet carbene by the isolation of its metal complexes. However, his attempts to isolate the free carbene failed and only the electron rich olefin, formed by dimerisation of the carbene, was identified.[17] The equilibrium between the free carbene and the dimer has recently been shown to exist for a few systems.[18,19,20] In addition, the stability of the carbenes against dimerisation was increased by the neighbouring π-systems (imidazol-2-ylidene and benzimidazol-2-ylidene), which demonstrated the delocalisation of the π-ring-system around these carbenes. With this additional electronic stabilisation, free sterically unhindered singlet carbenes have been isolated.[21] The aromaticity is due to the *4n+2* electrons contained within these π-ring-systems.

1.4 *N*-Heterocyclic carbenes

Nearly all stable singlet carbenes are *N*-heterocyclic, however there are a number of sub-families within this group (*Figure 1.5*). Most of the isolated free *N*-heterocyclic

carbenes are imidazol-2-ylidenes. The main reasons for their preponderance over others is that they can be synthesised *via* a number of different simple routes and are one of the most electronically stabilised of the types of singlet carbenes.

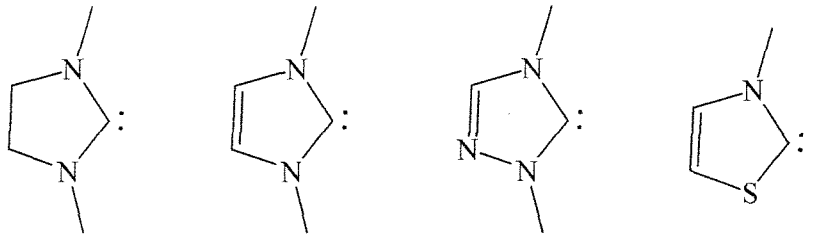

imidazolin-2-ylidenes	imidazol-2-ylidenes	1,2,4-triazol-5-ylidenes	1,3-thiazol-2-ylidenes

Figure 1.5. Types of stable *N*-heterocyclic carbenes.

Arduengo reported the first example of a stable singlet carbene, an imidazol-2-ylidene.[3] However, Wanzlick *et al.* demonstrated the formation of a stable singlet carbene (an imidazolin-2-ylidene) nearly two decades earlier, but were unable to isolate the free carbene.[17] The additional electronic stabilisation associated with the unsaturated heterocycles, created by the aromaticity of the ring, is regarded as the determining factor for Wanzlick only isolating the dimerised carbene.[22]

The heterocyclic carbenes are best represented as the combination of two resonance forms, which give some double bond character to the carbene-nitrogen bonds; this is demonstrated by the bond lengths being in the range between a single and a double bond. (*Figure 1.6*). Furthermore, unsaturated heterocycles have a further delocalisation around the ring, which gives the extra stabilisation of an aromatic system.

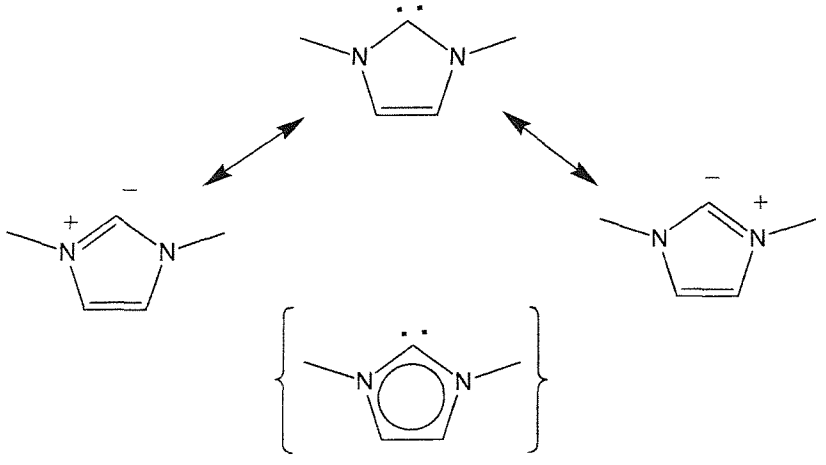

Figure 1.6. Resonance forms of imidazol-2-ylidenes.

The enormous variation of *N*-heterocyclic carbenes stems from the versatility of the different methods available for their synthesis.[11] The variety of methods used to synthesise these carbenes allowed a large number of different ligand designs to be developed. Some unusual ligand designs have been functionalised with ferrocenyl substituents,[23] long fluoroalkylated[24] and alkyl-chains,[25] and have been supported on polymers.[26] Stable free carbenes (*Figure 1.7*) have been reported to be functionalised with chiral groups, other donor groups, incoporated into ring structures, and linked to other carbenes giving bi- and tri-dentate carbenes to mention but a few. [20,27,28,29,30]

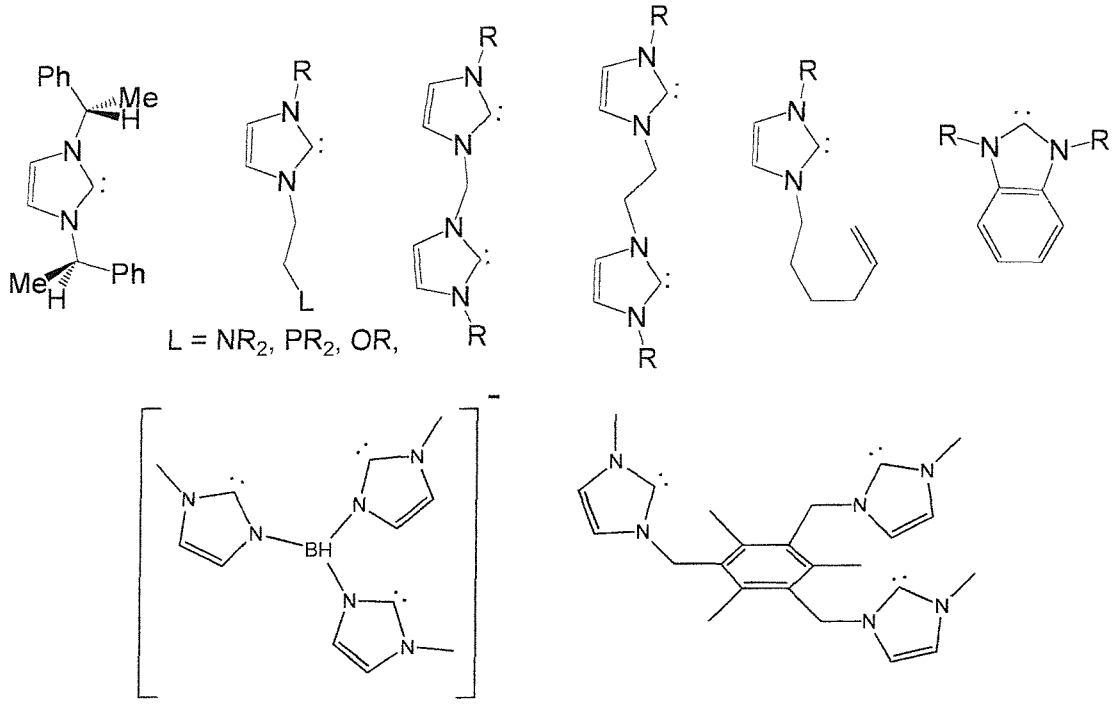

Figure 1.7. A variety of mono-, bi- and tri-dentate *N*-heterocyclic carbenes.

1.5 *N*-Heterocyclic carbenes as ligands

Although, *N*-heterocyclic carbenes are interesting stable species that have been previously difficult to isolate and characterise, currently the focus of attention has been on their properties as ligands and not as separate molecules.

N-Heterocyclic carbene ligands act as two-electron σ-donors and, in this respect, they are related to ethers, amines and phosphines with regards to their coordination chemistry. They bind strongly to transition metals and are considered stronger σ-donors than amines. In fact, it has been proposed[4,31,32] that their σ-donor properties are similar to the electron-rich phosphines and that π-back donation from the metal is insignificant.[31] The

π-acceptor properties of *N*-heterocyclic carbenes are not as expected from the simple notion of a singlet carbene with ambiphilic characteristics. *N*-Heterocyclic carbenes show almost no electrophilic character and are often referred to as nucleophilic carbenes. The highly stabilised nature of these singlet carbenes stems from the two adjacent nitrogen atoms donating electron density in to the carbenes "empty" *p*-orbital, which results in the loss of ambiphilic character.

The metal-carbon bond is much less reactive than in Fischer or Schrock type carbenes, as the ligand can be considered to have only nucleophilic character, with almost no double bond character to the metal. The thermal stability and chemical inertness[16] of the carbene-metal bond makes carbene ligands ideal as ancillary ligands in organometallic catalysis.

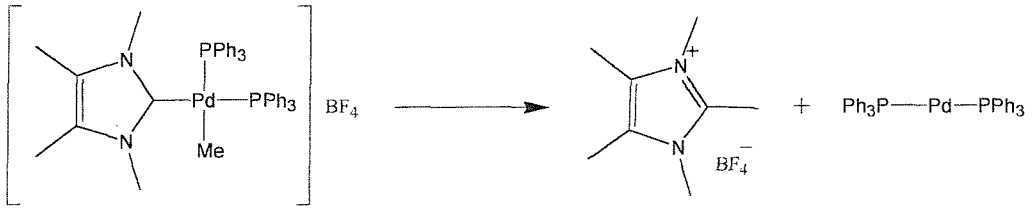

Scheme 1.2. Decomposition pathway for carbene complexes, proposed by Cavell *et al.*[33]

The bond between *N*-heterocyclic carbenes and late transition metals has been previously considered extremely inert towards decomposition and substitution; however, recent reports appeared which question this belief.[33,34] The decomposition pathway, shown in *Scheme 1.2*, has only been observed for a few systems and studied by theoretical methods, therefore the generality of the statements made above remains valid.

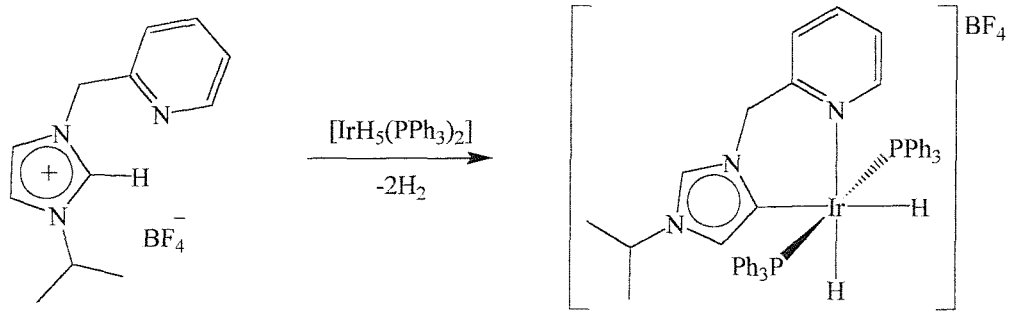

Scheme 1.3. Unusual binding of an imidazol-ylidene to iridium *via* the 4-position.[35]

In the last year, examples have been reported where a different proton of the imidazolium ring is removed in preference to the proton in the two-position. In the first example a ketone functionalised bis-imidazolium salt was observed to bind to palladium through a pseudo η^3-allyl group rather than through the normal carbene-bonding mode.[36] In another example, the imidazolium-ylidene ring was observed crystalographically to bond to the iridium through the 4-position of the ring rather than the usual, more electronically stabilised, 2-position (*Scheme 1.3*).[35] However, it is unknown why the ligand assumes these bonding modes. Both of the above compounds were synthesised by the direct addition of the imidazolium salts on to the metal and not *via* a free carbene.

1.6 *N*-Heterocyclic carbene complexes

The first *N*-heterocyclic carbene complexes were independently reported in 1968 by Öfele *et al.*[1] and Wanzlick *et al.*[2] (*Figure 1.8*). However, it was not until 1991, when the first free carbenes were isolated,[37] that the direct route to the complexes became available. This allowed the synthesis of complexes that would otherwise be unobtainable; since then, the area has developed into an important branch of organometallic chemistry.

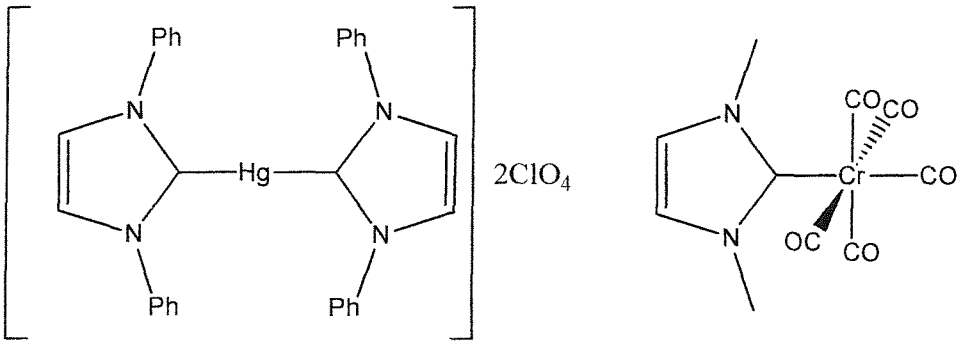

Figure 1.8. *N*-Heterocyclic carbene complexes synthesised by Wanzlick and Öfele in 1968.

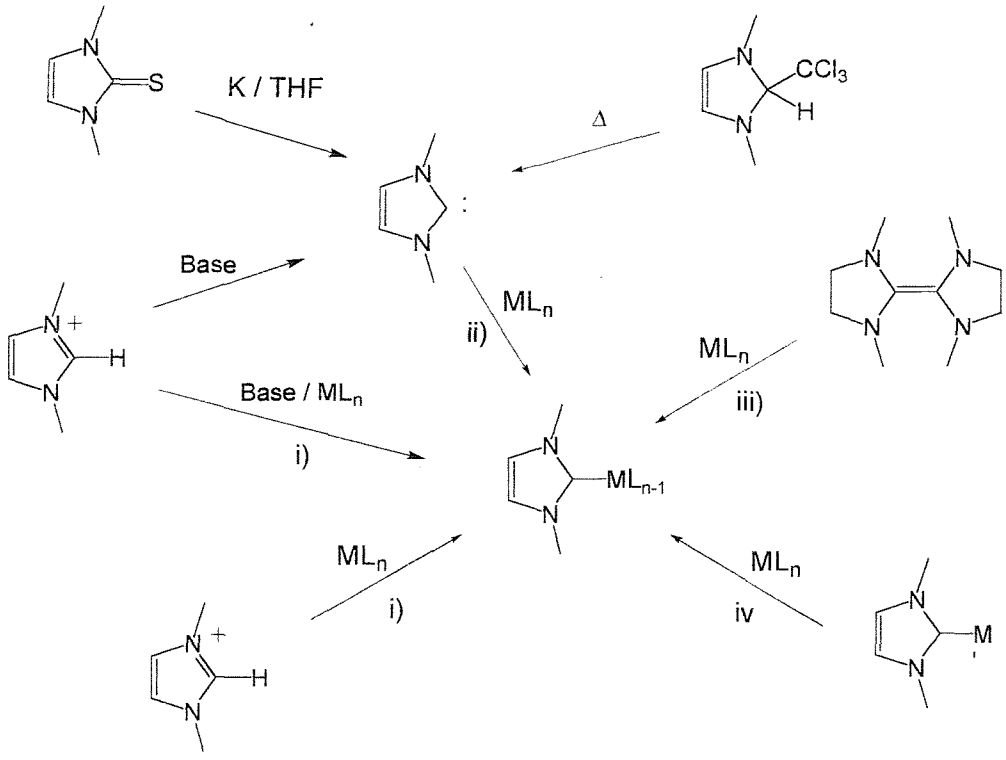

Scheme 1.4. General methods for the synthesis of *N*-heterocyclic carbene complexes.

Over the last few years, an enormous number of *N*-heterocyclic carbene complexes have been published, and they have utilised a number of different synthetic routes. The routes in which the complexes have been synthesised can be grouped into four general methods (*Scheme 1.4*):

i) *In situ* deprotonation of imidazolium salts by basic anions, by basic metallates or by an external base, in the presence of a suitable metal precursor.[38]

ii) Reaction of an isolated free *N*-heterocyclic carbene with a suitable metal precursor.[39]

iii) Thermal cleavage of electron rich olefins in the presence of a suitable metal precursor (applicable to imidazolin-2-ylidenes).[40]

iv) Transmetallation of the carbene ligand.[41]

However, there are a few examples of synthetic routes that do not fit in to one of these categories, such as metal-vapour-phase synthesis[42] and metal template synthesis (*Scheme 1.5*).[43,44]

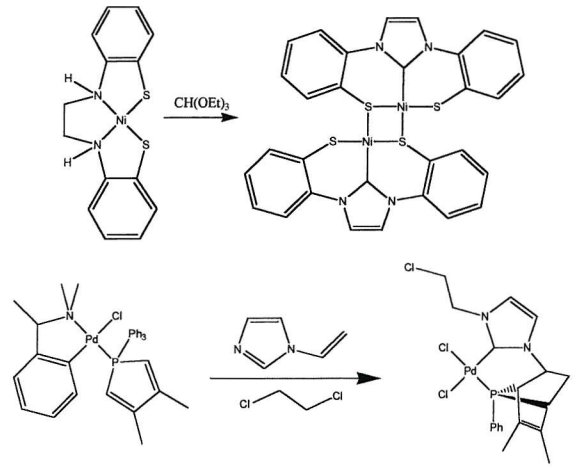

Scheme 1.5. Synthesis of carbene complexes using the metal as a template.

N-Heterocyclic carbene complexes, or their covalent compounds, have been made with elements from right across the periodic table (*Figure 1.9*). Carbene complexes with nearly all transition metals have been synthesised, including complexes of copper, silver and gold,[45] nickel and palladium,[46] rhodium and iridium,[47] iron,[48] ruthenium,[49] osmium,[50] rhenium,[51] chromium,[6] molybdenum and tungsten,[52] vanadium, niobium, tantalum, titanium, zirconium and hafnium.[53] A large proportion of these complexes contain mono-dentate carbenes, but there are also a number of examples with bi- and tri-dentate carbene ligands.[54,55,28]

H																	He
Li	Be											B	C	N	O	F	Ne
Na	Mg											Al	Si	P	S	Cl	Ar
K	Ca	Sc	Ti	V	Cr	Mn	Fe	Co	Ni	Cu	Zn	Ga	Ge	As	Se	Br	Kr
Rb	Sr	Y	Zr	Nb	Mo	Tc	Ru	Rh	Pd	Ag	Cd	In	Sn	Sb	Te	I	Xe
Cs	Ba	La	Hf	Ta	W	Re	Os	Ir	Pt	Au	Hg	Tl	Pb	Bi	Po	At	Rn
Fr	Ra	Ac	Rf	Ha	Sg	Ns	Hs	Mt	Unn	Unu							

Ce	Pr	Nd	Pm	Sm	Eu	Gd	Tb	Dy	Ho	Er	Tm	Yb	Lu
Th	Pa	U	Np	Pu	Am	Cm	Bk	Cf	Es	Fm	Md	No	Lr

Figure 1.9. Heterocyclic carbenes form complexes or covalent compounds with the elements marked in the periodic table.

1.7 *N*-Heterocyclic carbene complexes in catalysis

As mentioned above, *N*-heterocyclic carbenes have a number of characteristics that make them useful as ligands in homogeneous catalysis. The strong σ-donor properties of the ligand enable the formation of chemically and thermally inert metal-carbene bonds with high dissociation energies, which renders them as ideal spectator ligands. In comparison with phosphine complexes, these carbene complexes show good stability towards oxygen; and as dissociation of these carbenes is uncommon, no excess of ligand is required. Aryl phosphines show a tendency for phosphine-carbon bond cleavage, which is responsible for catalyst deactivation; however, this decomposition route is not present for carbene complexes.

N-Heterocyclic carbene complexes have been shown to have catalytic activity in a number of important transformations. These include: palladium-catalysed Heck, Suzuki, Kumada, Sonogashira and amination couplings,[56] palladium-catalysed CO-ethylene copolymerisations, [57] nickel-catalysed Sonogashira coupling,[58] iridium-catalysed hydrogenation,[59] ruthenium-catalysed furan synthesis and olefin metathesis[60] and rhodium-catalysed hydroformylation and hydrosilylations.[61]

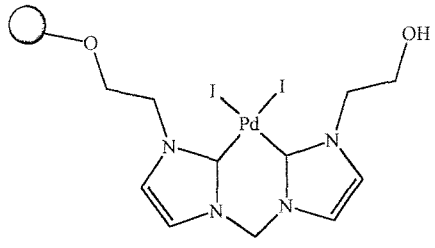

Figure 1.10. Immobilised carbene complex that is active as a Heck pre-catalyst.

The applications of carbene ligands in catalysis have been shown to be diverse, with a number of transformations being catalysed as efficiently as the best-known systems. In addition, the strong metal-carbene bonds allow the carbene ligand to be a suitable link for immobilised complexes. Carbene complexes have been successfully immobilised and they show good catalytic activity although not as good as their parent complexes (*Figure 1.10*).[26,62] Combinatorial type catalysis has been performed with imidazolium salts and it is proposed that the carbene complexes will form in *situ*.[63] Chiral carbene ligands have also been synthesised; most of which are monodentate ligands substituted with chiral groups. They show good activity towards a number of catalytic transformations but the enantiomeric excesses achieved show poor enantioselection.[64] There is also an example of

a bidentate chiral complex, which is based on a binaphthyl chiral auxiliary with a C_2 axis going through the metal centre; enabling the chiral information to be confered on the metal centre.[65] Unfortunately, this complex was isolated as a mixture of coordination isomers, which makes it unlikely to provided good enantioselection.

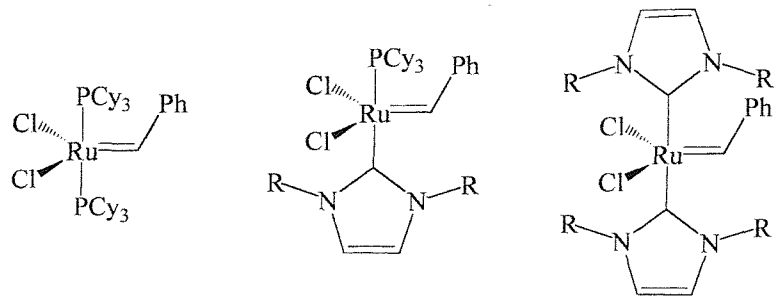

Figure 1.11. Similar carbene, phosphine and mixed complexes.

Phosphine complexes are widely used as pre-catalysts for important transformations and often produce the best catalytic activity.[66,67] As phosphine and carbene ligands have similar donor properties, it is therefore unsurprising that in the last few years carbene complexes for use in catalysis have been designed to mimic well-known phosphine complexes.[68] By comparing the activity of these complexes (*Figure 1.11*) in catalytic transformations, the role of the ligands in these systems can be understood in more detail.

1.8 Ligand design

N-Heterocyclic carbenes can be easily modified and functionalised, attributes making them suitable for novel ligand design. Carbene ligands are very unlikely to dissociate from a metal centre, which makes them effective spectator ligands, and they can be linked to almost any other functional group to exert electronic and steric tuning on the metal. Ligand design can influence the metal centre in a variety of ways; for example, a ligand can confer steric control with chiral information or steric bulk, causing molecules to coordinate in a particular orientation or restricting larger molecules from coordinating. Furthermore, the ligand can be designed to influence the properties of the coordination sites *trans* to the ligand.

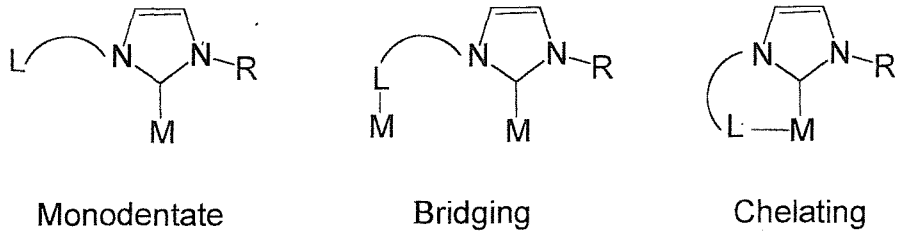

Figure 1.12. Binding modes of hybrid ligands.

Ligand designs can attempt to control the complexity of the transformations occurring in the coordination sphere of the metal during a catalytic cycle. The nature of the ancillary ligands can influence a catalytic site in subtle ways, changing the catalysts' activity, selectivity, and stability.

"Hybrid ligands" comprising two or more different donors; can be designed so that their donor moieties perform different roles during the catalytic cycle; for example, allowing the ligand to be in a monodentate, bridging or chelating mode (*Figure 1.12*). Asymmetric ligands may allow different metals to come into close proximity to one another, which could stabilise ligand-substrate interactions. Asymmetric ligands can also induce asymmetry on the coordination sites of the metal centre; helping to influence the transformations that occur on the metal.

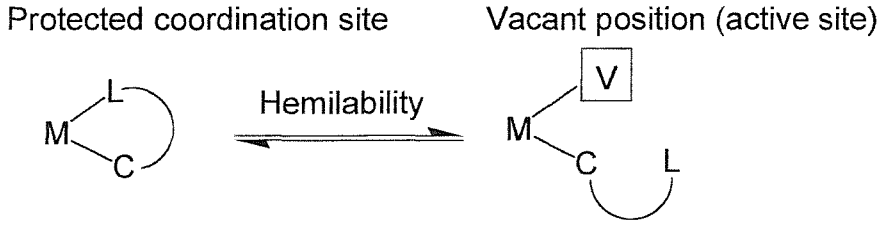

Figure 1.13. Hemilability: protecting or freeing a coordination site.

In addition, one of the donors can be selected to act as hemilabile, filling coordination sites and then dissociating when required, which can stabilise transition states and prevent decomposition (*Figure 1.13*).[69] Furthermore, steric asymmetry of the ligand can control the direction of incoming substrate molecules, which in turn can lower activation energies for conversions or simply select one particular stereochemistry for the product molecule. Potentially hemilabile mixed donor carbene ligands could prove useful in stabilising catalytic centres while creating a degree of coordinative and electronic

unsaturation, in the presence of substrates. These properties can be adjusted by changing a number of features of the ligand including chelate size and rigidity, donor properties, and steric bulk of the ligand (*Figure 1.14*).

Most *N*-heterocyclic carbene complexes comprise of symmetric ligands bound to the metal centre that in catalysis act only as spectator ligands. However, there are a number of complexes that have been synthesised with chiral and hybrid (mixed donor) ligands.

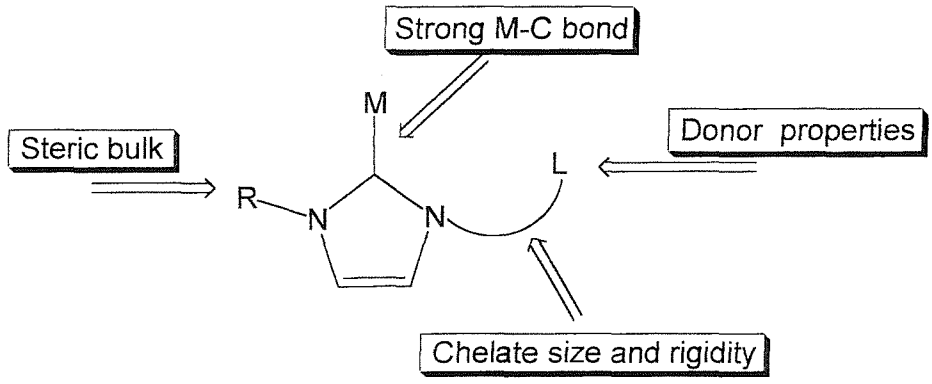

Figure 1.14. Features of mixed donor carbene ligands.

Until the last few years, there have been very few examples of mixed donor carbene complexes;[43,44,70] even though a report claimed the isolation of a range of mixed donor free carbenes.[71] Although, only one other report has been made recently of a free isolated mixed donor carbene,[30] a number of complexes have been synthesised in the last three years with mixed donor carbenes ligands.[30,35,72] These include nucleophilic carbenes linked to pyridine,[73] oxazoline,[74] alkoxide[75] and Schrock type carbene moieties.[30]

Similar mixed donor phosphine complexes have been synthesised and reported to be very effective pre-catalysts to important transformations, including mixed donor phosphine-pyridine ligands.[69,76,77]

1.9 Aims

The aims of the research were to investigate and develop novel mixed donor carbenes, including chiral carbene ligands, for use as ligands for palladium in catalysts, as well as to explore their use as ligands for other metals. These complexes were expected to have possible applications in the Heck reaction, the co-polymerization of carbon monoxide with ethylene, and the conversion of methyl-acetylene to methyl-methacrylate using carbon monoxide and methanol. Palladium complexes containing mixed donor nitrogen-

phosphine ligands have been shown to be effective pre-catalysts in these reactions. However, the disadvantages of the phosphine complexes as catalysts are the need for a large excess of the ligand, and the degradation of the catalysts leading to the loss of activity. It was hoped that by using carbenes as ligands, these problems could be overcome as they form much more stable bonds to transition metals. The investigations into these ligands and their complexes have given us reason to produce a number of publications as others have been involved in competing research.[78]

REFERENCES

1 K. Öfele, *J. Organomet. Chem.*, **1968**, *12*, 42.

2 H.W. Wanzlick, H.J. Schonherr, *Angew. Chem., Int. Ed. Engl.*, **1968**, *7*, 141.

3 A.J. Arduengo III, R.L. Harlow, M. Kline, *J. Am. Chem. Soc.*, **1991**, *113*, 361.

4 A.H. Cowley, *J. Organomet. Chem.*, **2001**, *617*, 105.

5 T. Weskamp, F.J. Kohl, W. Hieringer, D. Gleich, W.A. Herrmann, *Angew. Chem., Int. Ed. Engl.*, **1999**, *38*, 2416.

6 W.A. Herrmann, C. Köcher, *Angew. Chem., Int. Ed. Engl.*, **1997**, *36*, 2162.

7 M. Regitz, *Angew. Chem., Int. Ed. Engl.*, **1996**, *35*, 725.

8 A.J. Arduengo III, *Acc. Chem. Res.*, **1999**, *32*, 913.

9 D. Bourissou, O. Guerret, F.P. Gabbaï, G. Bertrand, *Chem. Rev.*, **2000**, *100*, 39.

10 C.J. Carmalt, A.H. Cowley, *Adv. Inorg. Chem.*, **2000**, *50*, 1.

11 T. Westamp, V.P.W. Böhm, W.A. Herrmann, *J. Organomet.Chem.*, **2000**, *600*, 12.

12 E.O. Fischer, A Maasböl, *Angew. Chem., Int. Ed. Engl.*, **1964**, 580.

13 R.R. Schrock, *J. Am. Chem. Soc.*, **1974**, *96*, 6796.

14 H. Tomioka, M. Hattori, K. Hirai, S. Murata, *J. Am. Chem. Soc.*, **1996**, *118*, 8723.

15 W.A. Herrmann, *Angew. Chem., Int. Ed. Engl.*, **2002**, *41*, 1290.

16 R.W. Alder, P.R. Allen, M. Murray, A.G. Orpen, *Angew. Chem., Int. Ed. Engl.*, **1996**, *35*, 1121.

17 H.W. Wanzlick, *Angew. Chem., Int. Ed. Engl.*, **1962**, *1*, 75.

18 Y. Liu, P.E. Lindner, D.M. Lemal, *J. Am. Chem. Soc.*, **1999**, *121*, 10626.

19 M.K. Denk, K. Hatano, M. Ma, *Tetrahedron Lett.*, **1999**, *40*, 2057.

20 F.E. Hahn, L. Wittenbecher, D. Le Van, R. Fröhlich, *Angew. Chem., Int. Ed. Engl.*, **2000**, *39*, 541.

21 A.J. Arduengo III, H.V.R. Dias, R.L. Harlow, M. Kline, *J. Am. Chem. Soc.*, **1992**, *114*, 1881.

22 V.P.W. Böhm, W.A. Herrmann, *Angew. Chem., Int. Ed. Engl.*, **2000**, *39*, 4037.

23 B. Bildstein, *J. Electroanal. Chem.*, **2001**, *617*, 28.

24 L. Xu, W. Chen, J.F. Bickley, A. Steiner, J. Xiao, *J. Organomet. Chem.*, **2000**, *598*, 409.

25 K.M. Lee, C.K. Lee, I.J.B. Lin, *Angew. Chem., Int. Ed. Engl.*, **1997**, *36*, 1851.

26 J. Schwarz, V.P.W. Böhm, M.G. Gardiner, M. Grosche, W.A. Herrmann, W. Hieringer, G. Raudaschl-Sieber, *Chem. Eur. J.*, **2000**, *6*, 1773.

[27] W.A. Herrmann, C. Köcher, L. Goossen, G.R.J. Artus, *Chem. Eur. J.*, **1996**, *2*, 1627.

[28] U. Kernbach, M. Ramm, P. Luger, W.P. Fehlhammer, *Angew. Chem., Int. Ed. Engl.*, **1996**, *35*, 310.

[29] H.V.R. Dias, W.Jin, *Tetrahedron Lett.*, **1994**, *35*, 1365.

[30] A. Fürstner, H. Krause, L. Ackermann, C.W. Lehmann, *Chem. Commun.*, **2001**, 2240.

[31] J.C. Green, R.G. Scurr, P.L. Arnold, F.G.N. Cloke, *Chem. Commun.*, **1997**, 1963; C. Boehme, G. Frenking, *Organometallics,* **1998**, *17*, 5801.

[32] M.F. Lappert, *J. Organomet. Chem*, **1988**, *358*, 185.

[33] D.S. McGuinness, N. Saendig, B.F. Yates, K.J. Cavell, *J. Am. Chem. Soc.*, **2001**, *123*, 4029.

[34] R.-Z. Ku, J.-C. Huang, J.-Y. Cho, F.-M. Kiang, K.R. Reddy, Y.-C. Chen, K.-J. Lee, J.-H. Lee, G.-H. Lee, S.-M. Peng, S.-T. Liu, *Organometallics*, **1999**, *18*, 2154.

[35] S. Gründemann, A. Kovacevic, M. Albrecht, J.W. Faller, R.H. Crabtree, *Chem. Commun.*, **2001**, 2274.

[36] D.J. Nielsen, K.J. Cavell, B.W. Skelton, A.H. White, *Organometallics*, **2001**, *20*, 995.

[37] A.J. Arduengo III, M. Kline, J.C. Calabrese, F. Davidson, *J. Am. Chem. Soc.*, **1991**, *113*, 9704.

[38] D. Enders, H. Gielen, G. Raabe, J. Runsink, J.H. Teles, *Chem. Ber.*, **1996**, *129*, 1483.

[39] A.J. Arduengo, III, F. Davidson, R. Krafczyk, W.J. Marshall, M. Tamm, *Organometallics*, **1998**, *17*, 3375.

[40] M.F. Lappert, *J. Organomet. Chem.*, **1998**, *358*, 185.

[41] H.M.J. Wang, I.J.B. Lin, *Organometallics*, **1998**,*17*, 972.

[42] P.L. Arnold, F.G.N. Cloke, T. Geldbach, P.B. Hitchcock, *Organometallics*, **1999**, *18*, 3228.

[43] D. Sellmann, W. Prechtal, F. Knoch, M. Moll, *Organometallics*, **1992**, *11*, 2346.

[44] H. Lang, J.J. Vittal, P.-H. Leung, *J. Chem. Soc., Dalton Trans.*, **1998**, 2109.

[45] C. Boehme, G. Frenking, *Organometallics*. **1998**, *17*, 5801.

[46] A.J. Arduengo, III, S.F. Gamper, J.C. Calabrese, F. Davidson, *J. Am. Chem. Soc.*, **1994**, *116*, 4391.

[47] C. Köcher, W.A. Herrmann, *J. Organomet. Chem*, **1997**, *532*, 261.

[48] U. Kernbach, M. Ramm, P. Luger, W.P. Fehlhammer, *Angew. Chem., Int. Ed. Engl.*, **1996**, *35*, 3.

[49] W.A. Herrmann, M. Elison, J. Fischer, C. Köcher, G.R.J. Artus, *Angew. Chem., Int. Ed. Engl.*, **1995**, *34*, 2371.

[50] W.A. Herrmann, C. Köcher, L. Goossen, G.R.J. Artus, *Chem. Eur. J.*, **1996**, *2*, 1627.

[51] D. Michalios, *Dissertation,* Technische Universität München, **1992**.

[52] K. Öfele, C.G. Kreiter, *Chem. Ber.*, **1972**, *105*, 529.

[53] W.A. Herrmann, K. Öfele, M. Elison, F.E. Kühn, P.W. Roesky, *J. Organomet. Chem.*, **1994**, *480,* C7.

[54] R.E Douthwaite, M.L.H. Green, P.J. Silcock, P.T. Gomes, *Organometallics*, **2001**, *20*, 2611.

[55] M.V. Baker, B.W. Skelton, A.H. White, C.C. Williams, *J. Chem. Soc., Dalton Trans.*, **2001**, 111.

[56] W. A. Herrmann, C-P. Reisinger, M. Spiegler, *J. Organomet. Chem.*, **1998**, *557*, 93; C. Zhang, J. Huang, M. L. Trudell, S. P. Nolan, *J. Org. Chem.*, **1999**, *64*, 3804; J. Huang, S. P. Nolan, *J. Am. Chem. Soc.*, **1999**, *121*, 9889; S. Caddick, F.G.N. Cloke, G.K.B. Clentsmith, P.B. Hitchcock, D. McKerrecher, L.R. Titcomb, M.R.V. Williams, *J. Organomet. Chem.*, **2001**, *617*, 635.

[57] M. G. Gardiner, W. A. Herrmann, C-P. Reisinger, J. Schwarz, M. Spiegler, *J. Organomet. Chem.*, **1999**, *572*, 239.

[58] V.P.W. Böhm T. Weskamp, C.W.K. Gstöttmayr, W.A. Herrmann, *Angew. Chem. Int. Ed. Engl.*, **2000**, *39*, 1602.

[59] A.C. Hillier, H.M. Lee, E.D. Stevens, S.P. Nolan, *Organometallics*, **2001**, *20*, 4246.

[60] B. Çetinkaya, I. Özdemir, C. Bruneau, P.H. Dixneuf, *J. Mol. Catal. A.*, **1997**, *118*, L1; T. Weskamp, W.C. Schattenmann, W.C. Spiegler, W.A. Herrmann, *Angew. Chem. Int. Ed. Engl.*, **1998**, *37*, 2490; J. Huang, E.D. Stevens, S.P. Nolan, J.L. Petersen, *J. Am. Chem. Soc.*, **1999**, *121*, 2674; J.G. Hamilton, U.Frenzel, F.J. Kohl, T.Westamp, J.J. Rooney, W.A. Herrmann, O. Nuyken, *J. Organomet. Chem.*, **2000**, *606*, 8; S.W. Craig, J.A. Manzer, E.B. Coughlin, *Macromolecules*, **2001**, *34*, 7929.

[61] A.C. Chen, L. Ren, A. Decken, C.M. Crudden, *Organometallics*, **2000**, *19*, 3459; W.A. Herrmann, L.J. Goossen, C. Køcher, G.R.J. Artus, *Angew. Chem., Int. Ed.*

Engl., **1996**, *35*, 2805; J. Huang, E.D. Stevens, S.P. Nolan, J.L. Petersen, *J. Am. Chem. Soc.*, **1999**, *121*, 2675.

62 S.C. Schürer, S. Gessler, N. Buschmann, S. Blechert, *Angew. Chem. Int. Ed. Engl.*, **2000**, *39*, 3898.

63 L. Xu, W. Chen, J. Xiao, *Organometallics*, **2000**, *19*, 1123.

64 D. Enders, H. Gielen, *J. Organomet. Chem.*, **2001**, *617*, 70; J. Huang, L. Jafarpour, A.C. Hillier, E.D. Stevens, S.P. Nolan, *Organometallics*, **2001**, *20*, 2878; T. Weskamp, W.C. Schattenmann, M. Spiegler, W.A. Herrmann, *Angew. Chem. Int. Ed. Engl.*, **1998**, *37*, 2490; D. Enders, H. Gielen, G. Raabe, J. Runsink, J.H. Teles, *Chem. Ber.*, **1996**, *129*, 1483; W.A. Herrmann, L.J. Goossen, C.Köcher, G.R.J. Artus, *Angew. Chem. Int. Ed. Engl.*, **1996**, *35*, 2805.

65 D.S. Clyne, J. Jin, E. Genest, J.C. Gallucci, T.V. RajanBabu, *Organic Lett.*, **2000**, *2*, 1125.

66 B. Cornils, W. A. Herrmann, *Applied Homogeneous Catalysis with Organometallic Compounds*, Wiley-VCH, Weinheim, **2000**.

67 G.W. Parshall, S.D. Ittel, *Homogeneous Catalysis*, 2nd Edition, Wiley Interscience NY, **1992**.

68 M. Scholl, T. M. Trnka, J. P. Morgan, R. H. Grubbs, *Tetrahedron Lett.*, **1999**, *40*, 2247; L. Ackermann, A. Fürst, T. Weskamp, F.J. Kohl, W.A. Herrmann, *Tetrahedron Lett.*, **1999**, *40*, 4787; U. Frenzel, T. Weskamp, F.J. Kohl, W.C. Schattenmann, O. Nuyken, W.A. Herrmann, *J. Organomet. Chem.*, **1999**, *586*, 263; W.A. Herrmann, V.P. W. Böhm, C.W.K. Gstöttmayr, M. Grosche, C.-P. Reisinger, T. Westamp, *J. Organomet. Chem.*, **2001**, *617*, 616.

69 P. Braunstein, F. Naud, *Angew. Chem., Int. Ed. Engl.*, **2001**, *40*, 680.

70 W.A. Herrmann, L. Goossen, M. Spiegler, *Organometallics*, **1998**, *17*, 2162; J.A. Chamizo, P.B. Hitchcock, H.A. Jasim, M.F. Lappert, *J. Organomet. Chem.*, **1993**, *451*, 89; B. Cetinkaya, I. Ozdemir, P.H. Dixneuf, *J. Organomet. Chem.*, **1997**, *534*, 153.

71 W.A. Herrmann, C. Køcher, L. Goossen, G.R.J. Artus, *Chem. Eur. J.*, **1996**, *2*, 1627.

72 J.C. Garrison, R.S. Simons, W.G. Kofron, C.A. Tessier, W.J. Youngs, *Chem. Commun.*, **2001**, 1780; D.S. Mcguinness, K.J. Cavell, *Organometallics*, **2000**, *19*, 741; E. Peris, J.A. Loch, J. Mata, R.H. Crabtree, *Chem. Commun.*, **2001**, 201.

[73] J.C.C. Chen, I.J.B. Lin, *Organometallics*, **2000**, *19*, 5113.

[74] M.T.Powell, D.-R. Hou, M.C. Perry, X. Cui, K. Burgess, *J. Am. Chem. Soc.*, **2001**, *123*, 8878.

[75] P.L.Arnold, A.C. Scarisbrick, A.J. Blake, C. Wilson, *Chem. Commun.*, **2001**, 2340.

[76] E. Drent, P. Arnoldy, P.H.M. Budzelaar, *J. Organomet. Chem.*, **1993**, *45*, 247.

[77] N. Rahmouni, J.A. Osborn, A. De Cian, J. Fisher. A. Ezzamarty, *Organometallics*, **1998**, *17*, 2470.

[78] S. Kleinhenz, A.A.D. Tulloch, A.A. Danopoulos, *Acta. Cryst.*, **2000**, *C56*, e476; A.A.D. Tulloch, A.A. Danopoulos, R.P. Tooze S.M. Cafferkey, S. Kleinhenz,M.B. Hursthouse, *Chem. Commun.*, **2000**, 1247; A.A.D. Tulloch, A.A. Danopoulos, S. Winston, S. Kleinhenz, G. Eastham, *J. Chem. Soc., Dalton Trans.*, **2000**, 4499; A.A.D. Tulloch, A.A. Danopoulos, S. Kleinhenz, M.E. Light, M.B. Hursthouse, G. Eastham, *Organometallics*, **2001**, *20*, 2027; A.A.D. Tulloch, A.A. Danopoulos, G.J. Tizzard, S.J. Coles, M.B. Hursthouse, R.S. Hay-Motherwell, W.B. Motherwell, *Chem. Commun.*, **2001**, 1270.

Chapter 2

Imidazolium Salts and Free Carbenes

Chapter 2

Imidazolium Salts and Free Carbenes

2.1 Introduction

The most frequently used method to synthesise stable free carbenes and nucleophilic carbene ligands is through their corresponding imidazolium salts.[1] Although a number of different types of stable carbenes have been isolated, including triazol-3-ylidenes,[2] thiazol-2-ylidenes,[3] imidazolin-2-ylidenes[4] and benzimidazol-2-ylidenes,[5] the majority are imidazol-2-ylidenes[6]. This is due to their increased stability[7,8] and their capacity for steric and electronic functionalising as well as their relative ease of synthesis. Because of these factors, in this chapter are described a wide range of new imidazolium salts as well as attempts to convert them to the corresponding free carbenes. Imidazolium salts can be made *via* a number of general routes:

i) By the reaction of primary amines with glyoxal and formaldehyde in the presence of an acid;[9]

ii) By the reaction of an *ortho*-ester with a secondary diamine in the presence of an ammonium salt;[10]

iii) By the treatment of benzimidazoles with trityl-tetrafluoroborate to generate benzimidazolium salt;[11]

iv) By a multi component reaction starting from glyoxal, formaldehyde, a primary amine and ammonium halide with the subsequent alkylation by an alkylhalide to form the imidazolium salt (*Scheme 2.1*);[12]

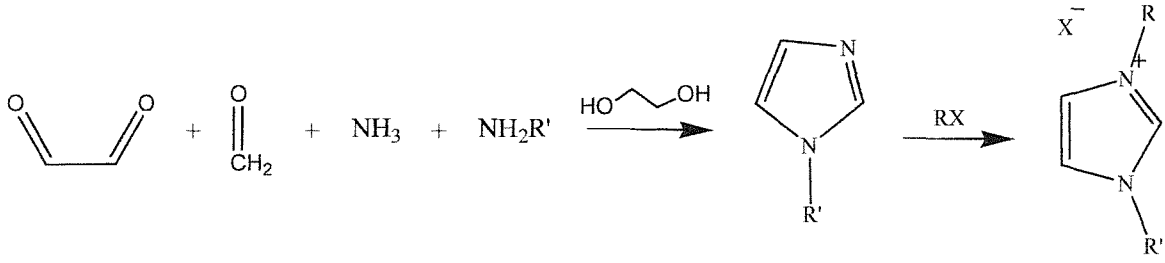

Scheme 2.1. General route iv): synthetic route to imidazolium salts

v) By a multi stage sequence initially forming an isothiocyanate, converting it to a acetalylthiourea, which is then ring closed to the mercapto-imidazole. This is

desulphurised by nitric acid giving the substituted imidazole[13] and finally reacted with an alkyl or aryl halide (*Scheme 2.2*).

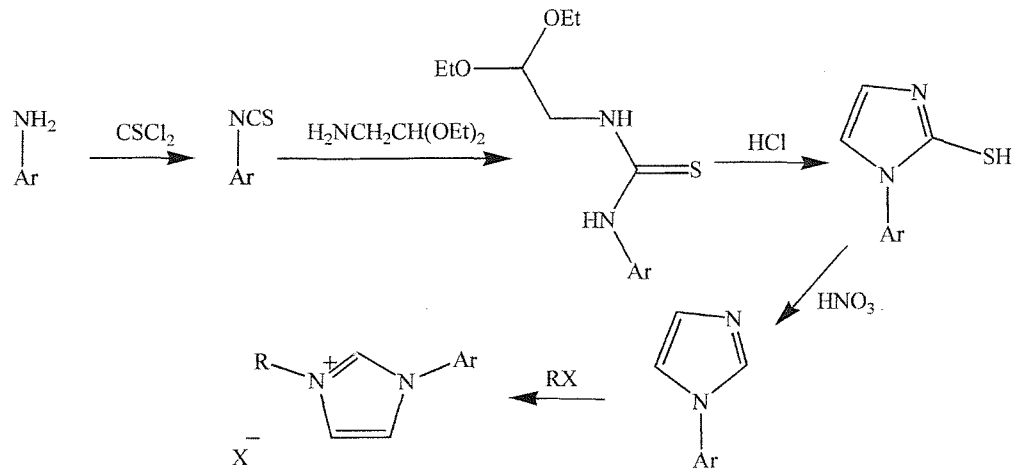

Scheme 2.2. General route v): synthetic route to imidazolium salts

The aryl substituted imidazolium salts described in this chapter were synthesised *via* general route v) (*Scheme 2.2*). However, the *tert*butyl substituted imidazolium salts were synthesised *via* general route iv) (*Scheme 2.1*) and some imidazolium salts were synthesised by quaternising imidazoles that were purchased from common chemical suppliers. The availability of starting materials was a determining factor in choosing these general methods, which involve the quaternisation of imidazoles.

The role in catalysis of the family of ligand precursors described in this chapter is very important. The architectures of the corresponding carbene ligands originating from these salts are designed to mimic systems extensively used in catalysis.[14,15] Furthermore, it has been shown by ourselves,[16,17] and others,[18,19,20,21,22] that they are suitable precursors to extremely good Heck catalysts. The incorporation of two donor atoms with different electronic characteristics into the ligand is believed to give the design its versatility, originating from the ability to control the coordination sphere of the metal during the various catalytic steps.

RESULTS AND DISCUSSION

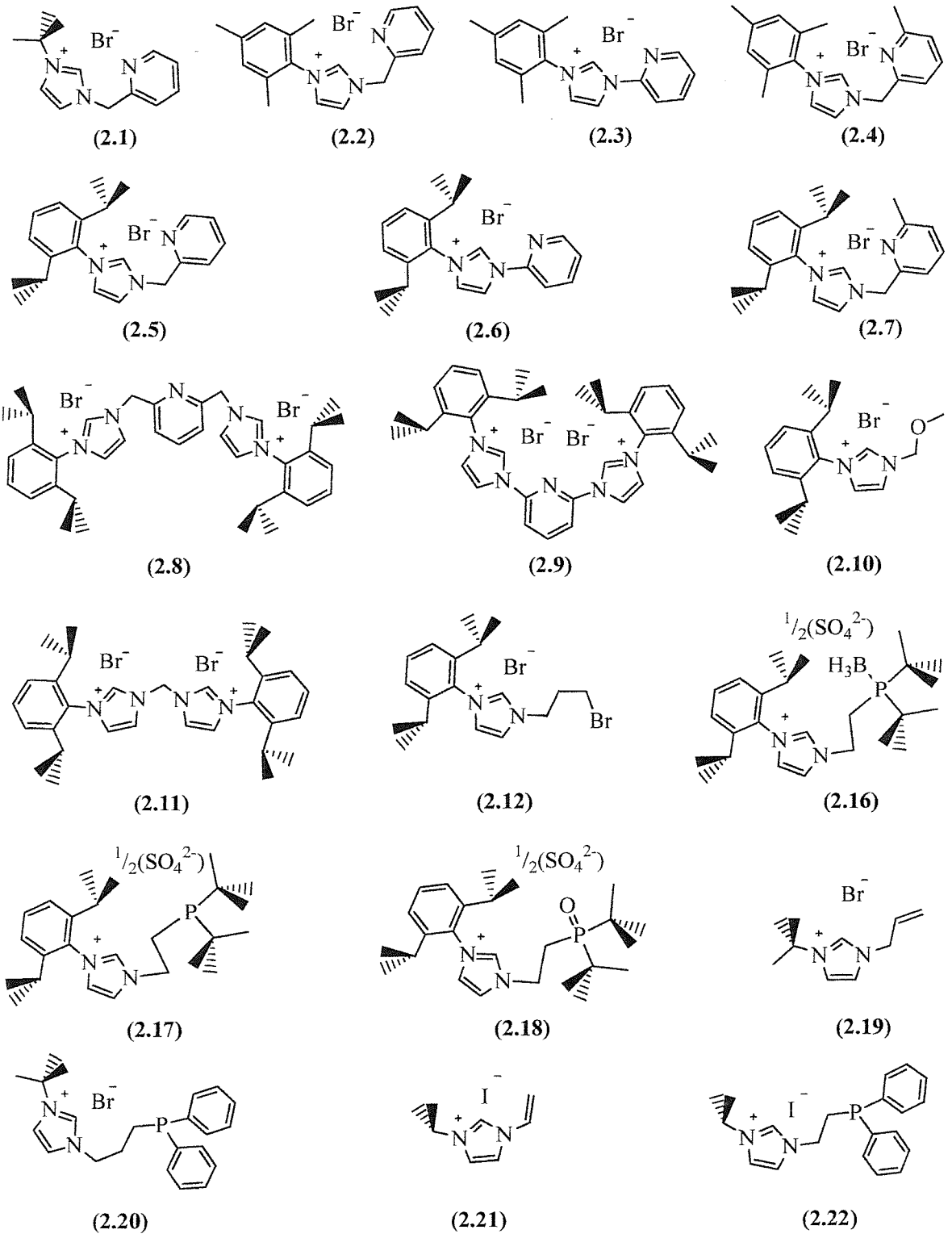

Figure 2.1. Imidazolium salts synthesised.

2.2 Ligand design

As mentioned in Chapter 1, *N*-heterocyclic carbene ligands have σ-donor properties that are similar to the electron-rich phosphines.[23,24] Due to their similarities as ligands, it follows that carbene ligand design should mimic ligands from the well-trodden field of phosphine chemistry. There are wide ranges of phosphine ligands that have been extensively used in catalysis; these include *monodentate*, *bidentate*, "pincer" type *tridentate* and hybrid ligands. The design of the imidazolium salts to be synthesised was directed to produce carbene ligands that mimic some of these phosphines (*Figure 2.2*).

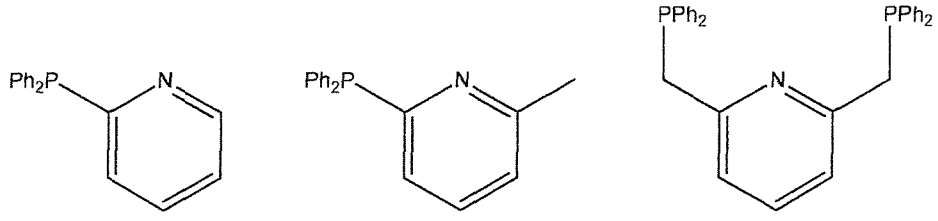

Figure 2.2. Compounds **(2.1)-(2.9)** were designed to mimic the above ligands, developed by Drent *et al.*[25] and Osborn *et al.*[27]

Compounds **(2.1)-(2.7)** were synthesised to mimic phosphine-pyridine ligands developed by Drent *et al.*[25] (ligands widely used in carbonylation chemistry).[26] Compounds **(2.8)** and **(2.9)** were designed to mimic "pincer" type phosphine ligands.[27,28] Compound **(2.10)** was developed as a variation of compounds **(2.1)-(2.7)**, functionalised with a weaker donor for late transition metals. Compound **(2.11)** was made as a modification of the bidentate carbene ligands developed by Herrmann *et al.*[29] Compounds **(2.12)**, **(2.19)** and **(2.21)** were synthesised as precursors for further functionalisation.

One of the limitations of phosphine ligands for use in catalytic systems is the requirement for an excess of ligand, due to the possibility of dissociation from the metal centre. As *N*-heterocyclic carbenes are similar donors to phosphines but do not dissociate from the metal centre, a mixed carbene-phosphine ligand could provide a stoichiometric amount of a phosphine donor linked to the metal by a carbene donor. This combination would allow the direct comparison of the donor types in one system. Compounds **(2.13)-(2.18)**, **(2.20)** and **(2.22)** were designed as precursors for mixed carbene-phosphine ligands.

2.3 Synthesis of imidazolium salts

In this chapter a range of synthetic methods, and characterisation of mixed donor functionalised imidazolium salts, are described. The new functionalised imidazolium salts were prepared by following one of three main synthetic methods detailed below:

i) *Quaternisation with bromomethyl pyridine in methanol at room temperature:* The manipulations were carried out with extreme caution, as the bromomethyl pyridine derivatives used are very powerful lachrymators. After neutralising the starting bromomethyl pyridinium derivative and extracting the liberated bromomethyl pyridines in ether, they were reacted with a methanolic solution of the corresponding imidazole. Following the completion of the quaternisation reaction in methanol, the resulting solid was washed with ether to give the products as white solids.

ii) *Quaternisation with bromopyridine in the melt:* The imidazole was quaternised in a melt with the respective bromopyridine compound for two to four days. After cooling, the brown residue was washed with ether to give the products as white solids.

iii) *Quaternisation in xylene, dioxane or ethanol at elevated temperatures:* The imidazole was quaternised in a xylene, dioxane or ethanol solution of the corresponding alkylhalide or allylhalide at elevated temperatures to give the product as a white solid.

In general, these quaternisation reactions proceeded selectively and at good rates in polar solvents like methanol, ethanol and dioxane. The white solid products were characterised by analytical and spectroscopic methods. In most cases, they were obtained as spectroscopically and analytically pure products. However, further purification was sometimes required. In these cases, recrystallisation was carried out from a saturated dichloromethane and diethyl ether solution or by cooling a saturated acetone solution. On occasions, the products were isolated as oils, which were analytically pure and were triturated with cold acetone or ether to obtain white powders. The imidazolium salts containing the *tert*butyl group were most prone to oiling and often required numerous attempts to isolate as a solid.

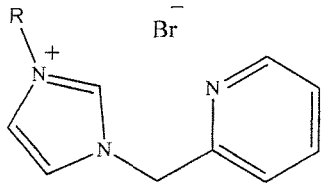

Figure 2.3. Picolyl-functionalised imidazolium salts, R = *tert*butyl, mesityl, 2,6-di*iso*propylphenyl.

The majority of the salts were isolated as their hydrates, having been washed with cold (undried) acetone. The process of washing with cold acetone in air has been identified as the source of the water. However, the imidazolium salts containing the 2,6-di*iso*propyl-phenyl groups have never shown any sign of oiling, were not washed with acetone and therefore were isolated as the anhydrous salts. The ability of water to aid crystallisation is thought to be due to the interaction between the bromide and the water, creating a large "pseudo-anion" to pack with the large cation. When the bromide was replaced with a much larger anion (tetraphenylborate) oiling never occurred and analytical data showed no water of crystallisation. However, the tetraphenylborate salts had low solubility in normal solvents and their use as ligand precursors was limited. Salts containing the 2,6-di*iso*propylphenyl groups generally showed good crystallinity even in the absence of counter-anions of comparable size.

2.4 Characterisation of nitrogen and oxygen functionalised imidazolium salts, compounds (2.1)-(2.12)

2.4.1. X-ray diffraction studies

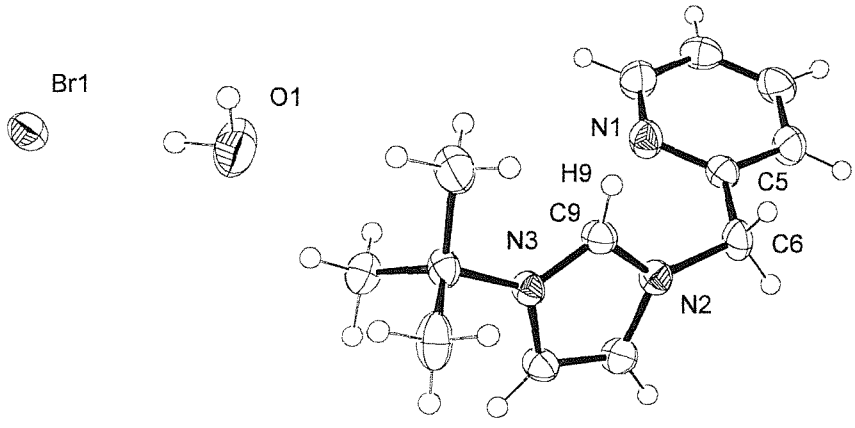

Figure 2.4. X-ray crystal structure of 3-(*tert*butyl)-1-(α-picolyl)-imidazolium bromide hydrate **(2.1)**.

X-ray diffraction quality crystals of **(2.1)** were obtained by cooling a saturated acetone solution to -35°C. An Ortep diagram of the salt is shown in *Figure 2.4* and bond lengths and important angles are shown in *Table 2.1* and *Table 2.2*.

O(1)-H(1O)	0.98(4)	C(2)-C(3)	1.374(4)
O(1)-H(2O)	0.98(4)	C(2)-H(21)	0.96(3)
N(3)-C(9)	1.326(3)	C(3)-C(4)	1.376(3)
N(3)-C(8)	1.383(3)	C(3)-H(31)	0.96(3)
N(3)-C(10)	1.502(2)	C(4)-H(41)	0.93(3)
C(9)-N(2)	1.327(3)	C(1)-H(11)	0.97(3)
C(9)-H(9)	0.89(2)	C(10)-C(12)	1.519(3)
N(1)-C(5)	1.327(3)	C(10)-C(11)	1.521(3)
N(1)-C(1)	1.348(3)	C(10)-C(13)	1.527(3)
N(2)-C(7)	1.373(3)	C(11)-H(111)	1.03(3)
N(2)-C(6)	1.467(3)	C(11)-H(112)	0.94(3)
C(8)-C(7)	1.344(3)	C(11)-H(113)	0.97(3)
C(8)-H(81)	0.92(2)	C(12)-H(121)	0.95(3)
C(7)-H(71)	0.96(3)	C(12)-H(122)	0.96(3)
C(5)-C(4)	1.390(3)	C(12)-H(123)	0.94(3)
C(5)-C(6)	1.516(3)	C(13)-H(131)	1.00(3)
C(6)-H(61)	0.97(3)	C(13)-H(132)	0.97(3)
C(6)-H(62)	0.97(2)	C(13)-H(133)	1.05(4)
C(2)-C(1)	1.370(4)		

Table 2.1. Bond lengths (Å) for 3-(*tert*butyl)-1-(α-picolyl)-imidazolium bromide hydrate, compound **(2.1)**.

C(9)-N(3)-C(8)	108.15(17)	C(8)-C(7)-N(2)	107.31(19)
C(9)-N(3)-C(10)	126.07(17)	N(1)-C(5)-C(6)	118.77(18)
N(3)-C(9)-N(2)	108.90(19)	N(2)-C(6)-C(5)	112.65(18)
C(9)-N(2)-C(7)	108.54(18)	N(3)-C(9)-H(9)	126.9(14)
C(9)-N(2)-C(6)	124.20(19)	N(2)-C(9)-H(9)	123.9(14)
C(7)-C(8)-N(3)	107.10(19)		

Table 2.2. Important angles (°) for 3-(*tert*butyl)-1-(α-picolyl)-imidazolium bromide hydrate, compound **(2.1)**.

The X-ray crystal structure of **(2.1)**, shows that the cation and bromide anion are linked *via* a water molecule through weak intermolecular hydrogen bonds (*Figure 2.5*).[30] Intermolecular hydrogen bonding is observed between one proton from each methyl of the *tert*butyl group and the oxygen atom of the water molecule. There are also weak hydrogen bonds to a pair of symmetry-equivalent bromide anions from the hydrogen atoms of the water molecule; these bond lengths and angles are shown in *Table 2.3*.

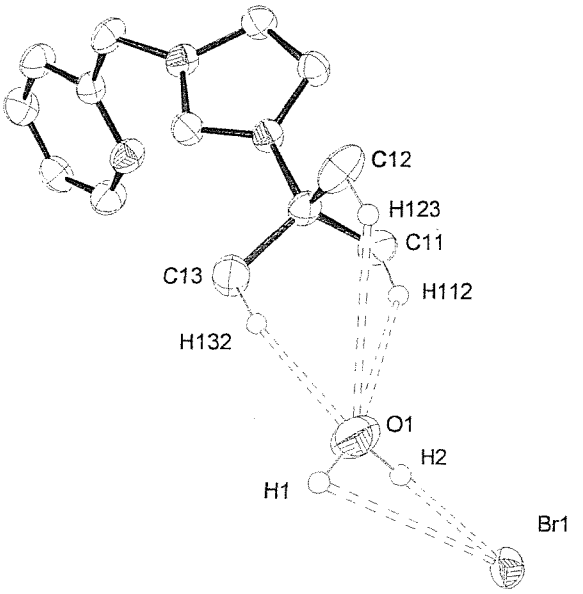

Figure 2.5. Dotted lines represent the weak hydrogen bonding in the X-ray crystal structure of 3-(*tert*butyl)-1-(α-picolyl)-imidazolium bromide hydrate **(2.1)**.

D	H	*A*	*D* – H	H ··· *A*	*D* ··· *A*	*D* – H ··· *A*
C13	H132	O1	0.97(3) Å	2.34(3) Å	3.292(3) Å	165(2)°
O1	H2	Br1	0.98(4) Å	2.33(4) Å	3.305(2) Å	175(3)°
O1	H1	Br1	0.98(4) Å	2.33(4) Å	3.301(2) Å	171(3)°

Table 2.3. Hydrogen-bonding geometry of compound **(2.1)**.

2.4.2. Electrospray mass spectrometry

The electrospray mass spectra of these salts are generally quite simple, showing either M^+ or $^1/_2M^+$ as the most intense peak with no other major fragments. However, even though this technique was useful to support the formulation of the cation, it did not give any information about the anion or the connectivity of the salt obtained. This limitation is because the parent ion being observed (the cation) is pre-ionised and therefore creates a more intense peak than any fragment ion that is formed by the ionisation method.

2.4.3. NMR spectroscopy

2.4.3.1. Characteristic peaks for pyridyl, picolyl and lutidyl functionalised salts, compounds (2.1)-(2.9)

The formation of the imidazolium salts was established by a low field peak assignable to the 2-imidazolium protons usually observed between 10.0 and 12.0 ppm in the ^{1}H NMR spectra in $CDCl_3$. Other characteristic peaks observed in the ^{1}H NMR spectra of this family of compounds are (*Figure 2.7*):

i) A singlet between 5.5 and 6.5 ppm assigned to the protons of the CH_2 bridge in the functionalised picolyl compounds, when n = 1;

ii) A singlet around 1.6 ppm assigned to the protons of the *tert*butyl group, when R = *tert*butyl;

iii) Singlets around 2.0, 2.3 and 7.0 ppm assigned to the protons of the mesityl group when R = mesityl;

iv) Doublets around 1.1 ppm; a septet around 2.3 ppm; and singlets around 7.3 and 7.5 ppm assigned to the protons of the 2,6-di*iso*propylphenyl group, when R = 2,6-di*iso*propylphenyl;

v) A singlet at 2.4 ppm assigned to the methyl of the lutidyl group when R' = .Me.

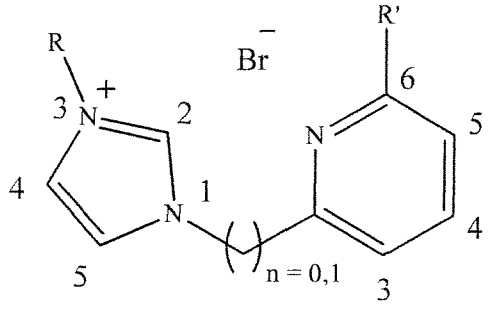

Figure 2.6. Connectivity and numbering order of the imidazolium and pyridine rings for the salts **(2.1)-(2.7)**. R = *tert*butyl, mesityl or 2,6-di*iso*propylphenyl R' = methyl or hydrogen.

The peaks around 1.1 ppm assigned to the methyl protons of the 2,6-di*iso*propylphenyl, when R = 2,6-di*iso*propylphenyl, appear as a pair of doublets when the *iso*propyl groups have restricted rotation; thus the methyls pointing in the direction of the double bond on the imidazolium ring are different to those that point away.

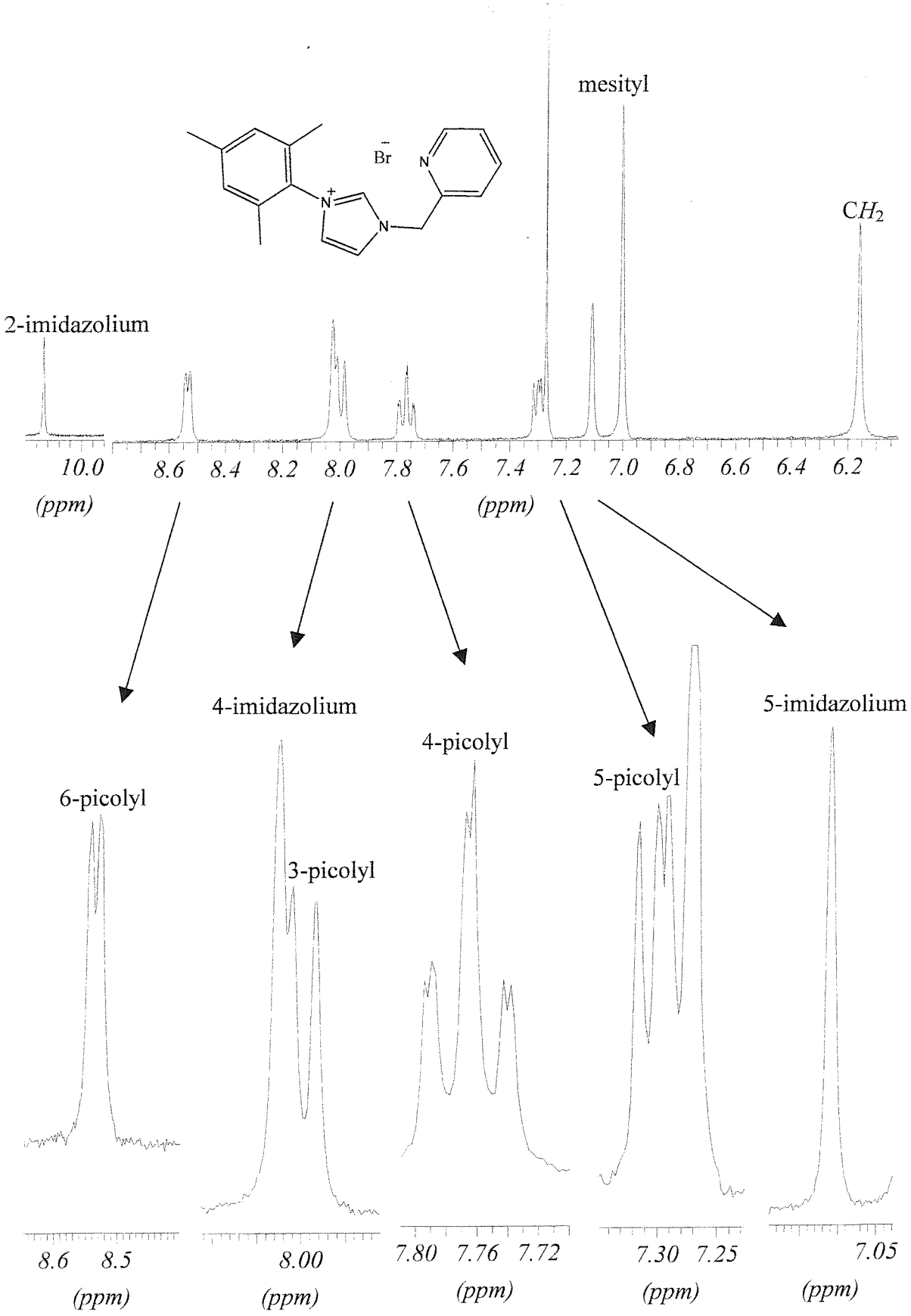

Figure 2.7. ^{1}H NMR spectrum of 3-(mesityl)-1-(α-picolyl)-imidazolium bromide, compound **(2.2)**.

The chemical shifts of the doublets assignable to the protons in the 4- and 5-positions on the imidazolium ring are diagnostic of the local environment (i.e. the substituents on the heterocyclic ring). In the case of the 3-*tert*butyl-imidazolium salts, these protons appear as two doublets of similar chemical shift, at 7.5 and 7.6 ppm in the ^{1}H NMR spectra. In contrast, for the mesityl substituted salts the doublets are seen much further apart in the ^{1}H NMR spectra at 7.1 ppm (5-*H*) and 8.1 to 8.9 ppm (4-*H*). This difference is even greater for the 2,6-di*iso*propylphenyl functionalised salts, at 7.1 ppm (5-*H*) and 8.3 to 10.0 ppm (4-*H*).

The peak assigned to the 3-position of the functionalised pyridine in the ^{1}H NMR spectra is also diagnostic of its environment, with a down field shift of up to 2 ppm between that of an imidazolium salt with a single carbon bridge to the functionalised pyridine, and that of a salt with no methylene bridge. The chemical shifts of the other peaks in the ^{1}H NMR spectra for these compounds were as expected and were relatively unchanged between the different salts.

2.4.3.2. Characteristic peaks for compounds (2.10), (2.11) and (2.12)

Most of the peaks that are characteristic for these salts are similar to those for compounds **(2.1)-(2.9)**. A peak at 3.6 ppm in the ^{1}H NMR spectrum of compound **(2.10)** was assigned to the protons of the methyl group and a peak at 6.2 ppm was assigned to the methylene bridge. A broad peak at 7.3 ppm in the ^{1}H NMR spectrum of compound **(2.11)** was assigned to the protons of the methylene bridge. The peak assigned to the protons in the 5-position on the imidazolium ring in the ^{1}H NMR spectra is shifted down field by 1 ppm from the most de-shielded protons in the 5-position in the other imidazolium salts (8.1 ppm) and the peak assigned to the proton in the 4-position is at 10.0 ppm. Peaks at 1.2, 3.5 and 4.9 ppm in the ^{1}H NMR spectrum of compound **(2.12)** were assigned to the protons of the γ-bromopropyl group. The chemical shifts of the other peaks in the ^{1}H NMR spectra for these compounds were as expected and were relatively unchanged between the different salts.

2.5 Characterisation of phosphine functionalised imidazolium salts

The accessibility of the new imidazolium compounds described above led us to develop methods to produce analogous phosphine functionalised imidazolium compounds.

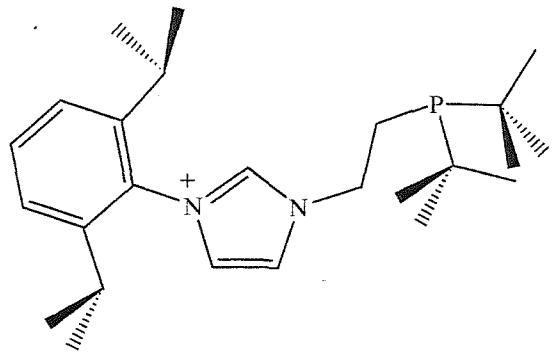

Figure 2.8. Connectivity of the imidazolium cation in 1-[3-(2,6-di*iso*propylphenyl)-imidazolium]-2-[di(tertbutyl) phosphine] ethane sulphate **(2.17)**.

2.5.1. Characterisation of compound (2.16)

Ethylene glycol cyclic sulphate (compound **(2.13)**) was synthesised by following a similar procedure to that described by Sharpless *et al.*,[31] and was characterised by ^{1}H NMR spectroscopy. Di-*tert*butylphosphine borane complex (compound **(2.14)**) was synthesised by following a procedure similar to that described by Livinghouse *et al.*,[32] and was used without further characterisation. 1-sulphato-2-(phosphineborane)-ethane lithium salt (compound **(2.15)**) was synthesised by a similar method to that described by Werner *et al.* from compounds **(2.13)** and **(2.14)**, and was characterised by ^{1}H and ^{31}P{H} NMR spectroscopy.[37]

1-[3-(2,6-di*iso*propylphenyl)-imidazolium]-2-[di(*tert*butyl)phosphineborane] ethane sulphate **(2.16)** was prepared by stirring **(2.15)** with 3-(2,6-di*iso*propylphenyl)-imidazole in ethanol for 12 hours, the product was obtained as a white solid. Analytical data confirmed the stoichiometry. However, the major peak in the electrospray mass spectrum in acetonitrile was assigned to the product with the loss of the borane. This is not surprising in view of the harsh ionisation technique used in this method. However, the existence of the coordinated borane was established by a doublet corresponding to a quaternary boron species in the ^{11}B{H} NMR spectrum at -40 ppm. Further conformation of this salt was given by the ^{31}P{H} NMR spectrum where a broad quartet at 43 ppm was observed, coupled to a boron atom ($I = {}^{3}/_{2}$) at the chemical shift range corresponding to a quaternary phosphorus species. The ^{1}H NMR spectrum was not particularly diagnostic as no peak corresponding to the 2-imidazolium proton was observed. However, the remainder of the spectrum consisted of assignable peaks at the expected positions. The ^{13}C{H} NMR spectrum contained characteristic peaks at 150 ppm assigned to the 2-imidazolium carbon and 22 and 69 ppm assigned to the ethylene bridge.

2.5.2. Characterisation of compound (2.17)

Removal of the borane from compound **(2.16)** resulted in the formation of 1-[3-(2,6-di*iso*propylphenyl)-imidazolium]-2-[di(*tert*butyl) phosphine] ethane sulphate **(2.17)** which is shown diagrammatically in *Figure 2.8*. The de-protection of **(2.16)** was carried out under nitrogen by stirring a solution of tetrafluoroboric acid dimethylether complex with **(2.16)** in dichloromethane. Ammonia was used to neutralise the reaction mixture as well as to de-protect the phosphine. The resulting oily solid was very air sensitive and attempts to get good analysis results failed. Electrospray mass spectrum contained peaks corresponding to the imidazolium phosphine as well as peaks for the phosphine oxide. The ^{1}H NMR spectrum contained characteristic peaks for the formation of compound **(2.17)**, however they showed the presence of unidentifiable impurities. In addition, no peak corresponding to the 2-imidazolium proton was observed. We reason that this proton is likely to give rise to a very broad peak due to its interaction with the strongly basic trialkyl phosphine, as shown in *Figure 2.9*. The ^{31}P{H} NMR spectrum provided strong evidence for the presence of the dibutyl alkyl phosphine from the characteristic chemical shift at 19 ppm.[33]

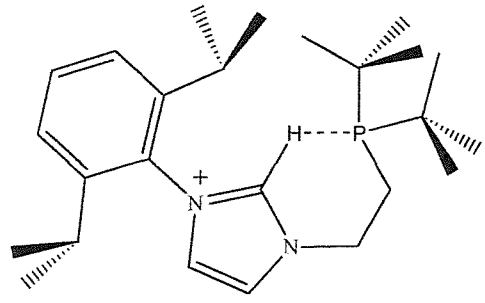

Figure 2.9. A plausible conformation of the cation in **(2.17)**, which could explain the lack of a peak assignable to the 2-imidazolium proton in the ^{1}H NMR spectrum.

2.5.3. Characterisation of compound (2.18)

When compound **(2.17)** was exposed to air and the resulting product, 1-[3-(2,6-di*iso*propylphenyl)-imidazolium]-2-[di(*tert*butyl) phosphinoxide] ethane **(2.18)** was obtained. The oily solid was initially characterised by electrospray mass spectroscopy; the spectrum had a peak that was assigned to the corresponding imidazolium phosphine oxide. The ^{31}P{H} NMR spectrum confirmed the formation of the oxide by a characteristic peak at 65 ppm.[33] Attempts to obtain the elemental analysis failed to give meaningful data, possibly due to residual ammonium salt impurities.

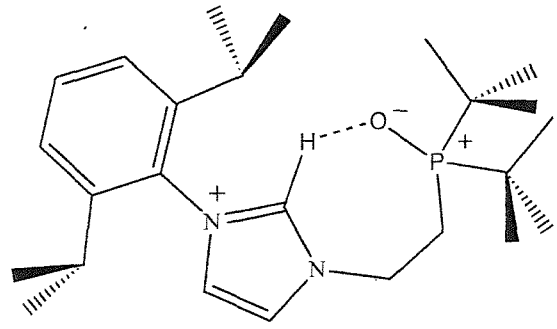

Figure 2.10. A plausible reason for the absence of the 2-imidazolium proton in the ^{1}H NMR spectrum for compound **(2.18)**.

The ^{1}H NMR spectrum of the oxide contained characteristic peaks for the compound. Again, the absence of a peak assignable to the 2-position of the imidazolium ring could be due to broadening as discussed for compound **(2.17)** (*Figure 2.10*).

2.5.4. Characterisation of compound (2.20)

Alternative routes to access phosphine imidazolium compounds were investigated, for example by hydrophosphination of **(2.19)** using $HPPh_2$ and 1,1'-azobis (cyclohexyl carbonitrile) producing 1-[3-(*tert*butyl) imidazolium]-3-diphenyl-phosphine-propane bromide **(2.20)** as an air sensitive white solid (*Scheme 2.3*). Compound **(2.19)** was synthesised by the quaternisation of 3-(*tert*butyl)-imidazole with allyl bromide in dioxane at 90°C and was characterised by electrospray mass spectrometry.

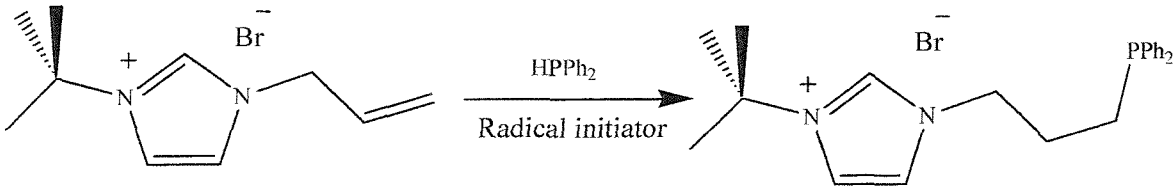

Scheme 2.3. The hydro-phosphination of **(2.19)** to synthesise **(2.20)**.

Compound **(2.20)** has a distinctive peak at -17 ppm in the $^{31}P\{H\}$ NMR spectrum. The electrospray mass spectrum provided further evidence for its existence by a peak at 351 *m/z*. The characteristic peaks in the ^{1}H NMR spectrum were observed but attempts to get conclusive elemental analysis failed, possibly due to its sensitivity towards air.

2.5.5. Characterisation of compound (2.22)

1-[3-(*iso*propyl)-imidazolium]-2-[diphenylphosphine]-ethane iodide **(2.22)** was made *via* a similar route to that use to synthesise **(2.20)** from a solution of **(2.21)**, $HPPh_2$ and 1,1'-azobis (cyclohexyl carbonitrile). Compound **(2.21)** was synthesised by the quaternisation of 1-vinyl-imidazole with *iso*propyl iodide neat at 90°C, and was characterised by electrospray mass spectrometry and ^1H NMR spectroscopy. The electrospray mass spectrum of compound **(2.22)** contained a peak at 323 *m/z* corresponding to the phosphine imidazolium salt. A peak at -20 ppm in the $^{31}P\{H\}$ NMR spectrum supported the formation of the product. Nevertheless, obtaining analytical and ^1H NMR data proved difficult. In the latter case, only broad signals were visible. We surmise that these phosphorus imidazolium salts are particularly difficult to isolate and purify due to:

i) The air sensitive nature of these phosphines;

ii) The difficulty in purifying the product salts from a mixture of salts;

iii) The oily nature of the compounds, as they are similar to a family of ionic liquids based on imidazolium salts, making them very difficult to purify by crystallisation;

iv) The increased acidity of the proton in the two position of the imidazolium ring hinders full characterisation by ^1H NMR spectroscopy.

These obstacles combined make it very difficult to obtain conclusive results from all of the possible analytical methods. These shortcomings have made phosphine imidazolium salts difficult to work with as ligand precursors for transition metals. This family of phosphine imidazolium salts has however been used in reactions described later in this thesis, and some data has been obtained to show that these compounds can be used as precursors for ligands on palladium.

2.6 Attempted deprotonation of imidazolium salts

Free carbenes that can be isolated and stored as powders or in solution are an enviable achievement. A "carbene in a bottle" could be used on a wide variety of metal starting materials as well as giving the opportunity to perform numerous reactions concurrently.

In an attempt to produce a stable free carbene from the imidazolium salts described above, anhydrous 3-(*tert*butyl)-1-(α-picolyl) imidazolium bromide was reacted with lithium di*iso*propylamide in THF. After careful work-up, a red solid was produced. The ^1H NMR spectrum of the resulting red solid was very broad and unassignable. Further attempts to purify and grow crystals of these solids failed. Similar results were obtained

when different bases, solvents and the number of equivalents of base were used, and also when similar experiments were performed with other imidazolium salts. Similar results were also observed at a variety of reaction and isolation temperatures.

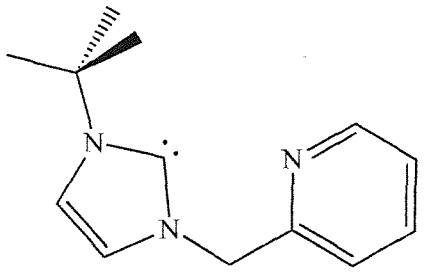

Figure 2.11. 3-(*tert*butyl)-1-(α-picolyl) imidazol-2-ylidene, the target compound for *reaction* ***2.9.1.***

However, when the reaction mixture was analysed *in situ* with minimal work-up, clean ^{1}H and $^{13}C\{H\}$ NMR spectra were obtained and the formation of the product was supported by electron impact mass spectroscopy. However, the characteristic peak in the $^{13}C\{H\}$ NMR spectrum for the carbon in the 2-position on the carbene ring was not observed as the compound decomposed very quickly in solution. Therefore, unfortunately, this is not a route to stable free carbenes but it does demonstrate the suitability of the reaction of these carbenes *in situ* with metal starting materials (*Figure 2.11*). The isolation attempts may have failed due to decomposition by a number of plausible routes, for example the *N*-heterocyclic carbene could be susceptible to electrophilic attack by the nitrogen donor atom.

2.7 Conclusions

Practical methods to synthesise and modify a large number of unusual imidazolium salts are reported in this chapter. These imidazolium salts are linked with a variety of other donors, including pyridyl, picolyl, lutidyl, phosphine, phosphine-borane, phosphine oxide, γ-bromopropane and methoxy moieties. A number of these imidazolium salts have been made with a variety of bulky aryl and alkyl groups. Bis-imidazolium salts have also been prepared with methylene, lutidyl and pyridyl bridges. From the adaptable methods described in this chapter, we were able to synthesis an even wider range of imidazolium salts. This has then led us to attempt the synthesis of a wide variety of metal complexes with these families of ligands and ligand precursors.

The use of bulky substituents is expected to differentiate the reactivity of the resulting carbene complexes from the known, easily available 1-methyl-imidazolium analogues. In addition, the crystallinity of the isolated compounds is expected to be better, allowing more detailed characterisation of the metal complexes to be obtained. Since this work was carried out, a paper has been published that describes the synthesis of a phosphine functionalised imidazolium salt.[34]

EXPERIMENTAL

2.8 Synthesis of imidazolium salts

The three general synthetic procedures used throughout are detailed below. The compounds **(2.1)-(2.9)** were synthesised following the general methods (i) and (ii) are given in *Scheme 2.4* Compounds synthesised by general method (iii) are given in *Figure 2.12*. The manipulations involving bromomethyl pyridine derivatives were carried out with extreme caution, as these are very powerful lachrymators.

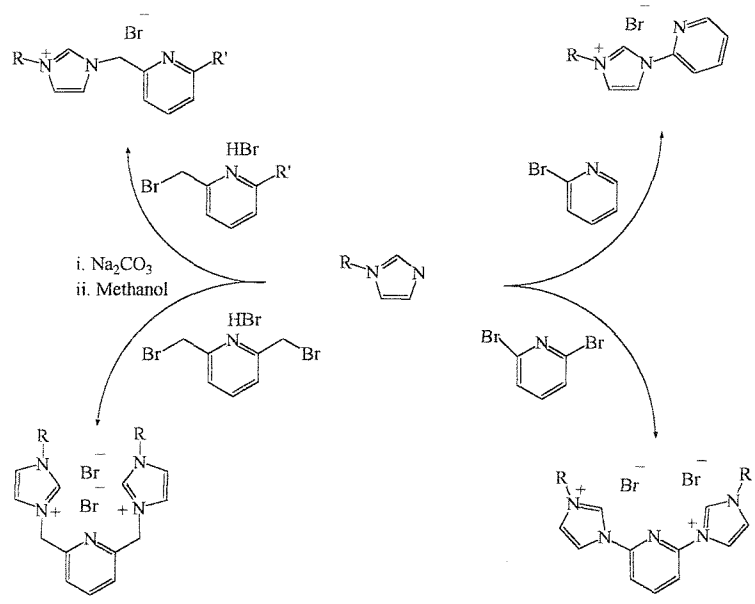

Scheme 2.4. Synthesis of compounds **(2.1)-(2.9)**. R = *tert*butyl, mesityl and 2,6-di*iso*propylphenyl R' = methyl and hydrogen.

2.8.2. General method (i) (*Scheme 2.5*)

A biphasic system at 0°C, consisting of an aqueous solution of bromomethyl pyridine hydrogen bromide derivative covered with diethyl ether, was neutralised by dropwise addition of an aqueous sodium carbonate solution. The liberated free pyridine was extracted into diethyl ether. The diethyl ether phase was dried with magnesium sulphate and filtered.

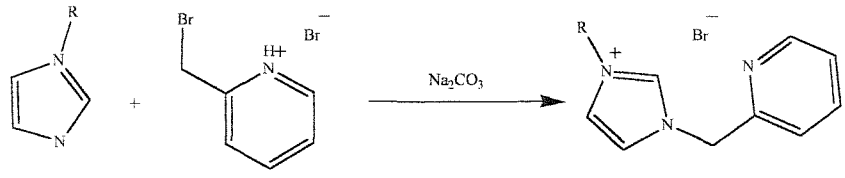

Scheme 2.5. General method (i): reaction of 2-(bromomethyl) pyridine hydrogen bromide with sodium carbonate and an imidazole.

To the diethyl ether phase was added while rapidly stirring the corresponding imidazole dissolved in methanol and the diethyl ether was removed under vacuum eventually leaving the reaction mixture in methanol. The resulting solution was stirred at room temperature for 12 hours or at reflux for 3 hours.

After filtering the reaction mixture, the volatiles were removed under vacuum and the resulting solid was washed with three portions of diethyl ether giving the products as white solids. In most cases, the products obtained at this stage were spectroscopically and analytically pure. If not, purification was carried out by recrystallisation from a saturated solution of dichloromethane layered with diethyl ether or from a saturated solution of hot acetone.

2.8.3. General method (ii) (*Scheme 2.6*)

In a sealed glass ampoule, completely immersed in an oil bath a mixture of the appropriate imidazole and 2-bromopyridine or 2,6-dibromopyridine was heated at 140°C for 48-96 hours. After cooling to room temperature, the ampoule was opened, the brown residue was washed three times with ether and the insoluble solid was isolated by filtration. In most cases, the products obtained at this stage were spectroscopically and analytically pure. If not, purification was carried out by recrystallisation from a saturated solution of dichloromethane layered with diethyl ether or from a saturated solution of hot acetone.

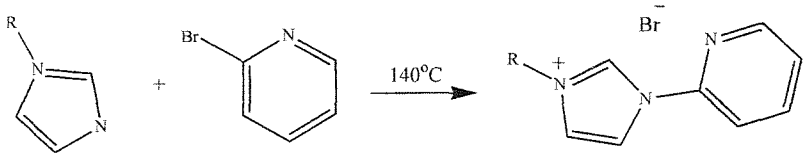

Scheme 2.6. General method (ii): reaction of 2-bromopyridine with an imidazole.

2.8.4. General method (iii)

A xylenes, dioxane or ethanol solution of the appropriate alkylhalide or allylhalide and the appropriate imidazole were heated at 90°C for 8 hours or stirred at room temperature for 12 hours. After completion, the reaction mixture was worked up as in general method (i).

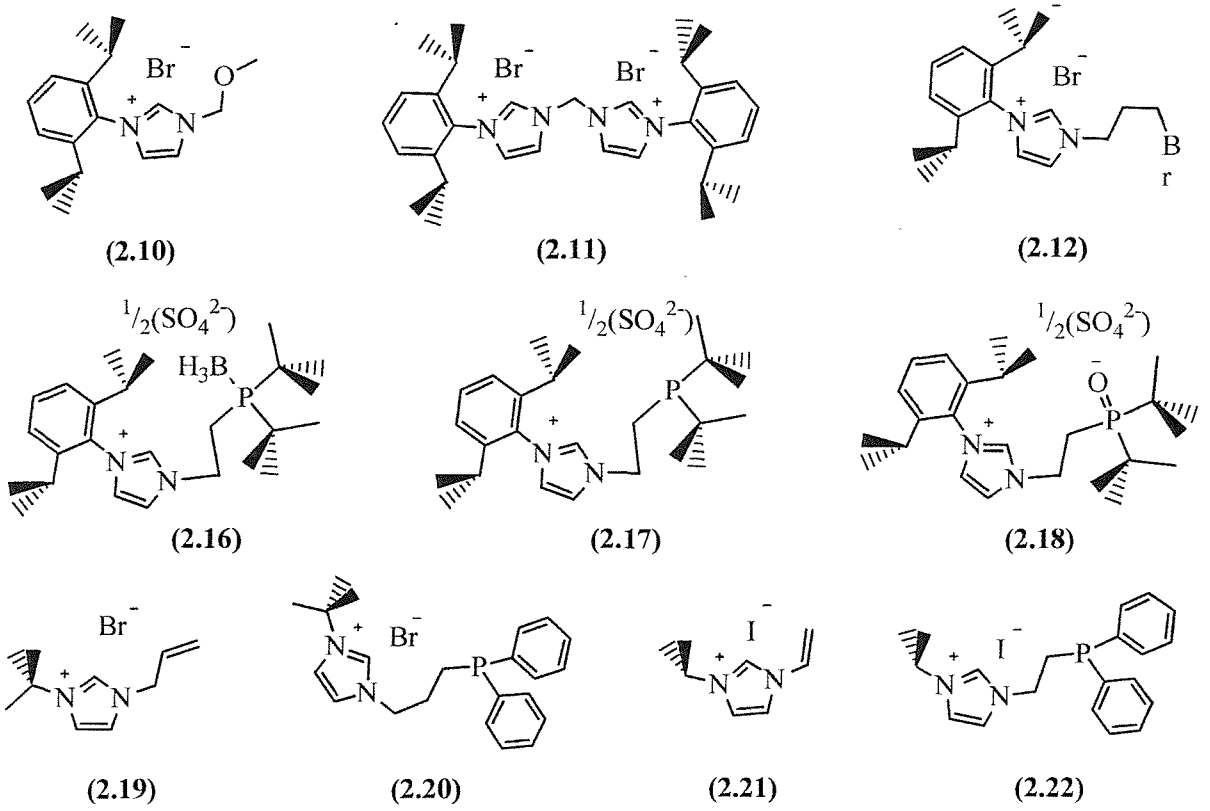

Figure 2.12. Imidazolium salts synthesised by following general method (iii).

(2.1) 3-(*tert*butyl)-1-(α-picolyl) imidazolium bromide hydrate

This was prepared following the general method (i) from 2-(bromomethyl)-pyridine hydrogen bromide (4.0g, 16.0mmol), which was neutralised with aqueous sodium carbonate and extracted into diethyl ether at 0°C (3 × 50ml). Stirring 1-*tert*butyl-imidazole (2.0g, 16.0mmol) in methanol (100ml) for 12 hours at room temperature gave the product as a white solid. X-ray diffraction quality crystals were obtained by cooling a saturated acetone solution to -35°C. Important bond lengths and angles are displayed in *Table 2.1* and *Table 2.2*, and an Ortep diagram is shown in *Figure 2.4.*

Yield: 3.80 g, 80%. Mp: 65°C.

MS (ES): *m/z* 216.1 $(M)^+$.

$\delta_H(CDCl_3)$ 1.6 [9H, s, $C(CH_3)_3$], 5.8 (2H, s, CH_2), 7.2 (1H, m, 5-picolyl *H*), 7.5 (1H, s, 5-imidazolium *H*), 7.6 (1H, s, 4-imidazolium *H*), 7.7 (1H, t, 4-picolyl *H*), 7.8 (1H, d, 3-picolyl *H*), 8.5 (1H, d, 6-picolyl *H*), 10.5 (1H, s, 2-imidazolium *H*).

(Found: C, 49.68; H, 6.43; N, 13.88. $C_{13}H_{20}BrN_3O$ calculated: C, 49.69; H, 6.42; N, 13.37%).

Compound	3-(*tert*butyl)-1-(α-picolyl)-imidazolium bromide hydrate
Chemical formula	$C_{13}H_{20}BrN_3O$
Formula weight	314.23
Crystal system	Monoclinic
Space group	$P\,2_1/c$
a/Å	9.7083(19)
b/Å	13.214(3)
c/Å	11.574(2)
α/°	90
β/°	92.11(3)
γ/°	90
V/Å^3	1483.8(5)
Z	4
T/K	150(2)
μ/mm^{-1}	2.764
F(000)	648
No. Data collected	30583
No. Unique data	3021
R_{int}	0.0476
Final R(|F|) for $F_O > 2\sigma(F_o)$	0.0287
Final R(F^2) for all data	0.0362

Table 2.4. Crystallographic parameters for 3-(*tert*butyl)-1-(α-picolyl)-imidazolium bromide hydrate, compound **(2.1)**.

(2.2) 3-(mesityl)-1-(α-picolyl) imidazolium bromide

This was prepared following the general method (i) from 2-(bromomethyl)-pyridine hydrogen bromide (3.0g, 12.0mmol), which was neutralised with aqueous sodium carbonate and extracted into diethyl ether at 0°C (3 × 40ml). Stirring 1-mesityl-imidazole (2.2g, 12.0mmol) in methanol (80ml) for 12 hours at room temperature gave the product as a white solid.

Yield 70%. Mp: 210°C (decomp.).

MS (ES): *m/z* 278.1 $(M)^+$.

$\delta_H(CDCl_3)$ 2.0 (6H, s, mesityl CH_3), 2.3 (3H, s, mesityl CH_3), 6.1 (2H, s, CH_2), 7.0 (2H, s, mesityl *H*), 7.1 (1H, d, 5-imidazolium *H*), 7.3 (1H, m, 5-picolyl *H*), 7.8 (1H, t, 4-picolyl *H*), 8.0 (1H, d, 3-picolyl *H*), 8.0 (1H, d, 4-imidazolium *H*), 8.5 (1H, d, 6-picolyl *H*), 10.3 (1H, s, 2-imidazolium *H*).

(Found: C, 57.42; H, 5.42; N, 11.03. $C_{18}H_{22}BrN_3O$ calculated: C, 57.45; H, 5.89; N, 11.17%).

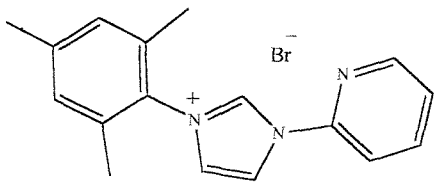

Figure 2.13. 3-(mesityl)-1-(2-pyridyl) imidazolium bromide, compound **(2.3)**.

(2.3) 3-(mesityl)-1-(2-pyridyl) imidazolium bromide

This was prepared following the general method (ii) from 2-bromopyridine (2.2g, 7.8mmol) and 1-mesityl-imidazole (1.8g, 10.0mmol) by heating 140°C for 48 hours. The product was obtained as a white solid (*Figure 2.13*).

Yield 85%. Mp: 250°C (decomp).

MS (ES): *m/z* 264 $(M)^+$.

$\delta_H(CDCl_3)$ 2.1 (6H, s, mesityl C*H*$_3$), 2.3 (3H, s, mesityl C*H*$_3$), 7.0 (2H, s, mesityl *H*), 7.3 (1H, d, 5-imidazolium *H*), 7.4 (1H, m, 5-pyridyl *H*), 8.0 (1H, t, 4-pyridyl *H*), 8.5 (1H, d, 3-pyridyl *H*), 8.9 (1H, d, 4-imidazolium *H*), 9.1 (1H, d, 6-pyridyl *H*), 11.2 (1H, s, 2-imidazolium *H*).

(Found: C, 55.99; H, 5.98; N, 11.35. $C_{17}H_{18}BrN_3(H_2O)$ calculated: C, 56.36; H, 5.56; N, 11.60%).

(2.4) 3-(mesityl)-1-(α-lutidyl) imidazolium bromide

This was prepared following the general method (i) from 2-(bromomethyl)-6-methylpyridine hydrogen bromide (3.3g, 13.0mmol), which was neutralised with aqueous sodium carbonate and extracted into diethyl ether at 0°C (3 × 50ml). Stirring 1-mesityl-imidazole (2.3g, 13.0mmol) in methanol (100ml) for 12 hours at room temperature gave the product as a white solid.

Yield: 80%.

MS (ES): *m/z* 292.3 $(M)^+$.

$\delta_H(CDCl_3)$ 2.0 (6H, s, mesityl C*H*$_3$), 2.3 (3H, s, mesityl C*H*$_3$), 2.4 (3H, s, CH_3), 6.0 (2H, s, CH_2), 7.0 (2H, s, mesityl *H*), 7.1 (1H, d, 5-imidazolium *H*), 7.1 (1H, m, 4-lutidyl *H*), 7.6 (1H, d, 5-lutidyl *H*), 7.6 (1H, d, 3-lutidyl *H*), 8.0 (1H, d, 4-imidazolium *H*), 10.0 (1H, s, 2-imidazolium *H*).

(Found: C, 61.17; H, 6.14; N, 10.89. $C_{19}H_{22}N_3Br$ calculated: C, 61.30; H, 5.96; N, 11.29%).

(2.5) 3-(2,6-di*iso*propylphenyl)-1-(α-picolyl)-imidazolium bromide

This was prepared following the general method (i) from 2-bromomethyl-pyridine hydrogen bromide (3.0g, 12.0mmol), which was neutralised with aqueous sodium carbonate and extracted into diethyl ether at 0°C (3 × 40ml). Stirring 1-(2,6-di*iso*propyl-phenyl)-imidazole (2.8g, 12.0mmol) in methanol (80ml) for 12 hours at room temperature gave the product as a white solid.

Yield: 3.4 g, 70%. Mp: 220°C (decomp).

MS (ES): *m/z* 320 $(M)^+$.

$\delta_H(CDCl_3)$ 1.1, 1.2 [2 × 6H, d, $CH(CH_3)_2$], 2.3 [2H, septet, $CH(CH_3)_2$], 6.2 (2H, s, CH_2), 7.1 (1H, s, 5-imidazolium *H*), 7.3 (2H, d, $^iPr_2C_6H_2H$), 7.3 (1H, m, 5-picolyl *H*), 7.5 (1H, t, $^iPr_2C_6H_2H$), 7.8 (1H, t, 4-picolyl *H*), 8.0 (1H, d, 3-picolyl *H*), 8.3 (1H, s, 4-imidazolium *H*), 8.5 (1H, d, 6-picolyl *H*), 10.1 (1H, s, 2-imidazolium *H*).

(Found: C, 62.73; H, 6.66; N, 10.45. $C_{21}H_{26}BrN_3$ calculated: C, 63.00; H, 6.55; N, 10.50%).

(2.6) 3-(2,6-di*iso*propylphenyl)-1-(2-pyridyl)-imidazolium bromide

This was prepared following the general method (ii) from 2-bromopyridine (2.2g, 7.8mmol) and 1-(2,6-di*iso*propylphenyl)-imidazole (2.2g, 9.8mmol) by heating 140°C for 48 hours. The product was obtained as a white solid.

Yield: 2.26 g, 95%. Mp: > 250°C.

MS (ES): *m/z* 306 $(M)^+$.

$\delta_H(CDCl_3)$ 1.2, 1.3 [2 × 6H, d, $CH(CH_3)_2$], 2.4 [2H, septet, $CH(CH_3)_2$], 7.3 (2H, d, $^iPr_2C_6H_2H$), 7.4 (1H, d, 5-imidazolium *H*), 7.5 (1H, m, 5-pyridyl *H*), 7.6 (1H, t, $^iPr_2C_6H_2H$), 8.1 (1H, t, 4-pyridyl *H*), 8.6 (1H, d, 3-pyridyl *H*), 9.3 (1H, d, 6-pyridyl *H*), 9.4 (1H, d, 4-imidazolium *H*), 10.9 (1H, s, 2-imidazolium *H*).

(Found: C, 62.15; H, 6.10; N, 10.73. $C_{20}H_{24}BrN_3$ calculated: C, 62.18; H, 6.26; N, 10.88%).

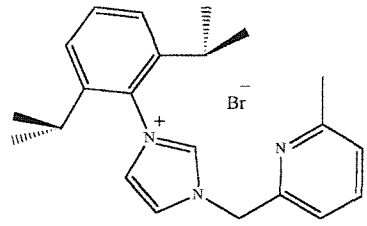

Figure 2.14. 3-(2,6-di*iso*propylphenyl)-1-(α-lutidyl) imidazolium bromide, compound **(2.7)**.

(2.7) 3-(2,6-di*iso*propylphenyl)-1-(α-lutidyl) imidazolium bromide

This was prepared following the general method (i) from 2-(bromomethyl)-6-methylpyridine hydrogen bromide (3.2g, 12.0mmol), which was neutralised with aqueous sodium carbonate and extracted into diethyl ether at 0^0C (3 × 50ml). Stirring 1-(2,6-di*iso*propylphenyl)imidazole (2.8g, 12.0mmol) in methanol (100ml) for 12 hours at room temperature gave the product as a white solid (*Figure 2.14*).

Yield: 75%. Mp: = 230°C (decomp).

MS (ES): *m/z* 334 $(M)^+$.

$\delta_H(CDCl_3)$ 1.1, 1.2 [2 × 6H, d, $CH(CH_3)_2$], 2.3 [2H, septet, $CH(CH_3)_2$], 2.5 (3H, s, CH_3), 6.1 (2H, s, CH_2), 7.1 (1H, d, 5-imidazolium *H*), 7.1 (1H, m, 5-lutidyl *H*), 7.3 (2H, d, $^iPr_2C_6H_2H$), 7.6 (1H, t, $^iPr_2C_6H_2H$), 7.7 (1H, t, 4-lutidyl *H*), 7.7 (1H, d, 3-lutidyl *H*), 8.2 (1H, d, 4-imidazolium *H*), 10.0 (1H, s, 2-imidazolium *H*).

(Found: C, 63.87; H, 6.33; N, 10.03. $C_{22}H_{28}BrN_3$ calculated: C, 63.77; H, 6.81; N, 10.14%).

(2.8) α,α'-bis-[3-(2,6-di*iso*propylphenyl)-imidazolium]-lutidine dibromide

This was prepared following the general method (i) from 2,6-di(bromomethyl)-pyridine hydrogen bromide (3.0g, 8.6mmol), which was neutralised with aqueous sodium carbonate and extracted into diethyl ether at 0°C (3 × 50ml). Stirring 1-(2,6-di*iso*propyl-phenyl)-imidazole (2.0g, 8.6mmol) in methanol (100ml) for 12 hours at room temperature gave the product as a white solid (*Figure 2.15*).

Yield: 75%. Mp: > 250°C.

MS (ES): *m/z* 281 $(1/2M)^+$.

$\delta_H(CDCl_3)$ 1.0, 1.1 [2 × 12H, d, $CH(CH_3)_2$], 2.2 [4H, septet, $CH(CH_3)_2$], 6.0 (2H, s, CH_2), 7.2 (4H, d, $^iPr_2C_6H_2H$), 7.2 (1H, d, 3,5-picolyl *H*), 7.3 (1H, s, 5-imidazolium *H*), 7.5 (2H, t, $^iPr_2C_6H_2H$), 7.7 (1H, t, 4-picolyl *H*), 8.6 (1H, s, 4-imidazolium *H*), 10.5 (1H, s, 2-imidazolium *H*).

(Found: C, 61.40; H, 6.18; N, 9.43. $C_{37}H_{47}Br_2N_5$ calculated: C, 61.58; H, 6.56; N, 9.71%).

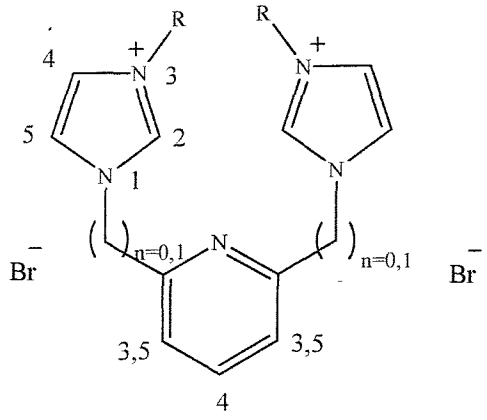

Figure 2.15. Connectivity and numbering order of the imidazolium and pyridine rings for the salts **(2.8)** and **(2.9)**. R = 2,6-di*iso*propylphenyl.

(2.9) 2,6-bis-[3-(2,6-di*iso*propylphenyl)-imidazolium]-pyridine dibromide

This was prepared following the general method (ii) from 2,6-dibromopyridine (2.0g, 8.4mmol) and 1-(2,6-di*iso*propylphenyl)-imidazole (4.7g, 21.1mmol) by heating 140°C for 48 hours. The product was obtained as a white solid (*Figure 2.15*).

Yield: 95%. Mp: > 250°C.

MS (ES): *m/z* 267 $(1/2M)^+$.

$\delta_H(CDCl_3)$ 1.1, 1.2 [2 × 12H, d, $CH(CH_3)_2$], 2.4 [4H, septet, $CH(CH_3)_2$], 7.3 (4H, d, $^iPr_2C_6H_2H$), 7.3 (1H, s, 5-imidazolium *H*), 7.5 (2H, t, $^iPr_2C_6H_2H$), 8.1 (1H, t, 4-pyridyl *H*), 9.1 (1H, d, 3,5-pyridyl *H*), 9.9 (1H, s, 4-imidazolium *H*), 12.0 (1H, s, 2-imidazolium *H*).

(Found: C, 60.99; H, 6.37; N, 9.68. $C_{35}H_{43}Br_2N_5$ calculated: C, 60.61; H, 6.25; N, 10.10%).

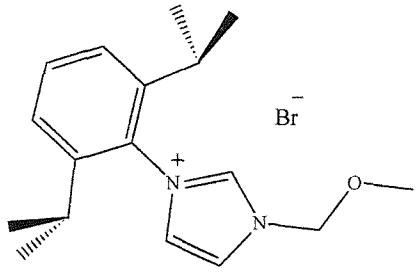

Figure 2.16. 1-[3-(2,6-di*iso*propylphenyl)-imidazolium]-1-methylether-methane bromide, compound **(2.10)**.

(2.10) 1-[3-(2,6-di*iso*propylphenyl)-imidazolium]-1-methylether-methane bromide

This was prepared following the general method (iii) from 1-methylether-1-bromo-methane (1.0g, 8.0mmol) and 3-(2,6-di*iso*propylphenyl)-imidazole (2.7g, 12.0mmol) in dioxane (80ml) by heating at 90°C for 8 hours. The product was obtained in quantitative yields as a white solid (*Figure 2.16*).

MS (ES): *m/z* 273 $(M)^+$.

$\delta_H(CDCl_3)$ 1.1, 1.2 [2 × 6H, d, $CH(CH_3)_2$], 2.3 [2H, septet, $CH(CH_3)_2$], 3.6 (3H, s, CH_3), 6.2 (2H, s, CH_2), 7.2 (1H, d, 5-imidazolium *H*), 7.3 (2H, d, $^iPr_2C_6H_2H$), 7.5 (1H, t, $^iPr_2C_6H_2H$), 7.9 (1H, d, 4-imidazolium *H*), 10.8 (1H, s, 2-imidazolium *H*).

(Found: C, 57.99; H, 6.96; N, 7.89. $C_{17}H_{25}ON_2Br$ calculated: C, 57.79; H, 7.13; N, 7.93%).

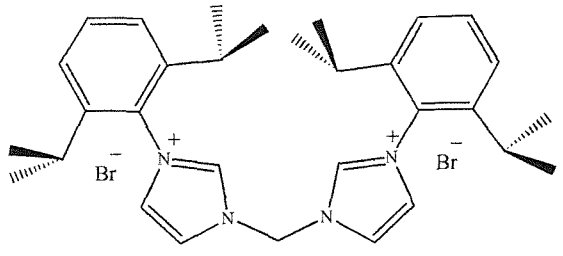

Figure 2.17. 1,1-bis[3-(2,6-di*iso*propylphenyl)-imidazolium]-methane dibromide, compound **(2.11)**.

(2.11) 1,1-bis[3-(2,6-di*iso*propylphenyl)-imidazolium]-methane dibromide

This was prepared following the general method (iii) from dibromomethane (0.5g, 2.9mmol) and 3-(2,6-di*iso*propylphenyl)-imidazole (1.6g, 7.1mmol) in xylene (40ml) by heating at 90°C for 8 hours. The product was obtained in quantitative yields as a white solid (*Figure 2.17*).

MS (ES): 235 $(1/2M)^+$.

$\delta_H(CDCl_3)$ 1.2, 1.3 [2 × 12H, d, $CH(CH_3)_2$], 2.2 [4H, septet, $CH(CH_3)_2$], 7.3 (2H, br., CH_2), 7.3 (4H, d, $^iPr_2C_6H_2H$), 7.6 (2H, t, $^iPr_2C_6H_2H$), 8.1 (2H, s, 5-imidazolium *H*), 10.0 (2H, s, 4-imidazolium *H*), 11.4 (2H, s, 2-imidazolium *H*).

(Found: C, 59.20; H, 6.47; N, 9.02. $C_{31}H_{42}Br_2N_4$ calculated: C, 59.05; H, 6.71; N, 8.89%).

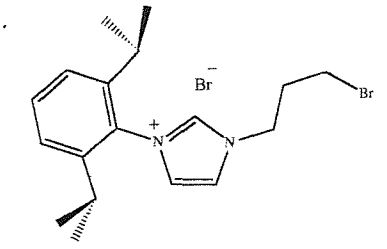

Figure 2.18. 1-[3-(2,6-di*iso*propylphenyl)-imidazolium]-3-bromopropane bromide, compound **(2.12)**.

(2.12) 3-(γ-bromopropyl)-1-[3-(2,6-di*iso*propylphenyl)-imidazolium] bromide

This was prepared following the general method (iii) from 1,3-dibromopropane (8g, 39.6mmol) and 3-(2,6-di*iso*propylphenyl)-imidazole (1.0g, 4.4mmol) in dioxane (20ml) by heating at 90°C for 8 hours. The product was obtained in quantitative yields as a white solid (*Figure 2.18*).

MS (ES): 349, 351 $(M)^+$.

$\delta_H(CDCl_3)$ 1.0, 1.1 [2 × 6H, d, $CH(CH_3)_2$], 1.2 (2H, d, CH_2), 2.2 [2H, septet, $CH(CH_3)_2$], 3.5 (2H, t, CH_2), 4.9 (2H, t, CH_2), 7.2 (1H, s, 5-imidazolium *H*), 7.3 (2H, d, $^iPr_2C_6H_2H$), 7.5 (1H, t, $^iPr_2C_6H_2H$), 8.4 (1H, s, 4-imidazolium *H*), 10.3 (1H, s, 2-imidazolium *H*).

(Found: C, 50.03; H, 5.89; N, 6.78. $C_{18}H_{26}Br_2N_2$ calculated: C, 50.25; H, 6.09; N, 6.51%).

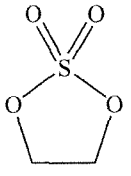

Figure 2.19. Ethylene glycol cyclic sulphate.

(2.13) Ethylene glycol cyclic sulphate

Synthesised by following a similar procedure to that described by Sharpless *et al.*[35] Thionyl chloride (8.8ml, 120mmol) was added drop-wise to a solution of ethylene glycol (6.2g, 100mmol) in tetrachloromethane (100ml), and the resulting solution was refluxed for 1.5 hours. The solution was then cooled to 0°C and diluted with acetonitrile (100ml). Ruthenium trichloride trihydrate (0.016g, 0.06mmol) and sodium periodate (32g, 150mmol) were added followed by water (150ml). The resulting orange mixture was

stirred at room temperature for 2 hours. The mixture was then diluted with diethyl ether (400ml) and the two phases were seperated. The organic layer was washed with 10ml of water and 10ml of saturated sodium carbonate. After drying over magnesium sulphate, the solution was filtered and the volatiles removed under vacuum. The product was obtained as a white solid and used without further purification (*Figure 2.19*).

$\delta_H(CDCl_3)$ 3.5 (br., CH_2).

(2.14) Di-*tert*butylphosphine borane complex

Synthesised by following a procedure similar to that described by Livinghouse *et al.*[36] for diphenylphosphine borane complex.

The manipulations were carried out under nitrogen. Borane methyl sulphide (16.3ml of a 2 molar solution, 15mmol) was added drop-wise to solution of di-*tert*-butylphosphine (1.8ml, 10mmol) in THF (20ml) at 0°C and stirred at room temperature for 2 hours. The volatiles were removed under vacuum and the resulting solid was washed with petrol (2 × 30ml). The product was obtained as a white solid and used without further purification.

(2.15) Synthesis of 1-sulphato-2-(phosphineborane)-ethane lithium salt

Synthesised by modification of the procedure described by Werner *et al.*[37]

A 2.45M solution of *n*BuLi in hexane (4.0ml, 10mmol) was added to a solution of the corresponding phosphine borane complex (10mmol) in THF (100ml) at -78°C. The mixture became yellow on warming. After stirring at room temperature for 30 min, the resulting solution was then added drop-wise at -78°C to a solution of **(2.13)** (10mmol) in THF (40ml). After the reaction was complete the colourless reaction was warmed to room temperature and after stirring for a further 30 min, the volatiles were removed under vacuum, the resulting solid was washed with petrol (2 × 20ml) and was used without further purification.

$\delta_H(CDCl_3)$ 1.3 [18H, br., $C(CH_3)_3$], 2.2 (2H, br., CH_2), 4.0 (2H, br., CH_2).

$\delta_P(CDCl_3)$ 40 (br. q).

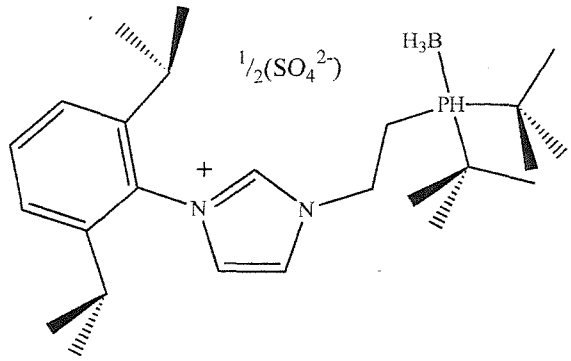

Figure 2.20. 1-[3-(2,6-di*iso*propylphenyl)-imidazolium]-2-[di(*tert*butyl)phosphine-borane]ethane sulphate, compound **(2.16)**.

(2.16) 1-[3-(2,6-di*iso*propylphenyl)-imidazolium]-2-[di(*tert*butyl)phosphine-borane]ethane sulphate

This was prepared following the general method (iv) from 1-sulphato-2-(di(*tert*-butyl)phosphineborane)ethane lithium salt (2g, 4.2mmol) and 3-(2,6-di*iso*propylphenyl)-imidazole (2.7g, 12mmol) in ethanol (60ml) by stirring at room temperature for 12 hours . After completion, the volatiles were removed under vacuum with gentle warming to remove the last traces of ethanol. To the resulting solid, diethyl ether was added and the suspension was cooled at -40°C for 12 hours. Finally, the product was isolated by filtration and dried under vacuum to give a white solid (*Figure 2.20*).

Yield = 70%

MS (ES): *m/z* 419 $(M - BH_3)^+$.

$\delta_H(CD_3OD)$ 1.2 [12H, d, $CH(CH_3)_2$], 1.4 [18H, d, $C(CH_3)_3$], 2.2 (2H, m, CH_2), 2.3 [2H, septet, $CH(CH_3)_2$], 4.2 (2H, m, CH_2), 7.2 (1H, s, 5-imidazolium *H*), 7.3 (2H, d, $^iPr_2C_6H_2H$), 7.5 (1H, t, $^iPr_2C_6H_2H$), 7.7 (1H, s, 4-imidazolium *H*).

$\delta_C(CD_3OD)$ 22 (d, CH_2), 27 [$CH(CH_3)_2$], 30 [$C(CH_3)_3$], 32 [$CH(CH_3)_2$], 36 [d, $C(CH_3)_3$], 69 (d, CH_2), 126 (4-imidazolium *C*),132 (5-imidazolium *C*), 128, 134, 136, 142 ($Pr^i_2C_6H_3$), 150 (2-imidazolium *C*).

$\delta_B(CDCl_3)$ -40 (br. d).

$\delta_P(CDCl_3)$ 43 (br. q).

(Found: C, 62.32; H, 9.31; N, 6.78. $C_{44}H_{78}B_2N_4O_4P_2S$ calculated: C, 62.71; H, 9.33; N, 6.65%).

(2.17) 1-[3-(2,6-di*iso*propylphenyl)-imidazolium]-2-[di(*tert*butyl)phosphine]ethane sulphate

The manipulations were carried out under nitrogen. Tetrafluoroboric acid dimethylether complex (0.16g, 0.97mmol) was added drop wise to a dichloromethane (20ml) solution of 1-[3-(2,6-di*iso*propylphenyl)-imidazolium]-2-[di(*tert*butyl)phosphine-borane]ethane sulphate (0.1g, 0.19mmol) at -15°C and stirred at room temperature 2 hours. The resulting solution was neutralised with a THF solution saturated with ammonia. Ammonia was bubbled through the reaction for 20mins, the solution was filtered, and the volatiles were removed under vacuum. The resulting solid was washed with ice-cold petrol (10ml) and used with out further purification.

MS (ES): *m/z* 419 $(M)^+$, 435 $(M + O)^+$.

$\delta_H(CD_2Cl_2)$ peaks including 1.1 [18H, d, $C(CH_3)_3$], 1.1 [12H, d, $CH(CH_3)_2$], 1.6 (2H, m, CH_2), 2.3 [2H, septet, $CH(CH_3)_2$], 3.8 (2H, m, CH_2), 7.2 (1H, s, 5-imidazolium *H*), 7.3 (2H, d, $^iPr_2C_6H_2H$), 7.5 (1H, t, $^iPr_2C_6H_2H$), 7.7 (1H, s, 4-imidazolium *H*).

$\delta_P(CD_2Cl_2)$ 19.

(2.18) 1-[3-(2,6-di*iso*propylphenyl)-imidazolium]-2-[di(*tert*butyl)phosphinoxide] ethane sulphate

A diethyl ether solution of 1-[3-(2,6-di*iso*propylphenyl)-imidazolium]-2-[di(*tert*-butyl)phosphine]ethane sulphate was exposed to air and the volatiles removed under vacuum. The solid was kept under air for 12h at room temperature. The solid was washed twice with diethyl ether to obtain an oily solid.

MS (ES): *m/z* 435 $(M)^+$.

$\delta_H(CDCl_3)$ 0.8 (2H, m, CH_2), 1.1 [18H, d, $C(CH_3)_3$], 1.2 [12H, d, $CH(CH_3)_2$], 2.3 [2H, septet, $CH(CH_3)_2$], 4.0 (2H, m, CH_2), 6.9 (1H, s, 5-imidazolium *H*), 7.2 (2H, d, $^iPr_2C_6H_2H$), 7.3 (1H, t, $^iPr_2C_6H_2H$), 7.4 (1H, s, 4-imidazolium *H*).

$\delta_P(CDCl_3)$ 65.

(2.19) 3-(*tert*butyl)-1-allyl-imidazolium bromide

A solution of 3-(*tert*butyl)-imidazole (2.0g, 1.6mmol) and allyl bromide (4.9g, 4.0mmol) in dioxane (25ml) was heated at 90°C for 2 hours in a thick walled Schlenk tube equipped with a PTFE stopcock. A small quantity of acetone was added to the biphasic system to crystallise the oil. The solvent was decanted off to leave a white crystalline solid, which was dried under vacuum.

Yield = 80%. Mp: 86°C.

MS (ES): *m/z* 165 $(M)^+$.

(2.20) 1-[3-(*tert*butyl) imidazolium]-3-diphenylphosphine-propane bromide

A solution of 3-(*tert*butyl)-1-allyl-imidazolium bromide (1g, 0.4mmol), $HPPh_2$ (3.5ml, 2mmol) and a small quantity of 1,1'-azobis(cyclohexane carbonitrile) was heated at 100°C for 12 hours. After stirring for the first two hours, another small quantity of 1,1'-azobis(cyclohexane carbonitrile) was added. The biphasic system was then allowed to cool to room temperature, washed with petrol (20ml) and diethyl ether (20ml). The lower phase was dried under vacuum and dissolved in THF. White crystals were obtained on cooling the THF.

Mp: 110°C.

MS (ES): *m/z* 351 $(M)^+$.

$\delta_H(D_2O)$ peaks including 1.4 [9H, s, $C(CH_3)_3$], 1.7 (2H, m, CH_2), 1.9 (2H, m, CH_2), 4.0 (2H, t, CH_2), 7.0-7.1 (10H, br. m, phenyl *H*), 7.4 (1H, m, 5-imidazolium *H*), 7.5 (1H, m, 4-imidazolium *H*), 8.7 (1H, s, 2-imidazolium *H*).

$\delta_P(D_2O)$ -17.

(2.21) 3-*iso*propyl-1-vinyl-imidazolium iodide

A mixture of 1-vinyl-imidazole (2.0g, 2.1mmol) and *iso*propyl iodide (7.2g, 4.3mmol) was heated at 90°C in a thick walled Schlenk tube equipped with a PTFE stopcock for 2 hours. The mixture was allowed to cool to room temperature and the mixture was washed with diethyl ether (2x30ml). The residue was dissolved into dichloromethane, filtered and the solvent evaporated to leave a yellow solid.

MS (ES): *m/z* 136.9 $(M)^+$.

$\delta_H(D_2O)$ 1.0 [6H, d, $CH(CH_3)_2$], 4.1 (1H, m, $CH(CH_3)_2$), 4.8 (1H, dd, $CH=CH_2$), 5.2 (1H, dd, $CH=CH_2$), 6.5 (1H, m, $CH=CH_2$), 7.1, 7.2 (1H, m, 4,5-imidazolium *H*), 8.5 (1H, s, 2-imidazolium *H*).

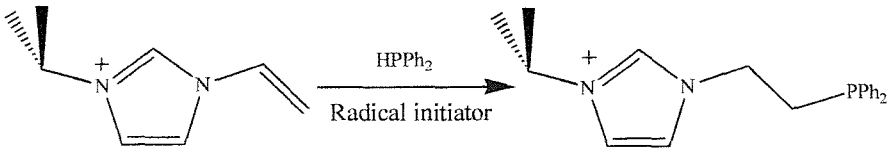

Scheme 2.7. The hydrophosphination of (2.21) to synthesise (2.22).

(2.22) 1-(3-*iso*propyl-imidazolium)-2-(diphenylphosphine)-ethane iodide

A mixture of 3-*iso*propyl-1-vinyl-imidazolium iodide (2.0g, 1.2mol), $HPPh_2$ (4.2ml, 2.4mol) and a small quantity of 1,1'-azobis(cyclohexane carbonitrile) was heated at 105°C for 12 hours. After stirring for the first two hours, another small quantity of 1,1'-azobis(cyclohexane carbonitrile) was added. The mixture was then allowed to cool to room temperature, washed with diethyl ether (2 × 20ml) and THF (20ml). The white sticky solid was left under vacuum for 2 hours (*Scheme 2.7*).

MS (ES): *m/z* 323 $(M)^+$.

$\delta_P(D_2O)$ -20.

2.9 Attempted deprotonation of imidazolium compounds

2.9.1. Attempted deprotonation of 3-(*tert*butyl)-1-(α-picolyl)imidazolium

1.1 equivalent of lithium di*iso*propylamide (0.19mmol) in THF (30ml) was added to a stirred suspension of anhydrous 3-(*tert*butyl)-1-(α-picolyl) imidazolium bromide (0.05g, 0.18mmol) at –78°C. The solution was allowed to slowly warm to room temperature; the analysis was performed at this stage. The solvent was removed *in vacuo* from the orange/red solution. The resulting solid was extracted into toluene, filtered and the solvent was removed under vacuum, leaving a red solid.

MS (EI): 215 $(M)^+$.

$\delta_H(C_6D_5)$ 1.4 [9H, s, $C(CH_3)_3$], 5.2 (2H, s, CH_2), 6.4 (1H, m, 5-picolyl *H*), 6.4 (1H, m, 5-imidazolium *H*), 6.5 (1H, s, 4-imidazolium *H*), 6.7 (1H, s, 4-picolyl *H*), 6.8 (1H, br., 3-picolyl *H*), 8.8 (1H, br., 6-picolyl *H*).

$\delta_H(NC_5D_5)$ 1.5 [9H, br., $C(CH_3)_3$], 5.4 (2H, br, CH_2), 6.9 (1H, br., 5-picolyl *H*), 7.2 (1H, br., 5-imidazolium *H*), 7.2 (1H, br., 4-imidazolium *H*), 7.2 (1H, br., 4-picolyl *H*), 7.4 (1H, br., 3-picolyl *H*), 8.6 (1H, br., 6-picolyl *H*).

$\delta_C(NC_5D_5)$ 30 [$C(CH_3)_3$], 56 [$C(CH_3)_3$], 68 (CH_2), 117 (4-imidazolium *C*), 120 (5-imidazolium *C*), 122 (5-picolyl *C*), 123 (3-picolyl *C*), 137 (4-picolyl *C*), 152 (2-picolyl *C*), 159 (6-picolyl *C*).

REFERENCES

1 Reviews: W.A. Herrmann, C. Köcher, *Angew. Chem., Int. Ed. Engl.*, **1997**, *36*, 2162; T. Weskamp, V.P.W. Böhm, W.A. Herrmann, *J. Organomet. Chem.*, **2000**, *600*, 12; D. Bourissou, O. Guerret, F.P. Gabbaï, G. Bertrand, **2000**, *100*, 39.

2 D. Enders, K. Breuer, G. Raabe, J. Runsink, J.H. Teles, J.P. Melder, K. Ebel, S. Brode, *Angew. Chem. Int. Ed. Engl.*, **1995**, *34*, 1021.

3 A.J. Arduengo III, J.R. Goerlich, W.J. Marshall, *Liebigs Ann.*, **1997**, 365.

4 A.J. Arduengo III, J.R. Goerlich, W.J. Marshall, *J. Am. Chem. Soc.*, **1995**, *117*, 11027.

5 F.E. Hahn, L. Wittenbecher, D. Le Van, R. Fröhlich, *Angew. Chem., Int. Ed. Engl.*, **2000**, *39*, 541.

6 A.J. Arduengo III, *Acc. Chem. Res.*, **1999**, *32*, 913.

7 Y. Liu, P.E. Linder, D.M. Lemal, *J. Am. Chem. Soc.*, **1999**, *121*, 10626.

8 V.P.W. Böhm, W.A. Herrmann, *Angew. Chem., Int. Ed.*, **2000**, *39*, 4037

9 W.A. Herrmann, C. Köcher, L. Goossen, G.R.J. Artus, *Chem. Eur. J.*, **1996**, *2*, 1627.

10 M. Scholl, S. Ding, C.W. Lee, R.H. Grubbs, *Org. Lett.*, **1999**, *1*,

11 B. Bildstein, M. Malaun, H. Kopacka, K-H. Ongania, K. Wurst, *J. Organomet. Chem.*, **1999**, *572*, 177.

12 H.V.R. Dias, W. Jin, *Tetrahedron Lett.*, **1994**, *35*, 1365.

13 A.L. Johnson, *U.S. Pat. 3,637,731*, **25/01/1972** (*E.I. du Pont*).

14 J.H. Groen, C.J. Elsevier, K. Vrieze, W.J.J. Smeets, A.L.Spek, *Organometallics*, **1996**, *15*, 3448.

15 T.R. Ward, *Organometallics*, **1996**, *15*, 2839.

16 A.A.D. Tulloch, A.A. Danopoulos, R.P. Tooze S.M. Cafferkey, S. Kleinhenz, M.B. Hursthouse, *Chem. Commun.*, **2000**, 1247.

17 A.A.D. Tulloch, A.A. Danopoulos, G.J. Tizzard, S.J. Coles, M.B. Hursthouse, R.S. Hay-Motherwell, W.B. Motherwell, *Chem. Commun.*, **2001**, 1270.

18 W.A. Herrmann, C. Køcher, L. Goossen and G.R.J. Artus, *Chem. Eur. J.*, **1996**, *2*, 1627.

19 W.A. Herrmann, L. Goossen, M. Spiegler, *Organometallics*, **1998**, *17*, 2162.

20 D.S. McGuinness, K.J. Cavell, *Organometallics*, **2000**, *19*, 741.

21 B. Cetinkaya, I. Ozdemir, P.H. Dixneuf, *J. Organomet. Chem.*, **1997**, *534*, 153.

22 E. Peris, J.A. Loch, J. Mata, R.H. Crabtree, *Chem. Commun.*, **2001**, 201.

23 J.C. Green, R.G. Scurr, P.L. Arnold, F.G.N. Cloke, *Chem. Commun.*, **1997**, 1963; C. Boehme, G. Frenking, *Organometallics*, **1998**, *17*, 5801.

24 M.F. Lappert, *J. Organomet. Chem.*, **1988**, *358*, 185.

25 E. Drent, P.H.M. Budzelaar, *J. Organomet. Chem.*, **2000**, 593, 211.

26 A. Dervisi, P.G. Edwards, P.D. Newman, R.P. Tooze, S.J. Coles, M.B. Hursthouse, *J. Chem. Soc., Dalton Trans.*, **1998**, 3771; A. Scrivanti, V. Beghetto, E. Campagna, M. Zanato, U. Matteoli, *Organometallics*, **1998**, *17*, 630.

27 N. Rahmouni, J.A. Osborn, A. De Cian, J. Fischer, A. Ezzamarty, *Organometallics*, **1998**, *17*, 2470.

28 K.K.M. Hii, M. Thornton-Pett, A. Jutand, R.P. Tooze, *Organometallics*, **1999**, *18*, 1887.

29 W.A. Herrmann, M.Elison, J. Fischer, C. Köcher, G.R. J. Artus, *Angew., Chem. Int. Ed.*, **1995**, *34*, 2371.

30 S. Kleinhenz, A.A.D. Tulloch, A.A. Danopoulos, *Acta Crystallogr., Sect. C*, **2000**, *56*, e476.

31 Y. Gao, K.B. Sharpless, *J. Am. Chem. Soc.* **1988**, *110*, 7538.

32 L. McKinstry, T. Livinghouse, *Tetrahedron.* **1985**, *51*, 7655.

33 G.M. Kosolapoff, L. Maier, *Organic phosphorus compounds*, J. Wiley, NY, **1972**, 105.

34 C. Yang, H.M. Lee, S.P. Nolan, *Org. Lett.*, **2001**, *3*, *No.10*, 1511.

35 Y. Gao, K.B. Sharpless, *J. Am. Chem. Soc.*, **1988**, *110*, 7538.

36 L. McKinstry, T. Livinghouse, *Tetrahedron.*, **1985**, *51*, 7655.

37 G. Fries, J. Wolf, M. Pfeiffer, D. Stalke, H. Werner, *Angew. Chem., Int. Ed. Engl.*, **2000**, *39*, 564.

Chapter 3

N-Heterocyclic Carbene Complexes of Silver (I) and Copper (I)

Chapter 3

N-Heterocyclic Carbene Complexes of Silver (I) and Copper (I)

3.1 Introduction

There is an enormous amount of interest in the use of Arduengo type carbenes as ligands on transition metals.[1,2] The thermodynamic stability of the resulting complexes, and the variety of opportunities for ligand design, promise the discovery of new metal compounds with applications in catalysis.

Silver *N*-heterocyclic carbene complexes are well known and some of them are structurally characterised.[3,4] However, the compounds described in this chapter are the first reported structurally characterised examples with mixed donor carbene ligands.

The only previously known copper (I) carbene complex is the homoleptic [Cu(1,3-dimesityl-imidazol-2-ylidene)$_2$]$^+$ $CF_3SO_3^-$, reported by Arduengo *et al.*,[4] prepared by interaction of the free 1,3-dimesityl-imidazol-2-ylidene with [Cu(CF_3SO_3)$\cdot^1/_2C_6H_6$] in THF. However, this complex was not structurally characterised. In this chapter are described the first reported structurally characterised copper (I) *N*-heterocyclic carbene complexes.[5]

RESULTS AND DISCUSSION

3.2 Synthesis of functionalised carbene complexes of silver (I)

The silver carbene complexes described in this Chapter were prepared by the adaptation of a method developed by Lin *et al.*[3] This route, to the silver complexes, involves the interaction of the imidazolium salts with Ag_2O or Ag_2CO_3. However, with the imidazolium salts described in chapter 2, much harsher conditions and longer reaction time were required to produce the silver complexes in good yields. The following findings were made.

i) Most imidazolium salts can be converted into their corresponding silver salts by refluxing them in dichloromethane for up to two days in the presence of Ag_2O (*Scheme 3.1*).

ii) Product yields are improved by addition of activated 4Å molecular sieves to the reaction.

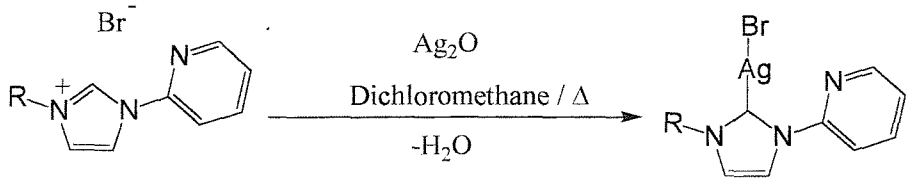

Scheme 3.1. Synthesis of silver carbene complexes.

iii) Ag_2CO_3 can be used instead of Ag_2O although the reaction times are usually longer.

iv) With the relatively unreactive bulky imidazolium salts, for example **(2.8)** and **(2.9)**, the reactions take place only in refluxing 1,2-dichloroethane over a four or five day period,[6] where as with all of the other imidazolium salts the reactions proceed much faster in refluxing 1,2-dichloroethane (*Scheme 3.2*).

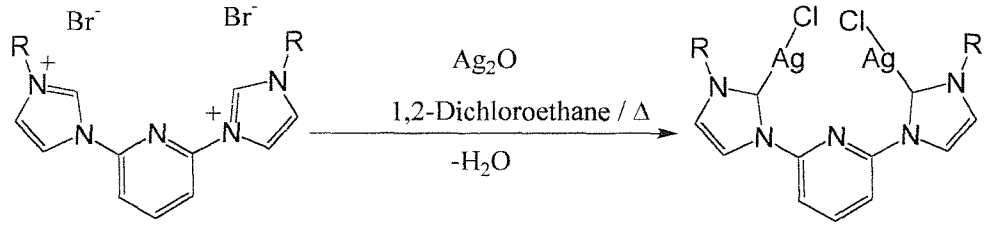

Scheme 3.2. Reaction of imidazolium salt **(2.8)** with silver oxide.[6]

v) However, under these harsher conditions (refluxing 1,2-dichloroethane), substantial exchange of bromide for chloride is observed, requiring longer reaction times to get complete conversion to the chloride (avoiding a mixture of halide anions). (See chemical analysis of compound **(3.6)**).

vi) When complexes **(3.2)** and **(3.3)** were synthesised in refluxing 1,2-dichloroethane, the formation of by-products was increased (see below).

vii) The preparation of silver (I) carbene complexes from silver halides, base and imidazolium salts under phase transfer catalysis as reported by Lin was not achieved.[3]

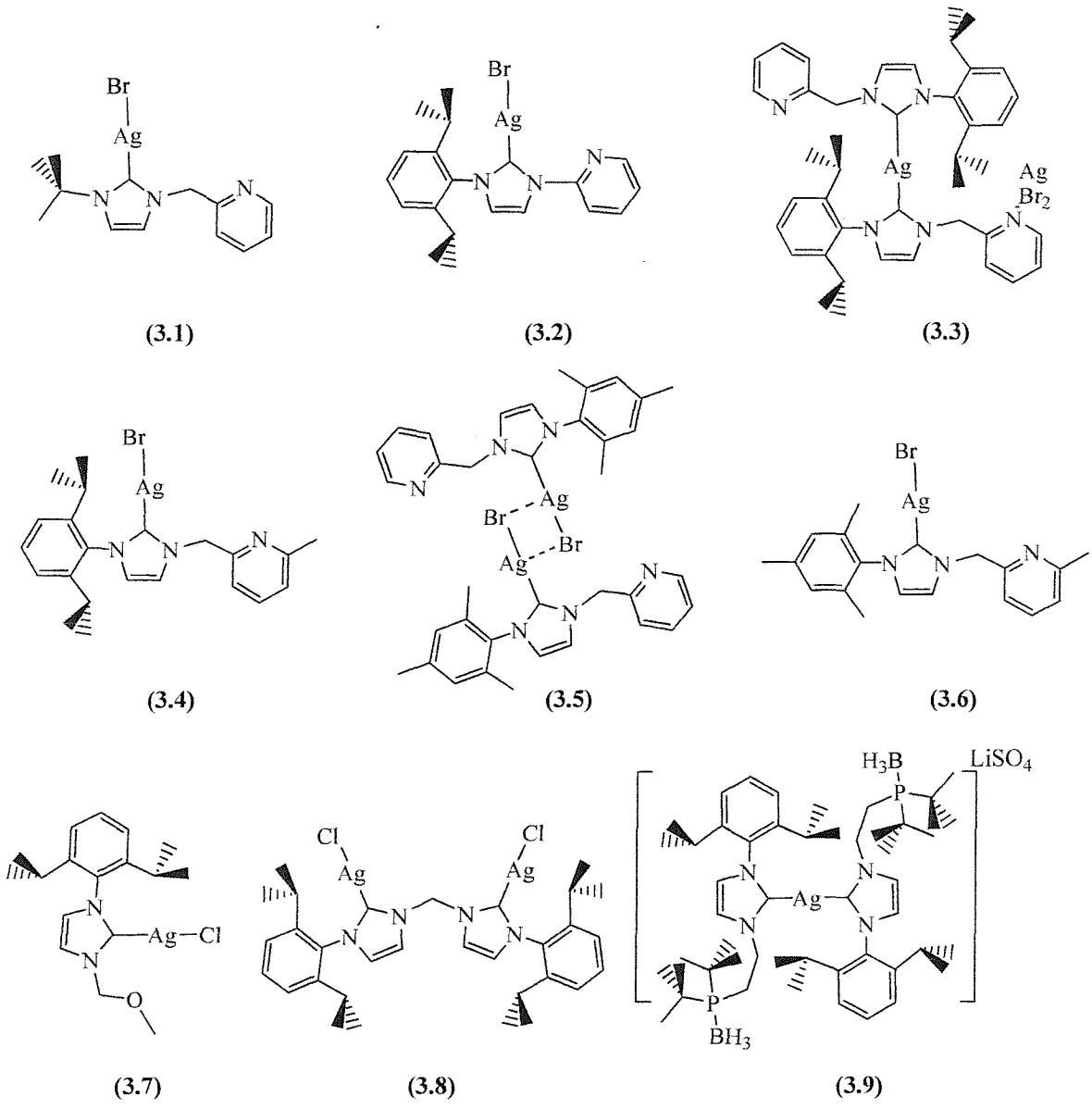

Figure 3.1. Silver complexes synthesised.

3.3 Characterisation of silver carbene complexes

A variety of analytical and spectroscopic techniques were used to identify the silver carbene complexes (*Figure 3.1*). These have at times appeared to be contradictory but when viewed together demonstrate some subtle characteristics of these silver complexes. Compounds **(3.1)-(3.6)** contain carbene ligands functionalised with pyridine type moieties; compound **(3.7)** contains a carbene ligand functionalised with a methoxy group; compound **(3.8)** contains a bidentate carbene ligand; and compound **(3.9)** contains a carbene ligand functionalised with a phosphine borane group.

3.3.1. Electrospray mass spectrometry

Electrospray mass spectrometry in acetonitrile solution was useful in identifying the formation of the silver complexes, with either a peak corresponding to $[Ag(ligand)_2]^+$ or $[Ag(ligand)MeCN]^+$. However, the technique was of low diagnostic value for structure elucidation; as under the sampling conditions employed [Ag(ligand)Br] converted to $[Ag(ligand)_2]^+$. This was demonstrated by sampling from a solution made from a crystal of **(3.2)**, which by X-ray diffraction was shown to be [Ag(ligand)Br]; the molecular ion observed in the spectra corresponded to $[Ag(ligand)_2]^+$. Although this showed that reliable structural information could not be obtained from the mass spectra in acetonitrile, it also demonstrated the lability of the silver carbene bond and suggested that silver carbene complexes could act as good transfer reagents for the ligands.

Chemical analysis could be only used to confirm the stoichiometry, which is the same for different coordination isomers, and could not complement mass spectrometry in structural elucidation.

3.3.2. NMR spectroscopy

The two most characteristic peaks in the ^1H and $^{13}C\{H\}$ NMR spectra, used to identify the formation of the silver carbene complexes are:

i) A weak peak downfield of 165ppm in the $^{13}C\{H\}$ NMR spectra which can be assigned to the carbene carbon (observed in these complexes between 174 and 179 ppm);

ii) The absence of the downfield peak usually observed between 10 and 12 ppm in the ^1H NMR spectra (assigned to the proton in the 2-position of the imidazolium ring).

Other peaks in the ^1H NMR spectra are less characteristic of the formation of the silver complexes, as their chemical shifts remained most unchanged from the imidazolium salts. However, one of the major changes in chemical shift between the imidazolium salts and their silver complexes is of the peak assigned to the protons in the 4,5-positions on the imidazol-2-ylidene ring, with an up-field shift of 1-2 ppm, The difference in shift of the protons in the 5-position is negligible.

The peaks assigned to the protons on the pyridyl ring in the ^1H NMR spectra lose their diagnostic value, with almost no difference in shift between the different silver complexes. The chemical shift of the protons on the methyl of the lutidyl group (see experimental, compounds **(3.4)** and **(3.6)**) also is almost unaffected by the coordination to silver.

The ^{1}H and $^{13}C\{H\}$ NMR spectra of compounds **(3.7)-(3.9)** were as expected and similar to their corresponding imidazolium salts. However, the $^{13}C\{H\}$ NMR spectrum of compound **(3.8)** was not characterisable; it is suggested that this is due to the compound being isolated as a mix of oligomers. Compound **(3.9)** was also characterised by its $^{31}P\{H\}$ NMR spectrum, which contained a broad peak at 41 ppm assigned to the phosphine borane complex, and its $^{11}B\{H\}$ NMR spectrum, which contained a broad peak at -39 ppm.

3.3.3. X-ray diffraction studies

X-Ray diffraction quality crystals of [3-(2,6-di*iso*propylphenyl)-1-(2-pyridyl) imidazol-2-ylidene] silver bromide **(3.2)** were obtained by layering a dichloromethane solution with diethyl ether.

X-Ray diffraction quality crystals of [3-(2,6-di*iso*propylphenyl)-1-(α-picolyl) imidazol-2-ylidene] silver bromide **(3.3)** were obtained by cooling a saturated solution of THF and diethyl ether to 4°C.

X-Ray diffraction quality crystals of [3-(mesityl)-1-(α-picolyl) imidazol-2-ylidene] silver bromide **(3.5)** were obtained by cooling a saturated solution of dichloromethane and petrol to 4°C.

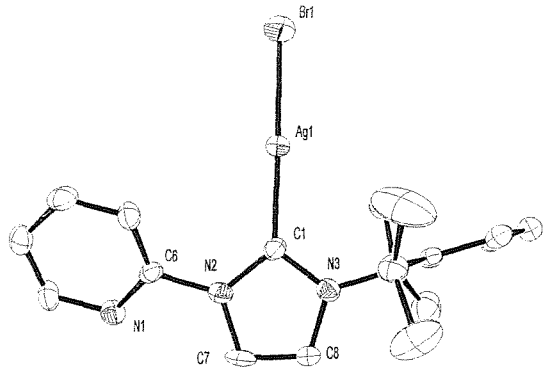

Figure 3.2. X-ray crystal structure of [3-(2,6-di*iso*propylphenyl)-1-(2-pyridyl) imidazol-2-ylidene] silver bromide **(3.2)**.

The single crystal X-ray structure of **(3.2)** comprises a silver atom coordinated by a bromide, and a carbene in a linear geometry (*Figure 3.2*). The silver-carbene bond length is 2.07Å, in the range of a single bond, which is similar to the complexes reported by Lin *et al.*[3] and Arduengo *et al.*[4] There are no close contacts to the pyridyl nitrogen and, the bond lengths and angles of the ligand are similar to that of the imidazolium salt **(2.1)**.

	Carbene-silver bond (Å)
Compound **(3.2)**	2.074(7)
Compound **(3.3)**	2.069(5) and 2.074(5)
Compound **(3.5)**	2.070(18)

Table 3.1. Carbene-silver bond lengths for compounds **(3.2)**, **(3.3)** and **(3.5)**.

In contrast, **(3.3)** comprises a silver atom coordinated by two carbenes in a linear geometry (*Figure 3.3*). In addition, a second silver atom coordinated by two bromides and one pyridine group in a trigonal geometry. The silver-carbene bond lengths in both structures are similar (*Table 3.1*). The rotational twist angle between the two planes defined by the carbene rings is 33.5°. The bond lengths and angles of the carbene rings remain relatively unchanged to those of the imidazolium salt **(2.1)**. In combination with the metal-carbon single bond length, this demonstrates that no significant back bonding from the silver to the carbene atom exists. The molecule adopts a conformation that keeps the picolyl rings away from each other.

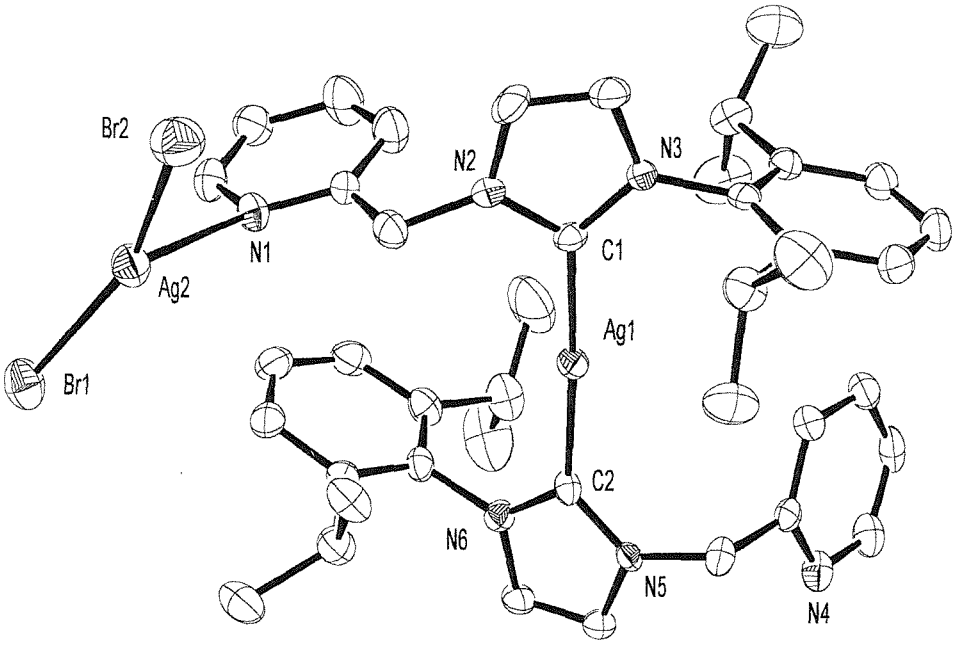

Figure 3.3. X-ray crystal structure of [3-(2,6-di*iso*propylphenyl)-1-(α-picolyl) imidazol-2-ylidene] silver bromide, compound **(3.3)**.

In addition, the structure of **(3.5)** was also solved, although twinned crystals were reproducibly obtained, which prevented the data to be refined to a suitable level (*Figure*

3.4). However, the connectivity of the molecule can be deduced unequivocally. An approximate carbene-silver bond length is shown in *Table 3.1*. The structure of the centro-symmetric dimer comprises two silver atoms bridged by bromides and two carbene ligands, one bound to each silver atom through the carbene end. The ligands are monodentate with no close contacts to the pyridyl nitrogen. The C-Ag-Br angle is only slightly bent away from linear. The geometry of the ring made up by the bridging bromides and the two silver atoms is rhombic with an silver-silver distance of 3.34 Å, indicating a weak metal-metal interaction. Why **(3.3)**, **(3.2)** and **(3.5)** adopt different solid state structures is not clear.

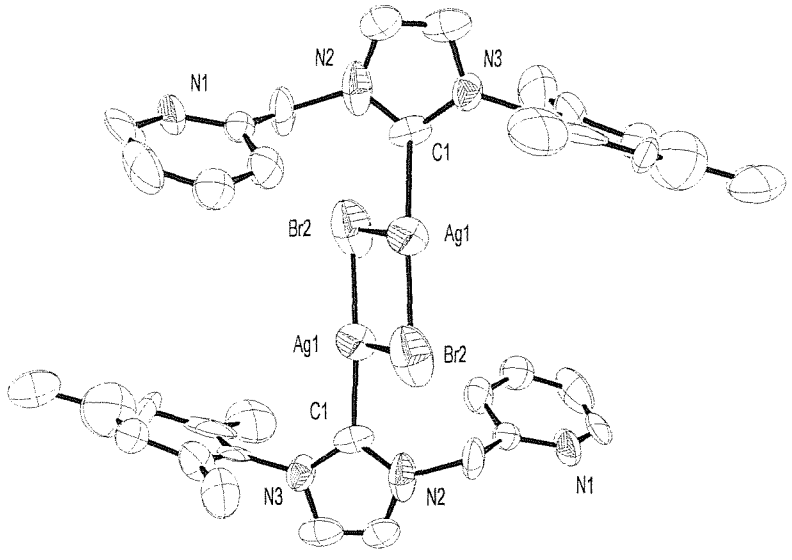

Figure 3.4. X-ray crystal structure of [3-(mesityl)-1-(α-picolyl) imidazol-2-ylidene] silver bromide, compound **(3.5)**.

3.3.4. Variable concentration and temperature ^{1}H NMR spectroscopy

Detailed NMR studies of **(3.3)** and **(3.2)** show many interesting features. The ^{1}H NMR spectra at room temperature of both **(3.3)** and **(3.2)** consists of very broad peaks. However, the appearance of the spectra is dependent on the concentration of the sample. When the solutions are diluted, the spectra show considerable sharpening of the peaks. This sharpening is probably due to the change, on dilution, of the intermolecular interactions in solution. Furthermore, the appearance of these spectra is temperature-dependent. An increase in temperature results in the sharpening of the peaks, which is believed to be due to increasing rate of rotation of the *iso*propyl groups.

3.3.5. Coordination isomers

When compounds **(3.3)** and **(3.2)** were prepared (as described in the experimental) pure solids were obtained, which had clean ^{1}H NMR spectra. However, when the complexes **(3.3)** and **(3.2)** were synthesised in refluxing 1,2-dichloroethane by-products were formed, as shown by NMR spectroscopy. Separation of these by-products from compounds **(3.3)** and **(3.2)** was not achieved. The ^{1}H NMR spectra of these impure mixtures each contain two sets of peaks, each assignable to a carbene complex (*Figure 3.5*). It was concluded that these peaks arise from the two different isostoichiometric silver carbene complexes for each of these mixtures. These coordination isomers of the compounds **(3.3)** and **(3.2)** are rationalised for the following reasons:

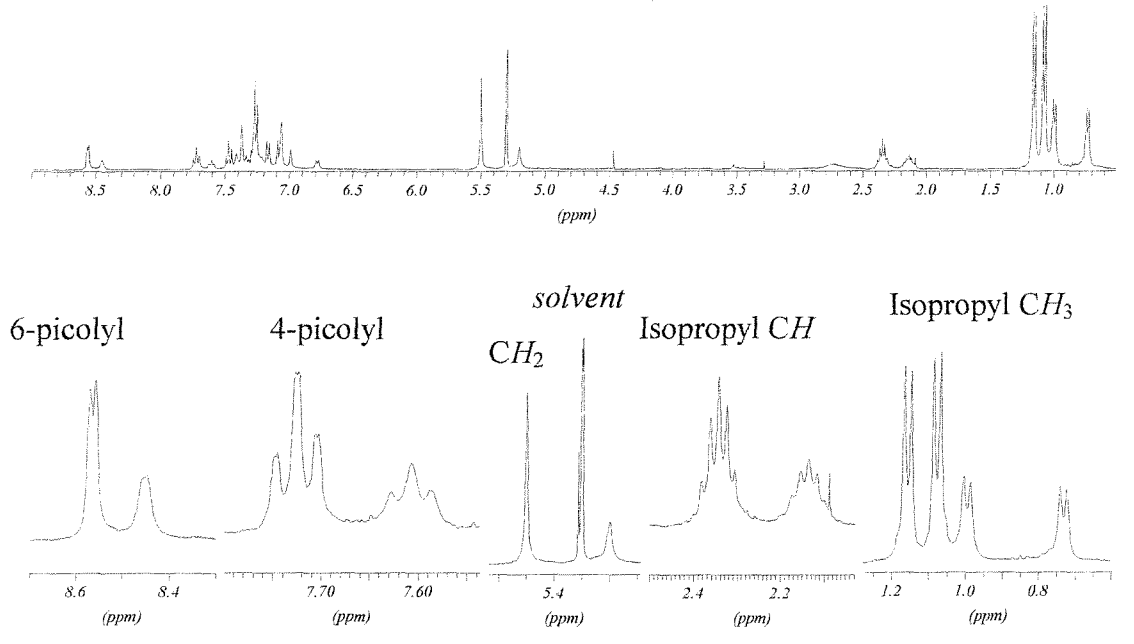

Figure 3.5. ^{1}H NMR spectrum (-30°C, CD_2Cl_2) of a sample of compound **(3.3)**, showing two sets of peaks.

i) In both cases, the major set of peaks was identical to those obtained by the low temperature preparations, described in the experimental.

ii) The peaks associated with the minor coordination isomer have the same appearance as the dominant peaks (slightly shifted).

iii) No interconversion was observed between the sets of peaks in the NMR time scale, over the temperature range -80 to +50°C for **(3.3)** and -80 to –10°C for **(3.2)**.

iv) The analytical data of the mixtures resulted in identical stoichiometry to that of the pure compounds.

The crystals of **(3.3)** and **(3.2)** that were used for X-ray diffraction studies were grown from solutions containing only one species. The crystal structures show that the isolated compound **(3.3)** is [Ag(ligand)$_2$AgBr$_2$] and compound **(3.2)** is [Ag(ligand)Br].

Therefore, it was deduced that the duplicate peaks are related to the coordination isomers [Ag(ligand)Br], in the case of **(3.3)**, and [Ag(ligand)$_2$AgBr$_2$], in the case of **(3.2)**. As X-ray diffraction is the only sure way of identifying the coordination geometry around the silver atoms, the type of coordination isomers that are isolated for compounds **(3.4)**, **(3.6)**, **(3.7)**, **(3.8)** and **(3.9)** was not identified.

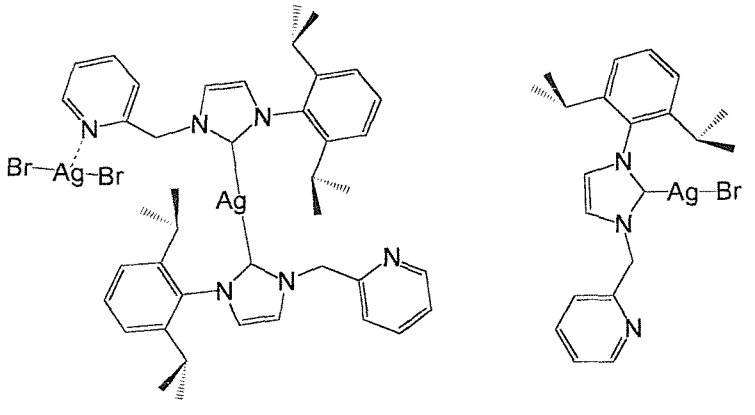

Figure 3.6. Coordination isomers of compound **(3.3)**.

The pyridyl carbene ligand in **(3.2)** is bulkier and more rotationally rigid (no methylene bridge) than the analogous picolyl carbene ligand in **(3.3)**. This difference in bulk is possibly why compounds **(3.3)** and **(3.2)** adopt different structures at low temperatures. The introduction of a second ligand to the silver in compound **(3.2)** would increase unfavourable steric inter-ligand interactions. However, these steric interaction do not appear to prevent the formation of [Ag(ligand)$_2$AgBr$_2$] when the compound is prepared at higher temperatures. Therefore, it can be concluded that, the structural differences in compounds **(3.3)** and **(3.2)** cause them to follow different reaction mechanisms in their low temperature syntheses.

3.4 *N*-functionalised Carbene Complexes of Copper (I), (3.10), (3.11) and (3.12)

Similar to the analogous silver complexes, the copper complexes (*Figure 3.7*) were prepared by the interaction of the imidazolium salts with Cu_2O. The reactions were carried out in chlorinated solvents in the presence of 4Å molecular sieves to give good yields of

the copper (I) complexes (*Scheme 3.3*). Using refluxing 1,2-dichloroethane rather than refluxing dichloromethane speeds up the reaction but does not appear to effect the purity or yields. The copper complexes are air sensitive white solids.

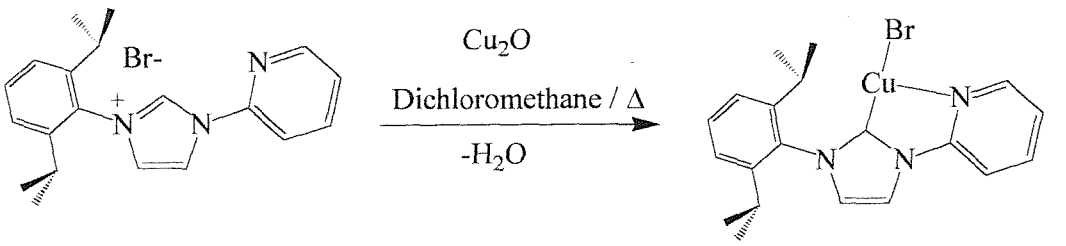

Scheme 3.3. Synthesis of compound **(3.12)**.

Their identification proved to be difficult by spectroscopic methods. However, the products stoichiometries were deduced by analytical methods, which supports the formulation of compounds **(3.10)**, **(3.11)** and **(3.12)** as having a ratio of one bromide to one copper to one ligand.

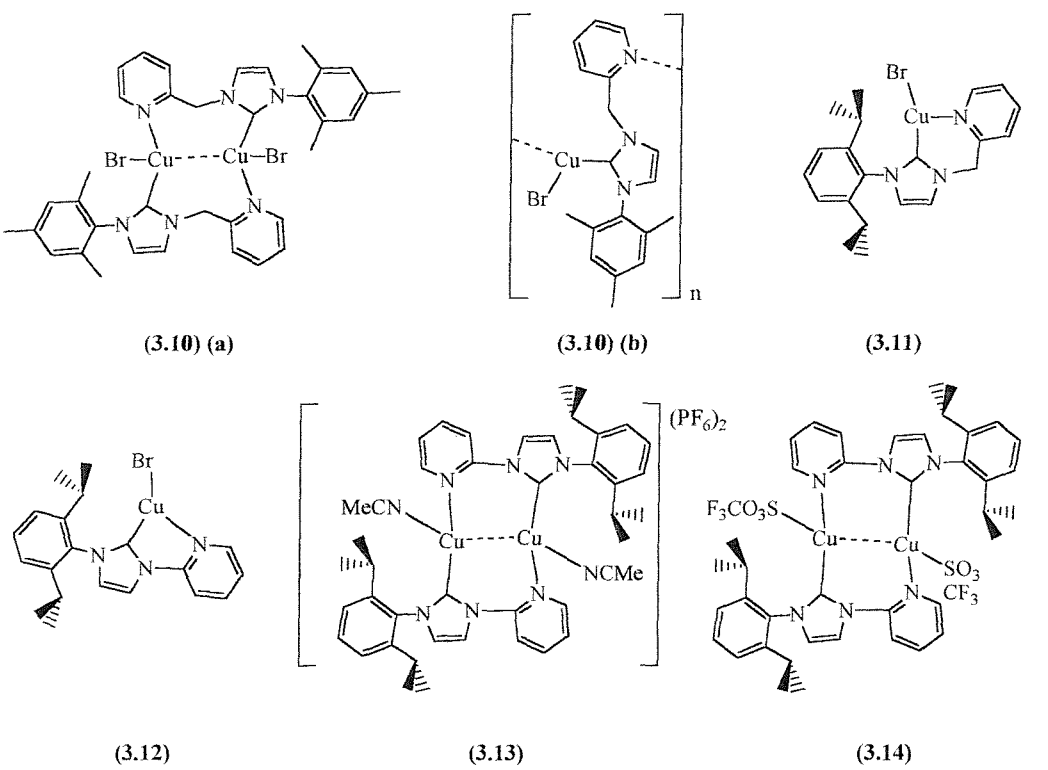

Figure 3.7. Copper complexes synthesised.

3.4.1. NMR spectroscopy

The ^{1}H NMR spectrum of compound **(3.10)** shows broad peaks at 2.1 and 2.3 ppm assignable to the methyls of the mesityl group. Very broad peaks were observed at 5.5 ppm (assigned to the bridging protons), 6.9 ppm (assigned to the aromatic protons on the mesityl ring), and the protons on the pyridine and imidazol-2-ylidene rings gave rise to broad *bands* between 6.2 and 8.6 ppm.

The ^{1}H NMR spectrum of compounds **(3.11)** shows two doublets at 1.1 and 1.2 ppm assignable to the diastereotopic methyls of the *iso*propyl groups (which delocalise at -70°C). Broad peaks were also observed at 2.4 ppm (assigned to the protons of the secondary *iso*propyl carbon); 5.5 ppm (assigned to the bridging protons); and between 7.0 and 8.5 ppm assigned to the protons on the pyridyl, imidazol-2-ylidene and phenyl rings.

The ^{1}H NMR spectrum of compound **(3.12)** shows two doublets at 1.2 and 1.3 ppm assignable to the diastereotopic methyls of the *iso*propyl groups (which split further at -80°C). Broad peaks were also observed at 2.6 ppm (which split at -80°C and are assigned to the protons of the secondary *iso*propyl carbon); and between 7.2 and 8.5 ppm assigned to the protons on the pyridyl, imidazol-2-ylidene and phenyl rings.

NMR spectroscopy proved to be of limited use in identifying these complexes, as the ^{1}H NMR spectra were very broad, and the ^{13}C{H} NMR were deceptively simple and unassignable. The chemical shifts for the broad peaks in the ^{1}H NMR spectra were very similar to that of the analogous silver complexes described previously. The carbene carbons were not observed in the ^{13}C{H} NMR spectra for **(3.10)**, **(3.11)** and **(3.12)**, even at temperatures above or below ambient, or when using long pulse delays. Variable-temperature studies from -80 to 60°C in deuterated dichloromethane did not allow any more information to be extracted, as they remained broad. The peak shapes changed noticeably at lower temperatures and were concentration dependant, however, they always remained broad and displayed limited coupling patterns. This is believed to be a manifestation of fluxional processes. These processes could be linked to:

i) Non-rigidity in the ligand framework when in solution;

ii) An equilibrium involving mono, bis or polymeric copper carbene species (*Scheme 3.4*);

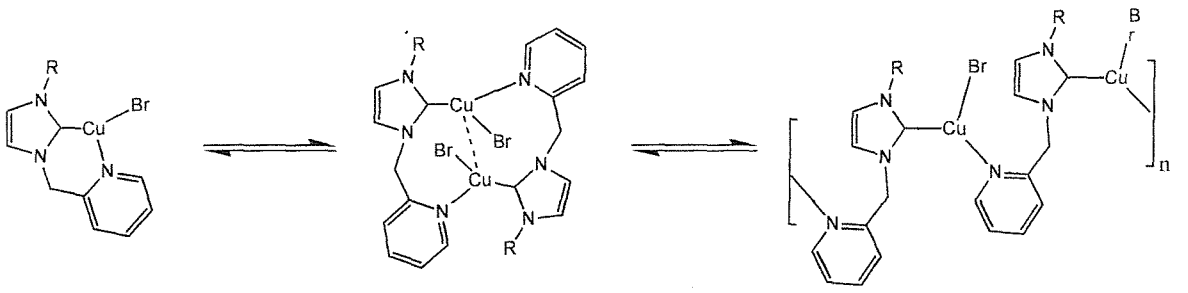

Scheme 3.4. An equilibrium involving mono, bis or polymeric copper carbene species.

iii) An equilibrium involving the transfer of a carbene ligand from one metal centre to another, creating a bis-carbene copper complex in solution (similar to the structure observed for the silver compound **(3.3)**).

3.4.2. X-ray diffraction studies on compound (3.10)

X-ray diffraction quality crystals of [3-(mesityl)-1-(α-picolyl) imidazol-2-ylidene] cuprous bromide, compound **(3.10)** were obtained by slowly cooling a saturated dichloromethane/ether solution to –30°C, giving **(3.10) (a)**; and from a saturated solution of deuterated chloroform, giving **(3.10) (b)**.

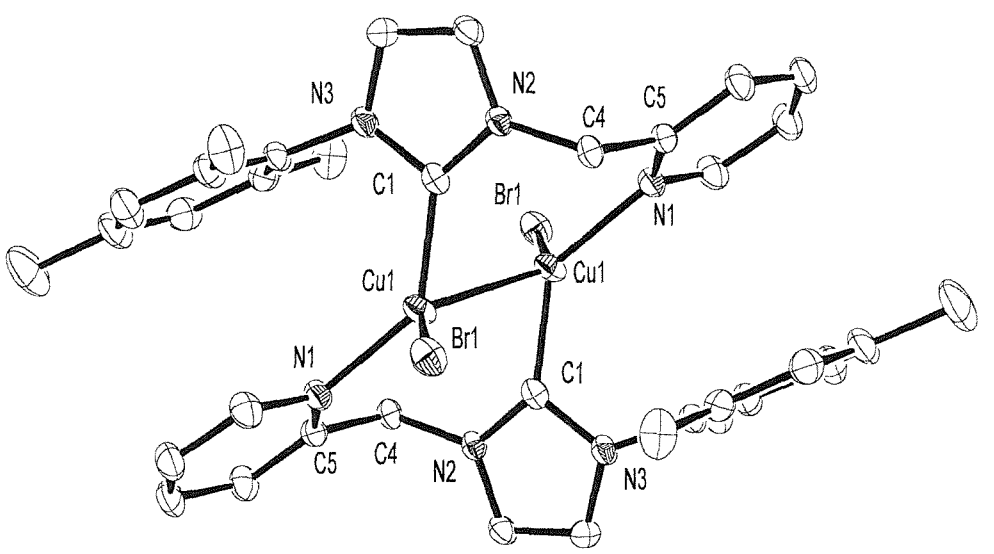

Figure 3.8. X-ray crystal structure of [3-(mesityl)-1-(α-picolyl) imidazol-2-ylidene] cuprous bromide, compound **(3.10) (a)**.

Compound **(3.10) (a)** crystallises as a centro-symmetric dimer with the two copper centres being bridged by two ligands (*Figure 3.8*). Each copper centre is surrounded by one carbene donor, one pyridine donor (from the other ligand), and one bromide atom as

well as having a copper-copper distance of 2.655Å. The geometry around the copper is best described as a distorted trigonal pyramid, with a weak metal-metal interaction.

	Carbene-copper bond (Å)	Nitrogen-copper bond (Å)
Compound **(3.10) (a)**	1.931(2)	2.029(2)
Compound **(3.10) (b)**	1.914(4)	2.044(3)
Compound **(3.12)**	1.880(6)	2.454(5)

Table 3.2. Carbene-copper bond lengths for compounds **(3.10) (a)**, **(3.10) (b)** and **(3.12)**.

The copper-carbon bond distance of 1.931Å is only slightly shorter than that of a single bond, supporting the accepted view that the carbene moiety is a good σ–donor and a poor π–acceptor. The mesityl and pyridyl rings orientate themselves above one another with a separation of 3.875Å, which is within the range for π-stacking interactions.

The structure of **(3.10) (b)** is best described as an organometallic coordination polymer. The chain comprises copper centres, in trigonal geometry, bridged by the ligands in a stretched-helical conformation (*Figure 3.9*).

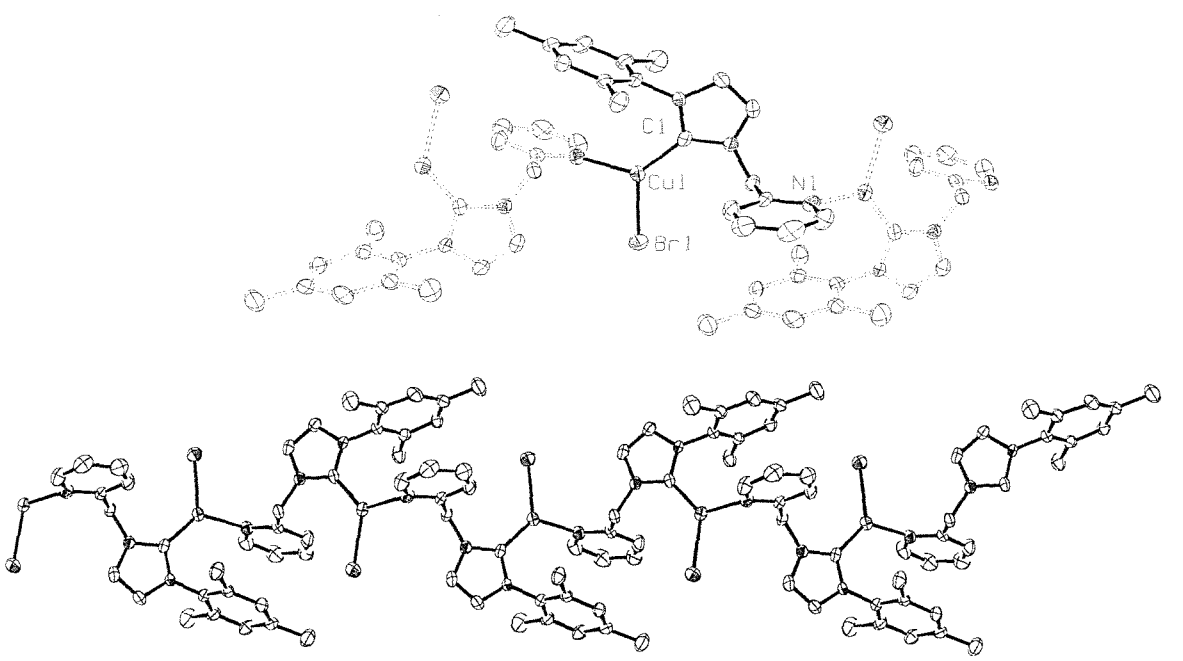

Figure 3.9. X-ray crystal structure of [3-(mesityl)-1-(α-picolyl) imidazol-2-ylidene] cuprous bromide, compound **(3.10) (b)**.

Each copper atom is bound to the carbene end of one ligand, the pyridine end of another ligand, and one bromine atom. The copper-carbon bond distance is 1.914Å (*Table 3.2*); all of the bond distances are comparable to those of the dimer **(3.10) (a)**. The mesityl and pyridyl rings orientate themselves above one another with a separation of 3.713Å, which is within the range for π-stacking interactions (*Figure 3.10*).

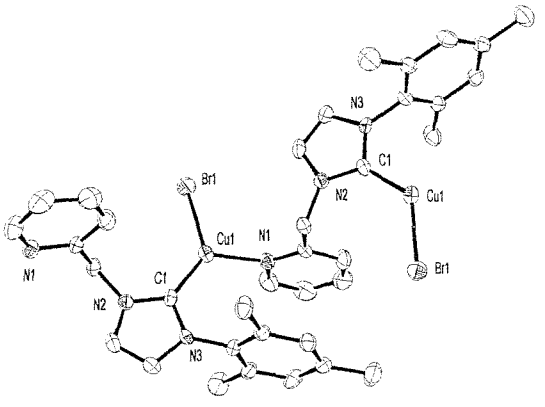

Figure 3.10. A section of the polymer chain from the X-ray crystal structure of [3-(mesityl)-1-(α-picolyl) imidazol-2-ylidene] cuprous bromide, compound **(3.10) (b)**.

3.4.3. X-ray diffraction studies on compound (3.12)

X-ray diffraction quality crystals of **(3.12)** were obtained by layering a saturated solution of deuterated chloroform with diethyl ether. Compound **(3.12)** crystallises as a monomer, the copper atom is chelated by the ligand and bound to a bromide atom (*Figure 3.11*). The geometry around the copper centre is T-shaped, with the copper displaced by 0.1359Å from the plane defined by the atoms in its coordination sphere.

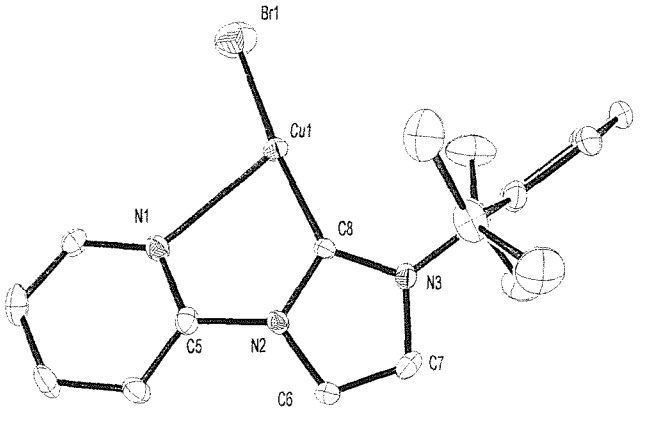

Figure 3.11. X-ray crystal structure of [3-(2,6-di*iso*propylphenyl)-1-(2-pyridyl) imidazol-2-ylidene] cuprous bromide, compound **(3.12)**.

The chelate ring made up of the ligand and the copper atom is close to planar, with a bite angle around the copper of 76.5°. The copper-carbon bond distance is 1.880Å (*Table 3.2*), which is comparable to that found in the thiazol-2-ylidene complexes.[7] The bond distance is shorter than that of **(3.10) (a)** and **(b)**, but longer than that of the theoretically predicted value of 1.848Å.[4] In compound **(3.12)** the conformation imposed by the ligand backbone as well as the increase in electron density on the metal may favour a small amount of metal-carbene back bonding, shortening the copper-carbene bond. The copper-nitrogen bond length of 2.454Å is longer that those in **(3.10) (a)** and **(b)**, possibly due to the effect of the tight angles in the chelate ring restricting the access of the nitrogen atom to the copper.

3.4.4. Structural differences between complexes of (3.10) (a), (3.10) (b) and (3.12)

Further insight into the identity of the isolated complexes in solution was obtained by comparing the crystallisation methods utilised, as **(3.12)** crystallised in a monomeric structure, **(3.10) (a)** crystallised in a dimeric structure, and **(3.10) (b)** crystallised in a polymeric structure. As the differences in the metrical data (carbon-copper distances for the complexes are in *Table 3.2*) of **(3.10) (a)** and **(b)** are minimal, it is assumed that the differences in the structures are due to the identity of the complex in solution. It is believed that the higher concentration of the complex in deuterated chloroform has the result that in solution the complex exists as higher oligomers, and therefore crystallises out as a chain, **(3.10) (b)**. The lower concentration of the complex in dichloromethane/ether means that in solution only the lower oligomers can form, and therefore the complex crystallises out as a dimer. As the crystals of compound **(3.12)** were obtained from quite a dilute solution and the ligand backbone has less conformational flexibility, it is plausible that the complex crystallised out at a monomer.

The compound **(3.12)** is the first published example of a structurally characterised monomeric imidazol-2-ylidene copper complex.[5]

3.4.5. By-products

When molecular sieves were not used in the synthesis of compound **(3.10)**, lower yields were observed and by-products were formed. X-ray diffraction quality crystals of this by-product were obtained by the slow evaporation of a diethyl ether solution. The quality of the best refinement was good enough to identify the connectivity, but not enough

to extract exact bond lengths and angles. However, the molecule is shown to contain four copper atoms in a tetrahedral arrangement around a central oxygen atom. Each copper atom is linked to the others by three bridging bromine atoms. The copper atoms are in trigonal bi-pyramidal geometries with the three bromides in the equatorial positions. The axial positions are filled on one end by the central oxygen atom, and on the other by an imidazole (*Figure 3.12*).

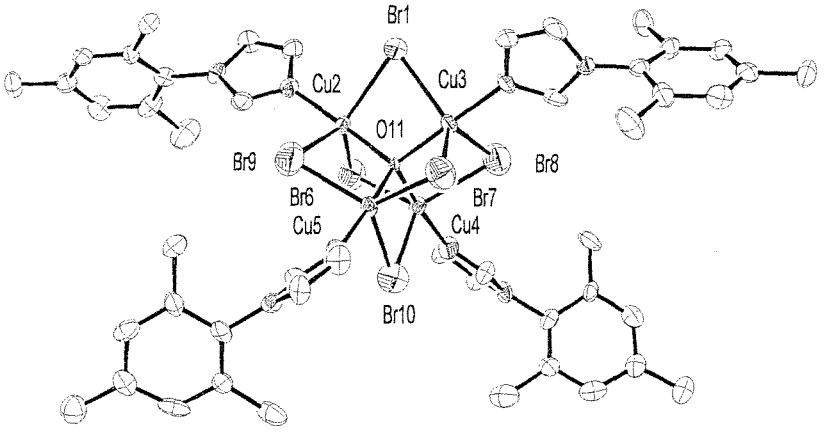

Figure 3.12. X-ray crystal structure of one of the by-products formed when compound **(3.10)** was synthesised in the absence of molecular sieves.

3.5 *N*-functionalised Carbene Complexes of Copper (I), (3.13) and (3.14)

Complexes **(3.13)** and **(3.14)** were synthesised by the interaction of [3-(2,6-di*iso*propylphenyl)-1-(2-pyridyl) imidazol-2-ylidene] cuprous bromide with the corresponding thallium salt in acetonitrile or dichloromethane respectively (*Scheme 3.5*). The products were obtained in good yields as moderately air sensitive white solids. The stoichiometries were determined by elemental analysis, showing complete displacement of the bromide anion.

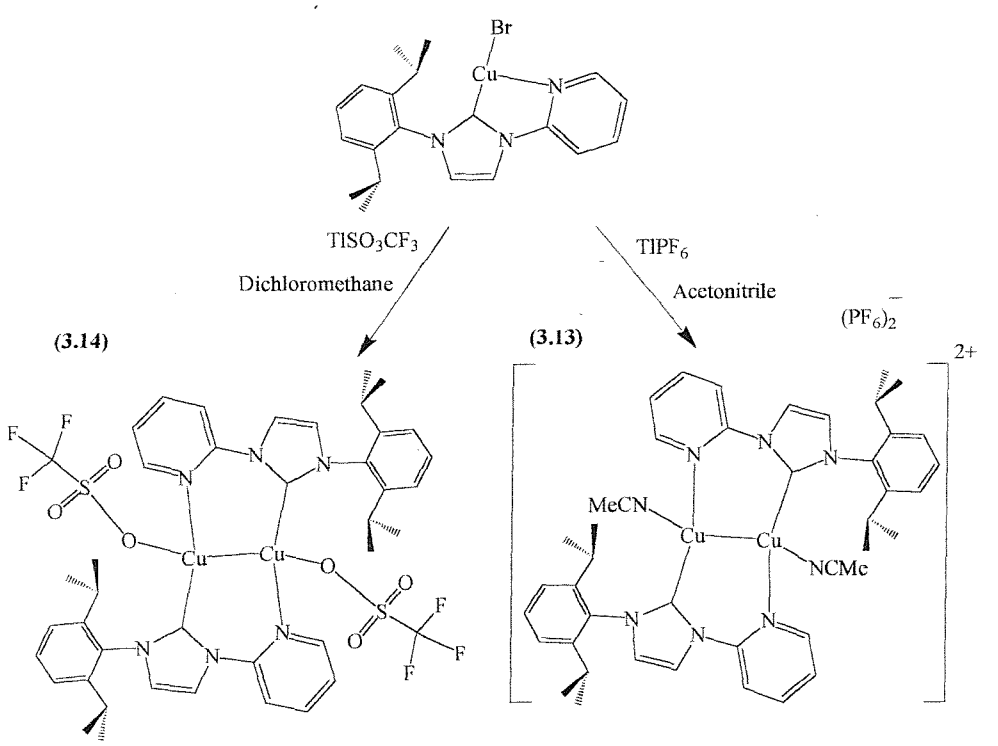

Scheme 3.5. Synthesis of compounds **(3.13)** and **(3.14)**.

3.5.1. NMR spectroscopy

The ^{1}H NMR spectra of the complexes were as broad and uninformative as that of the corresponding parent complex. The $^{13}C\{H\}$ NMR spectra were also deceptively simple, with characteristic peaks missing.

The ^{1}H NMR spectrum of **(3.13)** shows two doublets at 0.8 and 1.1 ppm assignable to the diastereotopic methyls of the *iso*propyl groups. Broad peaks were also observed at 2.1 ppm (assigned to acetonitrile); 2.4 ppm (assigned to the protons of the secondary *iso*propyl carbon) and between 7.1 and 8.1 ppm, assigned to the protons on the pyridyl, imidazol-2-ylidene and phenyl rings.

The ^{1}H NMR spectrum of **(3.14)** shows two doublets at 0.8 and 1.1 ppm assignable to the diastereotopic methyls of the *iso*propyl groups. Broad peaks were also observed at 2.3 ppm (assigned to the protons of the secondary *iso*propyl carbon); and between 6.9 and 8.0 ppm, assigned to the protons on the pyridyl, imidazol-2-ylidene and phenyl rings.

3.5.2. X-ray diffraction studies on compound (3.13)

X-ray diffraction quality crystals of [3-(2,6-di*iso*propylphenyl)-1-(2-pyridyl) imidazol-2-ylidene] cuprous hexafluorophosphate acetonitrile **(3.13)** were obtained by layering a saturated dichloromethane solution with petrol.

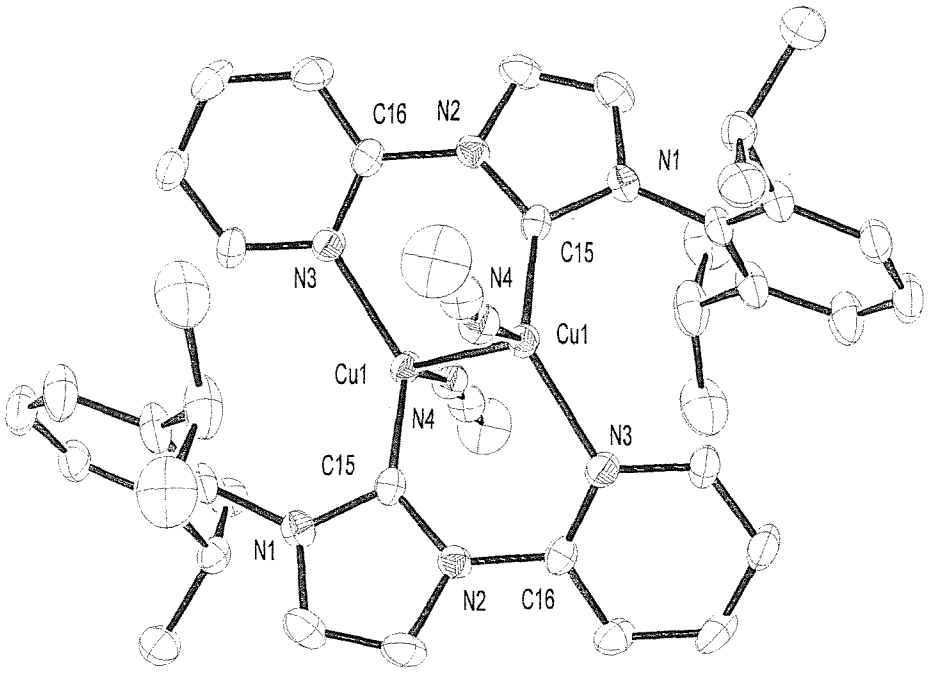

Figure 3.13. The dicationic complex from the X-ray crystal structure of [3-(2,6-di*iso*propylphenyl)-1-(2-pyridyl) imidazol-2-ylidene] cuprous hexafluorophosphate acetonitrile, compound **(3.13)**.

Compound **(3.13)** crystallises as a centro-symmetric dimer with the two copper centres being bridged by two ligands (*Figure 3.13*). Each copper centre is bound in a tetrahedral arrangement by one carbene donor, one pyridyl donor (from the other ligand), an acetonitrile, and the symmetry equivalent copper atom.

	Carbene-copper bond (Å)	Nitrogen-copper bond (Å)
Compound **(3.10) (a)**	1.931(2)	2.029(2)
Compound **(3.13)**	1.933(3)	2.036(2)
Compound **(3.14)**	1.916(2)	2.023(2)

Table 3.3. Carbene-copper bond lengths for compounds **(3.10) (a)**, **(3.13)** and **(3.14)**.

The copper-copper bond distance is 2.487Å. The copper-carbon bond distance of 1.93Å and the copper-nitrogen (pyridyl) bond distance of 2.04Å are similar to those of compound **(3.10) (a)** (*Table 3.3*).

3.5.3. X-ray diffraction studies on compound (3.14)

X-ray diffraction quality crystals of compound **(3.14)** were obtained by layering a saturated dichloromethane solution with diethyl ether. Compound **(3.14)** crystallises as a centro-symmetric dimer with the two copper centres being bridged by two ligands (*Figure 3.14* and *Figure 3.15*).

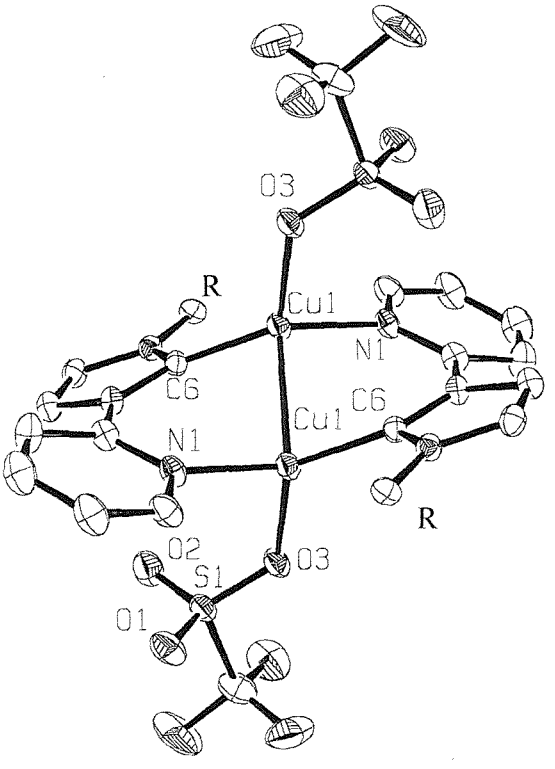

Figure 3.14. X-ray crystal structure of [3-(2,6-di*iso*propylphenyl)-1-(2-pyridyl) imidazol-2-ylidene] cuprous triflate, compound **(3.14)** (2,6-di*iso*propylphenyl groups removed and replaced with R for simplicity).

Each copper centre is bound in a tetrahedral arrangement by one carbene donor, one pyridine donor (from the second ligand), one oxygen atom (from a triflate), and the symmetry equivalent copper atom. The copper-copper bond distance is 2.521Å, which is slightly longer that that of compound **(3.13)**. The copper-carbon bond distance of 1.92Å and the copper-nitrogen (pyridyl) bond distance of 2.02Å are similar to that of compound **(3.13)** (*Table 3.3*). The copper-oxygen bond length of 2.13Å is in the range of a normal copper-oxygen bond.

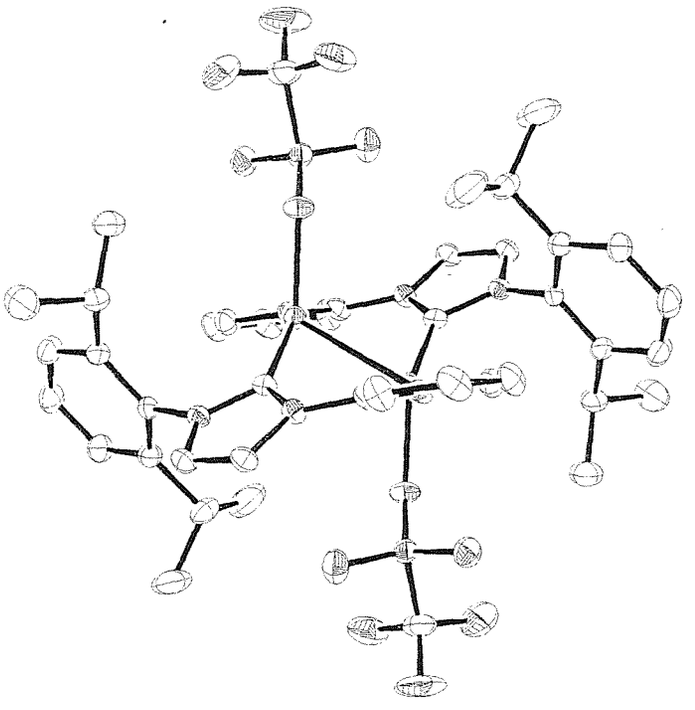

Figure 3.15. X-ray crystal structure of [3-(2,6-di*iso*propylphenyl)-1-(2-pyridyl) imidazol-2-ylidene] cuprous triflate, compound **(3.14)**.

3.6 Conclusions

The *N*-functionalised silver (I) carbene complexes can easily be prepared, and the first example of a silver (I) imidazol-2-ylidene complex with a mixed donor *N*-heterocyclic carbene ligand has been structurally characterised.

The *N*-functionalised copper (I) carbene complexes can also easily be prepared, and the first example of a monomeric copper (I) imidazol-2-ylidene complex has been structurally characterised.

The copper-carbon and silver-carbon bond lengths in these structures are shorter than copper-carbon or silver-carbon single bonds and comparable to the bond length observed in thiazol-2-ylidene complexes.[7]

Furthermore, by using picolyl-*N*-functionalised carbene ligands, which exhibit larger bite angles and increased backbone flexibility, dimeric and polymeric materials were obtained. The structures observed for the copper complexes demonstrate the versatility of the functionalised carbene ligands, as they can act as bridging ligands to form oligomers or polymers and in solution can exist in equilibrium with the monomer. It is hoped that this design principle (hemilability) could also operate in catalytically active transition metal complexes. The existence of similar equilibria could give rise to coordinativly unsaturated, and therefore catalytically more active, species.

EXPERIMENTAL

3.7 Synthesis of silver (I) complexes

3.7.1. General method:

The manipulations were carried out under nitrogen. In an ampoule, a suspension of the substituted imidazolium salt, excess of silver oxide or silver carbonate and 4Å molecular sieves in dichloromethane or 1,2-dichloroethane was heated at 35°C or 90°C respectively for 3-48 hours. After completion, the reaction mixture was filtered, the volatiles were removed under vacuum and the resulting solid was washed with diethyl ether and extracted into dichloromethane. Filtration of the solution and evaporation of the volatiles under vacuum produced white solids.

In most cases, the products obtained at this stage were spectroscopically and analytically pure. If not, the solids were purified by recrystallisation from a saturated solution of dichloromethane and diethyl ether.

(3.1) [3-(*tert*butyl)-1-(α-picolyl) imidazol-2-ylidene] silver bromide

This was prepared following the general method from 3-(*tert*butyl)-1-(α-picolyl) imidazolium bromide (0.24g, 0.77mmol) and silver oxide (0.16g, 0.58mmol) in dichloromethane (30ml) by heating at 35°C for 48 hours. The solid obtained was dissolved in toluene, the solution filtered and the solvent removed under reduced pressure. The resulting yellow powder was washed with ether and dried under vacuum.

Yield: 0.28g, 90%.

$\delta_H(CDCl_3)$ 1.6 (9H, s, $C(CH_3)_3$), 5.4 (2H, s, CH_2), 7.1 (1H, d, 5-imidazol-2-ylidene *H*), 7.2 (1H, d, 4-imidazol-2-ylidene *H*), 7.2 (2H, m, 3,5-picolyl *H*), 7.6 (1H, dt, 4-picolyl *H*), 8.5 (1H, dd, 6-picolyl *H*).

$\delta_C(CDCl_3)$ 32 [$C(CH_3)_3$], 54 [$C(CH_3)_3$)], 58 (CH_2), 119, 120, 122, 123 (picolyl *C*, 4,5-imidazol-2-ylidene *C*), 137, 150, 155 (picolyl *C*), 179 (2-imidazol-2-ylidene *C*).

(Found: C, 39.02; H, 4.68; N, 10.92. $C_{13}H_{17}AgBrN_3$ calculated: C, 38.74; H, 4.25; N, 10.43%).

(3.2) [3-(2,6-di*iso*propylphenyl)-1-(2-pyridyl) imidazol-2-ylidene] silver bromide

This was prepared following the general method from 3-(2,6-di*iso*propylphenyl)-1-(2-pyridyl) imidazolium bromide (2.0g, 4.78mmol) and silver carbonate (0.99g, 3.58mmol) in dichloromethane (80ml) by heating at 35°C for 48 hours. The product was obtained in

quantitative yields as a white solid. X-ray diffraction quality crystals were obtained by layering a dichloromethane solution with diethyl ether (*Figure 3.16* and *Table 3.4*).

MS (ES): *m/z* 455, $[Ag(ligand) + MeCN]^+$; 719, $[Ag(ligand)_2]^+$.

$\delta_H(CDCl_3)$ 1.0 and 1.3 [2 × 6H, d, $CH(CH_3)$], 2.5 (2H, septet, $CH(CH_3)_2$), 6.3(1H, d, 4-imidazol-2-ylidene *H*), 7.0 (2H, d, $^iPr_2C_6H_2H$), 7.1 (1H, t, $^iPr_2C_6H_2H$), 7.1 (2H, m, 3,5-pyridyl *H*), 7.8 (1H, d, 5-imidazol-2-ylidene *H*), 8.1 (1H, dd, 6-pyridyl *H*), 8.5 (1H, t, 4-pyridyl *H*).

$\delta_C(CDCl_3)$ 24 [$CH(CH_3)$], 28 [$CH(CH_3)$], 116, 120, 124, 124, 131, 135, 140, 146, 149, 150 ($^iPr_2C_6H_3$, pyridyl *C*, 4,5-imidazol-2-ylidene *C*), 174 (2-imidazol-2-ylidene *C*).

(Found: C, 49.35; H, 4.78; N, 8.52. $C_{20}H_{23}AgBrN_3$ calculated: C, 48.71; H, 4.70; N, 8.52%).

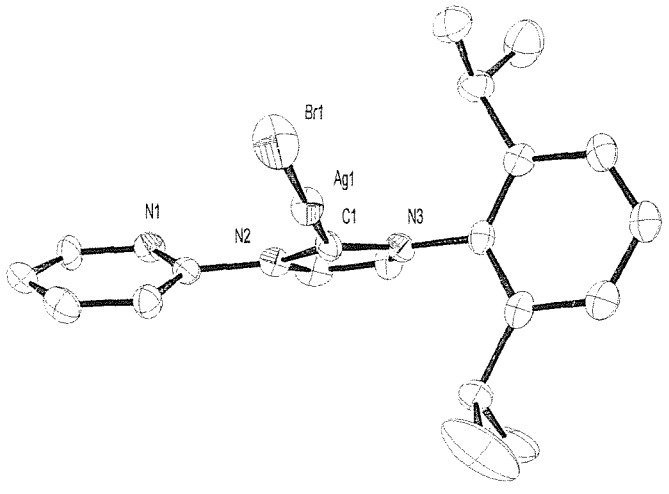

Figure 3.16. X-ray crystal structure of [3-(2,6-di*iso*propylphenyl)-1-(2-pyridyl) imidazol-2-ylidene] silver bromide **(3.2)**.

Ag(1)-C(1)	2.074(7)	C(7)-C(8)	1.332(11)
Ag(1)-Br(1)	2.4209(9)	C(8)-N(3)	1.377(9)
C(6)-N(1)	1.319(8)	N(2)-C(1)	1.377(9)
C(6)-N(2)	1.447(9)	N(3)-C(1)	1.359(9)
C(7)-N(2)	1.375(10)	N(3)-C(9)	1.451(8)
C(1)-Ag(1)-Br(1)	176.06(17)	C(1)-N(3)-C(8)	111.4(5)
N(1)-C(6)-N(2)	113.3(6)	C(1)-N(3)-C(9)	124.2(6)
C(8)-C(7)-N(2)	105.8(6)	N(3)-C(1)-N(2)	102.5(6)
C(7)-C(8)-N(3)	108.1(7)	N(3)-C(1)-Ag(1)	126.3(4)
C(7)-N(2)-C(1)	112.2(6)	N(2)-C(1)-Ag(1)	130.5(5)
C(6)-N(1)-C(2)	115.6(6)		

Table 3.4. Selected bond lengths (Å) and angles (°) for compound **(3.2)**.

(3.3) [3-(2,6-di*iso*propylphenyl)-1-(α-picolyl) imidazol-2-ylidene] silver bromide

This was prepared following the general method from 3-(2,6-di*iso*propylphenyl)-1-(α-picolyl) imidazolium bromide (2.0g, 5.17mmol) and silver carbonate (1.06g, 3.88mmol) in dichloromethane (80ml) by heating at 35°C for 48 hours. The product was obtained in quantitative yields as a white solid. X-Ray diffraction quality crystals were obtained by cooling a saturated solution of THF and diethyl ether to 4°C (*Figure 3.17* and *Table 3.5*).

MS (ES): *m/z* 469, $[Ag(ligand) + MeCN]^+$; 748, $[Ag(ligand)_2]^+$.

$\delta_H(CDCl_3)$ 1.1, 1.2 [2 × 6H, d, $CH(CH_3)_2$], 2.4 [2H, septet, $CH(CH_3)_2$], 5.5 (2H, s, CH_2), 7.0 (1H, d, 4-imidazol-2-ylidene *H*), 7.2 (2H, d, $^iPr_2C_6H_2H$), 7.3 (1H, m, 5- picolyl *H*), 7.3 (1H, d, 3-picolyl *H*), 7.4 (1H, d, 5-imidazol-2-ylidene *H*), 7.5 (1H, t, $^iPr_2C_6H_2H$), 7.8 (1H, dt, 4-picolyl *H*), 8.6 (1H, d, 6-picolyl *H*).

$\delta_C(CDCl_3)$ 24, 25 ($CH(CH_3)_2$), 28 ($CH(CH_3)_2$), 57 (CH_2), 122, 122, 123, 124, 124, 130, 135, 137, 146, 150, 155 ($^iPr_2C_6H_3$, picolyl *C*, 4,5-imidazol-2-ylidene *C*), 174 (2-imidazol-2-ylidene *C*).

(Found: C, 49.33; H, 4.59; N, 8.93. $C_{21}H_{25}AgBrN_3$ calculated: C, 49.73; H, 4.97; N, 8.28%).

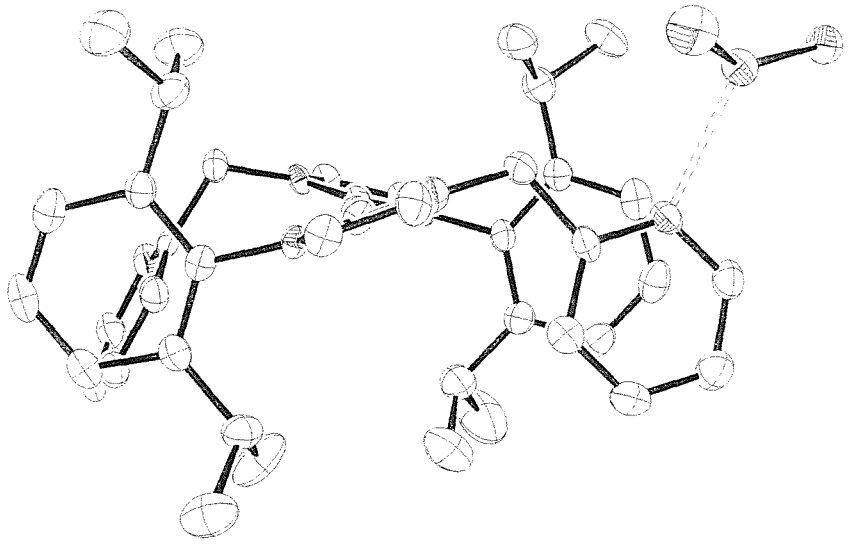

Figure 3.17. X-ray crystal structure of [3-(2,6-di*iso*propylphenyl)-1-(α-picolyl) imidazol-2-ylidene] silver bromide, compound **(3.3)**. View along the carbene-silver-carbene bonds.

Ag(1)-C(1)	2.069(5)	N(3)-C(11)	1.458(6)
Ag(1)-C(2)	2.074(5)	N(6)-C(2)	1.359(7)
Ag(2)-N(1)	2.467(4)	N(6)-C(30)	1.388(7)
Ag(2)-Br(1)	2.4909(7)	N(6)-C(31)	1.447(7)
Ag(2)-Br(2)	2.5090(8)	N(5)-C(2)	1.348(7)
N(3)-C(1)	1.339(6)	N(5)-C(29)	1.390(7)
N(3)-C(10)	1.370(7)	N(5)-C(28)	1.449(7)

N(2)-C(1)	1.373(7)	C(30)-C(29)	1.348(8)
N(2)-C(9)	1.383(8)	C(8)-C(7)	1.494(8)
N(2)-C(8)	1.457(7)	C(28)-C(27)	1.502(7)
N(1)-C(7)	1.340(7)	C(10)-C(9)	1.338(8)
N(4)-C(27)	1.327(7)		
C(1)-Ag(1)-C(2)	175.90(19)	C(29)-C(30)-N(6)	106.2(4)
N(1)-Ag(2)-Br(1)	108.82(11)	N(2)-C(8)-C(7)	114.0(4)
N(1)-Ag(2)-Br(2)	95.80(11)	N(1)-C(7)-C(8)	114.1(4)
Br(1)-Ag(2)-Br(2)	154.52(3)	N(3)-C(1)-N(2)	102.7(4)
C(1)-N(3)-C(10)	113.2(4)	N(3)-C(1)-Ag(1)	132.0(4)
C(1)-N(3)-C(11)	123.1(4)	N(2)-C(1)-Ag(1)	125.4(4)
C(2)-N(6)-C(30)	111.5(4)	C(9)-C(10)-N(3)	106.4(5)
C(2)-N(6)-C(31)	123.5(4)	C(10)-C(9)-N(2)	106.5(5)
C(2)-N(5)-C(29)	111.3(4)	C(30)-C(29)-N(5)	106.8(5)
C(2)-N(5)-C(28)	125.3(4)	N(4)-C(27)-C(28)	115.0(4)
C(1)-N(2)-C(9)	111.2(5)	N(5)-C(2)-N(6)	104.2(4)
C(1)-N(2)-C(8)	124.2(5)	N(5)-C(2)-Ag(1)	129.3(4)
C(7)-N(1)-Ag(2)	127.4(3)	N(6)-C(2)-Ag(1)	126.5(4)

Table 3.5. Selected bond lengths (Å) and angles (°) for compound **(3.3)**.

(3.4) [3-(2,6-di*iso*propylphenyl)-1-(α-lutidyl) imidazol-2-ylidene] silver bromide

This was prepared following the general method 3-(2,6-di*iso*propylphenyl)-1-(α-lutidyl) imidazolium bromide (1.0g, 2.42mmol) and silver oxide (0.80g, 3.48mmol) in dichloromethane (50ml) by heating at 35°C for 48 hours. The product was obtained in quantitative yields as a white solid.

MS (ES): *m/z* 473, $[Ag(ligand) + MeCN]^+$; 776, $[Ag(ligand)_2]^+$.

$_H$($CDCl_3$) 1.1, 1.2 [2 × 6H, d, $CH(CH_3)_2$], 2.4 [2H, septet, $CH(CH_3)_2$], 2.6 (3H, s, CH_3), 5.5 (2H, s, CH_2), 7.0 (1H, d, 5-imidazol-2-ylidene *H*), 7.1 (1H, d, 5- picolyl *H*), 7.2 (1H, d, 3-picolyl *H*), 7.3 (2H, d, $^iPr_2C_6H_2H$), 7.4 (1H, d, 4-imidazol-2-ylidene *H*), 7.5 (1H, t, $^iPr_2C_6H_2H$), 7.6 (1H, dt, 4-picolyl *H*).

δ_C($CDCl_3$) 24, 25, 25 [(CH_3)$_2$], 28 [$CH(CH_3)_2$], 57 (CH_2), 119, 121, 122, 123, 124, 124, 131, 138, 146, 154, 156, ($^iPr_2C_6H_3$, picolyl *C*, 4,5-imidazol-2-ylidene *C*), 175 (2-imidazol-2-ylidene *C*).

(Found: C, 50.83; H, 5.49; N, 8.29. $C_{22}H_{27}AgBrN_3$ calculated: C, 50.69; H, 5.22; N, 8.06%).

(3.5) [3-(mesityl)-1-(α-picolyl) imidazol-2-ylidene] silver bromide

This was prepared following the general method 3-(mesityl)-1-(α-picolyl) imidazolium bromide (2.0g, 5.35mmol) and silver carbonate (0.85g, 3.2mmol) in dichloromethane (80ml) by heating at 35°C for 48 hours. The product was obtained in quantitative yields as a pale yellow solid. X-ray diffraction quality crystals were obtained by cooling a saturated solution of dichloromethane and petrol to 4°C (*Figure 3.18* and *Table 3.6*).

MS (ES): *m/z* 427, $[Ag(ligand)MeCN]^+$; 663, $[Ag(ligand)_2]^+$.

$\delta_H(CDCl_3)$ 1.9 (6H, s, CH_3), 2.3 (3H, s, CH_3), 5.4 (2H, m, CH_2), 6.9 (2H, s, mesityl *H*), 6.9 (1H, m, 5-picolyl *H*), 7.2 (1H, d, 5-imidazol-2-ylidene *H*), 7.3 (1H, d, 4-imidazol-2-ylidene *H*), 7.2 (1H, d, 3-picolyl *H*), 7.7 (1H, dt, 4-picolyl *H*), 8.6 (1H, d, 6-picolyl *H*).

$\delta_C(CDCl_3)$ 18, 21 (CH_3), 57 (CH_2), 122, 123, 123, 124, 130, 135, 138, 140, 150 (mesityl *C*, picolyl *C*, 4,5-imidazol-2-ylidene *C*), 174 (2-imidazol-2-ylidene C).

(Found: C, 47.70; H, 4.22; N, 8.94. $C_{18}H_{19}AgBrN_3$ calculated: C, 46.48; H, 4.12; N, 9.03%).

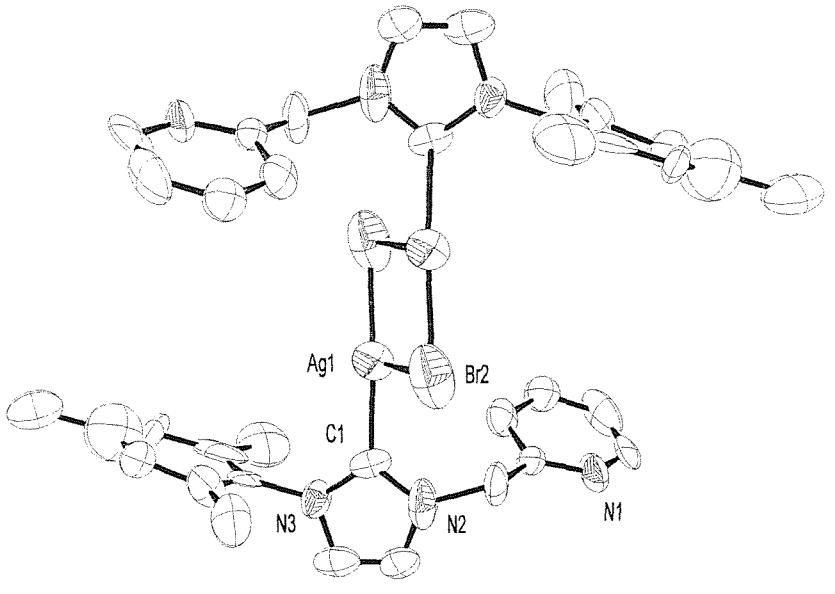

Figure 3.18. X-ray crystal structure of [3-(mesityl)-1-(α-picolyl) imidazol-2-ylidene] silver bromide, compound **(3.5)**.

Ag(1)-C(1)	2.070(18)	N(3)-C(10)	1.44(2)
Ag(1)-Br(2)#1	2.373(4)	N(2)-C(1)	1.31(2)
Ag(1)-Br(2)	2.952(4)	N(2)-C(8)	1.40(3)
Ag(1)-Ag(1)#1	3.367(6)	N(2)-C(7)	1.54(2)
Br(2)-Ag(1)#1	2.373(4)	N(1)-C(6)	1.32(2)
N(3)-C(9)	1.43(3)	N(1)-C(2)	1.36(4)
N(3)-C(1)	1.36(2)	C(9)-C(8)	1.29(3)

C(1)-Ag(1)-Br(2)#1	162.5(5)	C(6)-N(1)-C(2)	119.0(18)
C(1)-Ag(1)-Br(2)	94.6(5)	N(2)-C(1)-N(3)	103.5(16)
Br(2)#1-Ag(1)-Br(2)	102.40(13)	N(2)-C(1)-Ag(1)	128.6(16)
C(1)-Ag(1)-Ag(1)#1	138.0(5)	N(3)-C(1)-Ag(1)	125.7(12)
Ag(1)#1-Br(2)-Ag(1)	77.60(13)	C(8)-C(9)-N(3)	105(2)
C(9)-N(3)-C(1)	110.0(16)	C(6)-C(5)-C(4)	119.2(18)
C(1)-N(3)-C(10)	124.7(15)	C(6)-C(7)-N(2)	113.7(17)
C(1)-N(2)-C(8)	112.5(16)	N(1)-C(6)-C(7)	115.6(15)
C(1)-N(2)-C(7)	122(2)	C(9)-C(8)-N(2)	107.3(19)

Table 3.6. Selected bond lengths (Å) and angles (°) for compound **(3.5)**.

Compound	**(3.5)**	**(3.3)**	**(3.2)**
Chemical formula	$C_{18}H_{19}AgBrN_3$	$C_{42}H_{50}Ag_2Br_2N_6$	$C_{20}H_{23}AgBrN_3$
Formula weight	465.14	1014.44	493.19
Crystal system	Monoclinic	Othorhombic	Monoclinic
Space group	*P* 2/n	*P* 2_1 n b	*P* 2_1/n
a/Å	9.7752(13)	12.7737(1)	10.8837(4)
b/Å	16.867(3)	16.5530(1)	16.4154(6)
c/Å	10.909(2)	20.1344(2)	11.4127(4)
α/°	90	90.0	90.0
β/°	95.115(12)	90.0	103.155(2)
γ/°	90	90.0	90.0
V/Å^3	1791.5(5)	4257.28(6)	1985.5(2)
Z	4	4	4
T/K	293(2)	150	150
μ/mm^{-1}	3.358	2.833	3.035
F(000)	920	2032	984
No. Data collected	13805	37682	2801
No. Unique data	3686	8211	2167
R_{int}	0.2641	0.0660	0.0331
Final R(|F|) for $F_O > 2\sigma(F_o)$	0.2056	0.0386	0.0454
Final R(F^2) for all data	0.2842	0.0504	0.0519

Table 3.7. Crystallographic parameters for compounds **(3.2)**, **(3.3)** and **(3.5)**.

(3.6) [3-(mesityl)-1-(α-lutidyl) imidazol-2-ylidene] silver bromide

This was prepared following the general method 3-(mesityl)-1-(α-lutidyl) imidazolium bromide (0.3g, 0.8mmol) and silver carbonate (0.16g, 0.8mmol) in 1,2-dichloroethane (30ml) by heating at 90°C for 4 hours. The resulting solid was washed with cold diethyl ether and dissolved in toluene. The pale yellow solution was filtered and the solvent removed under vacuum. The product was obtained in quantitative yields as a pale yellow solid.

MS (ES): *m/z* 691.2, $[Ag(ligand)_2]^+$.

$\delta_H(CDCl_3)$ 1.8 (6H, s, mesityl C*H*$_3$), 2.2 (3H, s, mesityl C*H*$_3$), 2.4 (3H, s, C*H*$_3$), 5.3 (2H, m, C*H*$_2$), 6.8 (2H, s, mesityl *H*), 6.9 (1H, d, 5-imidazol-2-ylidene *H*), 6.9 (1H, d, 5-

picolyl *H*), 7.0 (1H, d, 3-picolyl *H*), 7.3 (1H, d, 4-imidazol-2-ylidene *H*), 7.5 (1H, t, 4-picolyl *H*).

δ_C($CDCl_3$) 18, 21, 25 (*C*H_3), 57 (*C*H_2), 119, 121, 122, 123, 130, 130, 135, 136, 138,140, 155 (mesityl *C*, picolyl *C*, 4,5-imidazol-2-ylidene *C*), 177 (2-imidazol-2-ylidene *C*).

(Found: C, 50.77; H, 4.76; N, 9.16. $C_{19}H_{21}AgN_3Br_{(2/5)}Cl_{(3/5)}$ calculated: C, 50.43; H, 4.68; N, 9.29%).

(3.7) {1-[3-(2,6-di*iso*propylphenyl) imidazol-2-ylidene]-1-methoxy-methane} silver chloride

This was prepared following the general method 1-[3-(2,6-di*iso*propylphenyl) imidazolium]-1-methylether-methane bromide (1.0g, 2.83mmol) and silver oxide (0.97g, 4.25mmol) in 1,2-dichloroethane (60ml) by heating at 90°C for 4 hours. The product was obtained in quantitative yields as a white solid.

MS (ES): *m/z* 653.4, $[Ag(ligand)_2]^+$.

δ_H($CDCl_3$) 1.1, 1.2 [2 × 6H, d, CH(C*H*$_3$)$_2$], 2.3 [2H, septet, C*H*(CH$_3$)$_2$], 3.4 (3H, s, C*H*$_3$), 5.5 (2H, s, C*H*$_2$), 7.0 (1H, d, 5-imidazol-2-ylidene *H*), 7.2 (2H, d, ^{i}Pr$_2$C$_6$*H*$_2$H), 7.3 (1H, d, 4-imidazol-2-ylidene *H*), 7.4 (1H, t, ^{i}Pr$_2$C$_6$H$_2$*H*).

δ_C($CDCl_3$) 24, 25 (*C* H$_3$), 28 (*C* H(CH$_3$)$_2$), 57 (*C*H$_2$), 83 (*C*H$_3$), 120, 125, 125, 131, 135, 146 (^{i}Pr$_2$*C*$_6$H$_3$, 4,5-imidazol-2-ylidene *C*), 176 (2-imidazol-2-ylidene *C*).

(Found: C, 48.65; H, 5.55; N, 6.72. $C_{17}H_{24}AgClN_2O$ calculated: C, 49.12; H, 5.82; N, 6.74%).

(3.8) {1,1-bis-[3-(2,6-di*iso*propylphenyl) imidazol-2-ylidene]-methane} disilver dichloride

This was prepared following the general method 1,1-bis-[3-(2,6-di*iso*propylphenyl) imidazolium]-methane dibromide (1.50g, 2.38mmol) and silver oxide (0.79g, 3.57mmol) in 1,2-dichloroethane (60ml) by heating at 90°C for 12 hours. The product was obtained in quantitative yields as a white solid.

δ_H($CDCl_3$) 1.0, 1.1 [2 × 12H, d, CH(C*H*$_3$)$_2$], 2.3 [4H, septet, C*H*(CH$_3$)$_2$], 6.5 (2H, v. br., C*H*$_2$), 6.9 (2H, d, 5-imidazol-2-ylidene *H*), 7.3 (4H, d, ^{i}Pr$_2$C$_6$*H*$_2$H), 7.5 (2H, t, ^{i}Pr$_2$C$_6$H$_2$*H*), , 8.2 (2H, v. br., 4-imidazol-2-ylidene *H*).

(Found: C, 49.65; H, 5.37; N, 7.27. $C_{31}H_{40}Ag_2Cl_2N_4$ calculated: C, 49.29; H, 5.34; N, 7.42%).

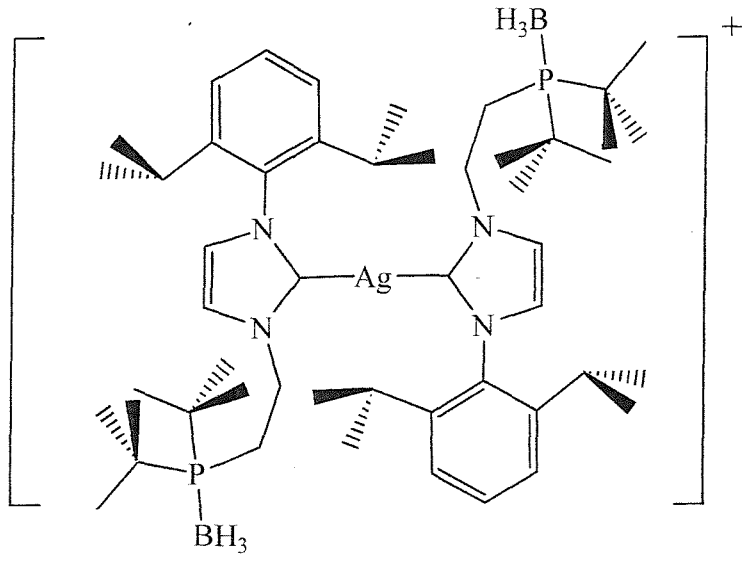

Figure 3.19. Possible coordination isomer for the cation of compound **(3.9)**.

(3.9) {1-[3-(2,6-diisopropylphenyl)-imidazol-2-ylidene]-2-[di(*tert*butyl)phosphine borane]-ethane} silver sulphate

This was prepared following the general method 1-[3-(2,6-diisopropylphenyl)-imidazolium]-2-[di(*tert*butyl)phosphine borane]-ethane lithium sulphate (0.10g, 0.19mmol) and silver oxide (0.04g, 0.10mmol) in dichloromethane (30ml) by heating at 35°C for 72 hours. The product was obtained in quantitative yields as a white solid (*Figure 3.19*).

MS (ES): *m/z* 565 [(ligandAg) + MeCN]$^+$.

δ_H($CDCl_3$) 1.1 [18H, s, C(CH_3)$_3$], 1.1 (3H, br., BH_3), 1.1, 1.2 [2 × 6H, d, CH(CH_3)$_2$], 2.2 (2H, m, CH_2), 2.3 [2H, septet, CH(CH_3)$_2$], 4.2 (2H, m, CH_2), 6.9 (1H, d, 5-imidazol-2-ylidene *H*), 7.2 (2H, d, ^{i}Pr$_2$C$_6$$H_2$H), 7.4 (1H, t, ^{i}Pr$_2C_6H_2$*H*), 7.8 (1H, d, 4-imidazol-2-ylidene *H*).

δ_C($CDCl_3$) 25 (CH(C H$_3$)$_2$), 28 (C(C H$_3$)$_3$), 28 (C H(CH_3)$_2$), 32 (d, CH_2), 65 (CH_2), 122, 124, 130, 130, 140, 146 (^{i}Pr$_2$$C_6H_3$, 4,5-imidazol-2-ylidene *C*), 175 (2-imidazol-2-ylidene *C*).

δ_B($CDCl_3$) -39 (br. s)

δ_P($CDCl_3$) 40.8. (br. s)

(Found: C, 50.61; H, 8.01; N, 4.68. ($C_{25}H_{45}AgBN_2P$)$_3$(SO_4)$_2$Li calculated: C, 50.92; H, 7.69; N, 4.75%).

3.8 Synthesis of copper (I) complexes

3.8.1. General method

The manipulations were carried out under nitrogen. A suspension of the substituted imidazolium salt, slight excess of copper oxide and 4Å molecular sieves in dichloromethane or 1,2-dichloroethane was heated at 35°C or 90°C for 3-12 hours, respectively. After completion, the volatiles were removed under vacuum and the resulting solid was washed with diethyl ether and extracted into THF. Filtration of the solution and evaporation of the volatiles under vacuum produced moderately air sensitive solids.

(3.10) [3-(mesityl)-1-(α-picolyl) imidazol-2-ylidene] cuprous bromide (a) and (b)

This was prepared following the general method from [3-(mesityl)-1-(2-picolyl) imidazolium] bromide (2.0g, 5.5mmol) and Cu_2O (0.4g, 2.7mmol) in dichloromethane (30ml) by heating at 35°C for 12 hours. The product was obtained as a moderately air sensitive white solid. X-ray diffraction quality crystals were obtained by cooling slowly a saturated dichloromethane/ether solution to –30°C **(a)** (*Figure 3.20* and *Table 3.8*) or from saturated $CDCl_3$ solution **(b)** (*Figure 3.21* and *Table 3.9*).

Yield: 60%. Mp: 170-5°C (dec)

$\delta_H(CDCl_3)$ 2.1 (6H, br., CH_3), 2.3 (3H, br., CH_3), 5.0 (2H, br., CH_2), 6.2 (1H, br., 5-imidazolium *H*), 6.4 (1H, br., 4-imidazolium *H*), 6.9 (2H, br., mesityl *H*), 7.2 (1H, br., 3-picolyl *H*), 7.3 (1H, br., 5-picolyl *H*), 7.7 (1H, br., 4-picolyl *H*), 8.6 (1H, v. br., 6-picolyl *H*).

(Found: C, 47.12; H, 4.16; N, 8.77. $(C_{18}H_{19}CuBrN_3)_2CH_2Cl_2$ calculated: C, 47.96; H, 4.35; N, 9.07%).

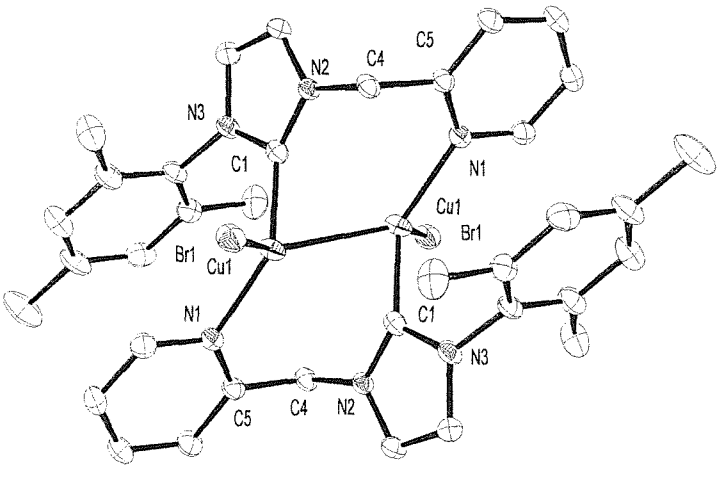

Figure 3.20. X-ray crystal structure of [3-(mesityl)-1-(α-picolyl) imidazol-2-ylidene] cuprous bromide, compound **(3.10) (a)**.

Br(1)-Cu(1)	2.5147(4)	N(3)-C(1)	1.368(3)
Cu(1)-C(1)	1.931(2)	N(3)-C(2)	1.385(3)
Cu(1)-N(1)#1	2.0299(18)	N(3)-C(10)	1.446(3)
Cu(1)-Cu(1)#1	2.6449(6)	C(2)-C(3)	1.348(3)
N(2)-C(1)	1.359(3)	C(4)-C(5)	1.507(3)
N(2)-C(3)	1.380(3)	C(5)-N(1)	1.341(3)
N(2)-C(4)	1.466(3)	N(1)-Cu(1)#1	2.0299(18)
C(1)-Cu(1)-N(1)#1	133.88(8)	C(3)-C(2)-N(3)	106.4(2)
C(1)-Cu(1)-Br(1)	106.14(7)	C(2)-C(3)-N(2)	106.7(2)
N(1)#1-Cu(1)-Br(1)	98.08(5)	N(2)-C(4)-C(5)	112.58(18)
C(1)-Cu(1)-Cu(1)#1	70.26(7)	N(2)-C(1)-N(3)	103.15(18)
N(1)#1-Cu(1)-Cu(1)#1	121.50(6)	N(2)-C(1)-Cu(1)	130.92(16)
Br(1)-Cu(1)-Cu(1)#1	128.777(17)	N(3)-C(1)-Cu(1)	122.34(15)
C(1)-N(2)-C(3)	112.05(18)	N(1)-C(5)-C(6)	122.4(2)
C(1)-N(2)-C(4)	123.57(18)	N(1)-C(5)-C(4)	116.58(19)
C(1)-N(3)-C(2)	111.66(19)	C(5)-N(1)-Cu(1)#1	125.03(15)
C(1)-N(3)-C(10)	122.19(18)		

Table 3.8. Selected bond lengths (Å) and angles (°) for compound **(3.10) (a)**. Symmetry transformations used to generate equivalent atoms: #1 -x+1,-y+2,-z+1

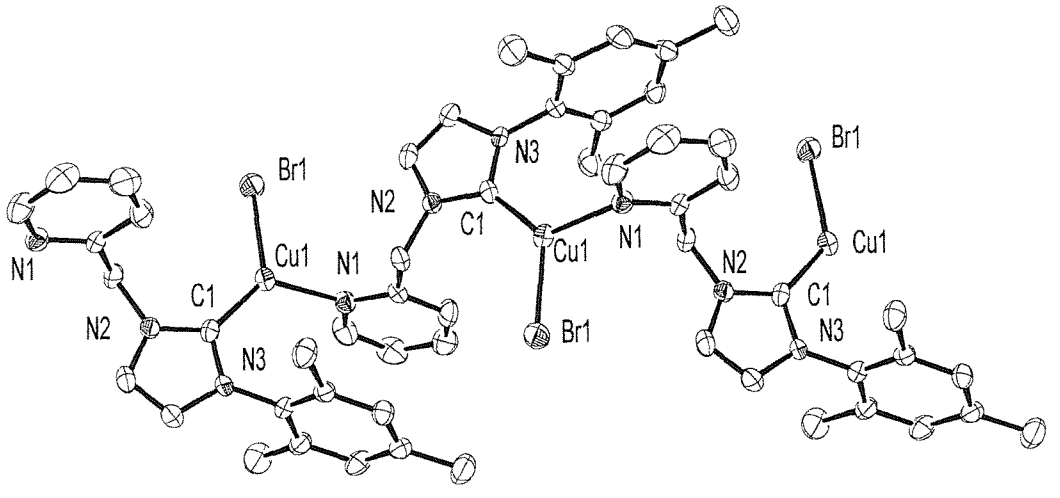

Figure 3.21. X-ray crystal structure of [3-(mesityl)-1-(α-picolyl) imidazol-2-ylidene] cuprous bromide, compound **(3.10) (b)**.

Br(1)-Cu(1)	2.3758(7)	C(1)-N(2)	1.356(5)
Cu(1)-C(1)	1.914(4)	N(2)-C(8)	1.382(6)
Cu(1)-N(1)#1	2.044(3)	N(2)-C(7)	1.470(5)
N(3)-C(1)	1.351(5)	C(6)-N(1)	1.346(5)
N(3)-C(9)	1.396(5)	C(6)-C(5)	1.379(6)
N(3)-C(10)	1.438(5)	C(6)-C(7)	1.498(6)
C(9)-C(8)	1.328(7)	N(1)-Cu(1)#2	2.044(3)

C(1)-Cu(1)-N(1)#1	125.24(16)	N(3)-C(1)-Cu(1)	124.2(3)
C(1)-Cu(1)-Br(1)	130.73(13)	N(2)-C(1)-Cu(1)	132.0(3)
N(1)#1-Cu(1)-Br(1)	103.43(10)	C(1)-N(2)-C(8)	111.8(4)
C(1)-N(3)-C(9)	111.2(4)	C(1)-N(2)-C(7)	124.2(4)
C(1)-N(3)-C(10)	123.1(3)	N(1)-C(6)-C(7)	117.3(4)
C(8)-C(9)-N(3)	106.7(4)	N(2)-C(7)-C(6)	111.3(3)
N(3)-C(1)-N(2)	103.6(4)	C(6)-N(1)-Cu(1)#2	127.4(3)

Table 3.9. Selected bond lengths (Å) and angles (°) for compound **(3.10) (b)**. Symmetry transformations used to generate equivalent atoms: #1 -x,y+1/2, -z+1/2; #2 -x,y-1/2,-z+1/2

(3.11) [3-(2,6-di*iso*propylphenyl)-1-(α-picolyl) imidazol-2-ylidene] cuprous bromide

This was prepared following the general method from [3-(2,6-di*iso*propylphenyl)-1-(2-picolyl) imidazolium] bromide (2.0g, 4.8mmol) and Cu_2O (0.5g, 4.0mmol) in 1,2-dichloroethane (30ml) by heating at 90°C for 3 hours. The product was obtained as a moderately air sensitive white solid.

Yield: 60%. Mp: 180-5°C (dec)

$\delta_H(CD_2Cl_2$, +60 to -50°C) 1.1, 1.2 [2 × 6H, br.d, CH (CH_3)$_2$], 2.4 [2H, br., C*H* (CH_3)$_2$], 5.5 (2H, br., CH_2), 7.0, 7.3 (4H, v. br, 4,5-imidazolium *H*, 3,5- picolyl *H*), 7.2 (2H, d, $^iPr_2C_6H_2H$), 7.4 (1H, br., $^iPr_2C_6H_2H$), 7.7 (1H, br., 4-picolyl *H*), 8.5 (1H, v. br, 6-picolyl *H*).

(Found: C, 54.15; H, 5.66; N, 8.66. $C_{21}H_{25}CuBrN_3$ calculated: C, 54.49; H, 5.44; N, 9.08%).

(3.12) [3-(2,6-di*iso*propylphenyl)-1-(2-pyridyl) imidazol-2-ylidene] cuprous bromide

This was prepared following the general method from [3-(2,6-di*iso*propyl-phenyl)-1-(2-pyridyl) imidazolium] bromide (1.0g, 2.6mmol) and Cu_2O (0.4g, 2.6mmol) in dichloromethane (20ml) by heating at 35°C for 12 hours. The product was obtained as a moderately air sensitive white solid. X-ray diffraction quality crystals were obtained by layering a saturated $CDCl_3$ solution with diethyl ether (*Figure 3.22* and *Table 3.10*).

Yield: 65%. Mp: 170°C.

$\delta_H(CD_2Cl_2$, +60 to -40°C) 1.2 [6H, br., CH (CH_3)$_2$], 1.3 [6H, v. br., CH (CH_3)$_2$], 2.6 [2H, v. br., C*H* (CH_3)$_2$], 7.2 (5H, br., $^iPr_2C_6H_2H$, 5-imidazolium *H*, 4,5-pyridyl *H*), 7.5 (1H, br., $^iPr_2C_6H_2H$), 8.0 (1H, br., 4-imidazolium *H*), 8.5 (2H, v. br., 3,6-pyridyl *H*).

(Found: C, 53.73; H, 5.48; N, 8.99. $C_{20}H_{23}BrN_3$ calculated: C, 53.52; H, 5.16; N, 9.36%).

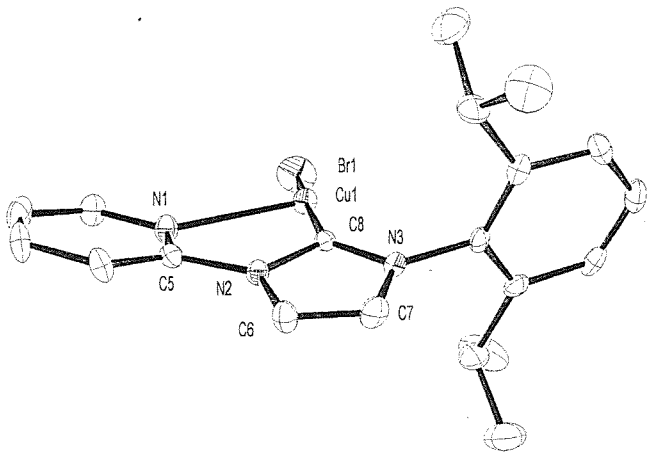

Figure 3.22. X-ray crystal structure of [3-(2,6-di*iso*propylphenyl)-1-(2-pyridyl) imidazol-2-ylidene] cuprous bromide, compound **(3.12)**.

C(5)-N(1)	1.330(8)	C(8)-N(2)	1.375(7)
C(5)-N(2)	1.429(8)	C(8)-Cu(1)	1.880(6)
C(6)-C(7)	1.337(9)	C(9)-N(3)	1.449(7)
C(6)-N(2)	1.379(8)	N(1)-Cu(1)	2.454(5)
C(7)-N(3)	1.398(8)	Cu(1)-Br(1)	2.2076(10)
C(8)-N(3)	1.356(7)		
N(1)-C(5)-N(2)	114.4(5)	C(1)-N(1)-Cu(1)	135.3(4)
C(7)-C(6)-N(2)	107.1(5)	C(8)-N(2)-C(6)	111.7(5)
C(6)-C(7)-N(3)	106.5(5)	C(8)-N(2)-C(5)	121.4(5)
N(3)-C(8)-N(2)	103.1(5)	C(8)-N(3)-C(7)	111.7(5)
N(3)-C(8)-Cu(1)	136.2(4)	C(8)-N(3)-C(9)	123.5(5)
N(2)-C(8)-Cu(1)	119.6(4)	C(8)-Cu(1)-Br(1)	170.33(17)
C(5)-N(1)-C(1)	116.8(5)	C(8)-Cu(1)-N(1)	76.5(2)
C(5)-N(1)-Cu(1)	106.1(3)	Br(1)-Cu(1)-N(1)	108.96(12)

Table 3.10. Selected bond lengths (Å) and angles (°) for compound **(3.12)**.

Compound	(3.12)	(3.10) (b)	(3.10) (a)
Chemical formula	$C_{20}H_{23}BrCuN_3$	$C_{20}H_{19}D_2BrCl_6CuN_3$	$C_{38}H_{42}Br_2Cl_4Cu_2N_6$
Formula weight	448.86	661.56	1011.48
Crystal system	Monoclinic	Monoclinic	Triclinic
Space group	$P\,2_1/c$	$P\,2_1/c$	P-1
a/Å	11.4666(3)	13.1826(2)	8.4260(1)
b/Å	12.4772(3)	12.8268(2)	11.0509(1)
c/Å	14.1522(3)	16.4122(3)	11.4536(1)
α/°	90.0	90.0	85.015(1)
β/°	99.7489(13)	105.964(1)	84.737(1)
γ/°	90	90.0	75.611(1)
V/Å^3	1995.53(8)	2668.12(8)	1.02644(2)
Z	4	4	2
T/K	150(2)	150	150
μ/mm^{-1}	3.104	2.931	3.279
F(000)	912	1312	508
No. Data collected	10430	26717	17262
No. Unique data	2853	7647	4186
R_{int}	0.0457	0.0926	0.0584
Final R(|F|) for $F_O > 2\sigma(F_o)$	0.0606	0.0560	0.0295
Final R(F^2) for all data	0.1898	0.1528	0.0756

Table 3.11. Crystallographic parameters for compounds **(3.10) (a)**, **(3.10) (b)** and **(3.12)**.

3.9 Anion exchange of copper complexes general method

The manipulations were carried out under nitrogen. A solution of [3-(2,6-di*iso*-propylphenyl)-1-(2-pyridyl) imidazol-2-ylidene] cuprous bromide was stirred with a solution of the corresponding thallium salt in acetonitrile or dichloromethane for 12 hours. After completion, the volatiles were removed under vacuum and the resulting solid was washed with diethyl ether and extracted into dichloromethane. Filtration of the solution and evaporation of the volatiles under vacuum produced moisture sensitive solids.

(3.13) [3-(2,6-di*iso*propylphenyl)-1-(2-pyridyl) imidazol-2-ylidene] cuprous hexafluorophosphate acetonitrile

This was prepared following the general method from [3-(2,6-di*iso*propylphenyl)-1-(2-pyridyl) imidazol-2-ylidene] cuprous bromide (0.08g, 0.17mmol) and thallium hexafluorophosphate (0.06g, 0.17mmol) in acetonitrile (30ml) by stirring for 12 hours. The product was obtained as a moisture sensitive white solid. X-ray diffraction quality crystals were obtained by layering a saturated dichloromethane solution with petrol (*Table 3.12*).

$\delta_H(CDCl_3)$ 0.8 [6H, br. d, $CH(CH_3)_2$], 1.1 [6H, d, $CH(CH_3)_2$], 2.1 (3H, s, CH_3CN), 2.4 [2H, septet, $CH(CH_3)_2$], 7.1 (1H, d, 5-imidazolium *H*), 7.2 (2H, d, $^iPr_2C_6H_2H$), 7.3 (1H, m, 5-pyridyl *H*), 7.4 (1H, t, $^iPr_2C_6H_2H$), 7.8 (1H, d, 3-pyridyl *H*), 7.9 (1H, d, 6-pyridyl *H*), 8.0 (1H, d, 4-imidazolium *H*), 8.1 (1H, t, 4-pyridyl *H*).

(Found: C, 47.21; H, 5.13; N, 9.80. $C_{22}H_{27}CuF_6N_4P$ calculated: C, 47.53; H, 4.89; N, 10.08%).

C(16)-N(3)	1.337(4)	C(13)-N(1)	1.380(4)
C(16)-C(17)	1.385(4)	C(15)-N(1)	1.361(4)
C(16)-N(2)	1.429(4)	C(15)-Cu(1)	1.933(3)
C(21)-N(4)	1.124(4)	Cu(1)-N(3)#1	2.036(2)
C(21)-C(22)	1.459(5)	Cu(1)-Cu(1)#1	2.4872(8)
N(2)-C(15)	1.374(4)	F(1)-P(1)	1.612(2)
N(2)-C(14)	1.395(4)	F(2)-P(1)	1.567(3)
N(3)-Cu(1)#1	2.036(2)	F(3)-P(1)	1.563(3)
N(4)-Cu(1)	1.968(3)	F(4)-P(1)	1.591(2)
C(1)-N(1)	1.446(4)	F(5)-P(1)	1.546(3)
C(13)-C(14)	1.326(5)	F(6)-P(1)	1.553(3)

N(3)-C(16)-N(2)	116.3(2)	N(1)-C(15)-Cu(1)	123.0(2)
N(4)-C(21)-C(22)	178.0(4)	N(2)-C(15)-Cu(1)	132.9(2)
C(15)-N(2)-C(14)	111.9(3)	C(15)-N(1)-C(13)	112.4(3)
C(15)-N(2)-C(16)	126.2(2)	C(15)-N(1)-C(1)	125.7(3)
C(16)-N(3)-C(20)	116.6(3)	C(15)-Cu(1)-N(4)	117.28(11)
C(16)-N(3)-Cu(1)#1	123.7(2)	C(15)-Cu(1)-N(3)#1	127.68(11)
C(21)-N(4)-Cu(1)	168.0(3)	N(4)-Cu(1)-N(3)#1	109.14(10)
C(14)-C(13)-N(1)	107.4(3)	C(15)-Cu(1)-Cu(1)#1	76.39(9)
C(13)-C(14)-N(2)	106.2(3)	N(4)-Cu(1)-Cu(1)#1	122.32(8)
N(1)-C(15)-N(2)	102.1(2)	N(3)#1-Cu(1)-Cu(1)#1	98.71(7)

Table 3.12. Selected bond lengths (Å) and angles (°) for compound **(3.13)**. Symmetry transformations used to generate equivalent atoms: #1 -x+1,-y,-z+1

(3.14) [3-(2,6-di*iso*propylphenyl)-1-(2-pyridyl) imidazol-2-ylidene] cuprous triflate

This was prepared following the general method from [3-(2,6-di*iso*propylphenyl)-1-(2-pyridyl) imidazol-2-ylidene] cuprous bromide (0.08g, 0.17mmol) and thallium triflate (0.06g, 0.17mmol) in dichloromethane (30ml) by stirring for 12 hours. The product was obtained as a moisture sensitive white solid. X-ray diffraction quality crystals were obtained by layering a saturated dichloromethane solution with diethyl ether (*Figure 3.23* and *Table 3.13*).

$\delta_H(CDCl_3)$ 0.8 [6H, br. d, $CH(CH_3)_2$], 1.1 [6H, d, $CH(CH_3)_2$], 2.3 [2H, br., $CH(CH_3)_2$], 6.9 (1H, d, 5-imidazolium *H*), 7.1 (2H, d, $^iPr_2C_6H_2H$), 7.2 (1H, d, 6-pyridyl *H*), 7.3 (1H, m, 5-pyridyl *H*), 7.4 (1H, t, $^iPr_2C_6H_2H$), 7.9 (1H, d, 3-pyridyl *H*), 8.0 (2H, br., 4-pyridyl *H*, 4-imidazolium *H*).

(Found: C, 48.17; H, 4,73; N, 8.24. $C_{21}H_{24}CuF_3N_3O_3S$ calculated: C, 48.59; H, 4.66; N, 8.10%).

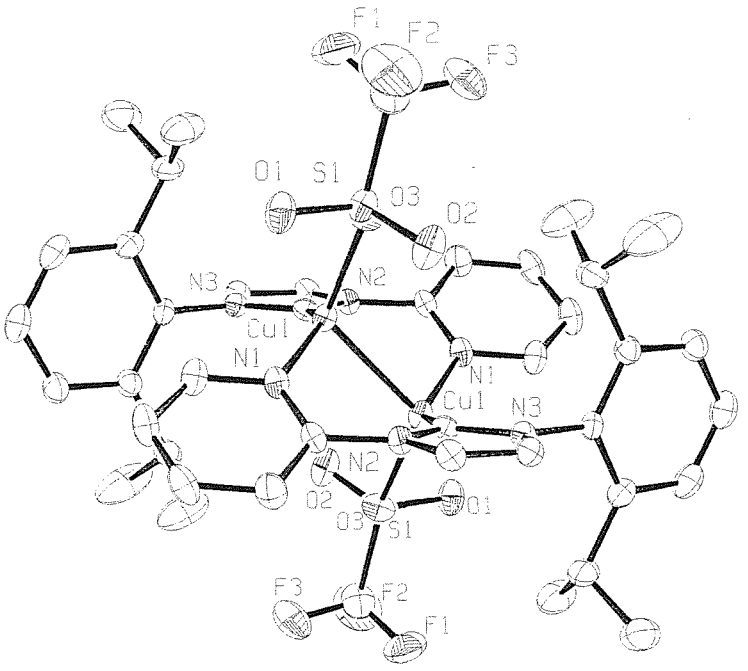

Figure 3.23. X-ray crystal structure of [3-(2,6-di*iso*propylphenyl)-1-(2-pyridyl) imidazol-2-ylidene] cuprous triflate, compound **(3.14)**.

C(5)-N(1)	1.335(4)	C(9)-N(3)	1.441(3)
C(5)-N(2)	1.427(3)	N(1)-Cu(1)	2.023(2)
C(6)-N(3)	1.355(3)	O(1)-S(1)	1.442(2)
C(6)-N(2)	1.370(3)	O(2)-S(1)	1.441(2)
C(6)-Cu(1)#1	1.916(2)	O(3)-S(1)	1.468(2)
C(7)-C(8)	1.342(4)	O(3)-Cu(1)	2.131(2)
C(7)-N(2)	1.395(3)	Cu(1)-C(6)#1	1.916(2)
C(8)-N(3)	1.382(3)	Cu(1)-Cu(1)#1	2.5211(9)
N(1)-C(5)-N(2)	117.4(2)	S(1)-O(3)-Cu(1)	123.65(12)
N(3)-C(6)-N(2)	103.0(2)	O(2)-S(1)-O(1)	115.78(13)
N(3)-C(6)-Cu(1)#1	122.1(2)	O(2)-S(1)-O(3)	114.28(12)
N(2)-C(6)-Cu(1)#1	134.6(2)	O(1)-S(1)-O(3)	114.75(13)
C(8)-C(7)-N(2)	105.9(2)	C(6)#1-Cu(1)-N(1)	135.31(10)
C(7)-C(8)-N(3)	107.2(2)	C(6)#1-Cu(1)-O(3)	120.14(9)
C(5)-N(1)-Cu(1)	128.0(2)	N(1)-Cu(1)-O(3)	99.14(8)
C(6)-N(2)-C(7)	111.8(2)	C(6)#1-Cu(1)-Cu(1)#1	83.30(8)
C(6)-N(2)-C(5)	127.4(2)	N(1)-Cu(1)-Cu(1)#1	97.26(7)
C(6)-N(3)-C(8)	112.1(2)	O(3)-Cu(1)-Cu(1)#1	117.85(7)
C(6)-N(3)-C(9)	126.1(2)		

Table 3.13. Selected bond lengths (Å) and angles (°) for compound **(3.14)**. Symmetry transformations used to generate equivalent atoms: #1 -x,-y+1,-z

Compound	**(3.14)**	**(3.13)**
Chemical formula	$C_{21}H_{23}CuF_3N_3O_3S$	$C_{22}H_{26}CuF_6N_4P$
Formula weight	518.02	493.31
Crystal system	Triclinic	Orthorombic
Space group	*P*-1	*P*bca
a/Å	10.251(2)	13.986(3)
b/Å	11.432(2)	16.370(3)
c/Å	12.347(3)	21.409(4)
α/°	69.32(3)	90.0
β/°	72.03(3)	90.0
γ/°	78.67(3)	90.0
V/Å^3	1281.4(5)	4901.7(17)
Z	2	9
T/K	150(2)	150(2)
μ/mm^{-1}	0.980	1.019
F(000)	532	2272
No. Data collected	26643	27000
No. Unique data	5795	5000
R_{int}	0.1080	0.0829
Final R(|F|) for $F_O > 2\sigma$ (F_o)	0.0513	0.0448
Final R(F^2) for all data	0.0639	0.0813

Table 3.14. Crystallographic parameters for compounds **(3.13)** and **(3.14)**.

REFERENCES

1 W.A. Herrmann, C. Køcher, *Angew. Chem., Int. Ed. Engl.*, **1997**, *36*, 2162.

2 D. Bourissou, O. Guerret, F.P. Gabbai, G. Bertrand, *Chem Rev.*, **2000**, *100*, 39.

3 H.M.J. Wang, I.J.B. Lin, *Organometallics,* **1998**, *17*, 972.

4 A.J. Arduengo III, H.V.R. Dias, J.C. Calabrese, F. Davidson, *Organometallics,* **1993**, *12*, 3405.

5 A.A.D. Tulloch, A.A. Danopoulos, S. Kleinhenz, M.E. Light, M.B. Hursthouse, G. Eastham, *Organometallics*, **2001**, *20*, 2027.

6 A.A. Danopoulos, S. Winston, personal communication.

7 H.G. Raubenheimer, S. Cronje, P.H. van Rooyen, P.J. Oliver, *Angew. Chem., Int. Ed. Engl.*, **1994**, *33*, 672.

Chapter 4

N-Heterocyclic Carbene Complexes of Palladium (II)

Chapter 4

N-Heterocyclic Carbene Complexes of Palladium (II)

4.1 Introduction

A new wave of interest in *N*-heterocyclic carbenes has emerged in the last ten years, from the understanding that this family of ligands have donor characteristics similar to those of phosphines.[1] The huge interest in transition metal carbene complexes has been ignited by the realisation that they can act as extremely good pre-catalyst for important catalytic reactions such as: Pd-catalysed Heck and Suzuki couplings.[2] Due to the variety of electronic and steric tuning which can be performed on these ligands, a large diversity of palladium complexes has been synthesised. Publications in this area have included reports of mixed donor functionalised *N*-heterocyclic carbene complexes (by ourselves,[3] and others[4,5,6]) as well as complexes containing multi-dentate carbenes[7] and polymer supported complexes.[8]

In this chapter, the syntheses of a number of *N*-heterocyclic carbene complexes of palladium are reported (*Figure 4.1*). They are substituted with large bulky alkyl and aryl groups and functionalised with pyridyl, picolyl, lutidyl and methoxy groups. In addition, reactions are described in which phosphine functionalised palladium complexes can be identified as well as reactions that demonstrate the limitations of the large-scale syntheses of some these palladium complexes. Described in this chapter are five X-ray crystal structures, which demonstrate the variety of coordination and geometry of the complexes of these ligands.

RESULTS AND DISCUSSION

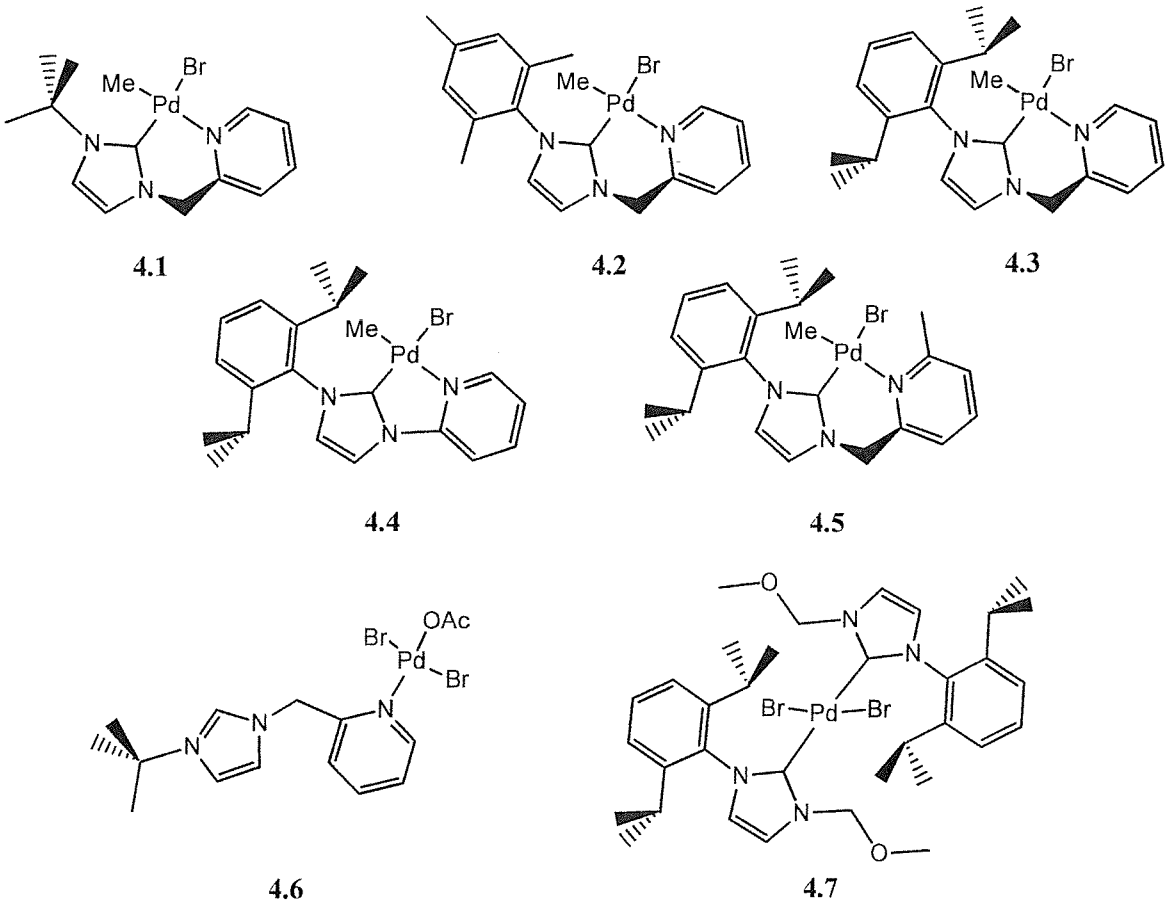

Figure 4.1. Palladium complexes (4.1)-(4.7).

4.2 Synthesis of palladium complexes

The palladium carbene complexes described in this chapter were prepared by two different methods. The first method (*Scheme 4.1*) involved trapping the free carbene (formed in *situ* by the careful deprotonation of the imidazolium salt), with [cyclooctadiene (COD) palladium methyl bromide].

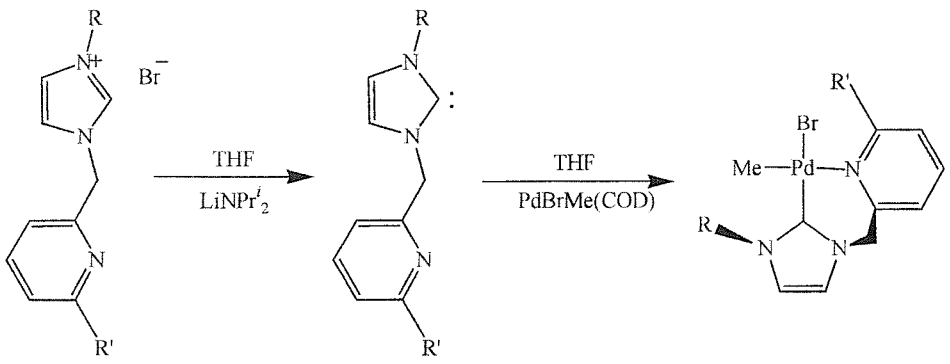

Scheme 4.1. Palladium carbene complex synthesised by trapping a carbene formed in *situ*.

The second of these methods (*Scheme 4.2*) involved the interaction of a silver carbene complex with [cyclooctadiene palladium methyl bromide/chloride] or [cyclooctadiene palladium dichloride] in dichloromethane.[6] The latter appeared to be much more adaptable, as it allowed easier scale-up of the reactions and involves simpler synthetic methods. The palladium complexes were each isolated as high melting point, air and moisture stable yellow solids.

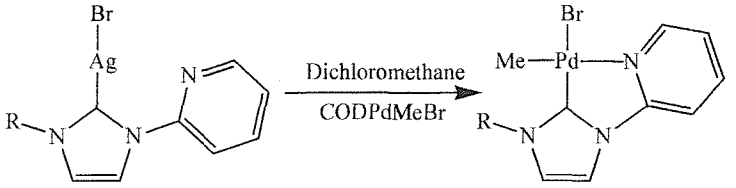

Scheme 4.2. Palladium carbene complex synthesised by ligand transfer from a silver carbene complex.

4.3 Characterisation of complexes (4.1)-(4.5)

4.3.1. Electrospray mass spectroscopy

Electrospray mass spectrometry in acetonitrile solution was useful in identifying the presence of the palladium complexes, by a peak corresponding to [(ligand)PdMe + MeCN]$^+$. A second peak in the electrospray mass spectrum was sometimes observed, corresponding to [(ligand)$_2$PdMe]$^+$, and is believed to originate from a by-product of the reaction (*Figure 4.2*).

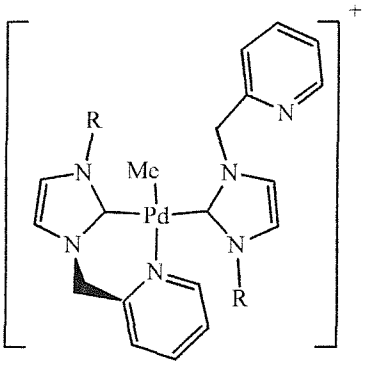

Figure 4.2. A plausible structure for the by-products.

The by-products were more abundant in the *reactions* ***4.8.3*** and ***4.8.4*** (see experimental), and the purity of the palladium complexes synthesised *via* general method

(ii) was dependant on the scale of the reactions. The factors affecting the purity of the products included the concentrations of the reactants and their rate of addition. However, impurities were largely reduced by using a very slight excess of the palladium starting material. The stoichiometry of the palladium carbene complexes was determined by chemical analysis. Depending on the final isolation step, a solvent of crystallisation was often observed in the analysis.

4.3.2. X-ray diffraction studies on complex (4.2)

X-ray diffraction quality crystals of [3-(mesityl)-1-(α-picolyl) imidazol-2-ylidene] palladium methyl bromide **(4.2)** were obtained by layering a dichloromethane solution with diethyl ether. The structure of compound **(4.2)** comprises a palladium atom coordinated by a methyl group, a bromide atom, and both the carbene and the picolyl ends of the ligand. The geometry around the palladium centre is square planar with a bite-angle between the carbene and the picolyl donors of 85.2° (*Table 4.2*). The ligand is orientated on the palladium centre so that the carbene end is disposed *trans* to the bromine atom (*Figure 4.3*).

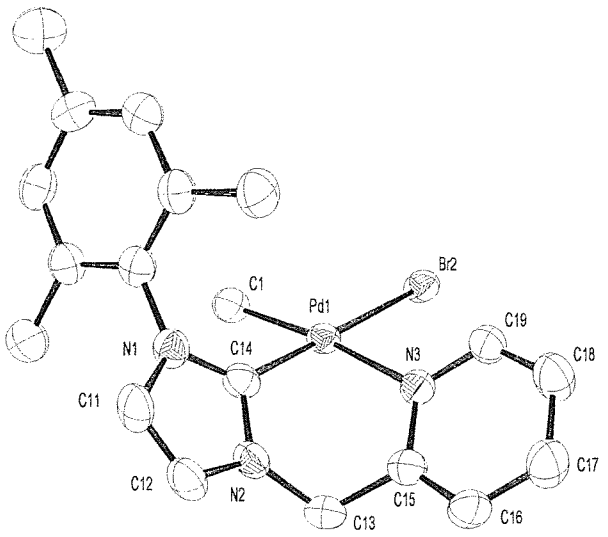

Figure 4.3. X-ray crystal structure of [3-(mesityl)-1-(α-picolyl) imidazol-2-ylidene] palladium methyl bromide, compound **(4.2)**.

The chelating ligand adopts a boat type puckered ring conformation, in order to release any conformational strain (*Figure 4.4*). The torsion angles around the chelate ring are as expected and the mesityl ring is orientated at right angles to the ring of the imidazol-2-ylidene. The palladium-carbene bond length (1.96Å) is shorter than that of the

palladium-methyl bond distance (2.20Å) (*Table 4.2*). Both bond lengths are in the range of normal palladium-carbon single bonds, and are similar to the other complexes described in this chapter (*Table 4.1*). The palladium carbon bond distance is slightly shorter than that of the theoretically predicted value for a monodentate carbene (2.08Å),[9] where the carbene-metal bond is considered to have purely σ-character and negligible metal-carbene π-back bonding. However, all the theoretically calculated bond lengths obtained by J.C. Green *et al.*[9] are slightly longer than the values observed in these complexes. The palladium-nitrogen (2.19Å) and the palladium bromine bond lengths (2.494Å) are normal for palladium (II) complexes.[4]

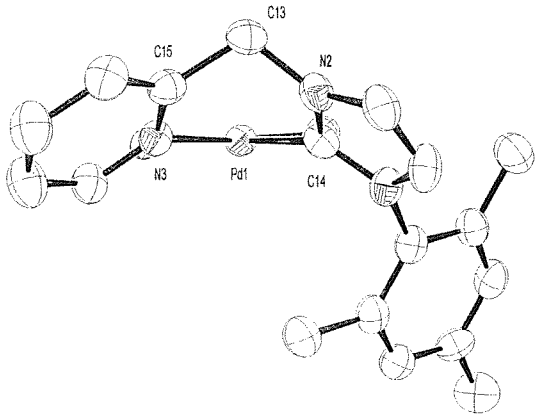

Figure 4.4. X-ray crystal structure of [3-(mesityl)-1-(α-picolyl) imidazol-2-ylidene] palladium methyl bromide, compound **(4.2)**. View along the palladium square plane.

4.3.3. X-ray diffraction studies on complex (4.3)

X-ray diffraction quality crystals of [3-(2,6-di*iso*propylphenyl)-1-(α-picolyl) imidazol-2-ylidene] palladium methyl bromide **(4.3)** were obtained by layering a saturated dichloromethane solution with petrol.

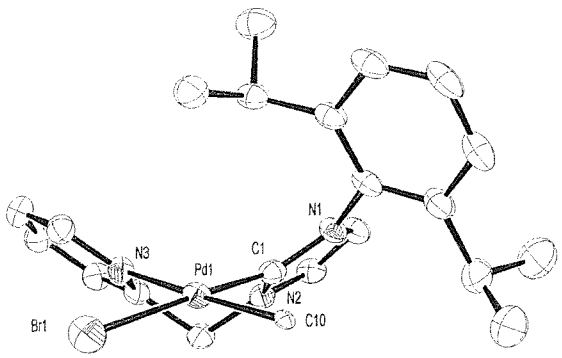

Figure 4.5. X-ray crystal structure of [3-(2,6-di*iso*propylphenyl)-1-(α-picolyl) imidazol-2-ylidene] palladium methyl bromide, compound **(4.3)**.

The structure of compound **(4.3)** (*Figure 4.5*) is similar to that of **(4.2)**, with the same bite-angle for the ligand and a similar conformation of the chelate ring (*Table 4.1*). The bond lengths and angles around the palladium are also almost identical to those in **(4.2)** with a palladium-carbene bond length of 1.97Å.

4.3.4. X-ray diffraction studies on complex (4.4)

X-ray diffraction quality crystals of [3-(2,6-di*iso*propylphenyl)-1-(2-pyridyl) imidazol-2-ylidene] palladium methyl bromide **(4.4)** were obtained by layering a saturated dichloromethane solution with petrol. The structure of compound **(4.4)** (like **(4.2)** and **(4.3)**) comprises a palladium atom coordinated by a methyl group, a bromide atom, and both the carbene and the pyridyl ends of the ligand (*Figure 4.6*). The geometry around the palladium centre is square planar with a bite-angle of 79.1° between the carbene and the pyridyl donors.

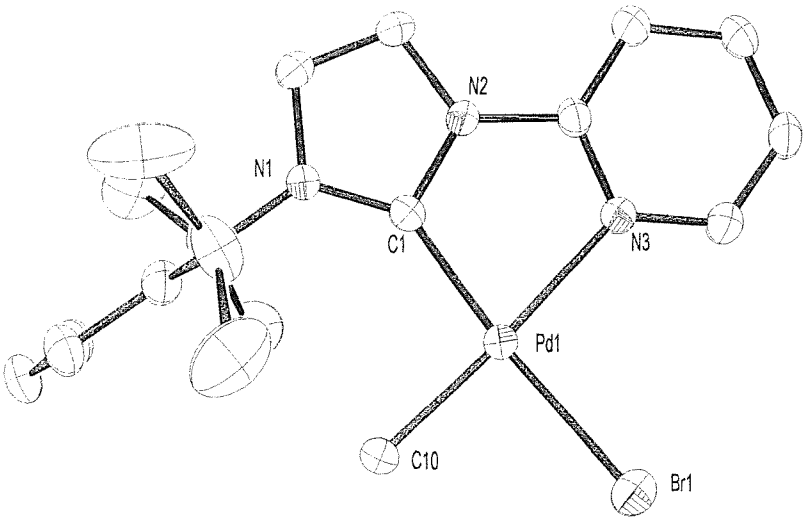

Figure 4.6. X-ray crystal structure of [3-(2,6-di*iso*propylphenyl)-1-(2-pyridyl) imidazol-2-ylidene] palladium methyl bromide, compound **(4.4)**.

The difference of the bite-angle to that of compounds **(4.2)**, **(4.3)** and **(4.5)** can be put down to the increased constraints of the ligand (*Table 4.1*). The ligand is orientated on the palladium centre so that the carbene end is disposed *trans* to the bromine atom. The chelating ligand is almost planar and is parallel with the square plane of the palladium. The aryl group is orientated at right angles to the imidazol-2-ylidene plane. The bond lengths around the palladium are almost identical to those in **(4.3)** with a palladium-carbene bond length of 1.97Å and the palladium-nitrogen bond length is 2.16Å (*Table 4.4*).

4.3.5. X-ray diffraction studies on complex (4.5)

X-ray diffraction quality crystals of [3-(2,6-di*iso*propylphenyl)-1-(α-lutidyl) imidazol-2-ylidene] palladium methyl bromide **(4.5)** were obtained by layering a saturated dichloromethane solution with petrol. The structure of compound **(4.5)** is similar to that of **(4.2)** and **(4.3)**, with a bite-angle for the ligand of 85.6Å and a similar conformation of the chelate ring (*Figure 4.7*). The bond lengths and angles around the palladium are slightly different to those in **(4.2)** and **(4.3)** (*Table 4.1*). This difference is probably due to the increased steric hindrance created by the methyl of the lutidyl group. This increased hindrance pushes the nitrogen further away from the palladium, giving a bond length of 2.22Å; thus, the methyl group (*trans* to the nitrogen) is pulled in closer to the palladium, giving a bond length of 2.04Å (*Table 4.5*). The palladium-carbene bond length is 1.98Å, which is similar to the bond lengths of compounds **(4.4)**, **(4.3)** and **(4.2)**.

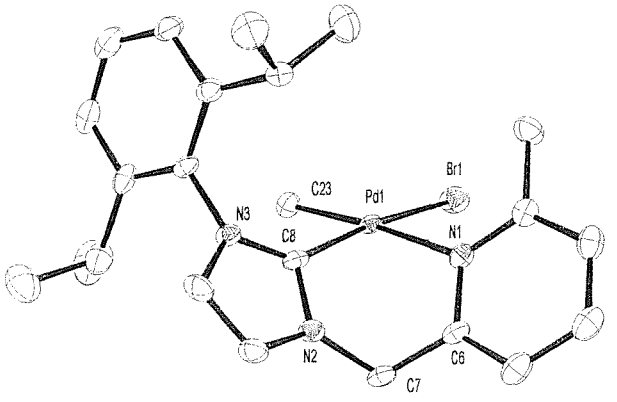

Figure 4.7. X-ray crystal structure of [3-(2,6-di*iso*propylphenyl)-1-(α-lutidyl) imidazol-2-ylidene] palladium methyl bromide, compound **(4.5)**.

	Pd–N (Å)	Pd–C (Å)	N–Pd–C (°)
Compound **(4.4)**	2.166(3)	1.970(4)	79.15(13)
Compound **(4.3)**	2.168(3)	1.969(4)	85.22(13)
Compound **(4.5)**	2.225(4)	1.976(5)	85.61(16)
Compound **(4.2)**	2.186(3)	1.962(4)	85.21(13)

Table 4.1. Palladium-carbon and palladium-nitrogen bond lengths, and nitrogen-palladium-carbon angle.

4.3.6. NMR spectroscopy

The peaks in the ^{1}H and $^{13}C\{H\}$ NMR spectra used to identify the formation of the palladium complexes are:

i) A weak peak downfield of 160 ppm in the $^{13}C\{^{1}H\}$ NMR spectra which can be assigned to the carbene carbon (observed in these complexes between 163 and 185 ppm);

ii) The disappearance upon complexation of a downfield peak at 10 and 12 ppm in the ^{1}H NMR spectra, which is assigned the proton in the 2-position of the imidazolium ring);

iii) A broad singlet or pair of doublets observed between 5.2 and 6.0 ppm in the ^{1}H NMR (*Figure 4.8*) (assigned to the protons on the methylene bridge of the picolyl complexes), and a peak observed between 55 and 59 ppm in the $^{13}C\{H\}$ NMR spectra (assigned to the carbon atom of the methylene bridge);

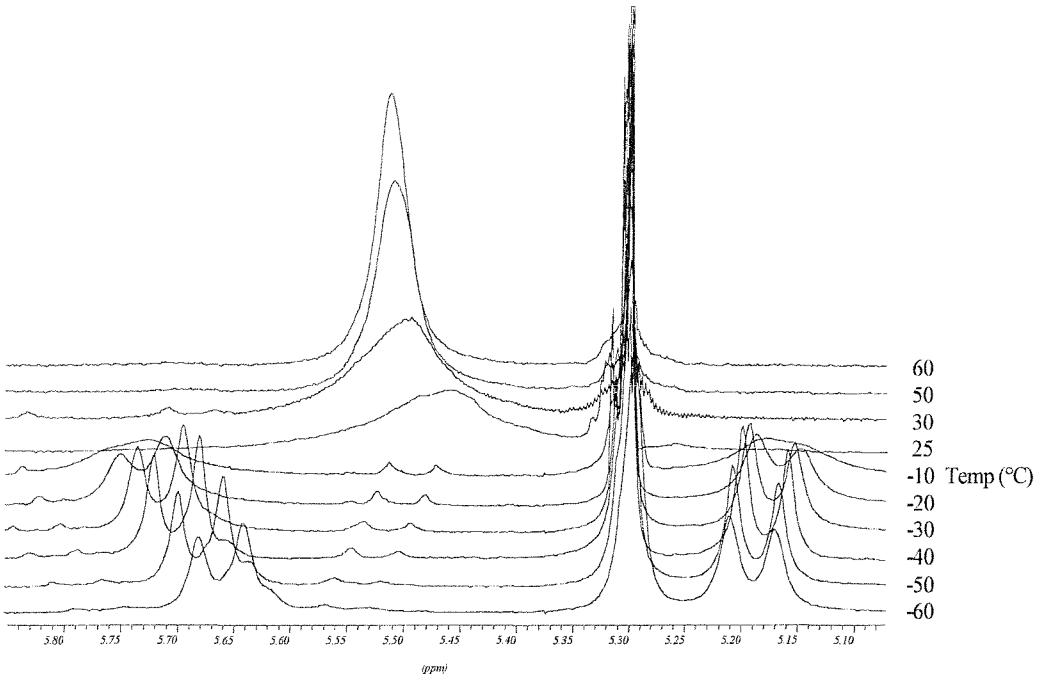

Figure 4.8. Variable temperature ^{1}H NMR spectrum of compound **(4.3)**; methylene bridge protons.

iv) A low field doublet or a doublet of doublets observed between 9.0 and 9.6 ppm and a triplet of doublets observed between 7.5 and 8.0 ppm in the ^{1}H NMR spectra for the picolyl or pyridyl carbene complexes (assigned to the protons in the 6- and 4-positions of the pyridine type rings);

v) A high field peak observed between -0.2 and 0.4 ppm in the ^{1}H NMR spectra (assigned to the protons of the methyl bound to palladium).

vi) The presence of two doublets, with very small coupling constants, between 6.7 and 7.1 ppm, and 7.2 and 8.0 ppm in the ^{1}H NMR spectra (assigned to the protons in the 5- and 4-position of the imidazol-2-ylidene ring, when the ligand is acting as a chelate);

vii) A multiplet (in most cases) or a doublet (in the case of compound **(4.5)**) between 7.2 and 7.4 ppm in the ^{1}H NMR spectra (assigned to the protons in the 5-position of the pyridine type rings);

viii) A doublet between 6.7 and 7.7 ppm in the ^{1}H NMR spectra (assigned to the protons in the 3-position of the pyridine type rings).

The other peaks in the ^{1}H NMR spectra are assigned to the protons of the R group on the imidazol-2-ylidene ring. When the R group is *tert*butyl a singlet is observed at around 2.0 ppm. When it is mesityl, singlets are observed around 2.1, 2.3 and 6.9 ppm; when it is 2,6-di*iso*propylphenyl, doublets are observed between 0.8 and 1.5 ppm, septets between 2.0 and 2.7 ppm, doublets between 7.1 and 7.2 ppm, and a triplet around 7.4 ppm (assigned to the protons of the aromatic ring and its substituents, see experimental). In the ^{1}H NMR spectrum of compound **(4.5)**, there is also a peak at 3.0 ppm, which is assigned to the methyl of the lutidyl group.

Variable temperature ^{1}H NMR spectroscopy was used to show that the diastereotopic protons of the methylene bridge exchanged, at elevated temperatures a sharp singlet was observed which on cooling changed to a pair of doublets (*Figure 4.8*). This observation clearly demonstrates that the chelate ring is relatively floppy and can flip at temperatures slightly above ambient. The rate of this dynamic process is affected by the bulky R groups, with the larger ones (2,6-di*iso*propylphenyl) slowing it down the most.

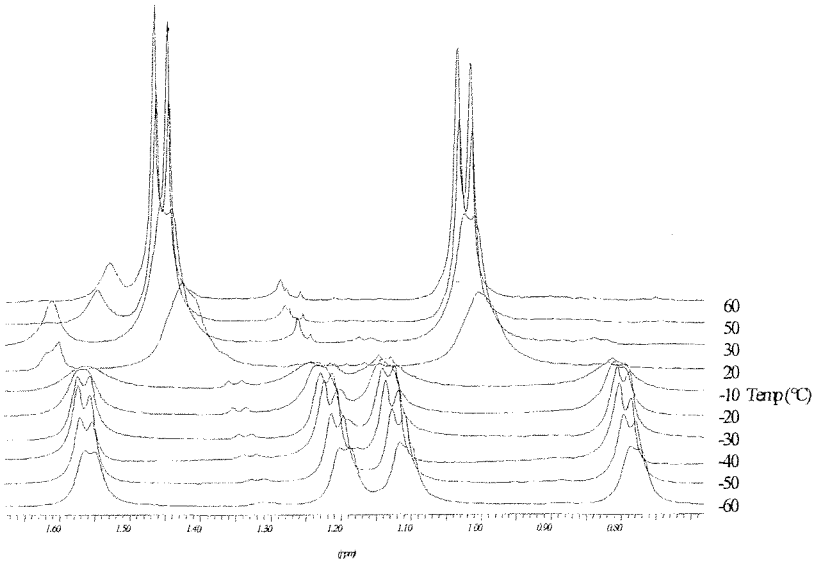

Figure 4.9. Variable temperature ^{1}H NMR spectrum of compound **(4.3)**; methyl protons (*iso*propyl).

When variable temperature ^{1}H NMR spectroscopy was performed on the compounds with a 2,6-di*iso*propylphenyl group, the *iso*propyls were observed to exchange at higher temperatures but they could also be "frozen out" under relatively mild conditions (*Figure 4.9* and *Figure 4.10*). The exchange process observed at higher temperatures is due to the chelate ring flipping, which makes the top and bottom of the complex equivalent. Surprisingly, at 60°C no other exchange processes are observed for the protons of the R group in the NMR time scale, including the rotation of the *iso*propyls.

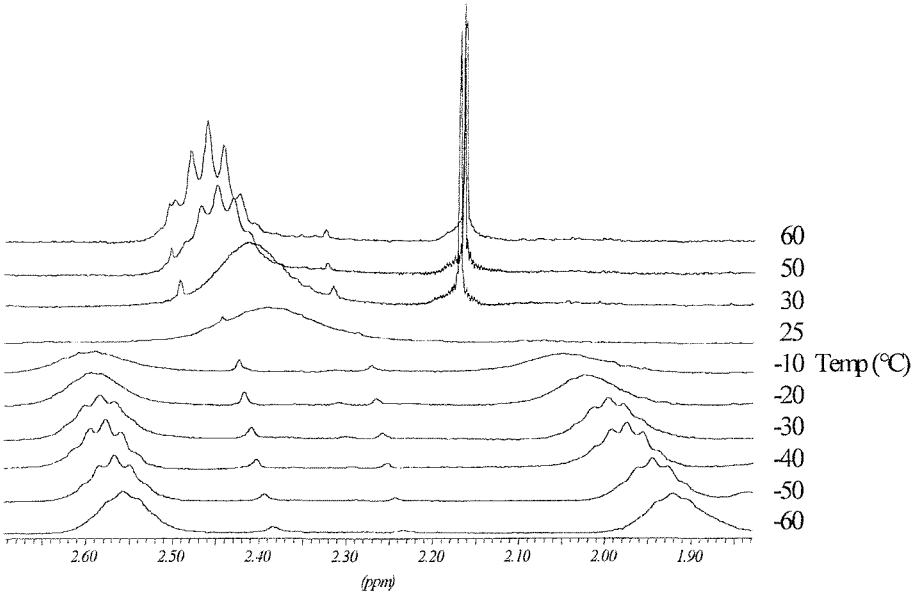

Figure 4.10. Variable temperature ^{1}H NMR spectrum of compound **(4.3)**; *iso*propyl C*H*$(CH_3)_2$ protons.

4.3.7. Isomers of compounds (4.2), (4.3) and (4.4)

When compounds **(4.2)**, **(4.3)** and **(4.4)** were synthesised from more concentrated solutions of the starting materials, a doubling of the peaks assigned to the protons of the methyl on the palladium and protons of the 6-position of the pyridine type rings was observed (in the ^{1}H NMR spectra). *Figure 4.11* shows the ^{1}H NMR spectrum of compound **(4.4)** with expanded sections that contain the peaks assigned to the protons of the methyl and the protons in the 6-position of pyridyl ring.

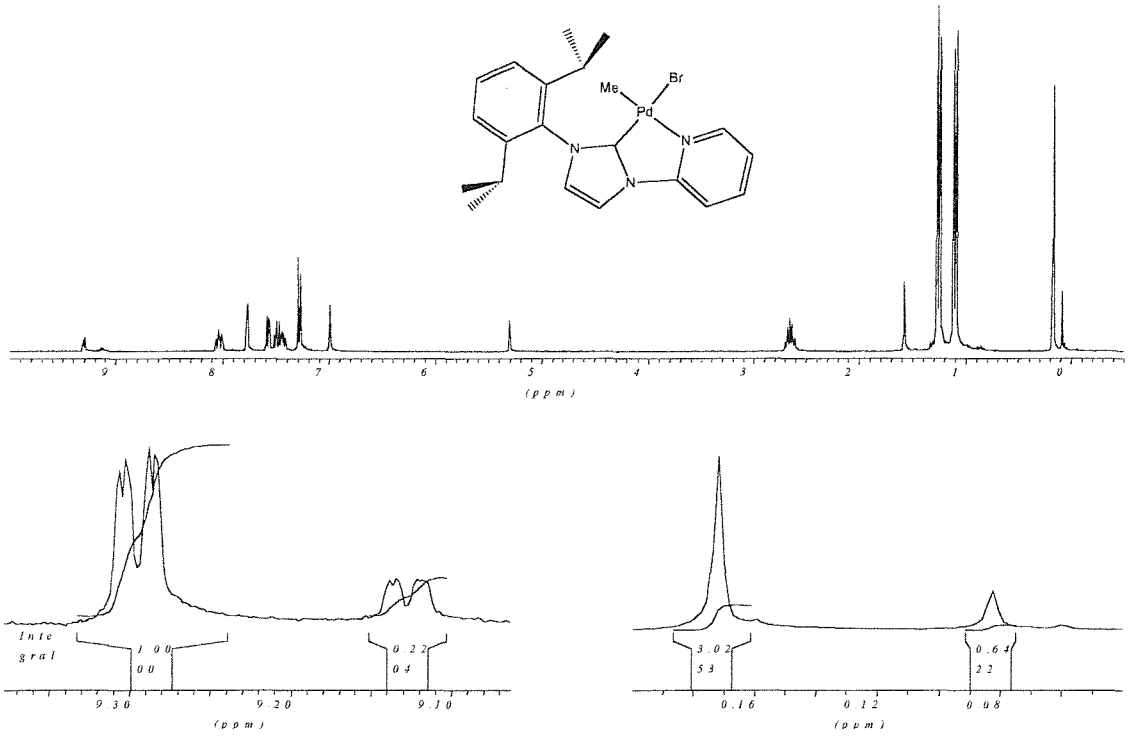

Figure 4.11. ^{1}H NMR spectrum of compound **(4.4)**, containing two peaks for both the 6-pyridyl and methyl protons.

These duplicate peaks (*Figure 4.11*) were observed in a ratio of between 1:3 and 1:6 with the original peaks. Nevertheless, when the integration of these peaks were combined, the total integration fitted with the rest of the ^{1}H NMR spectrum. These extra peaks were observed in the ^{1}H NMR spectrum for compound **(4.2)** at 0.1 and 9.2 ppm, for compound **(4.3)** at -0.2 and 9.0 ppm, and for compound **(4.4)** at 0.3 and 9.3 ppm. In a ^{13}C{H} NMR spectrum of compound **(4.4)** duplicate peaks were also observed for the methyl of the palladium at -9 ppm, for the six position of the pyridine ring at 149 ppm, and for the two position of the imidazol-2-ylidene at 174ppm. It is believed that these duplicate peaks relate to coordination isomers of the complexes (*Figure 4.11*).

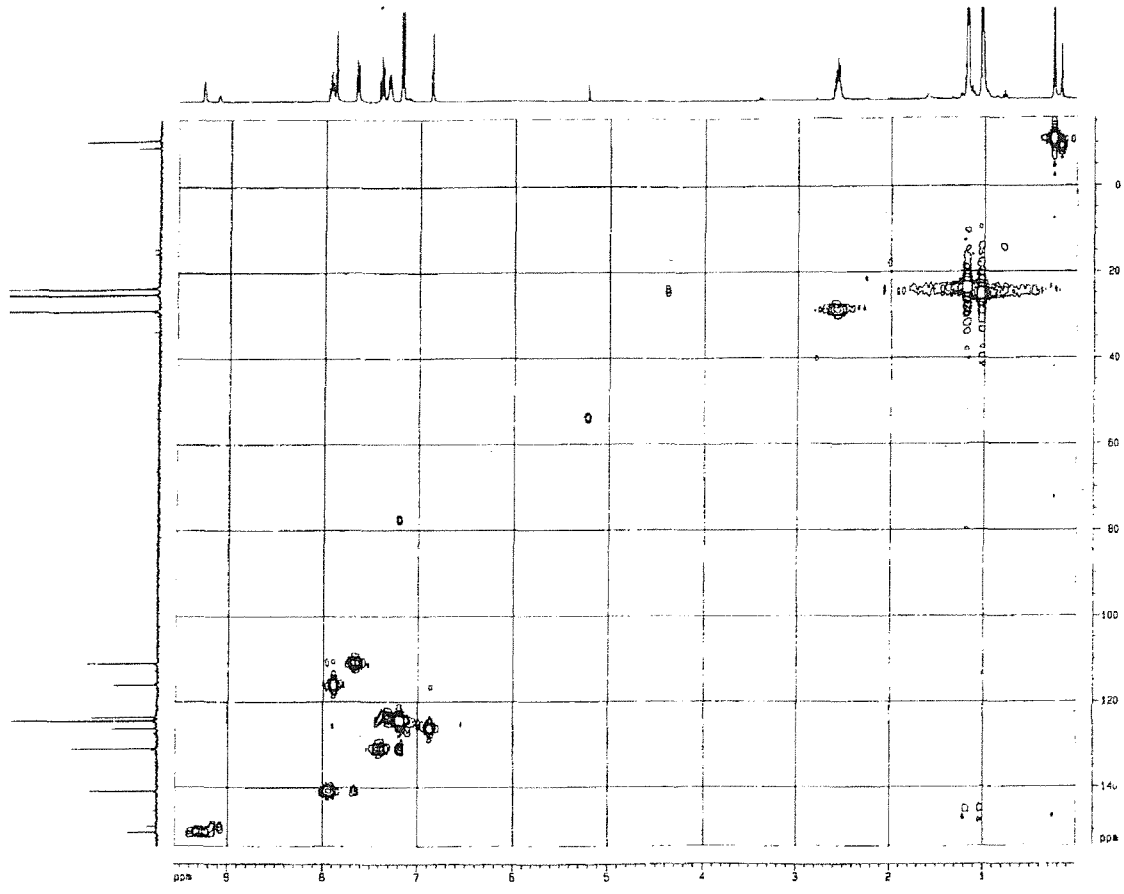

Figure 4.12. Spectrum of a C–H correlation NMR experiment performed on a sample of compound **(4.4)**, containing peaks for both the *cis* and *trans* isomers.

^{1}H 2D (NOESY) NMR experiments were performed on a sample of **(4.4)** that contained these duplicate peaks, in an attempt to show any through-space interaction between the protons of the methyl on palladium and either the proton in the 6-position of the picolyl ring or the protons of the *iso*propyl groups (*Figure 4.13*).[10] The NMR experiments showed interaction between protons positioned close to one another on the ligand, which confirmed the assignments that we made. However, none of the spectra obtained showed any increased interaction between the protons of either of the methyl group on palladium and any particular end of the ligand.

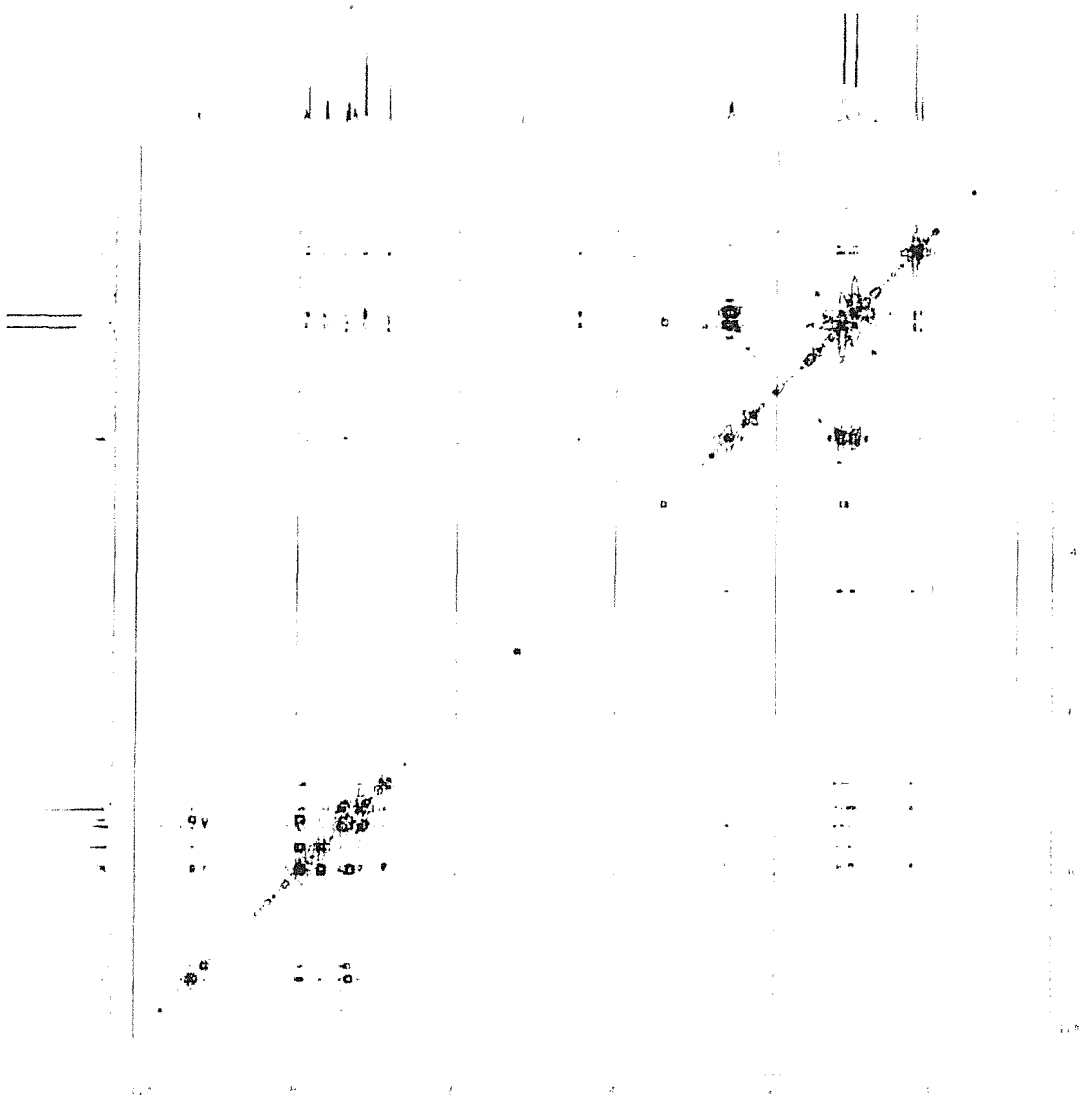

Figure 4.13. Spectrum of a 2D NOESY NMR experiment performed on a sample of compound **(4.4)**, containing peaks for both the *cis* and *trans* isomers.

Some X-ray diffraction quality crystals of compound **(4.2)** were obtained from a solution that contained these duplicate peaks, by layering a saturated dichloromethane solution with diethyl ether. The refinement of the data showed some disorder between the methyl and the bromine on palladium. The position-disposed *trans* to the carbene gave the best refinement when filled two-thirds by a bromine atom and one-third by a methyl group. This, in conjunction with observing duplicate peaks in the ^{1}H and $^{13}C\{H\}$ NMR spectra, has led us to conclude that the extra peaks are related to the *trans* and the *cis* isomers being formed when the compounds are synthesised from more highly concentrated solutions of starting materials. Attempts have been made to observe the two isomers interconverting in solution, but neither elevated temperatures nor polar solutions aided their interconversion.

The molecular weight of compound **(4.1)** in solution was measured by following the Signer method.[11] The procedure required that the compound was left in solution for weeks on end, at room temperature in a non-polar solvent. However, over these extended periods required, very small amounts of the sample decomposed. As the method relies on a pure sample of the compound to be in solution, accurate data for the molecular weight was not obtainable. However, it did conclusively identify that compound **(4.1)** does not exist solely as a monomer or a dimer in solution, but comprised of higher oligomers or mixtures of oligomers in solution.

4.4 Characterisation of complex (4.6)

When attempts were made to react deprotonated imidazolium salts with a palladium complex compound **(4.6)** was isolated. The compound was made by reacting the corresponding imidazolium salt with lithium di*iso*propylamide at -78°C stirring at room temperature for one hour and then mixing with palladium acetate.

The reason for the failure of the lithium salt to deprotonate the imidazolium salt is unclear. Possible reasons could be that a carbene initially formed but was unstable at room temperature in THF or the carbene formed reacted with the acetate anion. However, the complex was fully characterised. The electrospray mass spectrum included a peak corresponding to $[(\text{ligand})PdBr_2 + H_2O]^+$ and the chemical analysis confirmed the stoichiometry. The presence of water in the molecular ion observed in the mass spectrum probably originates from the carrier liquid (undried acetonitrile). The ^{1}H NMR spectrum contained a low field peak at 9.6 ppm corresponding to the proton in the 2-position of the imidazolium salt. Other peaks were as expected.

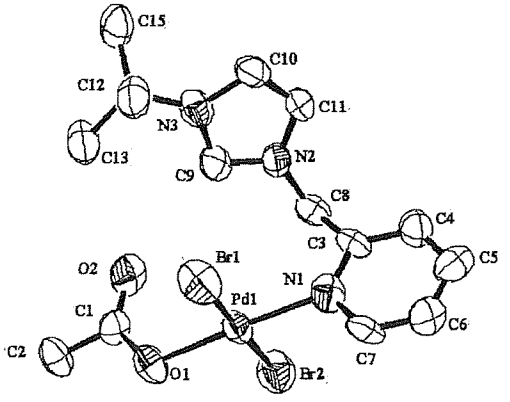

Figure 4.14. X-ray crystal structure of [3-(*tert*butyl)-1-(α-picolyl) imidazolium] palladium dibromide acetate, compound **(4.6)**.

4.4.2. X-ray diffraction studies on complex (4.6)

X-ray diffraction quality crystals of [3-(*tert*butyl)-1-(α-picolyl) imidazolium] palladium dibromide acetate **(4.6)** were obtained by cooling a saturated acetonitrile solution to -20°C. The crystal structure showed that the ligand on palladium was not a carbene but an imidazolium salt bound through the pyridyl functional group (*Figure 4.14*). The palladium-nitrogen bond length of 2.04Å is around 0.1Å shorter that others described in this chapter. The structure comprises a palladium atom in a square planar geometry with two bromine atoms disposed *trans* to one another and an acetate anion disposed *trans* to the picolyl end of the imidazolium salt.

4.5 Characterisation of complex (4.7)

The stoichometry of compound **(4.7)** was identified by the peak corresponding to $[(ligand)_2PdCl]^+$ in the electrospray mass spectrum. This compound was confirmed to have two carbene ligands for each palladium atom, by the results of the chemical analysis.

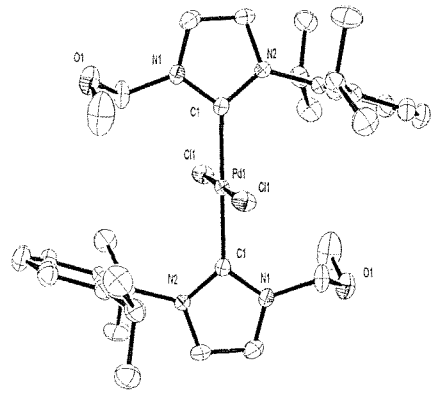

Figure 4.15. X-ray crystal structure of bis-{1-[3-(2,6-di*iso*propyl-phenyl)-imidazol-2-ylidene]-1-methoxy-methane} palladium dichloride, compound **(4.7)**.

4.5.2. X-ray diffraction studies on complex (4.7)

X-ray diffraction quality single crystals of bis-{1-[3-(2,6-di*iso*propylphenyl)-imidazol-2-ylidene]-1-methoxy-methane} palladium dichloride **(4.7)** were obtained by layering a saturated dichloromethane solution with diethyl ether. The complex comprises a palladium atom in a square planar geometry with two carbene ligands disposed *trans* to one another and with the other two sites filled by chloride atoms (*Figure 4.15*). The methoxy end of the carbene ligands is orientated to minimise steric interaction. The palladium-carbene bond length of 2.026Å is longer than the most other palladium complexes reported. Other complexes reported to have similar bond lengths are ones that

also comprise two carbene moieties orientated *trans* to one another.[12,13] This elongation is possibly due to the *trans* influence of the carbenes on one another.

4.5.3. NMR spectroscopy

The ^{1}H NMR spectrum contains characteristic peaks for the 2,6-di*iso*propylphenyl group at 1.0, 1.3, 2.8, 7.4 and 7.5 ppm. The peaks at 6.2 and 6.9 ppm, which correspond to the protons in the 4- and 5-positions of the imidazol-2-yliene ring, are higher field than those of the other palladium complexes synthesised. The reason for this difference in chemical shift of the protons is not fully understood, but could be related to the longer palladium-carbene bond length or to the ligand being monodentate. The other peaks observed in the ^{1}H NMR spectra were those assigned to the solvent (diethyl ether) and those assigned to the methylene and the methoxy protons at 5.6 and 3.0 ppm. The carbene carbon was assigned to a peak at 174 ppm in the ^{13}C{H} NMR spectrum.

4.6 Reactions

4.6.1. Discussion of the observations made for reactions 4.8.5 and 4.8.6

Reactions **4.8.5** and **4.8.6** were performed in an attempt to isolate a palladium complex with two *N*-functionalised carbene ligands (*Figure 4.16*). Reaction **4.8.6** was performed under similar conditions to method (i), using two equivalents of the silver carbene complex; and reaction **4.8.5** was performed under similar conditions to method (ii), using two equivalents of the imidazolium salt and excess base. Both methods when analysed by electrospray mass spectrometry revealed peaks associated with the stoichiometries (ligand to metal) one to one, two to one and three to one. The three stoichiometries thought to exist in these reaction mixtures meant that good spectroscopic and analytical data were not obtained.

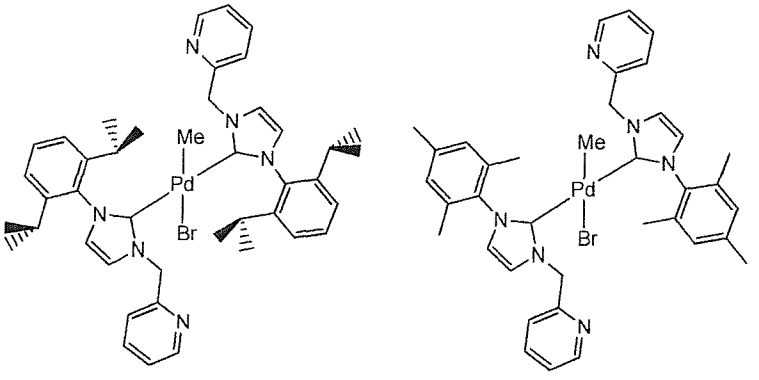

Figure 4.16. Target complexes for reactions **4.8.5** and **4.8.6**.

Unfortunately, no variations of the conditions used enabled the isolation of a pure sample of the two-ligands-on-a-palladium complexes. Attempts were made to separate the complexes but conditions were not found that gave pure samples of any particular complex. The ^{1}H NMR spectra obtained for these mixtures were not fully assignable but some characteristic peaks were observed, which confirmed the existence of palladium carbene complexes with more than one ligand on the metal centre.

4.6.2. Discussion of the observations made for reaction 4.8.7 and 4.8.8

Reactions **4.8.7** and **4.8.8** were performed in order to synthesise palladium complexes with phosphine functionalised carbene ligands (*Figure 4.17*). Although pure complexes were not obtained, characterisation methods used showed that these target complexes had been synthesised. However, normal separation and purification techniques failed to produce these target complexes as pure solids. Electrospray mass spectrometry proved to be very useful in identifying their formation, with peaks observed corresponding to [(ligand)PdMe + MeCN]$^{+}$ and [(ligand)PdMe]$^{+}$. The ^{1}H NMR spectra obtained were broad and inconclusive, however peaks in the ^{31}P{H} NMR spectra at 15 and 20 ppm are plausible for a phosphine coordinated to a palladium centre.

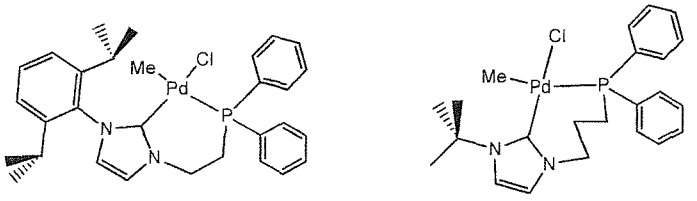

Figure 4.17. Target complexes for reactions **4.8.7** and **4.8.8**.

4.7 Conclusions

The synthesis and complete characterisation of a range of palladium mixed donor *N*-heterocyclic carbene complexes have been described in this chapter. These palladium complexes differ in subtle ways that are believed to adjust the catalytic activity when used as pre-catalysts. The properties of these complexes have been studied in detail. Fluxional processes have been identified and crystallographic differences have been noted. These differences include variations in steric bulk and in bite angle of the ligands. The palladium complexes and the reactions described in this chapter have laid out the ground rules that have allowed a variety of other palladium complexes to be synthesised, some of which are described in later chapters; others are ongoing work.[14]

EXPERIMENTAL

4.8 Synthesis of palladium complexes

4.8.1. General method (i)

A dichloromethane solution of the corresponding silver carbene complex was added drop wise to a solution of cyclooctadiene (COD) palladium methyl bromide/chloride or cyclooctadiene palladium dichloride and stirred at room temperature for 12-24 hours. After completion, the reaction mixture was filtered, the volatiles were removed under vacuum, and the resulting solid was washed with diethyl ether. Drying under vacuum gave the products as pale yellow solids.

In most cases, the products obtained at this stage were spectroscopically and analytically pure. If not, the solids were purified by recrystallisation from a saturated solution of dichloromethane and diethyl ether or by extraction into hot toluene.

4.8.2. General method (ii)

The manipulations were carried out under nitrogen. A THF solution of lithium di*iso*propylamide was added drop-wise to a dilute THF solution of the corresponding imidazolium salt and cyclooctadiene (COD) palladium methyl bromide at -78°C. The orange/red solution was then allowed to warm to room temperature and stirred for one hour. After completion, the reaction mixture was filtered; the volatiles were removed under vacuum, and washed with diethyl ether. The resulting solid was dissolved in methanol and filtered through a short silica column. The volatiles were removed under vacuum to give the air-stable complexes as pale yellow solids.

In most cases, the products obtained at this stage were spectroscopically and analytically pure. If not, the solids were purified by recrystallisation from a saturated solution of dichloromethane and diethyl ether.

(4.1) [3-(*tert*butyl)-1-(α-picolyl) imidazol-2-ylidene] palladium methyl bromide

This was prepared following the general method (ii) from 3-(*tert*butyl)-1-(α-picolyl) imidazolium bromide (2.0g, 7.5mmol) and (COD) palladium methyl bromide (0.9g, 7.5mmol) in THF (100ml) at -78°C. To this suspension was added a solution of lithium di*iso*propylamide (0.08g, 0.75mmol) in THF (50ml). The product was obtained as a yellow solid. Yield: 70%

MS (ES): *m/z* 377, $[(\text{ligand})\text{PdMe} + \text{MeCN}]^+$.

$\delta_H(CDCl_3)$ 0.2 (3H, s, PdCH_3), 2.0 [9H, s, C(CH_3)$_3$], 5.2, 5.9 (2H, 2 × d, CH_2), 6.7 (1H, d, 3-picolyl *H*), 7.1 (1H, d, 5-imidazol-2-ylidene *H*), 7.2 (1H, d, 4-imidazol-2-ylidene *H*), 7.3 (1H, m, 5-picolyl *H*), 7.7 (1H, td, 4-picolyl *H*), 9.2 (1H, d, 6-picolyl *H*).

$\delta_C(CDCl_3)$ -8 (PdCH$_3$), 32 [C(CH$_3$)$_3$], 59 (CH$_2$), 60 [C(CH$_3$)$_3$)], 119 (4-imidazol-2-ylidene *C*), 120 (5-imidazol-2-ylidene *C*), 122 (5-picolyl *C*H), 124 (3-picolyl *C*H), 138 (4-picolyl *C*H), 153 (6-picolyl *C*H), 160 (2-picolyl *C*), 175 (2-imidazol-2-ylidene *C*).

(Found: C, 40.45; H, 4.91; N, 10.05. $C_{14}H_{20}BrN_3Pd$ calculated: C, 40.36; H, 4.84; N, 10.09%).

(4.2) [3-(mesityl)-1-(α-picolyl) imidazol-2-ylidene] palladium methyl bromide

This was prepared following the general method (ii) from 3-(mesityl)-1-(α-picolyl) imidazolium bromide (3.0g, 12.0mmol) and (COD) palladium methyl bromide (2.2g, 12.0mmol) in THF (100ml) at -78°C. To this suspension was added a solution of lithium di*iso*propylamide (1.3g, 12.0mmol) in THF (50ml). The product was obtained as a yellow solid. X-ray diffraction quality crystals were obtained by layering a dichloromethane solution with diethyl ether (*Table 4.2*).

Quantitative yields were obtained when this was prepared following the general method (i) from [3-(mesityl)-1-(α-picolyl) imidazol-2-ylidene] silver bromide (0.3g, 0.64mmol) and (COD) palladium methyl bromide (0.2g, 0.64mmol) in dichloromethane (60ml) by stirring at room temperature for 12 hours.

MS (ES): *m/z* 439, $[(ligand)PdMe + MeCN]^+$.

$\delta_H(CDCl_3)$ 0.2 (3H, s, PdCH_3), 2.1 (6H, s, mesityl CH_3), 2.3 (3H, s, mesityl CH_3), 5.5 (2H, br., CH_2), 6.8 (1H, d, 5-imidazol-2-ylidene *H*), 6.9 (2H, s, mesityl *H*), 7.3 (1H, d, 4-imidazol-2-ylidene *H*), 7.4 (1H, m, 5-picolyl *H*), 7.5 (1H, d, 3-picolyl *H*), 7.8 (1H, td, 4-picolyl *H*), 9.3 (1H, d, 6-picolyl *H*).

$\delta_C(CDCl_3)$ -14 (PdCH$_3$), 19, 21 (mesityl CH$_3$), 55 (CH$_2$), 121 (4-imidazol-2-ylidene *C*), 122 (5-imidazol-2-ylidene *C*), 124 (5-picolyl *C*H), 124 (3-picolyl *C*H), 128 (mesityl *C*H), 129, 134, 135 (mesityl *C*), 139 (4-picolyl *C*H), 153 (6-picolyl *C*H), 153 (2-picolyl *C*), 173 (2-imidazol-2-ylidene *C*).

(Found: C, 47.69; H, 4.42; N, 8.77. $C_{19}H_{22}BrN_3Pd$ calculated: C, 47.67; H, 4.63; N, 8.78%).

Pd(1)-C(14)	1.962(4)	N(2)-C(13)	1.460(5)
Pd(1)-N(3)	2.186(3)	N(1)-C(11)	1.391(5)
Pd(1)-C(1)	2.207(2)	N(1)-C(5)	1.439(5)
Pd(1)-Br(2)	2.4942(6)	C(15)-C(16)	1.371(6)
C(14)-N(2)	1.349(5)	C(15)-C(13)	1.515(6)
C(14)-N(1)	1.358(5)	C(19)-C(18)	1.363(7)
N(3)-C(19)	1.333(5)	C(11)-C(12)	1.327(7)
N(3)-C(15)	1.349(5)	C(17)-C(18)	1.387(7)
N(2)-C(12)	1.391(5)	C(17)-C(16)	1.387(7)
C(14)-Pd(1)-N(3)	85.21(13)	C(19)-N(3)-Pd(1)	123.0(3)
C(14)-Pd(1)-C(1)	91.45(12)	C(15)-N(3)-Pd(1)	119.2(3)
N(3)-Pd(1)-C(1)	174.09(10)	C(14)-N(2)-C(12)	111.1(3)
C(14)-Pd(1)-Br(2)	178.10(11)	C(14)-N(2)-C(13)	122.3(3)
N(3)-Pd(1)-Br(2)	93.46(8)	C(14)-N(1)-C(11)	110.1(3)
C(1)-Pd(1)-Br(2)	90.00(6)	C(14)-N(1)-C(5)	125.3(3)
N(2)-C(14)-N(1)	104.7(3)	N(3)-C(15)-C(13)	116.5(3)
N(2)-C(14)-Pd(1)	119.9(3)	C(12)-C(11)-N(1)	107.6(4)
N(1)-C(14)-Pd(1)	135.0(3)	C(11)-C(12)-N(2)	106.5(4)
C(19)-N(3)-C(15)	117.8(3)		

Table 4.2. Selected bond lengths (Å) and angles (°) for compound **(4.2)**.

(4.3) [3-(2,6-di*iso*propylphenyl)-1-(α-picolyl) imidazol-2-ylidene] palladium methyl bromide. Method (i)

This was prepared following the general method (i) from [3-(2,6-di*iso*propyl-phenyl)-1-(α-picolyl) imidazol-2-ylidene] silver bromide (1.5g, 3.2mmol) and (COD) palladium methyl bromide (1.0g, 3.2mmol) in dichloromethane (200ml) by stirring at room temperature for 12 hours. The product was obtained in quantitative yields as a yellow solid. X-ray diffraction quality crystals were obtained by layering a saturated dichloromethane solution with petrol (*Figure 4.18* and *Table 4.3*).

MS (ES): *m/z* 481, [(ligand)PdMe + MeCN]$^+$.

δ_H(CD_2Cl_2, -40°C) -0.1 (3H, s, PdC*H*$_3$), 0.8, 1.1, 1.2, 1.6 [4 × 3H, d, CH(C*H*$_3$)$_2$], 2.0, 2.6 [2 × 1H, septet, C*H*(CH$_3$)$_2$], 5.2, 5.7 (2 × 1H, 2 × d,, C*H*$_2$), 6.8 (1H, d, 5-imidazol-2-ylidene *H*), 7.2, 7.2 (2 × H, d, ^{i}Pr$_2$C$_6$*H*$_2$H), 7.3 (1H, d, 4-imidazol-2-ylidene *H*), 7.3 (1H, m, 5-picolyl *H*), 7.4 (1H, t, ^{i}Pr$_2$C$_6$H$_2$*H*), 7.5 (2H, d, 3-picolyl *H*), 7.8 (1H, dt,4-picolyl *H*), 9.1 (1H, br. d, 6-picolyl *H*).

δ_C($CDCl_3$) -2 (PdCH$_3$), 23, 25 (CH(*C* H$_3$)$_2$), 29 (*C* H(CH$_3$)$_2$), 56 (C*H*$_2$), 111 (3-picolyl *C*H), 114 (4-imidazol-2-ylidene *C*), 121 (5-picolyl *C*H), 123, 124, 131, 147 (^{i}Pr$_2$*C*$_6$H$_3$), 124 (5-imidazol-2-ylidene *C*), 138 (4-picolyl *C*H), 153 (6-picolyl *C*H), 154 (2-picolyl *C*), 174 (2-imidazol-2-ylidene *C*).

(Found: C, 50.63; H, 5.53; N, 7.94. $C_{22}H_{28}PdBr$ calculated: C, 50.74; H, 5.42; N, 8.07%).

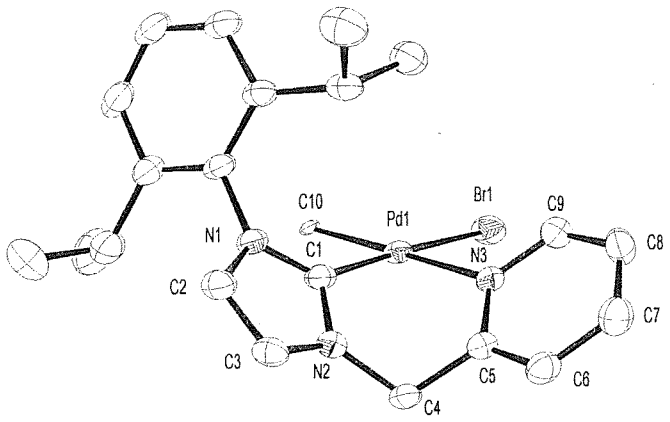

Figure 4.18. X-ray crystal structure of [3-(2,6-di*iso*propylphenyl)-1-(α-picolyl) imidazol-2-ylidene] palladium methyl bromide, compound **(4.3)**.

Pd(1)-C(1)	1.969(4)	N(1)-C(1)	1.356(4)
Pd(1)-C(10)	2.126(3)	N(1)-C(2)	1.391(4)
Pd(1)-N(3)	2.168(3)	N(1)-C(11)	1.443(4)
Pd(1)-Br(1)	2.4890(5)	C(9)-C(8)	1.378(6)
N(3)-C(9)	1.341(5)	C(6)-C(7)	1.377(6)
N(3)-C(5)	1.344(4)	C(6)-C(5)	1.381(5)
N(2)-C(1)	1.349(4)	C(2)-C(3)	1.343(5)
N(2)-C(3)	1.383(5)	C(8)-C(7)	1.382(6)
N(2)-C(4)	1.467(4)	C(4)-C(5)	1.507(5)
C(1)-Pd(1)-C(10)	91.44(12)	C(1)-N(1)-C(2)	110.9(3)
C(1)-Pd(1)-N(3)	85.22(13)	C(1)-N(1)-C(11)	126.4(3)
C(10)-Pd(1)-N(3)	176.58(11)	N(2)-C(1)-N(1)	104.4(3)
C(1)-Pd(1)-Br(1)	176.89(10)	N(2)-C(1)-Pd(1)	119.4(3)
C(10)-Pd(1)-Br(1)	90.01(8)	N(1)-C(1)-Pd(1)	136.0(2)
N(3)-Pd(1)-Br(1)	93.37(8)	C(3)-C(2)-N(1)	106.6(3)
C(5)-N(3)-Pd(1)	119.8(2)	N(2)-C(4)-C(5)	109.2(3)
C(1)-N(2)-C(3)	111.5(3)	N(3)-C(5)-C(4)	116.3(3)
C(1)-N(2)-C(4)	122.3(3)	C(2)-C(3)-N(2)	106.7(3)

Table 4.3. Selected bond lengths (Å) and angles (°) for compound **(4.3)**.

(4.3) [3-(2,6-di*iso*propylphenyl)-1-(α-picolyl) imidazol-2-ylidene] palladium methyl bromide. Method (ii)

This was prepared following the general method (ii) from 3-(2,6-di*iso*propylphenyl)-1-(α-picolyl) imidazolium bromide (0.14g, 0.32mmol) and (COD) palladium methyl bromide (0.1g, 0.32mmol) in THF (50ml) at -78°C. To this suspension was added a solution of lithium di*iso*propylamide (0.09g, 0.88mmol) in THF (20ml). The product was obtained in good yields as a yellow solid.

MS (ES): *m/z* 481, $[(\text{ligand})\text{PdMe} + \text{MeCN}]^+$; 759, $[(\text{ligand})_2\text{PdMe}]^+$.

(4.4) [3-(2,6-di*iso*propylphenyl)-1-(2-pyridyl) imidazol-2-ylidene] palladium methyl bromide

This was prepared following the general method (i) from [3-(2,6-di*iso*propylphenyl)-1-(2-pyridyl) imidazol-2-ylidene] silver bromide (1.5g, 3.2mmol) and (COD) palladium methyl bromide (1.0g, 3.2mmol) in dichloromethane (200ml) by stirring at room temperature for 12 hours. The product was obtained in quantitative yields as a yellow solid. X-ray diffraction quality crystals were obtained by layering a saturated dichloromethane solution with petrol (*Figure 4.19* and *Table 4.4*).

MS (ES): *m/z* 455, $[(\text{ligand})\text{PdMe} + \text{MeCN}]^+$.

$\delta_H(CDCl_3)$ 0.4 (3H, s, $PdCH_3$), 1.1, 1.3 [2 × 6H, d, $CH(CH_3)_2$], 2.7 [2H, septet, $CH(CH_3)_2$], 7.0 (1H, d, 5-imidazol-2-ylidene *H*), 7.3 (2H, d, $^iPr_2C_6H_2H$), 7.4 (1H, m, 5-pyridyl *H*), 7.5 (1H, t, $^iPr_2C_6H_2H$), 7.7 (2H, d, 3-pyridyl *H*), 8.0 (1H, d, 4-imidazol-2-ylidene *H*), 8.0 (1H, dt,4-pyridyl *H*), 9.4 (1H, br. d, 6-pyridyl *H*).

$\delta_C(CDCl_3)$ -11 ($PdCH_3$), 23, 25 ($CH(CH_3)_2$), 29 ($CH(CH_3)_2$), 110 (3-picolyl *C*H), 116 (4-imidazol-2-ylidene *C*), 123 (5-picolyl *C*H), 124, 131, 134, 146 ($^iPr_2C_6H_3$), 126 (5-imidazol-2-ylidene *C*), 141 (4-picolyl *C*H), 150 (6-picolyl *C*H), 150 (2-picolyl *C*), 174 (2-imidazol-2-ylidene *C*).

(Found: C, 49.79; H, 5.25; N, 8.15. $C_{21}H_{25}PdBr$ calculated: C, 49.77; H, 5.17; N, 8.29%).

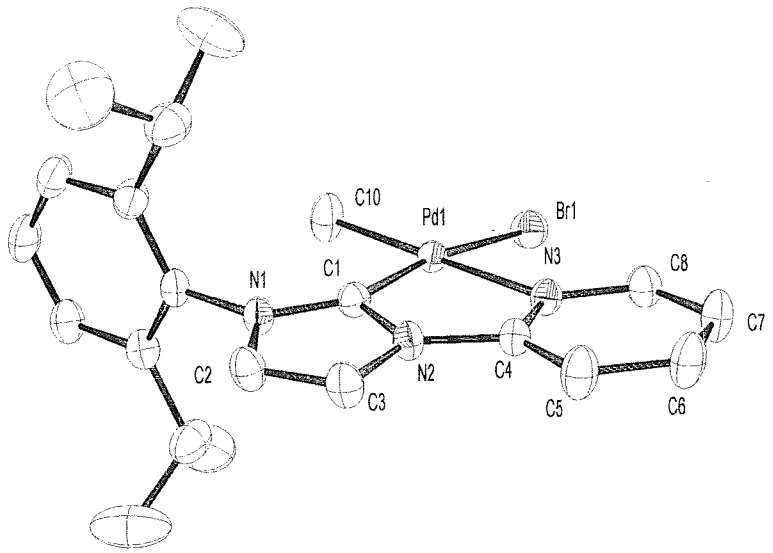

Figure 4.19. X-ray crystal structure of [3-(2,6-di*iso*propylphenyl)-1-(2-pyridyl) imidazol-2-ylidene] palladium methyl bromide, compound **(4.4)**.

Pd(1)-C(1)	1.970(4)	N(1)-C(11)	1.443(5)
Pd(1)-C(10)	2.034(4)	N(2)-C(1)	1.369(5)
Pd(1)-N(3)	2.166(3)	N(2)-C(3)	1.392(5)
Pd(1)-Br(1)	2.4528(5)	N(2)-C(4)	1.410(5)
N(1)-C(1)	1.348(5)	N(3)-C(4)	1.332(5)
N(1)-C(2)	1.391(5)	C(2)-C(3)	1.342(6)
C(1)-Pd(1)-C(10)	96.91(17)	C(3)-N(2)-C(4)	127.3(3)
C(1)-Pd(1)-N(3)	79.15(13)	C(4)-N(3)-Pd(1)	112.8(2)
C(10)-Pd(1)-N(3)	175.17(17)	C(8)-N(3)-Pd(1)	129.4(3)
C(1)-Pd(1)-Br(1)	171.53(11)	N(1)-C(1)-N(2)	103.5(3)
C(10)-Pd(1)-Br(1)	88.07(13)	N(1)-C(1)-Pd(1)	142.3(3)
N(3)-Pd(1)-Br(1)	96.18(8)	N(2)-C(1)-Pd(1)	113.7(3)
C(1)-N(1)-C(2)	111.5(3)	Pd(1)-C(1)-N(3)	53.71(11)
C(1)-N(1)-C(11)	127.4(3)	N(3)-C(4)-N(2)	113.2(3)
C(2)-N(1)-C(11)	121.1(3)	C(3)-C(2)-N(1)	107.4(3)
C(1)-N(2)-C(3)	111.9(3)	C(2)-C(3)-N(2)	105.7(3)
C(1)-N(2)-C(4)	120.8(3)		

Table 4.4. Selected bond lengths (Å) and angles (°) for compound **(4.4)**.

(4.5) [3-(2,6-di*iso*propylphenyl)-1-(α-lutidyl) imidazol-2-ylidene] palladium methyl bromide

This was prepared following the general method (i) from [3-(2,6-di*iso*propylphenyl)-1-(α-lutidyl) imidazol-2-ylidene] silver bromide (0.5g, 1.1mmol) and (COD) palladium methyl bromide (0.3g, 1.1mmol) in dichloromethane (100ml) by stirring at room temperature for 12 hours. The product was obtained in quantitative yields as a yellow solid. X-ray diffraction quality crystals were obtained by layering a saturated dichloromethane solution with petrol (*Figure 4.20* and *Table 4.5*).

MS (ES): *m/z* 482, [(ligand)PdMe + MeCN]$^+$.

δ_H($CDCl_3$) 0.2, 0.3 (3H, s, PdC*H*$_3$), 0.8, 1.1, 1.2, 1.5 [4 × 3H, d, CH(C*H*$_3$)$_2$], 2.4, 2.7 [2 × 1H, septet, C*H*(CH$_3$)$_2$], 3.0 (3H, s, lutidyl C*H*$_3$), 5.1, 6.0 (2 × 1H, dd, C*H*$_2$), 6.7 (1H, d, 5-imidazol-2-ylidene *H*), 7.1 (2H, br. d, ^{i}Pr$_2$C$_6$*H*$_2$H), 7.3 (1H, d, 4-imidazol-2-ylidene *H*), 7.2 (1H, d, 5-lutidyl *H*), 7.3 (1H, t, ^{i}Pr$_2$C$_6$H$_2$*H*), 7.3 (1H, d, 3-lutidyl *H*), 7.5 (1H, t, 4-lutidyl *H*).

δ_C($CDCl_3$) -5 (PdCH$_3$), 22, 24, 25, 26 (CH(*C*H$_3$)$_2$), 28 (lutidyl *C*H$_3$), 29 (*C*H(CH$_3$)$_2$), 57 (C*H*$_2$), 120 (3-lutidyl *C*H), 120 (4-imidazol-2-ylidene *C*), 123 (5-lutidyl *C*H), 123, 125, 130, 145 (^{i}Pr$_2$*C*$_6$H$_3$), 128 (5-imidazol-2-ylidene *C*), 138 (4-lutidyl *C*H), 152 (6-lutidyl *C*H), 152 (2-lutidyl *C*), 163 (2-imidazol-2-ylidene *C*).

(Found: C, 52.06; H, 5.80; N, 7.91. $C_{23}H_{30}BrN_3Pd$ calculated: C, 51.65; H, 5.65; N, 7.86%).

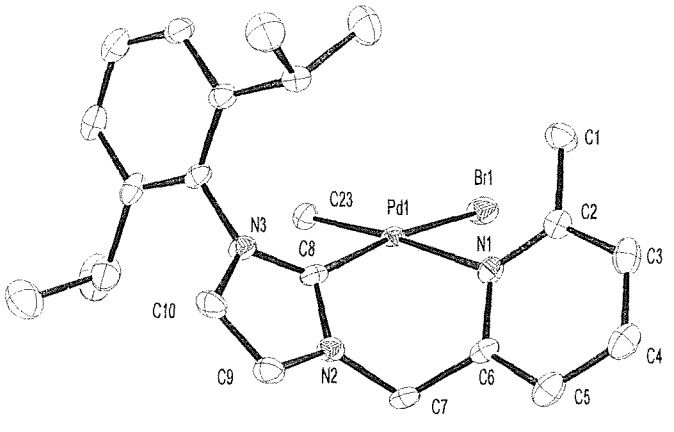

Figure 4.20. X-ray crystal structure of [3-(2,6-di*iso*propylphenyl)-1-(α-lutidyl) imidazol-2-ylidene] palladium methyl bromide, compound **(4.5)**.

C(1)-C(2)	1.499(7)	C(8)-N(3)	1.350(6)
C(2)-N(1)	1.332(6)	C(8)-N(2)	1.362(6)
C(2)-C(3)	1.403(7)	C(8)-Pd(1)	1.976(5)
C(3)-C(4)	1.379(8)	C(9)-C(10)	1.353(7)
C(4)-C(5)	1.393(8)	C(9)-N(2)	1.380(6)
C(5)-C(6)	1.367(7)	C(10)-N(3)	1.398(6)
C(6)-N(1)	1.375(6)	C(23)-Pd(1)	2.044(5)
C(6)-C(7)	1.510(7)	N(1)-Pd(1)	2.225(4)
C(7)-N(2)	1.461(6)	Br(1)-Pd(1)	2.4968(8)
N(1)-C(2)-C(1)	118.9(4)	C(8)-N(2)-C(7)	122.1(4)
N(3)-C(8)-N(2)	104.6(4)	C(9)-N(2)-C(7)	126.9(4)
N(3)-C(8)-Pd(1)	138.3(3)	C(8)-N(3)-C(10)	111.2(4)
N(2)-C(8)-Pd(1)	117.0(3)	C(8)-N(3)-C(11)	125.9(4)
C(10)-C(9)-N(2)	107.1(4)	C(8)-Pd(1)-C(23)	90.69(19)
C(9)-C(10)-N(3)	106.0(4)	C(8)-Pd(1)-N(1)	85.61(16)
C(2)-N(1)-C(6)	118.3(4)	C(23)-Pd(1)-N(1)	175.36(17)
C(2)-N(1)-Pd(1)	126.6(3)	C(8)-Pd(1)-Br(1)	172.30(13)
C(6)-N(1)-Pd(1)	115.1(3)	C(23)-Pd(1)-Br(1)	88.60(14)
C(8)-N(2)-C(9)	111.0(4)	N(1)-Pd(1)-Br(1)	94.69(10)

Table 4.5. Selected bond lengths (Å) and angles (°) for compound **(4.5)**.

Compound	**(4.2)**	**(4.3)**	**(4.5)**
Chemical formula	$C_{20}H_{22}BrN_3Pd$	$C_{22}H_{28}BrN_3Pd$	$C_{24}H_{32}BrCl_2N_3Pd$
Formula weight	490.72	520.78	619.74
Crystal system	Rhombohedral	Monoclinic	Monoclinic
Space group	*R*-3	$P\,2_1/n$	$P\,2_1/n$
a/Å	15.5514(18)	7.79810(10)	7.7892(16)
b/Å	15.5514(18)	21.8591(2)	23.120(5)
c/Å	15.5514(18)	13.48780(10)	14.536(3)
α/°	102.993(17)	90	90
β/°	102.993(17)	90.60	94.15(3)
γ/°	102.993(17)	90	90
V/Å^3	3417.4(7)	2299.00(4)	2610.9(9)
Z	6	4	4
T/K	150(2)	150(2)	150(2)
μ/mm^{-1}	2.574	2.556	2.462
F(000)	1464	1048	1248
No. Data collected	38472	24498	17717
No. Unique data	4523	6659	5320
R_{int}	0.0463	0.0434	0.0824
Final R(|F|) for $F_O > 2\sigma(F_o)$	0.0393	0.0444	0.0529
Final R(F^2) for all data	0.0530	0.0612	0.0614

Table 4.6. Crystallographic parameters for compounds **(4.2)**, **(4.3)** and **(4.5)**.

(4.6) [3-(*tert*butyl)-1-(α-picolyl) imidazolium] palladium dibromide acetate

The manipulations were carried out under nitrogen. A THF (20ml) solution of lithium di*iso*propylamide (0.075g, 0.7mmol) was added drop-wise to a THF solution (20ml) of 3-(*tert*butyl)-1-(α-picolyl) imidazolium bromide (0.2g, 0.7mmol) at -78°C. After warming to room temperature, the solution was stirred for one hour, the reaction mixture was filtered, the volatiles were removed under vacuum, and the solid was redissolved in cold THF (20ml). This THF solution was added slowly to a THF (20ml) solution of palladium acetate (0.144g, 0.64mmol) at -78°C, and the solution was stirred for one hour. On warming to room temperature a precipitate formed. The supernatant was decanted off and the solid was washed with toluene. The volatiles were removed under vacuum to give the air-stable complex as an orange/yellow solid. X-ray diffraction quality crystals were obtained by cooling a saturated acetonitrile solution to -20°C (*Table 4.7*).

MS (ES): *m/z* 495, $[(\text{imidazolium})PdBr_2 + H_2O]^+$.

$\delta_H(CDCl_3)$ 1.6 [9H, s, $C(CH_3)_3$], 1.8 (3H, s, CO_2CH_3), 6.1 (2H, s, CH_2), 7.5 (1H, s, 5-imidazolium *H*), 7.5 (1H, d, 3-picolyl *H*), 7.7 (1H, s, 4-imidazolium *H*), 7.7 (1H, m, 5-picolyl *H*), 8.0 (1H, dt, 4-picolyl *H*), 9.0 (1H, d, 6-picolyl *H*), 9.6 (br., 2-imidazolium *H*).

(Found: C, 33.78; H, 3.69; N, 8.10. $C_{15}H_{21}Br_2N_3O_2Pd$ calculated: C, 33.33; H, 3.73; N, 7.77%).

Pd(1)-O(1)	2.017(8)	N(2)-C(9)	1.300(16)
Pd(1)-N(1)	2.043(11)	N(2)-C(11)	1.355(16)
Pd(1)-Br(1)	2.389(2)	N(2)-C(8)	1.462(17)
Pd(1)-Br(2)	2.416(2)	N(3)-C(9)	1.373(17)
N(1)-C(3)	1.339(18)	N(3)-C(10)	1.384(16)
N(1)-C(7)	1.383(18)	N(3)-C(12)	1.485(17)

O(1)-Pd(1)-N(1)	177.0(6)	O(1)-Pd(1)-Br(2)	89.9(3)
O(1)-Pd(1)-Br(1)	91.4(3)	N(1)-Pd(1)-Br(2)	89.9(3)
N(1)-Pd(1)-Br(1)	88.7(3)	Br(1)-Pd(1)-Br(2)	178.09(9)

Table 4.7. Selected bond lengths (Å) and angles (°) for compound **(4.6)**. (Symmetry transformations used to generate equivalent atoms: #1 -x+1,-y+2,-z; #2 -x,-y+1,-z+1).

(4.7) bis-{1-[3-(2,6-di*iso*propylphenyl)-imidazol-2-ylidene]-1-methoxy-methane} palladium dichloride

This was prepared following the general method (i) from {1-[3-(2,6-di*iso*propyl-phenyl) imidazol-2-ylidene]-1-methoxy-methane} silver chloride (0.39g, 1.05mmol) and (COD) palladium dichloride (0.15g, 0.53mmol) in dichloromethane (75ml) by stirring at room temperature for 12 hours. The product was obtained in good yields as a orange/yellow solid. X-ray diffraction quality crystals were obtained by layering a saturated dichloromethane solution with diethyl ether (*Table 4.8*).

MS (ES): *m/z* 455, $[(ligand)_2PdCl]^+$.

$\delta_H(CDCl_3)$ 1.0, 1.3 [2 × 6H, d, $CH(CH_3)_2$], 2.8 [2H, septet, $CH(CH_3)_2$], 3.0 (3H, s, OCH_3), 5.6 (2H, d, CH_2), 6.2 (1H, d, 5-imidazol-2-ylidene *H*), 6.9 (1H, d, 4-imidazol-2-ylidene *H*), 7.4 (2H, d, $^iPr_2C_6H_2H$), 7.5 (1H, t, $^iPr_2C_6H_2H$).

$\delta_C(CDCl_3)$ 22, 26 ($CH(CH_3)_2$), 26 (OCH_3), 29 ($CH(CH_3)_2$), 58 (CH_2), 117 (4-imidazol-2-ylidene *C*), 119, 1126, 130, 147 ($^iPr_2C_6H_3$), 124 (5-imidazol-2-ylidene *C*), 174 (2-imidazol-2-ylidene *C*).

(Found: C, 57.49; H, 7.41; N, 6.89. $(C_{34}H_{48}Cl_2N_4O_2PdCl_2)C_4H_{10}O$ calculated: C, 57.18; H, 7.58; N, 7.02%).

C(1)-N(2)	1.355(3)	C(4)-O(1)	1.396(3)
C(1)-N(1)	1.354(3)	C(4)-N(1)	1.469(3)
C(1)-Pd(1)	2.026(2)	C(5)-O(1)	1.392(4)
C(2)-C(3)	1.344(3)	Cl(1)-Pd(1)	2.3070(9)
C(2)-N(1)	1.382(3)	Pd(1)-C(1)#1	2.026(2)
C(3)-N(2)	1.390(3)	Pd(1)-Cl(1)#1	2.3070(10)
N(2)-C(1)-N(1)	104.42(18)	C(1)-N(2)-C(6)	124.23(18)
N(2)-C(1)-Pd(1)	129.20(15)	C(3)-N(2)-C(6)	124.76(18)
N(1)-C(1)-Pd(1)	126.38(15)	C(4)-O(1)-C(5)	113.6(2)
C(3)-C(2)-N(1)	106.7(2)	C(1)#1-Pd(1)-C(1)	180.00(8)
C(2)-C(3)-N(2)	106.7(2)	C(1)#1-Pd(1)-Cl(1)#1	91.10(6)
O(1)-C(4)-N(1)	111.1(2)	C(1)-Pd(1)-Cl(1)#1	88.90(6)
C(1)-N(1)-C(2)	111.33(18)	C(1)#1-Pd(1)-Cl(1)	88.90(6)
C(1)-N(1)-C(4)	125.1(2)	C(1)-Pd(1)-Cl(1)	91.10(6)
C(2)-N(1)-C(4)	123.5(2)	Cl(1)#1-Pd(1)-Cl(1)	180. 00(8)
C(1)-N(2)-C(3)	110.87(18)		

Table 4.8. Selected bond lengths (Å) and angles (°) for compound **(4.7)**. (Symmetry transformations used to generate equivalent atoms: #1 -x,-y,-z+1).

Compound	(4.4)	(4.7)	(4.6)
Chemical formula	$C_{21}H_{26}BrN_3Pd$	$C_{34}H_{48}Cl_2N_4O_2Pd$	$Cl_{5.66}H_{21}Br_2N_{3.34}O_2Pd$
Formula weight	506.76	722.06	554.25
Crystal system	Monoclinic	Triclinic	Triclinic
Space group	$P\,2_1/c$	P-1	P-1
a/Å	11.29100(10)	8.1263(16)	69.85(3)
b/Å	13.06100(10)	9.1631(18)	78.62(3)
c/Å	14.7203(2)	12.565(3)	88.00(3)
α/°	90	74.36(3)	7.783(2)
β/°	90.93	78.00(3)	11.248(2)
γ/°	90	79.56(3)	12.976(3)
V/Å^3	2170.54(4)	873.5(3)	1044.8(4)
Z	4	1	2
T/K	150(2)	150(2)	150(2)
μ/mm^{-1}	2.705	0.719	4.725
F(000)	1016	376	541
No. Data collected	25345	12135	15676
No. Unique data	6245	3884	4330
R_{int}	0.0471	0.0487	0.1791
Final R(|F|) for $F_O > 2\sigma(F_o)$	0.0497	0.0352	0.0929
Final R(F^2) for all data	0.0658	0.0387	0.2661

Table 4.9. Crystallographic parameters for compounds **(4.4)**, **(4.6)** and **(4.7)**.

4.8.3. Reaction between [3-(*tert*butyl)-1-(α-lutidyl) imidazolium bromide, (COD) palladium methyl bromide and excess lithium di*iso*propylamide

This was prepared following the general method (ii) from 3-(*tert*butyl)-1-(α-lutidyl) imidazolium bromide) (0.13g, 0.32mol) and (COD) palladium methyl bromide (0.1g, 0.32mmol) in THF (50ml) at -78°C. To this suspension was added a solution of lithium di*iso*propylamide (0.09g, 0.88mmol) in THF (20ml). The product was obtained in good yields as a yellow solid.

MS (ES): *m/z* 391, $[(ligand)PdMe + MeCN]^+$; 565, $[(ligand)_2PdMe]^+$.

4.8.4. Reaction between 3-(mesityl)-1-(α-lutidyl) imidazolium bromide, (COD) palladium methyl bromide and excess lithium di*iso*propylamide

This was prepared following the general method (ii) from 3-(mesityl)-1-(α-lutidyl) imidazolium bromide (0.13g, 0.32mmol) and (COD) palladium methyl bromide (0.1g, 0.32mmol) in THF (50ml) at -78°C. To this suspension was added a solution of lithium di*iso*propylamide (0.09g, 0.88mmol) in THF (20ml). The product was obtained in good yields as a yellow solid.

MS (ES): *m/z* 453, $[(ligand)PdMe + MeCN]^+$; 703, $[(ligand)_2PdMe]^+$.

4.8.5. Reaction between two equivalents of 3-(mesityl)-1-(2-picolyl) imidazolium bromide, (COD) palladium methyl bromide and excess lithium di*iso*propylamide

This was performed following the general method (ii) from 3-(2,6-di*iso*propyl-phenyl)-1-(α-picolyl) imidazolium bromide (0.28g, 0.76mmol) and (COD) palladium methyl bromide (0.1g, 0.32mmol) in THF (50ml) at -78°C. To this suspension was added a solution of lithium di*iso*propylamide (0.18g, 1.7mmol) in THF (30ml). The product obtained at this stage was not spectroscopically or analytically pure. However, attempts to purify the solid by standard separation and purification techniques gave no further increase in purity.

MS (ES): *m/z* 439, $[(\text{ligand})\text{PdMe} + \text{MeCN}]^+$; 674, $[(\text{ligand})_2\text{PdMe}]^+$; 952, $[(\text{ligand})_3\text{PdMe}]^+$.

$\delta_H(CDCl_3)$ including -0.4 (3H, s, $PdCH_3$), 5.3, 5.6 (2 × 2H, d, CH_2), 6.5 (2H, t, $^iPr_2C_6H_2H$), 6.8 (2H, s, 5-imidazol-2-ylidene *H*), 6.9 (4H, d, $^iPr_2C_6H_2H$), 7.1 (2H, s, 4-imidazol-2-ylidene *H*), 7.7 (2H, br.,4-picolyl *H*), 8.6 (2H, br. d, 6-picolyl *H*).

4.8.6. Reaction between two equivalents of [3-(2,6-di*iso*propylphenyl)-1-(α-picolyl) imidazol-2-ylidene] silver bromide and (COD) palladium methyl bromide

This was performed following the general method (i) from [3-(2,6-di*iso*propyl-phenyl)-1-(α-picolyl) imidazol-2-ylidene] silver bromide (0.36g, 0.64mmol) and (COD) palladium methyl bromide (0.1g, 0.32mmol) in dichloromethane (40ml) by stirring at room temperature for 12 hours. The product obtained at this stage was not spectroscopically or analytically pure. However, attempts to purify the solid by standard separation and purification techniques gave no further increase in purity.

MS (ES): *m/z* 469, $[(\text{ligand})\text{PdMe} + \text{MeCN}]^+$; 735, $[(\text{ligand})_2\text{PdMe}]^+$; 1042, $[(\text{ligand})_3\text{PdMe}]^+$.

$\delta_H(CDCl_3)$ including -0.4 (3H, s, $PdCH_3$), 0.6, 0.8, 0.9, 1.0 [4 × 6H, d, $CH(CH_3)_2$], 1.8, 2.4 [2 × 2H, septet, $CH(CH_3)_2$], 4.1, 5.9 (2 × 2H, d, CH_2), 6.9 (2H, s, 5-imidazol-2-ylidene *H*), 7.1 (4H, d, $^iPr_2C_6H_2H$), 7.2 (2H, s, 4-imidazol-2-ylidene *H*), 7.7 (2H, br., picolyl *H*), 8.1 (2H, br. d, 6-picolyl *H*).

4.8.7. Reaction between {1-[3-(di*iso*propyl)-imidazolium]-2-[diphenylphosphine]-ethane} iodide, (COD) palladium methyl chloride and lithium di*iso*propylamide

This was performed following the general method (ii) from {1-[3-(di*iso*propyl) imidazolium]-2-[diphenylphosphine]-ethane} iodide (0.19g, 0.38mmol) and (COD) palladium methyl chloride (0.1g, 0.38mmol) in THF (20ml) at -78°C. To this suspension was added a solution of lithium di*iso*propylamide (0.045g, 0.4mmol) in THF (20ml). The yellow product obtained at this stage was not spectroscopically or analytically pure. However, attempts to purify the solid by standard separation and purification techniques gave no further increase in purity.

MS (ES): *m/z* 484, $[(\text{ligand})\text{PdMe} + \text{MeCN}]^+$, 441, $[(\text{ligand})\text{PdMe}]^+$.

$\delta_H(CD_3CN)$ broad peaks including 0.5 (3H, br., $PdCH_3$), 2.08 [6H, br. d, $CH(CH_3)_2$], 2.1 (2H, br., PCH_2), 2.5 (2H, s, CH_2), 2.6 [1H, br. m, $CH(CH_3)_2$],7.2-7.9 (12H, phenyl *H*, 4,5-imidazol-2-ylidene *H*).

$\delta_P(CD_3CN)$ 15.

4.8.8. Reaction between {1-[3-(*tert*butyl)-imidazolium]-3-[diphenylphosphine]-propane} bromide, (COD) palladium methyl chloride and lithium di*iso*propylamide

This was performed following the general method (ii) from 1-[3-(*tert*butyl) imidazolium]-3-[diphenylphosphine]-propane} bromide (0.2g, 0.4mmol) and (COD) palladium methyl chloride (0.12g, 0.4mmol) in THF (20ml) at -78°C. To this suspension was added a solution of lithium di*iso*propylamide (0.05g, 0.42mmol) in THF (20ml). The yellow product obtained at this stage was not spectroscopically or analytically pure. However, attempts to purify the solid by standard separation and purification techniques gave no further increase in purity.

MS (ES): *m/z* 498, $[(\text{ligand})\text{PdMe} + \text{MeCN}]^+$.

$\delta_H(CDCl_3)$ broad peaks including 1.2 (3H, s, $PdCH_3$), 1.65 [9H, s, $C(CH_3)_3$], 1.7 (2H, s, CH_2), 2.1 (2H, s, CH_2), 2.3 (2H, s, CH_2), 7.4-8.0 (12H, phenyl *H*, 4,5-imidazol-2-ylidene *H*).

$\delta_P(CDCl_3)$ 20.

REFERENCES

1 Review: W.A. Herrmann, C. Køcher, *Angew. Chem., Int. Ed. Engl.*, **1997**, *36*, 2162.

2 B. Cornils, W.A. Herrmann, *Applied Homogeneous Catalysis with Organometallic Compounds*, Wiley-VCH, Weinheim, **2000**; C. Zhang, J. Huang, M.L. Trudell, S.P. Nolan, *J. Org. Chem.*, **1999**, *64*, 3804.

3 A.A.D. Tulloch, A.A. Danopoulos, R.P. Tooze S.M. Cafferkey, S. Kleinhenz, M.B. Hursthouse, *Chem. Commun.*, **2000**, 1247.

4 W.A. Herrmann, C. Køcher, L. Goossen, G.R.J. Artus, *Chem. Eur. J.*, **1996**, *2*, 1627.

5 W.A. Herrmann, L. Goossen, M. Spiegler, *Organometallics*, **1998**, *17*, 2162.

6 D.S. McGuinness, K.J. Cavell, *Organometallics*, **2000**, *19*, 741.

7 M.G. Gardiner, W.A. Herrmann, C-P. Reisinger, J. Schwarz, M. Spiegler, *J. Organomet. Chem.*, **1999**, *572*, 239; F.E. Hahn, M. Foth, *J. Organomet. Chem.*, **1999**, *585*, 241; M.V. Baker, B.W. Skelton, A.H. White, C.C. Williams, *J. Chem. Soc., Dalton Trans.*, **2001**, 111.

8 J. Schwarz, V.P.W. Böhm, M.G. Gardiner, M. Grosche, W.A. Herrmann, W. Hieringer, G. Raudaschl-Sieber, *Chem. Eur. J.*, **2000**, *6*, 1773.

9 J.C. Green, R.G. Scurr, P.L. Arnold, F.G.N. Cloke, *Chem. Commun.*, **1997**, 1963.

10 2D NMR experiments were performed by Mrs J.M. Street; including 2D NOESY, gradient NOESY and NOE difference experiments.

11 B.J. Burger, J.E. Bercaw, *Experimental Organometallic Chemistry; A Practicum in Synthesis and Characterization*, A. L. Wayda, M.Y. Darensbourg, American Chemical Society, **1985**.

12 L. Xu, W. Chen, J.F. Bickley, A. Steiner, J. Xiao, *J. Organomet. Chem.*, **2000**, *598*, 409.

13 M.V. Baker, B.W. Skelton, A.H. White, C.C. Williams, *J. Chem. Soc., Dalton trans.*, **2001**, 111.

14 A.A. Danopoulos, S. Winston, personal communication.

Chapter 5

N-Heterocyclic Bis-Carbene Complexes of Palladium (II)

Chapter 5

N-Heterocyclic Bis-Carbene Complexes of Palladium (II)

5.1 Introduction

The pressing need for precise ligand design incorporating *N*-heterocyclic carbenes has opened a new area of research in homogeneous catalysis.[1] This research interest has been stimulated by the fact that carbenes are good ligand for late transition metals (strong σ-donors) as well as the observation that their complexes are able to promote a variety of catalytic reactions. *N*-Heterocyclic carbenes also show a number of other attractive characteristics including ease of electronic and steric tuning, formation of relatively strong and inert bonds to late transition metals and electronic similarity to the alkyl phosphines.[2] One of the most significant limitations of some homogeneous catalysts, especially phosphine based catalysts, is their relatively rapid deactivation, particularly when high temperatures or harsh conditions are needed. Compared with the electronically similar phosphine ligands, *N*-heterocyclic carbenes appear not to dissociate easily from the metal centre and are less prone to metal assisted decomposition leading to catalyst deactivation.

The growing importance of transition metal catalysed asymmetric synthesis has stimulated considerable efforts towards the development of new types of chiral ligands.[3] Chiral diphosphines, especially those with C_2 symmetry, have proven to be especially useful, resulting in good enantioselective control of the catalytic reactions. The potential of chiral auxiliary ligands that bind to the metal through nitrogen and carbon atoms is now being explored.[4] A limited number of examples of transition metal complexes containing chiral carbene ligands have been reported.[5]

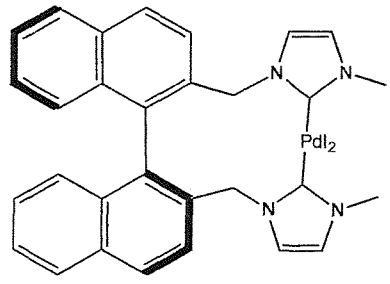

Figure 5.1. *N*-Heterocyclic carbene complex containing a chiral C_2 axis, reported by RajanBabu.[6]

Chiral information has been incorporated in a number of different ways on to *N*-heterocyclic carbenes:

i) A chiral centre on alkyl substituents directly linked to the imidazolin-2-ylidenes or imidazol-2-ylidenes rings,[7]

ii) A chiral centre integrated directly in to the imidazolin-2-ylidene ring,[8]

iii) A chiral centre on the functional group of *N*-functionalised imidazol-2-ylidenes,[9]

iv) A chiral C_2 axis built in to the framework of the *N*-heterocyclic carbenes attached to the chiral auxiliaries of binaphthyl or biphenyl type (*Figure 5.1*).[6]

As a logical extension of pyridine and picoline functionalised carbene complexes of palladium described in the previous chapters and those reported by McGuiness and Cavell,[10,11] the use of tridentate pincer architectures bearing carbene ligands was explored.

The compounds **(5.1)** and **(5.3)** are only the second examples of racemic mixtures of carbene complexes with a chiral C_2 axis, comparable with chiral phosphines of the BINAP family. The chiral nature of these complexes originates from the helical structures formed by the two-carbene moieties, which are linked by a lutidine backbone.

RESULTS AND DISCUSSION

5.2 Palladium (II) tridentate carbene complexes

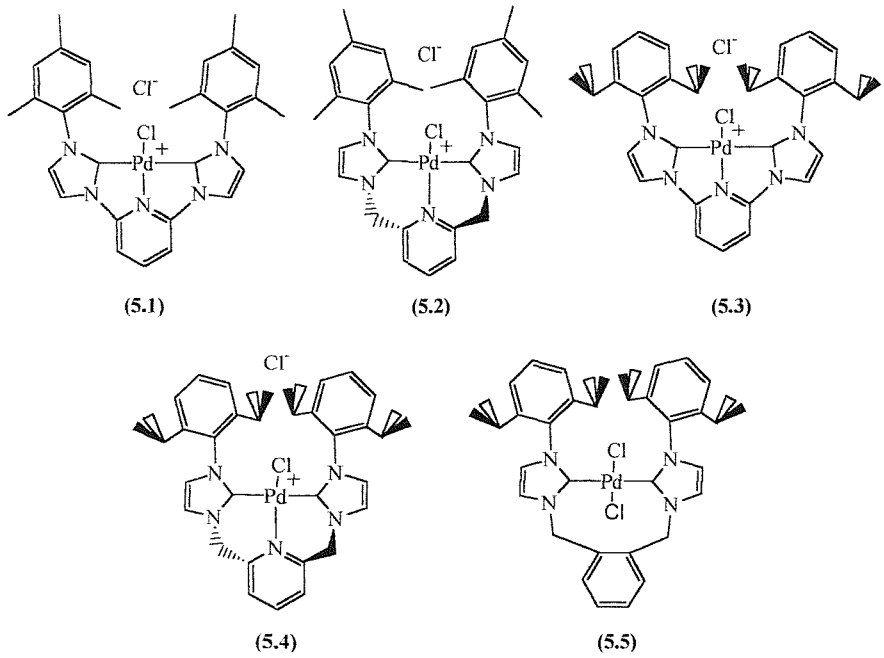

Figure 5.2. Palladium complexes **(5.1)-(5.5)**.

5.2.1. Synthesis of bis-carbene palladium complexes

The complexes described in this chapter were prepared by a similar method to that described in the previous chapter, general method (i), by the interaction of the analogous silver complexes[12] with cyclooctadiene (COD) palladium dichloride in dichloromethane.

Compounds **(5.1)**, **(5.2)**, **(5.3)**, **(5.4)** and **(5.5)** were isolated as air stable, pale yellow/colourless solids (*Figure 5.2*).

5.2.2. Electrospray mass spectroscopy

The electrospray mass spectra obtained for all the compounds contained a peak corresponding to the molecular ion $[Pd(ligand)Cl]^+$. This demonstrated that the ligand was chelating the palladium centre. However, the spectrum obtained for compound **(5.5)** also contained peaks corresponding to $[Pd(ligand)Cl + MeCN]^+$, $[Pd(ligand)Cl_2 + MeCN]^+$ and $[Pd_2(ligand)_2Cl_4 - 1]^+$. This suggested that the geometry of the complex was not as straight forward as in the other cases, possibly with the ligand bridging two metal centres.

5.2.3. Chemical analysis

The overall stoichiometry of the complexes was determined by chemical analysis, which showed that in all cases there was only one ligand for each palladium. However, the analysis of compounds **(5.1)**, **(5.2)**, **(5.3)** and **(5.4)** implied that, to a varying degree, silver chloride was also present in the compounds. Diethyl ether was also believed to be present in some of the analysis samples, this was due to it being used as a solvent for the fractional-crystallisation. The silver was removed from the complexes when repeated fractional-crystallisations were performed. The presence of silver in the analysis was due to the complex containing silver dichloride as the anion $[(AgCl_2)^-]$ rather than a chloride ion. The silver dichloride anion was later shown to be present in the X-ray crystal structure of compound **(5.3)**. In contrast, the crystal structure data for the compounds **(5.1)** and **(5.4)** were collected on crystals that had been repeatedly re-crystallised and showed only a chloride as the anion.

5.2.4. X-ray diffraction studies on complex (5.4)

X-ray diffraction quality crystals of {2,6-bis-[3-(2,6-di*iso*propylphenyl) imidazol-2-ylidene] pyridine} palladium dichloride **(5.4)** were obtained by layering a saturated dichloromethane solution with petrol (*Figure 5.3*).

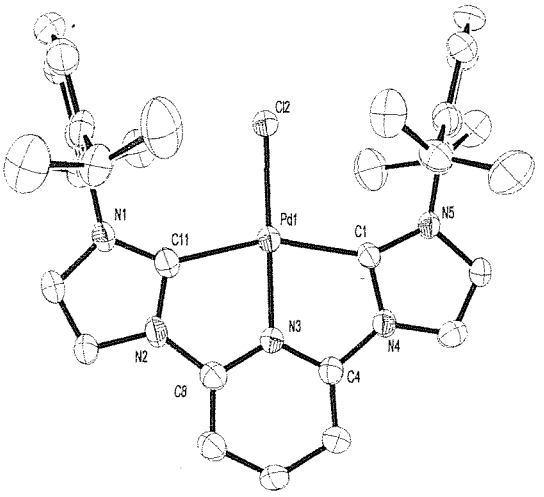

Figure 5.3. Cation from the X-ray crystal structure of {2,6-bis-[3-(2,6-di*iso*propylphenyl) imidazol-2-ylidene] pyridine} palladium dichloride, compound **(5.4)**.

The structure of **(5.4)** is very similar to that of a related complex, with methyl substituted carbene functionalities that has been reported since this work was carried out.[13] The structure comprises a palladium centre coordinated by the "pincer" type ligand and a chloride, which makes up the cation; and a chloride ion as the anion. The "pincer" ligand is coordinated to the square planar palladium centre with the carbene ends disposed *trans* to each other and the lutidine nitrogen *trans* to the chloride. The molecule is virtually planar except for the phenyl groups that are nearly perpendicular to the square plane of the palladium (twisted from the plane to reduce steric interactions, *Figure 5.4*).

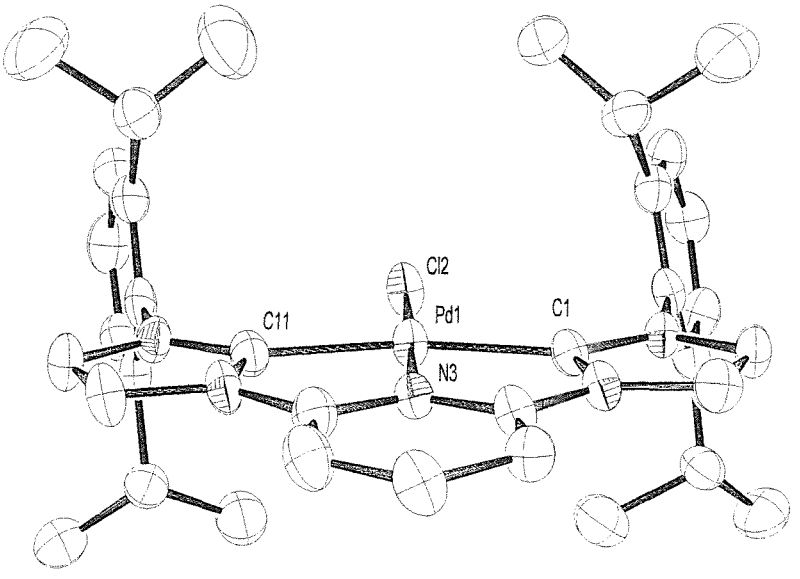

Figure 5.4. Cation from the X-ray crystal structure of {2,6-bis-[3-(2,6-di*iso*propylphenyl) imidazol-2-ylidene] pyridine} palladium dichloride, compound **(5.4)**.

The bite-angles between the carbene moieties and the nitrogen are very similar to that of compound **(4.4)**. However, the bond lengths around the palladium are not very similar; the palladium-nitrogen bond length is 0.2Å shorter at 1.98Å, and the palladium carbene bond lengths are about 0.05Å longer at 2.01 and 2.03Å (*Table 5.1*). This difference in bond length probably arises from the increased constraints built into the "pincer" ligand or possibly from the *trans* influence of the carbenes on one another. The carbene-palladium-carbene angle is only 158°, which shows that the square plane of the palladium is considerably distorted by the ligands constraints. All other metrical data are very similar to **(4.4)**.

5.2.5. X-ray diffraction studies on complex (5.3)

X-ray diffraction quality crystals of {α,α'-bis-[3-(2,6-di*iso*propylphenyl) imidazol-2-ylidene] lutidine} palladium dichloride **(5.3)** were obtained by layering a saturated dichloromethane solution with petrol (*Figure 5.4*). The coordination sphere of compound **(5.3)** is similar to that of **(5.4)**, comprising the square planar palladium centre coordinated by the two carbene ends of a ligand (disposed *trans* to each other), and the lutidine nitrogen *trans* to the chloride. However, there are two major differences in the structure Firstly, the anion comprises a silver atom coordinated by two chloride atoms; Secondly, and more interestingly, the ligand adopts a helical arrangement around the palladium centre. The beautiful helical structure of the cation is a direct result of the rigidity of the carbene and lutidyl rings and the flexibility of the methylene bridges, which create two puckered six-membered chelate rings with a C_2 axis along the nitrogen-palladium bond (*Figure 5.5*).

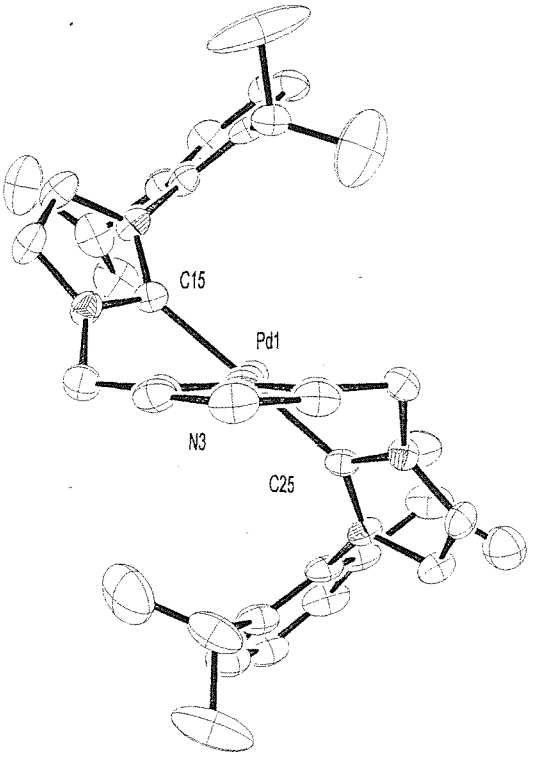

Figure 5.5. Cation from the X-ray crystal structure of {α,α'-bis-[3-(2,6-di*iso*propylphenyl) imidazol-2-ylidene] lutidine} palladium dichloride, compound **(5.3)**.

The helical conformation of the cation is most simply described by considering the angles that the carbene and lutidyl rings are twisted from the coordination plane of the palladium (*Figure 5.6*), when looking down the donor-palladium bond. Starting at a carbene end of the ligand of one enantiomer: the carbene ring is twisted clockwise by 38.9° from the coordination plane of the palladium; moving along the ligand, the lutidyl ring is twisted anticlockwise by 40.2° from the coordination plane of the palladium; moving along the ligand, the second carbene ring is twisted clockwise by 39.3°. As a consequence of the centro-symmetric nature of the space group ($P2_1/c$), the second enantiomer is generated through an inversion centre leading to a racemic mixture in the crystal lattice.

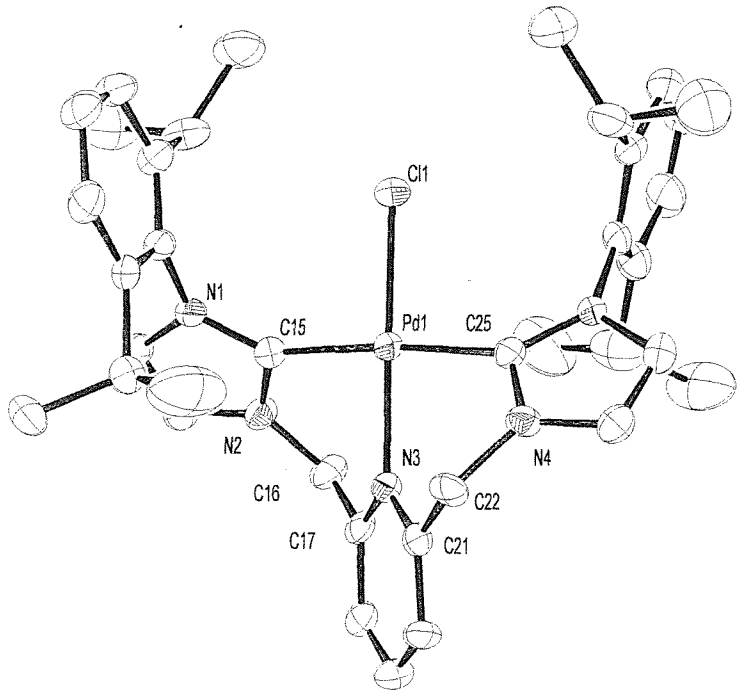

Figure 5.6. Cation from the X-ray crystal structure of {α,α'-bis-[3-(2,6-di*iso*propylphenyl) imidazol-2-ylidene] lutidine} palladium dichloride, compound **(5.3)**.

The phenyl rings are twisted by 81.9° and 79.9° from the planes of the carbene rings. The palladium-nitrogen bond length is 2.074Å (*Table 5.1*) and the palladium-carbene bond lengths are both 2.03Å; similarly different from its bidentate counterpart **(4.3)**, as **(5.4)** is from its counterpart **(4.4)**. The bite-angles between the nitrogen and the carbenes are 87.4° and 87.7°, just over 2° larger than **(4.3)**. The carbene-palladium-carbene angle is 175.0°, but all other metrical data are very similar to **(4.3)**.

Compound	Pd–N (Å)	Pd–C (Å)	N–Pd–C (°)	C–Pd–C (°)
(5.1)	2.071(4)	1.999(6), 2.021(6)	87.1(2), 87.7(2)	174.5(2)
(5.3)	2.074(3)	2.025(4), 2.029(4)	87.4(1), 87.7(1)	175.1(2)
(5.4)	1.975(7)	2.014(9), 2.033(9)	78.9(3), 79.2(3)	158.1(4)
(5.5)	—	1.98(2), 1.981(18), 2.00(2), 2.03(2)	—	163.7(8), 170.9(7)

Table 5.1. Palladium-carbon and palladium-nitrogen bond lengths, and nitrogen-palladium-carbon and carbon-palladium-carbon angles.

5.2.6. X-ray diffraction studies on complex (5.1)

X-ray diffraction quality crystals of {α,α'-bis-[3-(mesityl) imidazol-2-ylidene] lutidine} palladium dichloride **(5.1)** were obtained by layering a saturated dichloromethane solution with petrol (*Figure 5.7*). The helical conformation of the structure is similar to that in compound **(5.3)**.

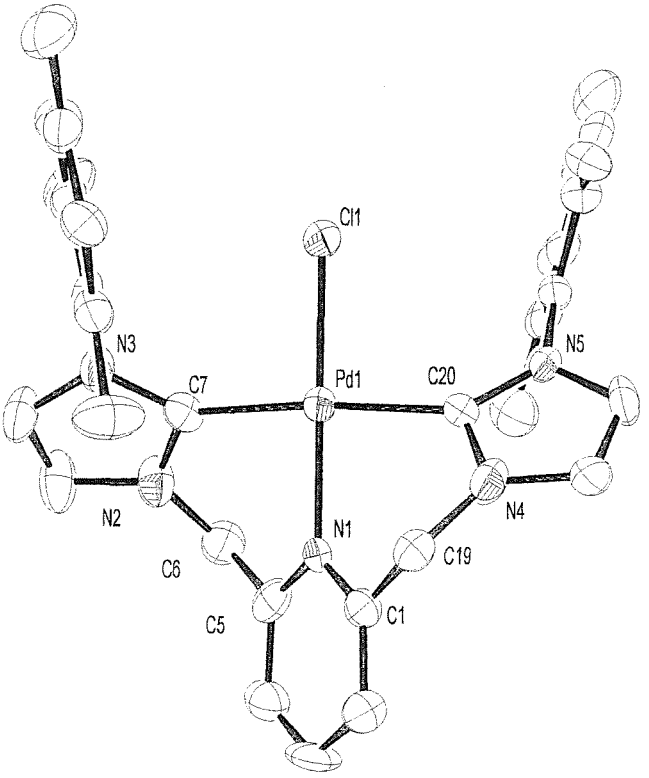

Figure 5.7. Cation from the X-ray crystal structure of {α,α'-bis-[3-(mesityl) imidazol-2-ylidene] lutidine} palladium dichloride, compound **(5.1)**.

The palladium-nitrogen and palladium-carbene bond lengths are similar to that of **(5.3)** and the carbene-palladium-carbene angle is 174° (*Table 5.1*). The helical conformation of the cation is most simply described by considering the angles that the carbene and lutidyl rings are twisted from the coordination plane of the palladium (*Figure 5.7*), when looking down the donor-palladium bond. Starting at a carbene end of one enantiomer: the carbene ring is twisted clockwise by 36.8° from the coordination plane of the palladium; moving along the ligand, the lutidyl ring is twisted anticlockwise by 40.0° from the coordination plane of the palladium; moving along the ligand, the second carbene ring is twisted clockwise by 39.9° form the coordination plane of the palladium. All other metrical data are very similar to **(4.2)**.

5.2.7. NMR spectroscopy

Similarly to the palladium complexes described in Chapter Four, the peaks in the ^{1}H and $^{13}C\{H\}$ NMR spectra used to characterise compounds **(5.1)**, **(5.2)**, **(5.3)**, and **(5.4)** are:

i) A weak peak downfield of 160 ppm in the $^{13}C\{^{1}H\}$ NMR spectra which can be assigned to the carbene carbon (observed in these complexes between 168 and 175 ppm);

ii) The pair of doublets observed between 5.4 and 6.5 ppm in the ^{1}H NMR spectra for the lutidyl carbene complexes (assigned to the diastereotopic protons on the methylene bridge), and a peak observed at 55 ppm in the $^{13}C\{H\}$ NMR spectra (assigned to the carbon of the methylene bridge);

iii) A doublet observed between 8.4 and 9.0 ppm, and a triplet observed between 8.0 and 8.5ppm in the ^{1}H NMR spectra (assigned to the protons in the 3,5- and 4-positions of the lutidyl or pyridyl ring);

iv) The presence of two doublets, with very small coupling constants, between 6.7 and 7.0 ppm, and 7.9 and 9.3 ppm in the ^{1}H NMR spectra (assigned to the protons in the 5- and 4-position on the imidazol-2-ylidene ring).

The other peaks in the ^{1}H NMR spectra are assigned to the protons of the R group on the imidazol-2-ylidene ring. The ^{1}H NMR spectra obtained for **(5.2)** and **(5.4)** are relatively simple as the complexes in solution retain their high degree of symmetry observed in the crystal structure of compound **(5.4)**.

The peaks associated with the methyls of the *iso*propyls of **(5.4)** are a pair of doublets, one doublet assigned to the four methyls pointing towards the lutidyl ring, and the other assigned to the methyls pointing away (at elevated temperatures these methyls exchange, which is shown by the peaks becoming one doublet). A septet is observed in the ^{1}H NMR spectrum assigned to the protons on the secondary carbons of the *iso*propyls. A doublet and a triplet are observed, which can be assigned to the protons of the phenyl ring.

The ^{1}H NMR spectrum for **(5.2)** contains peaks assigned to the protons on the methyls of the mesityl substituent at 2.0 and 2.2 ppm as well as a peak at 6.9 ppm assigned to the *CH* protons on the mesityl substituent. The $^{13}C\{H\}$ NMR spectra of complexes **(5.2)** and **(5.4)** are similarly simple, and the chemical shifts are comparable to those of the comparable *bidentate* complexes described in Chapter Four.

The peaks assigned to the R groups in the ^{1}H NMR spectra of complexes **(5.1)** and **(5.3)** are not as straight forward as the analogous planar complexes **(5.2)** and **(5.4)**. The

complexity of these spectra are caused by the solid-state structures of **(5.1)** and **(5.3)** being persistent in solution.

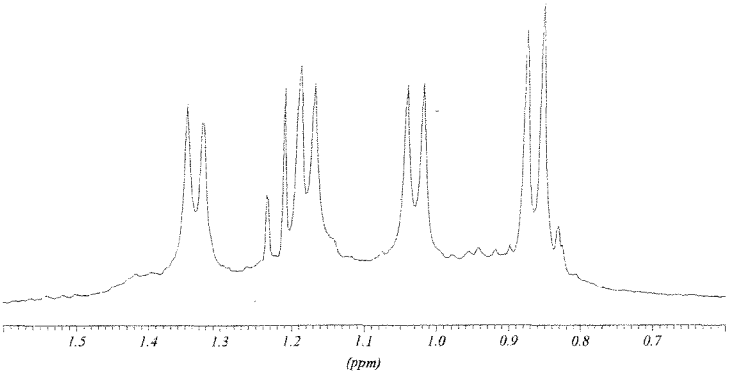

Figure 5.8. The *iso*propyl methyl region of the ^{1}H NMR spectrum of compound **(5.3)**.

The ^{1}H NMR spectrum of **(5.3)** contains four doublets that can be assigned to the protons on the four types of *iso*propyl methyl (*Figure 5.8*). These four categories of *iso*propyl methyls are best defined by labelling them as pointing towards (T) or away (A) from the lutidyl ring, and by labelling them as being above/below (O) the helix or level with the centre (C) of the helix. Therefore, the four types of methyl are TO, TC, AO and AC; each associated to one of the doublets in the *iso*propyl methyl region of the ^{1}H NMR spectrum.

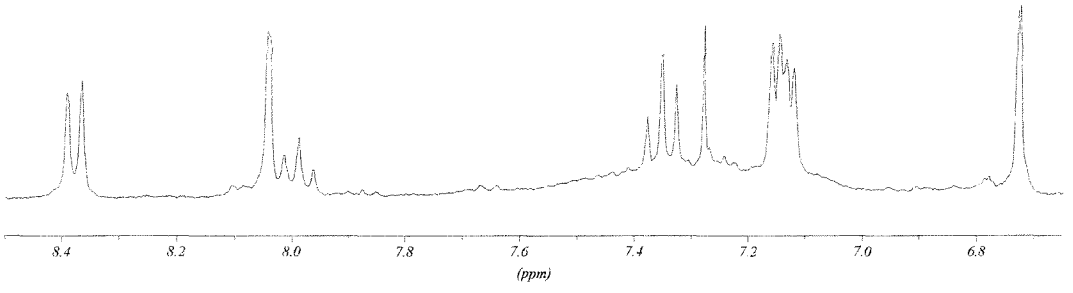

Figure 5.9. The aromatic regions of the ^{1}H NMR spectrum of compound **(5.3)**.

The protons in the *meta* positions on the phenyl ring can also be divided into two categories; those that are above/below the helix of the structure and those that are level with the central region of the helix of the structure; which lead to two doublets in the ^{1}H NMR spectrum (*Figure 5.9*).

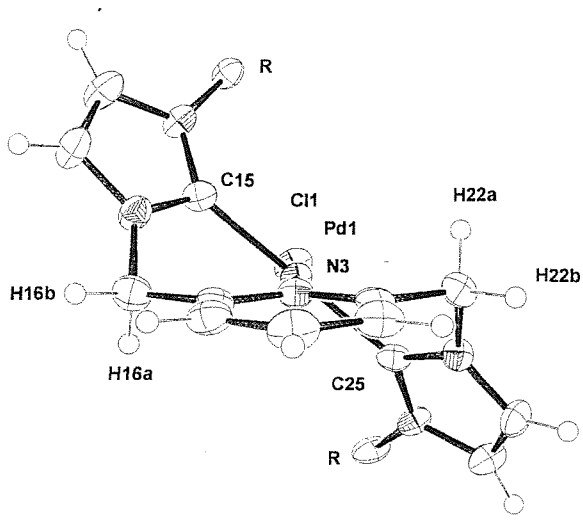

Figure 5.10. Cation from the X-ray crystal structure of {α,α'-bis-[3-(2,6-di*iso*-propylphenyl) imidazol-2-ylidene] lutidine} palladium dichloride, compound **(5.3)**. R = 2,6-di*iso*propylphenyl.

The solid-state structure of compound **(5.3)** is also shown to be persistent in solution by the peaks assigned to the methylene-bridge protons in the ^{1}H NMR spectra, which appear as a pair of doublets. Each of these doublets can be assigned to either the protons pointing in an axial (H22a, H26a) or in an equatorial direction (H22b, H26b), in relation to the plane of the lutidyl ring (*Figure 5.10* and *Figure 5.11*).

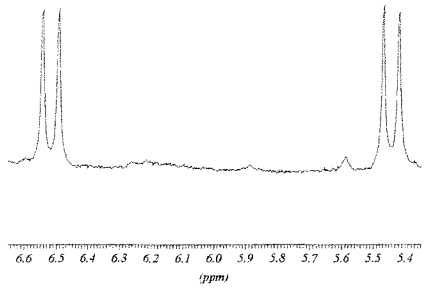

Figure 5.11. The bridging methylene regions of the ^{1}H NMR spectrum of compound **(5.3)**.

The helical C_2 symmetrical structure of **(5.3)** is persistent in solution at least up to 80 °C in C_6D_5Cl as shown by variable temperature ^{1}H NMR spectroscopy. However, at these elevated temperatures the *iso*propyls rotate, resulting in the methyls labelled TO and AO, and TC and AC exchange to give only two doublets in the ^{1}H NMR spectrum, related to those above/below (O) or in the centre (C). This supports the assumption that a high

activation barrier exists for any enantiomeric interconversion of this complex, and therefore leads to the realistic possibility of resolving the racemic mixture by chemical or chromatographic means. The $^{13}C\{H\}$ NMR spectrum is equally complex, with analogous peaks to that of the ^{1}H NMR spectrum.

The ^{1}H NMR spectrum of compound **(5.1)** contains three peaks that can be assigned to the protons of the three categories of methyls of the mesityl groups. Firstly, the two methyls in the *para* position of the mesityl rings, secondly, the two methyls that are above/below the helix of the structure, and lastly, the two methyls that are level with the central region of the helix (*Figure 5.12*). The protons on the mesityl ring can also be divided into two groups; those that are above/below the helix of the structure and those that are level with the central region of the helix; which results in two peaks in the ^{1}H NMR spectrum.

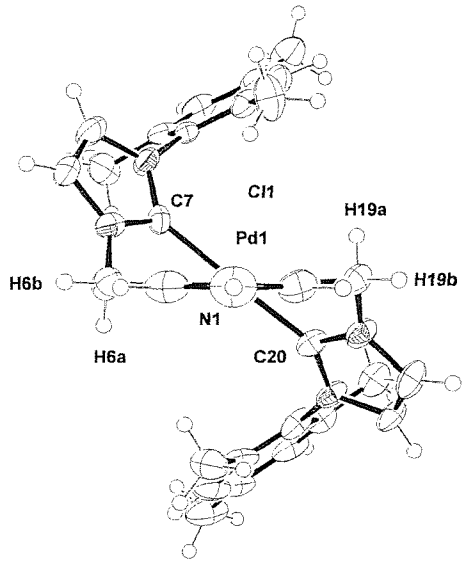

Figure 5.12. Cation from the X-ray crystal structure of {α,α'-bis-[3-(mesityl) imidazol-2-ylidene] lutidine} palladium dichloride, compound **(5.1)**.

Like compound **(5.3)**, the peaks (in the ^{1}H NMR spectrum of **(5.1)**) assigned to the methylene-bridge protons appear as a pair of doublets. Each of these doublets can be assigned to either the two protons pointing in an axial or the protons in an equatorial direction, in relation to the plane of the lytidyl ring (*Figure 5.12*). In addition, like compound **(5.3)**, the conformation of **(5.1)** is rigid at elevated temperatures. The $^{13}C\{H\}$ NMR spectrum is similarly complex and contains analogous peaks to that of the ^{1}H NMR spectrum.

5.2.8. Chirality of (5.3) and (5.1) in solution

In order to demonstrate the chiral nature of compounds **(5.3)** and **(5.1)** in solution, Pirkle's acid [TFAE, S-(+)-2,2,2-trifluoro-1-(9-anthryl)ethanol] (*Figure 5.14*) was used as a chiral discriminating agent on a sample of **(5.3)**.[14] The regions of the ^{1}H NMR spectrum, corresponding to the protons of the methyls of the *iso*propyl groups and the protons of the methylene bridge, after addition of 3.4 equivalents of TFAE to a solution of **(5.3)** in deuterated dichloromethane (*Figure 5.13*). The four doublets (*Figure 5.8*) are split to give eight doublets of equal intensity (four for each enantiomer). The doublet, corresponding to the axially pointing protons of the methylene bridge (H22a and H16a in *Figure 5.10*), is split into a pair of doublets (one for each enantiomer). The splitting of these peaks originates from the interaction of the chiral discriminating agent with the two enantiomers of **(5.3)**. The other peaks in the ^{1}H NMR spectrum are unchanged, as the TFAE does not allow the differentiation of the other protons on the two enantiomers.

(a)

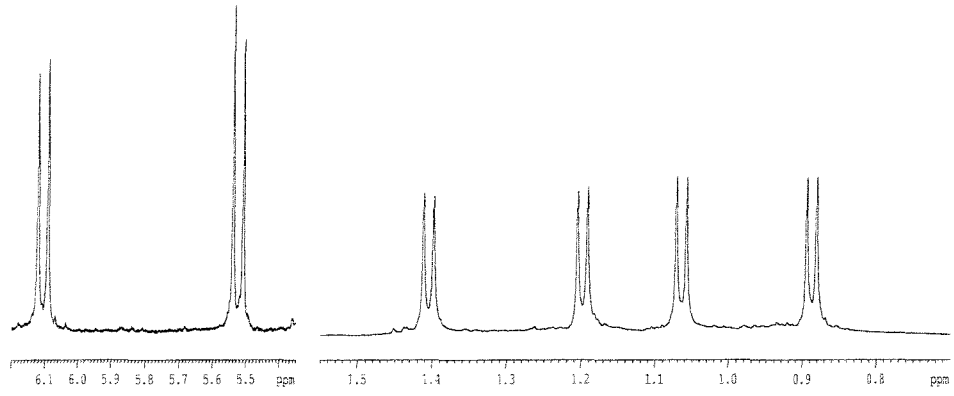

(b)

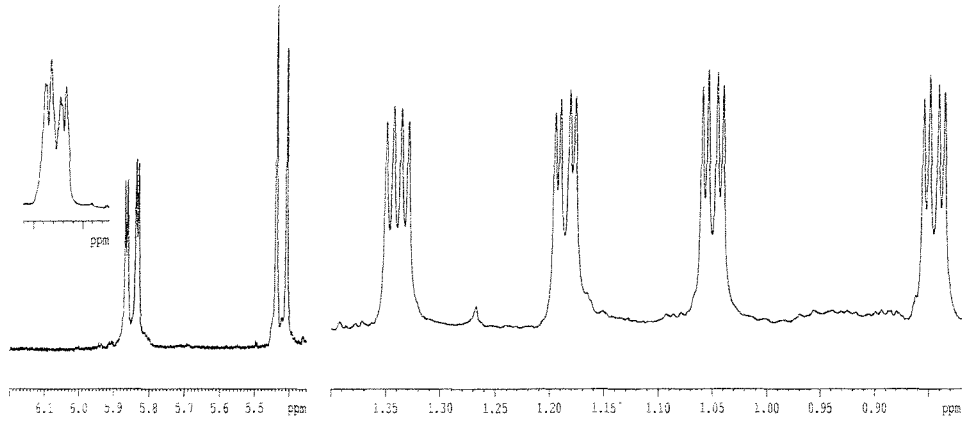

Figure 5.13. The *iso*propyl methyl- and bridging methylene-regions of the ^{1}H NMR spectrum of **(5.3)**, before (a) and after (b) the addition of Pirkle's acid.

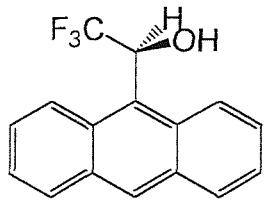

Figure 5.14. Pirkle's acid. [TFAE, S-(+)-2,2,2-trifluoro-1-(9-anthryl)ethanol]

5.2.9. X-ray diffraction studies on complex (5.5)

X-ray diffraction quality crystals of {α,α'-bis-[3-(2,6-di*iso*propylphenyl) imidazol-2-ylidene] *o*-xylene} palladium dichloride **(5.5)** were obtained by layering a saturated dichloromethane solution with petrol (*Figure 5.15* and *Figure 5.16*). The asymmetric unit contains a monomeric complex, comprising a palladium centre ligated by two chlorides and a chelating ligand, and half a centro-symmetric dimeric complex. The dimer comprises two symmetry equivalent palladium atoms each ligated by two chlorides and bridged by two symmetry equivalent ligands.

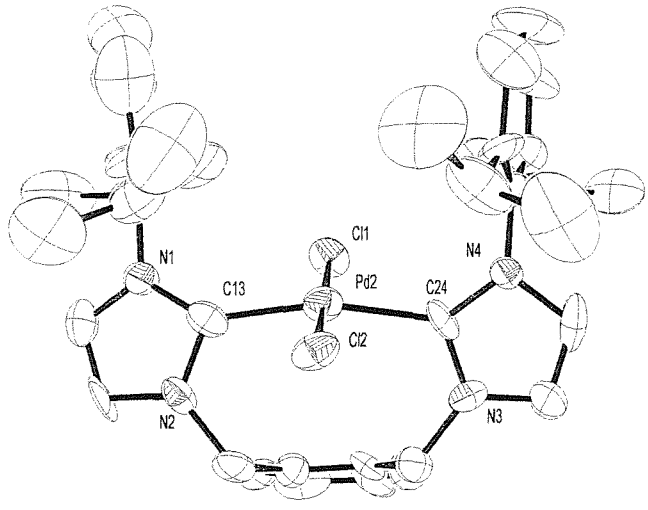

Figure 5.15. The monomeric complex from the X-ray crystal structure of {α,α'-bis-[3-(2,6-di*iso*propylphenyl) imidazol-2-ylidene] *o*-xylene} palladium dichloride, compound **(5.5)**.

In the monomeric complex (*Figure 5.15*), the two carbenes of the chelating ligand are disposed *trans* across the palladium centre. The geometry around the palladium is square planar, with two chlorides filling the other two positions. The palladium-carbon bonds in this fragment are 1.98 and 2.03Å (*Table 5.1*), and the palladium-chlorine bonds are 2.28 and 2.35Å (*Table 5.5*).

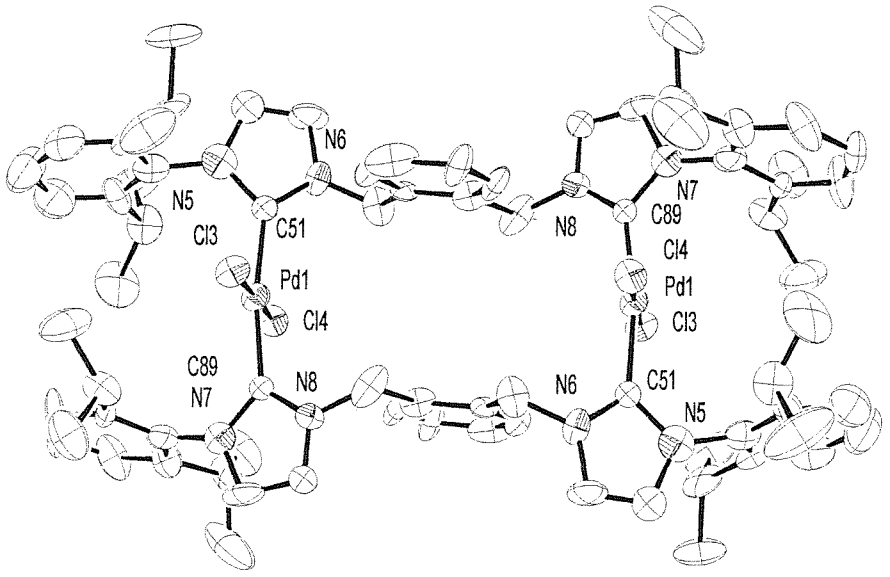

Figure 5.16. The dimeric complex from the X-ray crystal structure of {α,α'-bis-[3-(2,6-di*iso*propylphenyl) imidazol-2-ylidene] *o*-xylene} palladium dichloride, compound **(5.5)**.

In the dimeric complex (*Figure 5.16*), two bridging ligands coordinate to the two palladium centres, so that the carbene ends are disposed *trans* to one another. The other positions of each of the palladium square planes are filled by chlorides. The palladium-carbon bond lengths in this fragment are 1.97 and 1.99Å (*Table 5.1*) and the palladium-chlorine bond lengths are 2.31Å (*Table 5.5*). The remainder of the bond lengths and angles are as expected. The ^{1}H NMR spectrum proved to be unassignable because of the number, and broadness, of the peaks. The ^{1}H NMR spectrum of the reaction mixture appeared to contain peaks for a number of other oligomers. The ^{13}C{H} NMR spectrum was also unassignable due to the large numbers of similar peaks.

5.2.10. Reaction *5.4.2*

Reaction ***5.4.2*** comprised of stirring {{1,1-bis-[3-(2,6-di*iso*propylphenyl)-imidazol-2-ylidene]-methane}disilver dichloride} with (cyclooctadiene palladium dichloride) in dichloromethane in an attempt to synthesise {1,1-bis-[3-(2,6-di*iso*propylphenyl) imidazol-2-ylidene]-methane} palladium dichloride. Although pure complexes were not obtained, characterisation methods suggested that these target complexes were present within the reaction mixture. However, normal separation and purification techniques failed to produce them as pure solids. Electrospray mass spectrometry proved to be useful in identifying the products of the reaction, with peaks

observed corresponding to $[(ligand)_2Pd(MeCN)_2]^{2+}$, $[(ligand)_2Pd]^{2+}$ and $[(ligand)PdCl(MeCN)]^{+}$. The ^1H NMR spectrum in deuterated chloroform contained broad peaks around 1.0, 2.5, 5.0, 7.0 and 8.0 ppm. The broad ^1H NMR spectrum and the mass spectrum suggests that the impurities in the reaction could be a palladium complex comprising two ligands bound to the metal centre, and that a mixture of coordination isomers of the target molecule were formed.

5.3 Conclusion

The synthesis and characterisation of a number of palladium complexes with "pincer" type mixed donor *N*-heterocyclic carbene ligands have been described in this chapter, as well as a palladium complex with a bis-carbene xylyl bridged ligand.

Compounds **(5.1)** and **(5.3)** are the first examples of *N*-heterocyclic carbene complexes that contain a stereogenic C_2 axis that was not pre-formed in the ligand. Furthermore, the chiral nature of the complex in solution has been confirmed by the use of a chiral-discriminating agent implying that the separation of the two enantiomers is possible. Most importantly, these complexes have been shown to be conformationally rigid in solution at temperatures as high as 80°C. This could be developed into a convenient method to a single enantiomer of the complex by using a recoverable chiral salt in the reaction mixture in order to imprint the chiral information on the complex.

Although compounds **(5.2)** and **(5.4)** are similar to the pincer complex reported by Crabtree,[13] they were developed independently and submitted for publication[15] prior to their paper being published.

EXPERIMENTAL

5.4 Synthesis of bis-carbene palladium complexes

5.4.1. General method:

A dichloromethane solution of the corresponding silver carbene complex was added drop wise to a solution of cyclooctadiene (COD) palladium dichloride and stirred at room temperature for 12-24 hours (*Scheme 5.1*). After completion, the reaction mixture was filtered, the volatiles were removed under vacuum, and the resulting solid was washed with diethyl ether. Drying under vacuum gave the products as pale yellow solids.

In most cases, the solids were purified by recrystallisation from a saturated solution of dichloromethane and diethyl ether or by extraction into hot toluene.

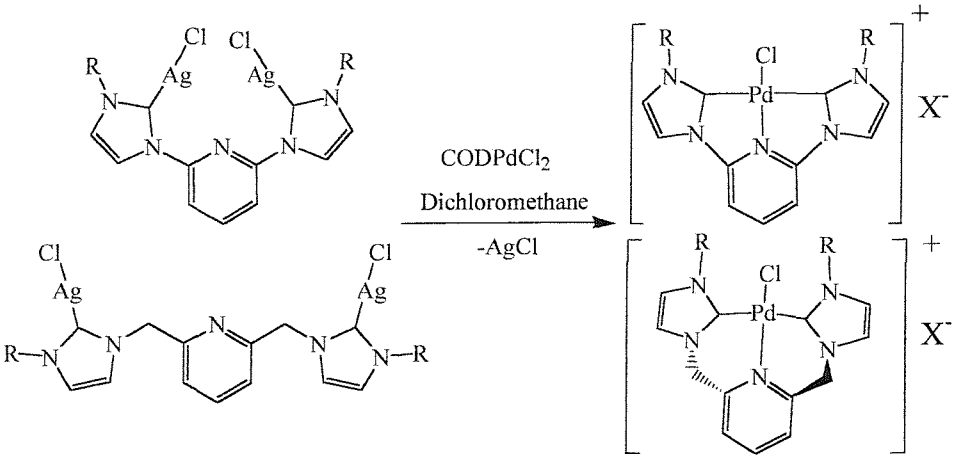

Scheme 5.1. Synthesis of complexes **(5.1)-(5.4)**, R = mesityl or 2,6-di*iso*propylphenyl, X^- = Cl^-, $AgCl_2^-$.

(5.1) {α,α'-bis-[3-(mesityl) imidazol-2-ylidene] lutidine} palladium dichloride

This was prepared following the general method from {α,α'-bis-[3-(mesityl)-imidazol-2-ylidene]-lutidine} disilver dichloride (0.2g, 0.26mmol) and (COD) palladium dichloride (0.08g, 0.26mmol) in dichloromethane (100ml) by stirring at room temperature for 24 hours. The product was obtained in quantitative yields as a yellow solid. X-ray diffraction quality crystals were obtained by layering a saturated dichloromethane solution with petrol (*Table 5.2*).

Yield: 80%.

MS (ES): *m/z* 618.0, $[Pd(ligand)Cl]^+$.

δ_H($CDCl_3$) 1.9 (6H, s, CH_3), 2.1 (6H, s, CH_3), 2.3 (6H, s, CH_3), 6.3, 5.5 (4H, dd, CH_2), 6.7 (1H, d, 4-imidazol-2-ylidene *H*), 6.9 (2H, s, mesityl *H*), 6.9 (2H, s, mesityl *H*), 7.9 (1H, d, 5-imidazol-2-ylidene *H*), 8.1 (1H, t, 4-lutidyl *H*), 8.4 (1H, d, 3,5-lutidyl *H*).

δ_C($CDCl_3$) 19, 19 21, (mesityl CH_3), 55 (CH_2), 122 (5-imidazol-2-ylidene *C*), 123 (mesityl *C*), 127 (3,5-lutidyl *C*), 129, 129, 134, 135, 136, (mesityl *C*), 139 (4-imidazol-2-ylidene *C*), 141 (4-lutidyl *C*), 155 (2,6-lutidyl *C*), 168 (2-imidazol-2-ylidene C).

(Found: C, 50.27; H, 4.81; N, 8.71. $(C_{31}H_{33}Cl_2N_5Pd)_3Ag_2Cl_2$ calculated: C, 49.74; H, 4.44; N, 9.36%).

C(1)-N(1)	1.339(8)	C(10)-N(3)	1.441(8)
C(1)-C(19)	1.500(9)	C(19)-N(4)	1.427(8)
C(5)-N(1)	1.338(8)	C(20)-N(5)	1.345(7)
C(5)-C(6)	1.525(9)	C(20)-N(4)	1.374(8)
C(6)-N(2)	1.446(8)	C(20)-Pd(1)	2.021(6)
C(7)-N(2)	1.363(8)	C(21)-C(22)	1.338(9)
C(7)-N(3)	1.371(8)	C(21)-N(4)	1.385(8)
C(7)-Pd(1)	1.999(6)	C(22)-N(5)	1.368(8)
C(8)-C(9)	1.322(10)	C(23)-N(5)	1.431(8)
C(8)-N(2)	1.386(8)	N(1)-Pd(1)	2.071(4)
C(9)-N(3)	1.384(8)	Cl(1)-Pd(1)	2.2880(15)

N(1)-C(1)-C(19)	116.9(5)	C(1)-N(1)-Pd(1)	120.4(4)
N(1)-C(5)-C(6)	119.0(5)	C(7)-N(2)-C(8)	111.0(5)
N(2)-C(6)-C(5)	109.1(5)	C(7)-N(2)-C(6)	120.8(5)
N(2)-C(7)-N(3)	103.8(5)	C(7)-N(3)-C(9)	110.3(5)
N(2)-C(7)-Pd(1)	120.3(4)	C(7)-N(3)-C(10)	124.9(5)
N(3)-C(7)-Pd(1)	135.1(4)	C(20)-N(4)-C(21)	111.0(5)
C(9)-C(8)-N(2)	107.0(6)	C(20)-N(4)-C(19)	120.5(5)
C(8)-C(9)-N(3)	107.8(6)	C(20)-N(5)-C(22)	111.6(5)
N(4)-C(19)-C(1)	112.9(5)	C(20)-N(5)-C(23)	125.1(5)
N(5)-C(20)-N(4)	103.7(5)	C(7)-Pd(1)-C(20)	174.5(2)
N(5)-C(20)-Pd(1)	138.3(4)	C(7)-Pd(1)-N(1)	87.1(2)
N(4)-C(20)-Pd(1)	118.1(4)	C(20)-Pd(1)-N(1)	87.76(19)
C(22)-C(21)-N(4)	105.9(5)	C(7)-Pd(1)-Cl(1)	92.85(16)
C(21)-C(22)-N(5)	107.8(5)	C(20)-Pd(1)-Cl(1)	92.27(15)
C(5)-N(1)-C(1)	119.4(5)	N(1)-Pd(1)-Cl(1)	179.82(15)
C(5)-N(1)-Pd(1)	120.2(4)		

Table 5.2. Selected bond lengths (Å) and angles (°) for compound **(5.1)**.

(5.2) {2,6-bis-[3-(mesityl) imidazol-2-ylidene] pyridine} palladium dichloride

This was prepared following the general method from {2,6-bis-[3-(mesityl)-imidazol-2-ylidene]-pyridine}disilver dichloride (0.2g, 0.27mmol) and (COD) palladium dichloride (0.08g, 0.27mmol) in dichloromethane (100ml) by stirring at room temperature for 24 hours. The product was obtained in quantitative yields as a yellow solid (*Figure 5.17*).

MS (ES): *m/z* 589.7, $[Pd(ligand)Cl]^+$.

$\delta_H(CDCl_3)$ 2.0 (12H, s, mesityl CH_3), 2.2 (6H, s, mesityl CH_3), 6.9 (4H, s, mesityl *H*), 6.9 (2H, d, 5-imidazol-2-ylidene *H*), 8.5 (1H, d, 4-picolyl *H*), 9.0 (2H, d, 3,5-picolyl *H*), 9.3 (2H, d, 4-imidazol-2-ylidene *H*).

$\delta_C(CDCl_3)$ 18, 21 (CH_3), 111 (5-imidazol-2-ylidene C), 121 (mesityl *C*), 125 (3,5-pyridyl *C*), 129, 133, 134 (mesityl *C*), 140 (4-imidazol-2-ylidene C), 151 (4-pyridyl *C*), 169 (2,6-pyridyl *C*), 175 (2-imidazol-2-ylidene C).

(Found: C, 49.64; H, 6.12; N, 7.01. $[C_{29}H_{29}Cl_2N_5Pd(C_4H_{10}O)_3]AgCl$ calculated: C, 49.71; H, 6.00; N, 7.07%).

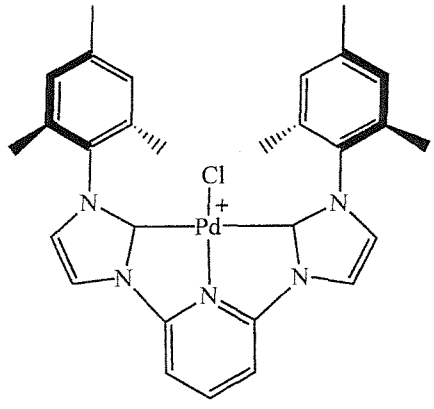

Figure 5.17. Cationic part of compound **(5.2)**.

(5.3) {α,α'-bis-[3-(2,6-di*iso*propylphenyl) imidazol-2-ylidene] lutidine} palladium dichloride

This was prepared following the general method from {α,α'-bis-[3-(2,6-di*iso*propylphenyl)-imidazol-2-ylidene]-lutidine}disilver dichloride (0.5g, 0.59mmol) and (COD) palladium dichloride (0.17g, 0.59mmol) in dichloromethane (150ml) by stirring at room temperature for 24 hours. The product was obtained in quantitative yields as a yellow solid. X-ray diffraction quality crystals were obtained by layering a saturated dichloromethane solution with petrol (*Table 5.3*).

MS (ES): *m/z* 702.2, $[Pd(ligand)Cl]^+$.

$\delta_H(CDCl_3)$ 0.9, 1.0, 1.2, 1.3 (24H, 4 × d, *iso*propyl C*H*$_3$), 1.9, 2.6 (4H, 2 × septet, *iso*propyl C*H*), 5.4, 6.5 (4H, 2 × d, C*H*$_2$), 6.7 (2H, d, 5-imidazol-2-ylidene *H*), 7.1, 7.2 (4H, 2 × d, ^{i}Pr$_2$C$_6$*H*$_2$H), 7.3 (2H, t, ^{i}Pr$_2$C$_6$H$_2$*H*), 8.0 (1H, t, 4-lutidyl *H*), 8.0 (2H, d, 4-imidazol-2-ylidene *H*), 8.4 (2H, d, 3,5-lutidyl *H*).

$\delta_C(CDCl_3)$ 23, 24, 25, 26 [CH(*C*H$_3$)], 28, 29 [*C*H(CH$_3$)], 55 (C*H*$_2$), 122 (5-imidazol-2-ylidene *C*), 123 (^{i}Pr$_2$*C*$_6$H$_3$ *C*), 124 (3,5-pyridyl *C*), 125, 127, 130, 135 (Pr$^i_2$*C*$_6$H$_3$ *C*), 142 (4-pyridyl *C*), 145 (4-imidazol-2-ylidene *C*), 147 (Pr$^i_2$*C*$_6$H$_3$ *C*), 155 (2,6-pyridyl *C*), 168 (2-imidazol-2-ylidene *C*).

(Found: C, 54.39; H, 5.95; N, 8.22. $(C_{38}H_{47}Cl_2N_5Pd)_5Ag_3Cl_3$ calculated: C, 54.52; H, 5.66; N, 8.37%).

C(1)-N(1)	1.445(5)	C(23)-C(24)	1.331(6)
C(13)-C(14)	1.341(6)	C(23)-N(4)	1.364(5)
C(13)-N(1)	1.379(5)	C(24)-N(5)	1.393(5)
C(14)-N(2)	1.373(5)	C(25)-N(5)	1.351(5)
C(15)-N(2)	1.345(5)	C(25)-N(4)	1.356(5)
C(15)-N(1)	1.350(5)	C(25)-Pd(1)	2.029(4)
C(15)-Pd(1)	2.025(4)	C(26)-N(5)	1.443(5)
C(16)-N(2)	1.455(5)	N(3)-Pd(1)	2.074(3)
C(16)-C(17)	1.493(6)	Cl(1)-Pd(1)	2.2756(11)
C(17)-N(3)	1.347(5)	Cl(6)-Ag(1)	2.3712(12)
C(21)-N(3)	1.346(5)	Cl(7)-Ag(1)	2.341(3)
C(21)-C(22)	1.512(5)	Cl(7')-Ag(1)	2.422(9)
C(22)-N(4)	1.464(5)		

N(2)-C(15)-N(1)	104.5(3)	C(15)-N(2)-C(16)	122.6(3)
N(2)-C(15)-Pd(1)	118.3(3)	C(14)-N(2)-C(16)	125.7(3)
N(1)-C(15)-Pd(1)	137.0(3)	C(17)-N(3)-Pd(1)	119.8(3)
N(2)-C(16)-C(17)	111.8(3)	C(25)-N(4)-C(23)	111.7(3)
N(3)-C(17)-C(18)	120.6(4)	C(25)-N(4)-C(22)	122.2(3)
N(3)-C(17)-C(16)	118.9(4)	C(23)-N(4)-C(22)	125.9(3)
C(18)-C(17)-C(16)	120.6(4)	C(25)-N(5)-C(24)	110.2(3)
N(3)-C(21)-C(22)	117.1(4)	C(25)-N(5)-C(26)	128.9(3)
N(4)-C(22)-C(21)	110.4(3)	C(15)-Pd(1)-C(25)	175.07(16)
C(24)-C(23)-N(4)	106.8(4)	C(15)-Pd(1)-N(3)	87.41(14)
C(23)-C(24)-N(5)	107.1(4)	C(25)-Pd(1)-N(3)	87.67(14)
N(5)-C(25)-N(4)	104.1(3)	C(15)-Pd(1)-Cl(1)	92.44(12)
N(5)-C(25)-Pd(1)	137.8(3)	C(25)-Pd(1)-Cl(1)	92.48(12)
N(4)-C(25)-Pd(1)	117.9(3)	N(3)-Pd(1)-Cl(1)	177.78(9)
C(15)-N(1)-C(13)	110.5(3)	Cl(7)-Ag(1)-Cl(6)	164.12(15)
C(15)-N(1)-C(1)	127.3(3)	Cl(7)-Ag(1)-Cl(7')	17.9(5)
C(15)-N(2)-C(14)	111.6(3)	Cl(6)-Ag(1)-Cl(7')	160.7(5)

Table 5.3. Selected bond lengths (Å) and angles (°) for compound **(5.3)**.

(5.4) {2,6-bis-[3-(2,6-di*iso*propylphenyl) imidazol-2-ylidene] pyridine} palladium dichloride

This was prepared following the general method from {2,6-bis-[3-(2,6-di*iso*propylphenyl)-imidazol-2-ylidene]-pyridine}disilver dichloride (0.5g, 0.61mmol) and (COD) palladium dichloride (0.17g, 0.61mmol) in dichloromethane (150ml) by stirring at room temperature for 24 hours. The product was obtained in quantitative yields as a yellow solid. X-ray diffraction quality crystals were obtained by layering a saturated dichloromethane solution with petrol (*Table 5.4*).

MS (ES): *m/z* 674.1, $[Pd(ligand)Cl]^+$.

$\delta_H(CDCl_3)$ 1.1, 1.2 (24H, 2 × d, *iso*propyl C*H*$_3$), 2.5 (4H, septet, *iso*propyl C*H*), 7.0 (2H, d, 5-imidazol-2-ylidene *H*), 7.2 (4H, d, $^iPr_2C_6H_2H$), 7.4 (2H, t, $^iPr_2C_6H_2H$), 8.5 (1H, t, 4-pyridyl *H*), 9.0 (2H, d, 3,5-lutidyl *H*), 9.3 (2H, d, 4-imidazol-2-ylidene *H*).

$\delta_C(CDCl_3)$ 23, 24 [CH(*C*H$_3$)], 28 [*C*H(CH$_3$)], 111 (5-imidazol-2-ylidene *C*), 120 ($Pr^i_2C_6H_3$ *C*), 124 (3,5-pyridyl *C*), 126, 132, 135 ($Pr^i_2C_6H_3$ *C*), 145 (4-midazol-2-ylidene *C*), 151 (4-pyridyl *C*), 170 (2,6-pyridyl *C*), 174 (2-imidazol-2-ylidene *C*).

(Found: C, 53.22; H, 5.60; N, 8.61. $(C_{36}H_{43}Cl_2N_5Pd)_5Ag_3Cl_3$ calculated: C, 53.44; H, 5.36; N, 8.66%).

Pd(1)-N(3)	1.975(7)	N(4)-C(3)	1.379(12)
Pd(1)-C(1)	2.014(9)	N(4)-C(1)	1.385(12)
Pd(1)-C(11)	2.033(9)	N(4)-C(4)	1.416(11)
Pd(1)-Cl(2)	2.283(2)	N(3)-C(4)	1.322(12)
N(5)-C(1)	1.342(11)	N(3)-C(8)	1.345(12)
N(5)-C(2)	1.404(12)	N(2)-C(11)	1.336(12)
N(5)-C(12)	1.456(12)	N(2)-C(9)	1.384(12)
N(1)-C(11)	1.344(12)	N(2)-C(8)	1.427(12)
N(1)-C(10)	1.395(12)	C(3)-C(2)	1.338(13)
N(1)-C(24)	1.450(13)	C(10)-C(9)	1.343(14)

N(3)-Pd(1)-C(1)	79.2(3)	C(4)-N(3)-C(8)	120.9(8)
N(3)-Pd(1)-C(11)	78.9(3)	C(4)-N(3)-Pd(1)	119.7(6)
C(1)-Pd(1)-C(11)	158.1(4)	C(8)-N(3)-Pd(1)	119.4(6)
N(3)-Pd(1)-Cl(2)	179.4(2)	C(11)-N(2)-C(9)	113.0(8)
C(1)-Pd(1)-Cl(2)	101.3(2)	C(11)-N(2)-C(8)	119.9(7)
C(11)-Pd(1)-Cl(2)	100.6(3)	C(9)-N(2)-C(8)	127.1(8)
C(1)-N(5)-C(2)	111.4(7)	C(2)-C(3)-N(4)	105.8(8)
C(1)-N(5)-C(12)	124.6(8)	C(3)-C(2)-N(5)	107.5(8)
C(11)-N(1)-C(10)	110.5(8)	N(5)-C(1)-N(4)	103.1(7)
C(11)-N(1)-C(24)	127.0(8)	N(5)-C(1)-Pd(1)	144.7(7)
C(3)-N(4)-C(1)	112.3(7)	N(4)-C(1)-Pd(1)	112.0(6)
C(3)-N(4)-C(4)	129.7(8)	C(9)-C(10)-N(1)	107.5(9)
C(1)-N(4)-C(4)	117.9(7)	C(10)-C(9)-N(2)	104.8(8)

N(1)-C(11)-N(2)	104.2(7)	N(3)-C(4)-N(4)	111.2(8)
N(1)-C(11)-Pd(1)	143.7(7)	N(3)-C(8)-N(2)	109.7(8)
N(2)-C(11)-Pd(1)	112.1(7)		

Table 5.4. Selected bond lengths (Å) and angles (°) for compound **(5.4)**. Symmetry transformations used to generate equivalent atoms: #1 -x+2,-y+1,-z

(5.5) {α,α'-bis-[3-(2,6-di*iso*propylphenyl) imidazol-2-ylidene] *o*-xylene} palladium dichloride

This was prepared following the general method from {α,α'-bis-[3-(2,6-di*iso*propylphenyl)-imidazol-2-ylidene]-*o*-xylene} disilver dichloride (0.2g, 0.24mmol) and COD palladium dichloride (0.07g, 0.24mmol) in dichloromethane (100ml) by stirring at room temperature for 24 hours. The product was obtained in quantitative yields as a yellow solid. X-ray diffraction quality crystals were obtained by layering a saturated dichloromethane solution with petrol (*Figure 5.18* and *Table 5.5*).

MS (ES): *m/z* 617.2, $[Pd(ligand)Cl]^+$,656.3, $[Pd(ligand)Cl+MeCN]^+$, 694.2, $[Pd(ligand)Cl_2+MeCN]^+$, 1302.1, $[Pd_2(ligand)_2Cl_4 -1]^+$.

$\delta_H(CDCl_3)$ very broad spectrum (see discussion)

(Found: C, 62.64; H, 6.74; N, 6.92. $C_{39}H_{48}Cl_2N_4Pd$ calculated: C, 62.44; H, 6.45; N, 7.47%).

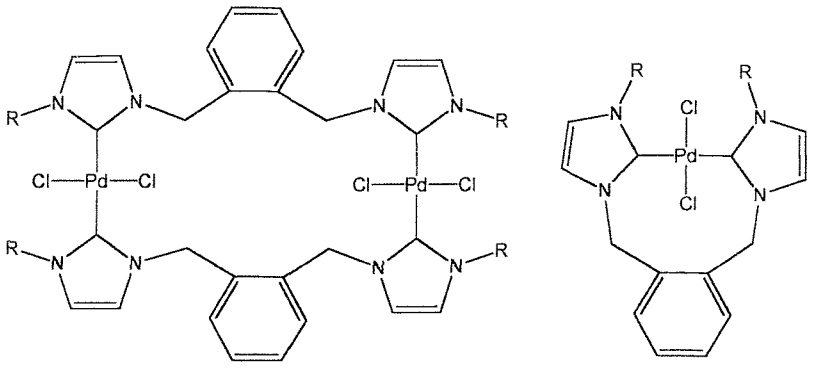

Figure 5.18. Coordination isomers of {α,α'-bis-[3-(2,6-di*iso*propylphenyl) imidazol-2-ylidene] *o*-xylene} palladium dichloride, compound **(5.5)**.

C(13)-N(1)	1.337(19)	C(89)-N(8)#1	1.319(17)
C(13)-N(2)	1.407(18)	C(89)-N(7)	1.372(18)
C(13)-Pd(2)	1.981(18)	C(89)-Pd(1)	1.998(16)
C(24)-N(4)	1.335(16)	N(8)-C(89)#1	1.319(17)
C(24)-N(3)	1.370(19)	Cl(1)-Pd(2)	2.283(4)
C(24)-Pd(2)	2.033(17)	Cl(2)-Pd(2)	2.352(4)
C(51)-N(6)	1.338(18)	Cl(3)-Pd(1)	2.312(4)
C(51)-N(5)	1.444(18)	Cl(4)-Pd(1)	2.308(4)
C(51)-Pd(1)	1.976(16)		

N(1)-C(13)-N(2)	100.0(15)	C(51)-N(6)-C(53)	113.6(15)
N(1)-C(13)-Pd(2)	141.6(15)	C(51)-N(6)-C(54)	119.6(15)
N(2)-C(13)-Pd(2)	117.9(14)	C(53)-N(6)-C(54)	125.7(15)
N(4)-C(24)-N(3)	107.1(15)	C(89)#1-N(8)-C(91)	118.2(16)
N(4)-C(24)-Pd(2)	136.0(15)	C(89)#1-N(8)-C(61)	122.5(16)
N(3)-C(24)-Pd(2)	116.8(13)	C(91)-N(8)-C(61)	118.7(17)
N(6)-C(51)-N(5)	100.7(14)	C(51)-Pd(1)-C(89)	170.9(7)
N(6)-C(51)-Pd(1)	127.4(13)	C(51)-Pd(1)-Cl(4)	88.5(5)
N(5)-C(51)-Pd(1)	131.6(13)	C(89)-Pd(1)-Cl(4)	91.6(4)
N(8)#1-C(89)-N(7)	100.1(14)	C(51)-Pd(1)-Cl(3)	91.5(5)
N(8)#1-C(89)-Pd(1)	127.2(13)	C(89)-Pd(1)-Cl(3)	88.8(4)
N(7)-C(89)-Pd(1)	132.5(14)	Cl(4)-Pd(1)-Cl(3)	177.61(17)
C(15)-N(2)-C(13)	113.4(16)	C(13)-Pd(2)-C(24)	163.7(8)
C(15)-N(2)-C(16)	125.4(16)	C(13)-Pd(2)-Cl(1)	90.7(5)
C(13)-N(2)-C(16)	121.2(15)	C(24)-Pd(2)-Cl(1)	89.3(5)
C(24)-N(3)-C(25)	112.0(16)	C(13)-Pd(2)-Cl(2)	90.0(5)
C(24)-N(3)-C(23)	122.8(16)	C(24)-Pd(2)-Cl(2)	90.9(4)
C(25)-N(3)-C(23)	125.2(16)	Cl(1)-Pd(2)-Cl(2)	176.92(16)

Table 5.5. Selected bond lengths (Å) and angles (°) for compound **(5.5)**. Symmetry transformations used to generate equivalent atoms: #1 -x,-y,-z

Compound	(5.1)	(5.3)	(5.4)	(5.5)
Chemical formula	$C_{31}H_{33}Cl_2N_5Pd$	$C_{40}H_{45}AgCl_9N_5Pd$	$C_{36}H_{41}Cl_{4.5}N_5Pd$	$C_{38}H_{46}Cl_2N_4Pd$
Formula weight	652.92	1129.13	809.66	535.34
Crystal system	Monoclinic	Monoclinic	Triclinic	Monoclinic
Space group	$P\,2_1/n$	$P\,2_1/c$	P -1	$P\,2_1/c$
a/Å	10.823(2)	11.559(2)	8.4782(4)	16.948(3)
b/Å	20.571(4)	42.043(8)	11.8790(6)	33.444(7)
c/Å	19.286(4)	10.631(2)	20.8146(11)	16.958(3)
α/°	90	90	75.077(3)	90
β/°	90.86(3)	112.51(3)	83.364(3)	98.70(3)
γ/°	90	90	71.322(2)	90
V/Å^3	4293.5(15)	4772.6(16)	1917.65(17)	9501(3)
Z	4	4	2	11
T/K	150(2)	150(2)	150(2)	150(2)
μ/mm^{-1}	0.577	1.325	0.829	0.527
F(000)	1336	2264	829	3056
No. Data collected	30684	28393	14147	33749
No. Unique data	9674	10436	6524	12829
R_{int}	0.0863	0.0867	0.0839	0.2453
Final R(|F|) for $F_O > 2\sigma(F_o)$	0.0855	0.0514	0.0838	0.1012
Final R(F^2) for all data	0.1250	0.0897	0.1316	0.3391

Table 5.6. Crystallographic parameters for compounds **(5.1)**, **(5.3)**, **(5.4)** and **(5.5)**.

5.4.2. Reaction between {1,1-bis-[3-(2,6-di*iso*propylphenyl) imidazol-2-ylidene]-methane} disilver dichloride and (COD) palladium dichloride

This was performed following the general method from {1,1-bis-[3-(2,6-di*iso*propylphenyl)-imidazol-2-ylidene]-methane}disilver dichloride (0.16g, 0.22mmol) and (COD) palladium dichloride (0.08g, 0.22mmol) in dichloromethane (60ml) by stirring at room temperature for 12 hours. The yellow product obtained at this stage was not spectroscopically or analytically pure. However, attempts to purify the solid by standard separation and purification techniques gave no further increase in purity.

MS (ES): *m/z* 377, $[(\text{ligand})Pd_2 + 2MeCN]^{2+}$; 517, $[(\text{ligand})_2Pd]^{2+}$; 650, $[(\text{ligand})PdCl + MeCN]^{+}$.

$\delta_H(CDCl_3)$ very broad spectra containing peaks at 1.0, 2.5, 5.0, 7.0, 8.0 (d, $^iPr_2C_6\mathit{H}_2H$).

REFERENCES

1 D. Bourisou, O. Guerret, F.P. Gabbai, G. Bertrand, *Chem. Rev.*, **2000**, *100*, 39; W. A. Herrmann, C. Kocher, *Angew. Chem., Int. Ed. Engl.*, **1997**, *36*, 2162.

2 J.C. Green, R.G. Scurr, P.L. Arnold, F.G.N. Cloke, *Chem. Commun.*, **1997**, 1963.

3 I. Ojima, *Catalytic Asymmetric Synthesis*, Wiley-VCH, 2^{nd} edition, **2000**.

4 F. Fache, E. Schulz, M.L. Tommasino, M. Lemaire, *Chem. Rev.*, **2000**, *100*, 2159; A.H. Hoveida, J. P. Moren, *Metallocenes*, ed. A. Togni, R. L. Halterman, Wiley-VCH, Weinheim, **1998**.

5 D. Enders, H. Gielen, G. Raabe, J. Runsink, J.H. Teles, *Chem. Ber.*, **1996**, *129*, 1483.

6 D.S. Clyne, J. Jin, E. Genest, J.C. Gallucci, T.V. RajanBabu, *Org. Lett.*, **2000**, *2*, 1125.

7 A.W. Coleman, P.B. Hitchcock, M.F. Lappert, R.K. Maskell, J.H. Muller, *J. Organomet. Chem.*, **1985**, *296*, 173; W.A. Herrmann, L.J. Goosen, C. Koecher, G.R.J. Artus, *Angew. Chem., Int. Ed. Engl.*, **1996**, *35*, 2805; J. Huang, L. Jafarpour, A.C. Hillier, E.D. Stevens, S.P. Nolan, *Organometallics*, **2001**, *13*, 2878.

8 M. Scholl, S. Ding, C.W. Lee, R.H. Grubbs, *Org. Lett.*, **1999**, *1*, 953.

9 W.A. Herrmann, L.J. Goosen, M. Spiegler, *Organometallics*, **1998**, *17*, 2162; M.T. Powell, D.-R. Hou, M.C. Perry, X. Cui, K. Burgess, *J. Am. Chem. Soc.*, **2001**, *123*, 8878.

10 A.A.D. Tulloch, A.A. Danopoulos, R.P. Tooze, S.M. Cafferkey S. Kleinhenz, M.B. Hursthouse, *Chem. Commun.*, **2000**, 1247.

11 D.S. McGuiness, K.J. Cavell, *Organometallics*, **2000**, *19*, 741.

12 A.A.D. Tulloch, A.A. Danopoulos, S. Winston, S. Kleinhenz, G. Eastham, *J. Chem. Soc., Dalton Trans.*, **2000**, 4499; S. Winston, personal communication.

13 E. Peris, J.A. Loch, J. Mata, R.H. Crabtree, *Chem. Commun.*, **2001**, 201.

14 H. Pirkle, M.S. Hoekstra, *J. Am. Chem. Soc.*, **1976**, *98*, 1832.

15 A.A.D. Tulloch, A.A. Danopoulos, G.J. Tizzard, S.J. Coles, M.B. Hursthouse, R.S. Hay-Motherwell, W.B. Motherwell, *Chem. Commun.*, **2001**, 1270.

Chapter 6

Reactions of Palladium (II) *N*-Heterocyclic Carbene Complexes

Chapter 6

Reactions of Palladium (II) *N*-Heterocyclic Carbene Complexes

6.1 Introduction

The avalanche of publications on transition metal *N*-heterocyclic carbene complexes has been encouraged by the realisation that they can act as catalysts or pre-catalysts for important transformations, including; Pd-catalysed Heck and Suzuki reactions,[1] CO–ethylene copolymerisation,[2] Ru-catalysed olefin metathesis[3] and Rh catalysed hydrosilylations.[4]

Following on from complexes described in Chapter Four, this chapter focuses on reactions of palladium carbene complexes aiming at studying some of their properties and to synthesise complexes with a range of weakly coordinating anions. There are few examples of palladium *N*-heterocyclic carbene complexes that undergo anion exchange[2,5] and few publications that show examples of dissociation of either the carbene moiety or a linked donor group of a *N*-functionalised heterocyclic carbene ligand.[5,6]

Within this chapter are described a number of anion exchange reactions and their characterised products (*Figure 6.1*), including three X-ray crystal structures. One of these crystal structures contains the second example of a mixed donor functionalised *N*-heterocyclic carbene acting as a bridging ligand. The other structures included here all contain functionalised *N*-heterocyclic carbene ligands that act as chelates. This chapter also reports on some interesting reactions of the complexes described in Chapter Four with phosphines and amines, in an attempt to demonstrate the hemilability of the ligands.[7]

RESULTS AND DISCUSSION

6.2 Anion exchange reactions of palladium (II) carbene complexes

6.2.1. Synthesis of palladium complexes (6.1)-(6.10)

The palladium complexes described in this chapter were synthesised by the interaction of the corresponding parent palladium carbene complex [either compound **(4.1)**, **(4.2)**, **(4.3)** or **(4.4)**] with the respective silver salt of the replacement anion (*Scheme 6.1*).

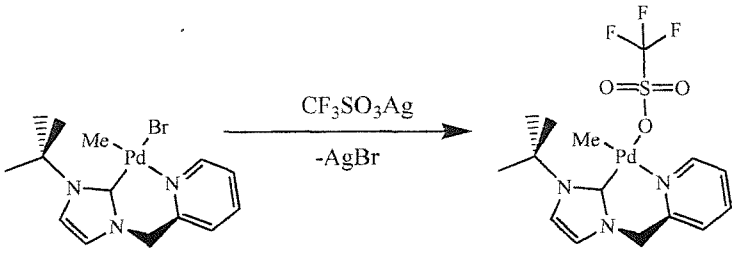

Scheme 6.1. Synthesis of compound **(6.2)** from **(4.1)**.

The reactions were performed in either dichloromethane or acetonitrile and stirred at room temperature until completion, giving the products as pale yellow air stable solids. In most cases, the products obtained at this stage were spectroscopically and analytically pure. However, in some cases, small excesses of the silver salt used proved difficult to remove. In these cases, the solids were purified by repeated recrystallisation from saturated solutions of dichloromethane and diethyl ether.

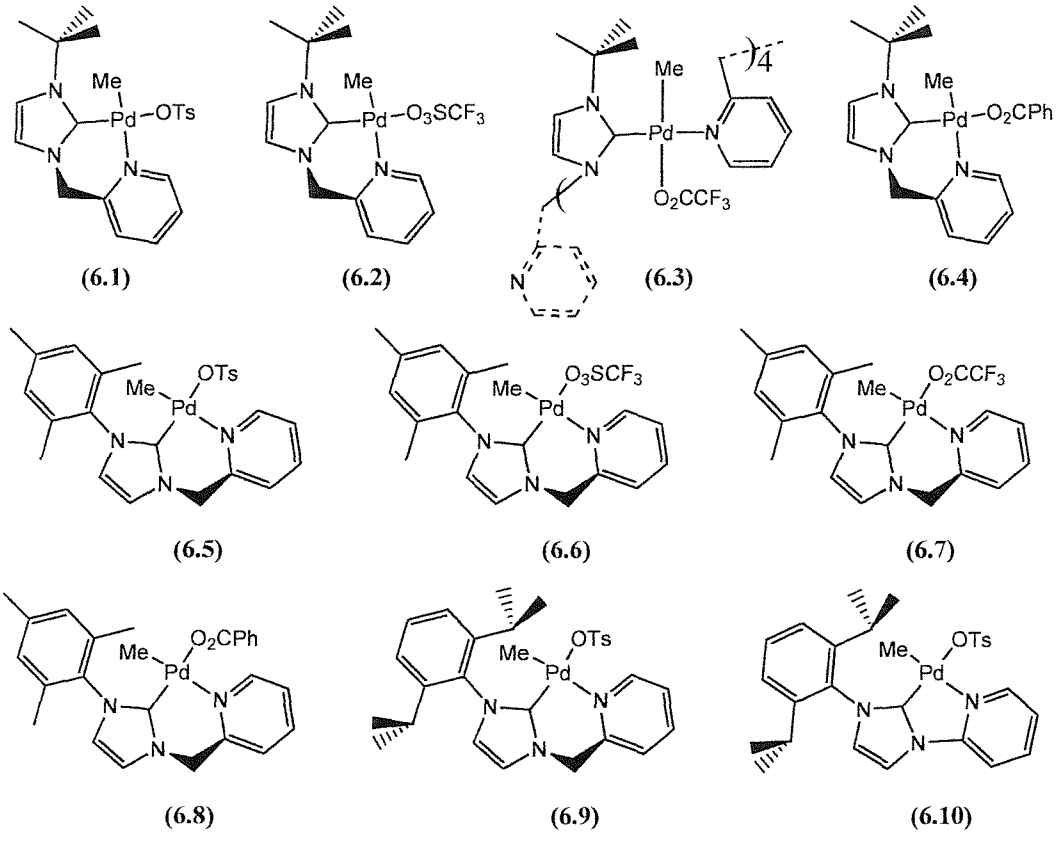

Figure 6.1. Palladium complexes **(6.1)-(6.10)**.

6.2.2. X-ray diffraction studies on compound (6.7)

X-ray diffraction quality crystals of [3-(mesityl)-1-(α-picolyl) imidazol-2-ylidene] palladium methyl trifluoroacetate **(6.7)** were obtained by layering a dichloromethane solution with diethyl ether. The crystal structure demonstrates the difficulty of removing any excess silver salt (*Figure 6.2*). These crystals were grown from a sample that had not been recrystallised. The structure comprises two palladium atoms and one central silver atom with two bridging trifluoroacetate ligands and one trifluoroacetate bound only to the silver.

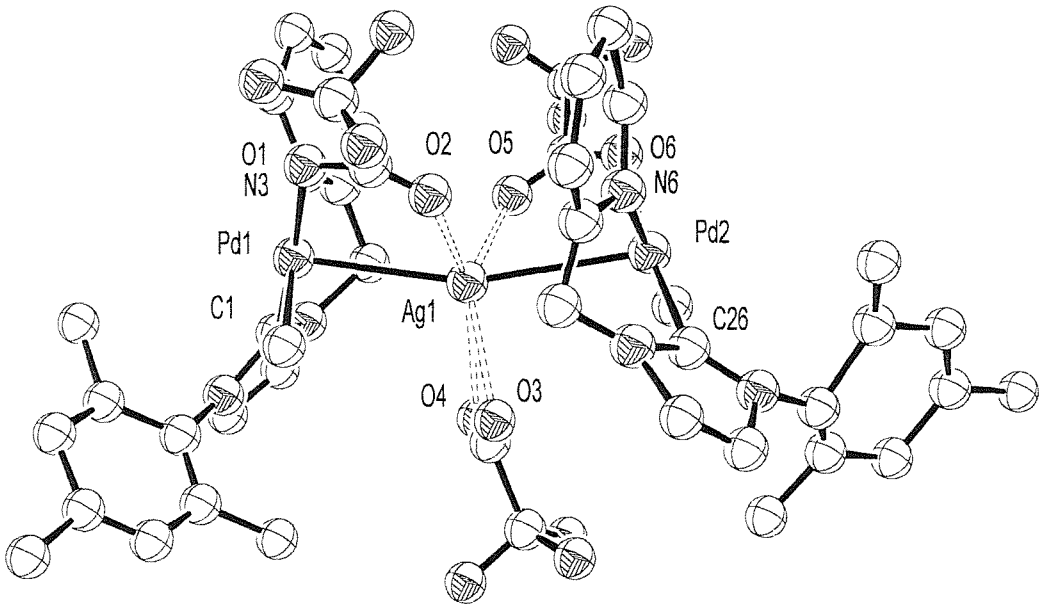

Figure 6.2. X-ray crystal structure of [3-(mesityl)-1-(α-picolyl) imidazol-2-ylidene] palladium methyl trifluoroacetate, compound **(6.7)**.

The coordination sphere of each palladium comprises of a trifluoroacetate, a methyl group and a chelating ligand with the carbene end disposed *trans* to the trifluoroacetate (*Figure 6.2*). The palladium centres are in square planar geometry, with close contacts with the silver atom, and the silver is in a much-distorted tetrahedral geometry. The palladium-silver close contacts are 2.94 and 3.07Å. The palladium-carbene bond lengths are 1.84 and 1.89Å, the palladium-nitrogen bond lengths are 2.18 and 2.13Å, and the palladium-carbon (methyl) bond lengths are 2.08 and 2.14Å. These bond lengths are not dramatically different to those of compound **(4.2)**, with the palladium-carbene bond length being only around 0.1Å shorter. The other bond lengths and angles of the ligand are very similar.

6.2.3. X-ray diffraction studies on compound (6.3)

X-ray diffraction quality crystals of [3-(*tert*butyl)-1-(α-picolyl) imidazol-2-ylidene] palladium methyl trifluoroacetate **(6.3)** were obtained by layering a dichloromethane solution with diethyl ether (*Figure 6.4*). These crystals were grown from a sample that had been repeatedly recrystallised. This structure is the second structurally characterised example of a pyridine *N*-functionalised carbene acting as a bridging ligand rather than a chelate (*Figure 6.3*).

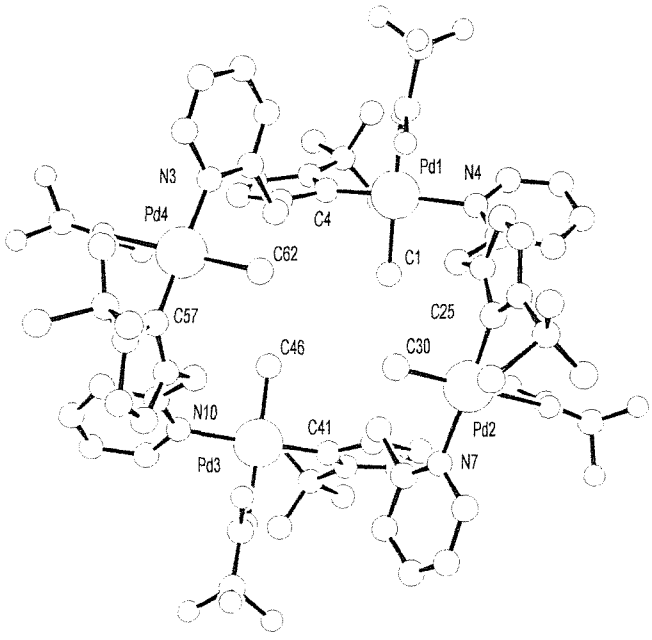

Figure 6.3. X-ray crystal structure of [3-(*tert*butyl)-1-(α-picolyl) imidazol-2-ylidene] palladium methyl trifluoroacetate, compound **(6.3)**.

This tetrameric structure comprises four palladium atoms that occupy the corners of a distorted tetrahedron with four ligands bridging four of the six sides, in a way that completes the chain (*Figure 6.4*). Each palladium is coordinated by a carbene end of one ligand, a pyridine end of another ligand, a methyl group, and an oxygen of a trifluoroacetate. The pyridine and carbene moieties occupy mutually *trans* positions of the palladium square plane. The palladium-carbene bond lengths are 1.89, 1.91, 1.94 and 1.96Å, which are all in the range of carbene-palladium bond lengths found in these type of complexes.[8] The palladium-nitrogen bond lengths are in the range 1.99–2.11Å, the palladium-carbon (methyl) bond lengths are in the range 1.94–2.10Å, and the palladium-oxygen (trifluoroacetate) bond lengths are in the range 2.15–2.17Å, which are as expected for these types of complexes.

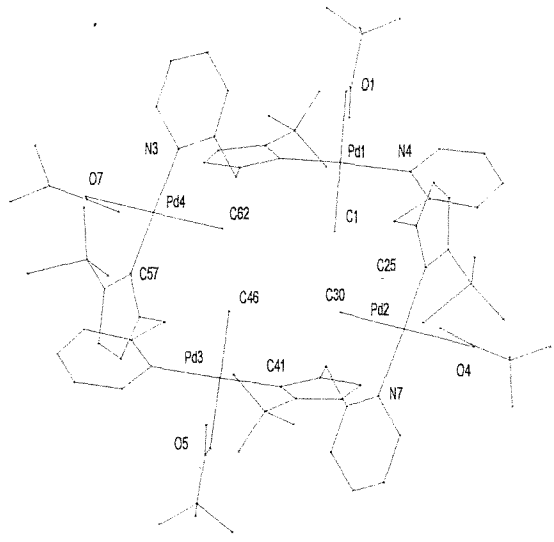

Figure 6.4. X-ray crystal structure of [3-(*tert*butyl)-1-(α-picolyl) imidazol-2-ylidene] palladium methyl trifluoroacetate, compound **(6.3)**.

6.2.4. X-ray diffraction studies on compound (6.10)

X-ray diffraction quality crystals of [3-(2,6-di*iso*propylphenyl)-1-(2-pyridyl) imidazol-2-ylidene] palladium methyl tosylate **(6.10)** were obtained by layering a saturated solution of dichloromethane with diethyl ether (*Figure 6.5*). These crystals were grown from a sample that had been carefully recrystallised.

The structure comprises a central palladium atom coordinated by a chelating ligand, a methyl group and a tosylate anion, in a square planar geometry. The carbene end of the ligand is disposed *trans* to the oxygen of the tosylate and therefore the pyridine end is disposed *trans* to the methyl group, similar to that of compound **(4.4)**. The palladium-carbene, palladium-methyl, and the palladium-nitrogen bond lengths are similar to those in compound **(4.4)** at 1.95, 2.02 and 2.14Å. The palladium-oxygen bond length of 2.12Å is similar to those in compounds **(6.3)** and **(6.7)**.

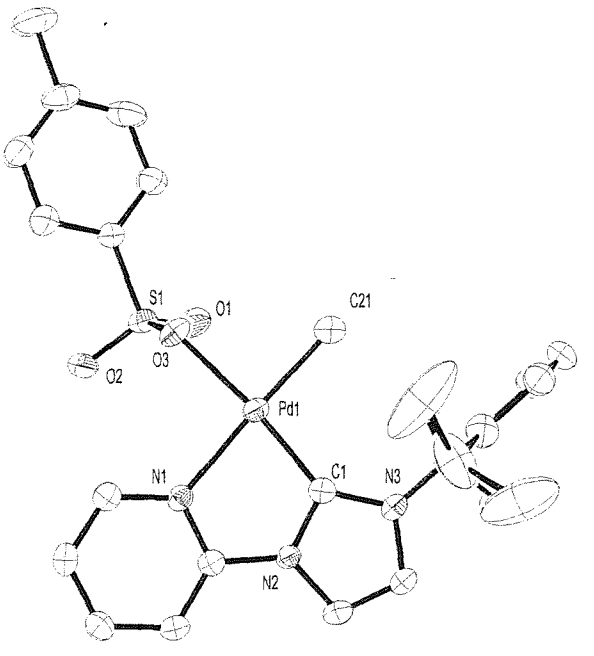

Figure 6.5. X-ray crystal structure of [3-(2,6-di*iso*propylphenyl)-1-(2-pyridyl) imidazol-2-ylidene] palladium methyl tosylate, compound **(6.10)**.

Crystals were also obtained of compounds **(6.1)** and **(6.4)**, by cooling saturated THF solutions. However, the X-ray data obtained for these crystals were of poor quality; unfortunately, crystals of better quality were not obtained.

6.2.5. Electrospray mass spectrometry

Electrospray mass spectrometry (positive) was of limited diagnostic value as the starting palladium complex and the product give the same parent peak. The peaks observed in the spectra were assigned to $[(\text{ligand})\text{PdMe} + \text{MeCN}]^+$ in all cases, a peak corresponding to a parent ion $[(\text{ligand})\text{PdMe}]^+$ was also observed in the spectrum of compound **(6.3)**. Elemental analysis was very useful in determining the stoichiometries especially as it demonstrated the need for repeated recrystallisation. In the case of compound **(6.7)**, the elemental analysis disagreed with the stoichiometry determined by the crystal structure. However, the difference can be explained by further recrystallisations being performed before a sample for analysis was taken. This further purification step removed the final traces of the silver salt.

6.2.6. NMR spectroscopy

NMR spectroscopy proved itself the most the useful technique to determine the formation of the products and their characteristics.

6.2.6.1. Characteristic peaks

The complexes **(6.1)-(6.10)** were identified by the following peaks in the ^{1}H and $^{13}C\{H\}$ NMR spectra, similar to the those for the palladium complexes described in Chapter Four:

i) A weak peak downfield of 159 ppm in the $^{13}C\{H\}$ NMR spectra which can be assigned to the carbene carbon (observed in these complexes between 159 and 174 ppm);

ii) For the compounds **(6.1)-(6.9)**, a broad singlet or pair of doublets were observed between 5.3 and 5.7 ppm in the ^{1}H NMR spectra (assigned to the protons on the methylene bridge), and a peak observed between 55 and 58 ppm in the $^{13}C\{H\}$ NMR spectra (assigned to the carbon of the methylene bridge);

iii) A low field doublet observed between 8.5 and 9.1 ppm and a triplet or triplet of doublets observed between 7.5 and 8.1 ppm in the ^{1}H NMR spectra (assigned to the protons in the 6- and 4-positions of the pyridine type rings);

iv) A high field peak observed between -0.1 and 0.6 ppm in the ^{1}H NMR spectra (assigned to the protons of the methyl bound to palladium) and a corresponding peak in the $^{13}C\{H\}$ NMR spectra between -10 and -5 ppm.

v) The presence of two doublets, with very small coupling constants, between 6.9 and 7.2 ppm, and 7.2 and 7.9 ppm in the ^{1}H NMR spectra (assigned to the protons in the 5- and 4- positions of the imidazol-2-ylidene ring, when the ligand is acting as a chelate);

vi) A multiplet between 7.2 and 7.6 ppm in the ^{1}H NMR spectra (assigned to the protons in the in the 5-position of the pyridine ring);

vii) A doublet between 7.1 and 7.9 ppm in the ^{1}H NMR spectra (assigned to the protons in the in the 3-position of the pyridine ring).

6.2.6.2. Chelating or bridging?

Compound **(6.3)** has a tetrameric structure in the solid-state with the ligands bridging between the four metal centres. The peaks in the ^{1}H NMR spectrum assigned to the protons in the 5- and 4-position of the imidazol-2-ylidene ring appear at considerably

higher field (6.4 and 7.0 ppm) than in similar complexes with chelating ligands. No other peaks in the ^{1}H NMR spectrum appear to show characteristic chemical shift differences between a chelating and a bridging ligand. Although the chemical shifts of the protons of the methylene bridge might be expected to be different, no clear trend has been observed. However, when the diastereotopic protons of the methylene bridge give rise to a pair of doublets it can be concluded that the ligand is chelating as when the ligand is bridging, the flexibility of the methylene linker would be greatly increased.

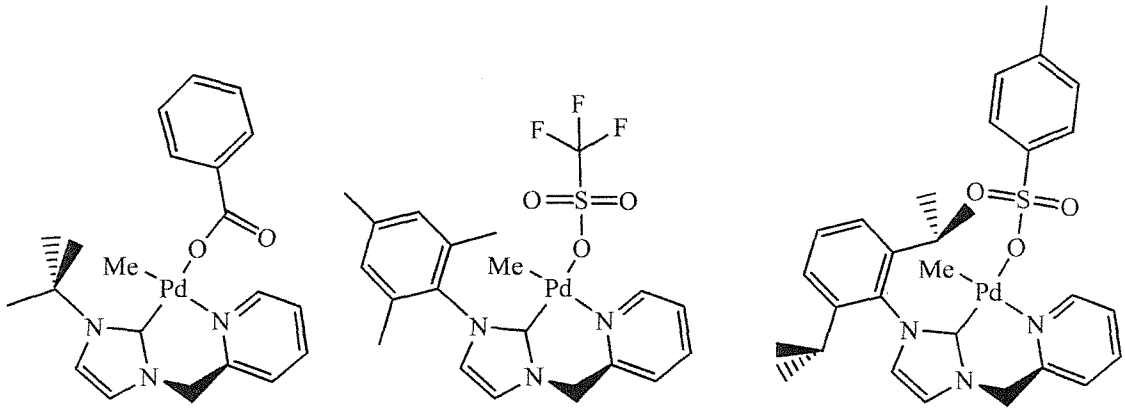

Figure 6.6. Compounds **(6.4)**, **(6.6)** and **(6.9)** are all believed to be monomeric complexes in solution at room temperature.

From this deduction, we can say that compounds **(4.1)-(4.3)**, **(4.5)**, **(6.1)**, **(6.2)**, and **(6.4)-(6.10)** all contain ligands that are chelating a metal centre as they all have a doublet of doublets assignable to the protons of the methylene bridge (*Figure 6.6*).

6.2.6.3. Other peaks

The other peaks in the ^{1}H NMR spectra are either associated to the protons of the R group on the imidazol-2-ylidene ring or to the protons on the anion. The peaks associated to the R groups are at similar shifts to those complexes described in Chapter Four: for *tert*butyl, a singlet around 1.7 ppm; for mesityl, singlets around 2.1, 2.3 and 7.0 ppm; and for 2,6-di*iso*propylphenyl, two doublets between 1.0 and 1.4 ppm, a septet at around 2.4 ppm, a doublet at 7.2 ppm and a triplet at around 7.4 ppm. For compounds **(6.1)**, **(6.5)**, **(6.9)** and **(6.10)** three peaks were observed in the ^{1}H NMR spectra for the tosylate group. These peaks were observed around 2.3 ppm (singlet) for the methyl group and between 7.0

and 7.3 ppm (doublet), and between 7.5 and 7.8 ppm (doublet). The protons of the benzoate group were observed around 8.0 and 7.3 ppm for compounds **(6.4)** and **(6.8)**.

The $^{13}C\{H\}$ NMR spectra, although complicated, were fully assigned (see experimental) and the chemical shifts were similar to those of the complexes described in Chapter Four, and the peaks corresponding to the anions were in the normal ranges.

6.2.7. Coordination isomers of (6.1) and (6.4)

When compounds **(6.1)** and **(6.4)** were synthesised using more concentrated solutions of the starting materials, duplicate peaks were observed in the ^{1}H NMR spectra, assigned to the protons of the methyl on palladium and of the 6-position of the pyridine ring. These peaks were assigned to the *cis* and *trans* coordination isomers, similar to those observed for **(4.2)**, **(4.3)** and **(4.4)** (*Figure 6.7*).

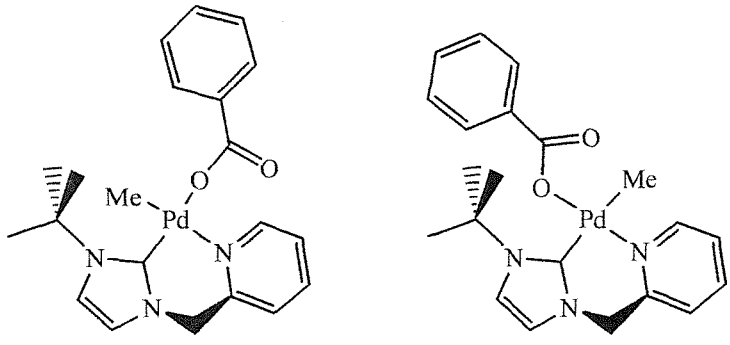

Figure 6.7. Cis and *trans* coordination isomers of compound **(6.4)**.

6.2.8. Hemilability of the pyridine moiety

From the deduction that compound **(4.1)** contains a chelating ligand in solution, and the fact that compound **(6.3)** in the solid state is a tetramer; we can speculate that at some point in the synthesis of **(6.3)** the pyridine end of the ligand became detached from the palladium centre, demonstrating its lability (*Scheme 6.2*).

The reactions ***6.5.2-6.5.6*** were performed in an attempt to displace the pyridine end of the ligand from its coordination to the palladium centre to show the lability of this group. The reactions were carried out by careful addition of a solution of the phosphine or amine to a solution of the corresponding palladium complex [either compound **(4.2)**, **(4.3)** or **(4.4)**]. Simple work-up and purification methods were carried out in order to remove any excess phosphine or amine.

Attempts to obtain suitable chemical analysis failed, possibly due to small excesses of the phosphine or amine still being present or due to side reactions that took place. Slow

decomposition was observed in these samples (much slower for reactions ***6.5.4*** and ***6.5.6***) producing palladium black as a fine precipitate. The palladium complexes **(4.1)**, **(4.2)**, **(4.3)** and **(4.4)** also decompose when under an atmosphere of carbon monoxide; however, the complexes with a picolyl group decompose much faster than compound **(4.4)** which has a pyridyl group. This decomposition is possibly related to the de-ligation of the metal by the pyridine moiety, and therefore demonstrates that the picolyl group is more labile than the pyridyl groups.

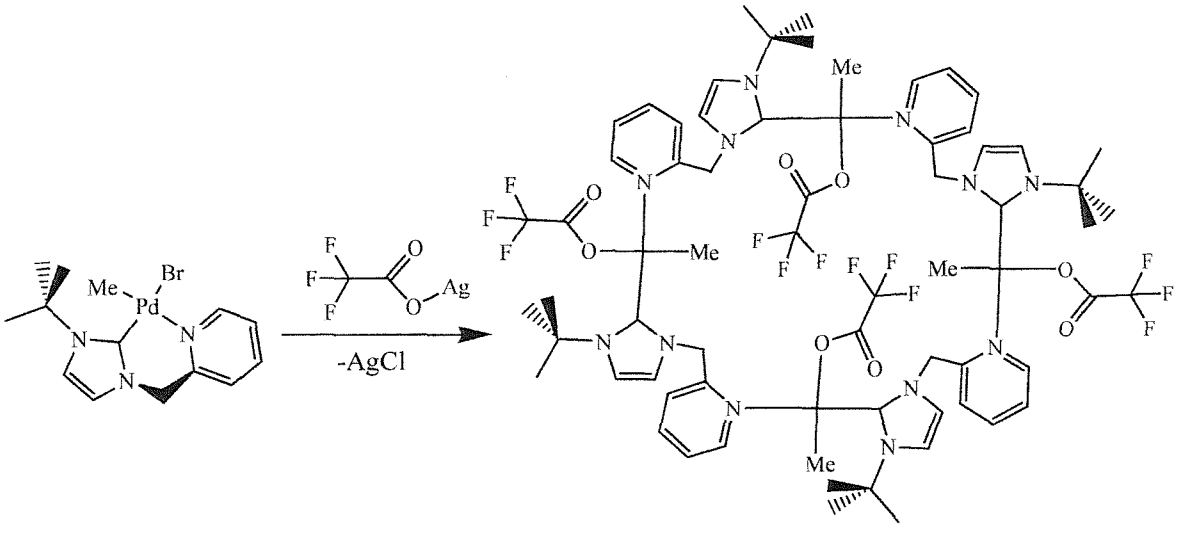

Scheme 6.2. Synthesis of compound **(6.3)** from **(4.1)**.

Electrospray mass spectrometry showed that the phosphines and amines were coordinated to the metal centre, by the existence of a peak assigned to the parent ion $[(ligand)PdMe + PPh_3]^+$ or $[(ligand)PdMe + NEt_3]^+$. However, this information on its own can not prove any lability of the pyridine end of the ligand. The ^1H NMR spectra of the product show that in reaction ***6.5.3*** the ligand is acting as a chelate, based on the pair of doublets assigned to the protons of the methylene bridge. The symmetry of the spectra of the starting complex and the isolated product are similar, but the peaks of the product are slightly shifted from that of the starting complexes, with additional peaks that can be assigned to the phosphine or the amine used. The peaks assigned to the protons in the 6-position of the picolyl and pyridyl rings did shift dramatically in the *reactions* ***6.5.3*** and ***6.5.4***. This shift was up to 0.9 ppm; the reason for this change is unknown but implies a considerable difference in the environment of the protons in that position.

The protons in the 6-position of the picolyl and pyridyl rings become a pair of doublets when the complexes are reacted with triethylamine. These duplicate peaks can be assigned to *cis/trans* type species, which implies that some form of coordination

isomerisation has taken place during the reaction. Although the exact identity of the species has not been clarified, this observation suggests that there is considerable lability in the complex. The $^{31}P\{H\}$ NMR spectrum of reaction ***6.5.4*** contain peaks that can be assigned to phosphine coordinated to a metal centre.

6.3 Conclusion

The synthesis and characterisation of a number of palladium mixed donor *N*-heterocyclic carbene complexes with weakly coordinating anions have been described in this chapter. Compound **(6.3)**, is the second structurally characterised example of a mixed donor *N*-heterocyclic carbene that acts as a bridging ligand rather than either a chelate or a mono-dentate ligand.[8] The X-ray crystal structure shows that the complex is a tetramer with the carbene moiety disposed *trans* to the picolyl group. From the ^{1}H NMR data collected, we can show that all the other complexes described in this chapter contain chelating ligands (except **(6.3)**); this is clearly shown in the symmetry of the NMR peaks assigned to the methylene bridging protons.

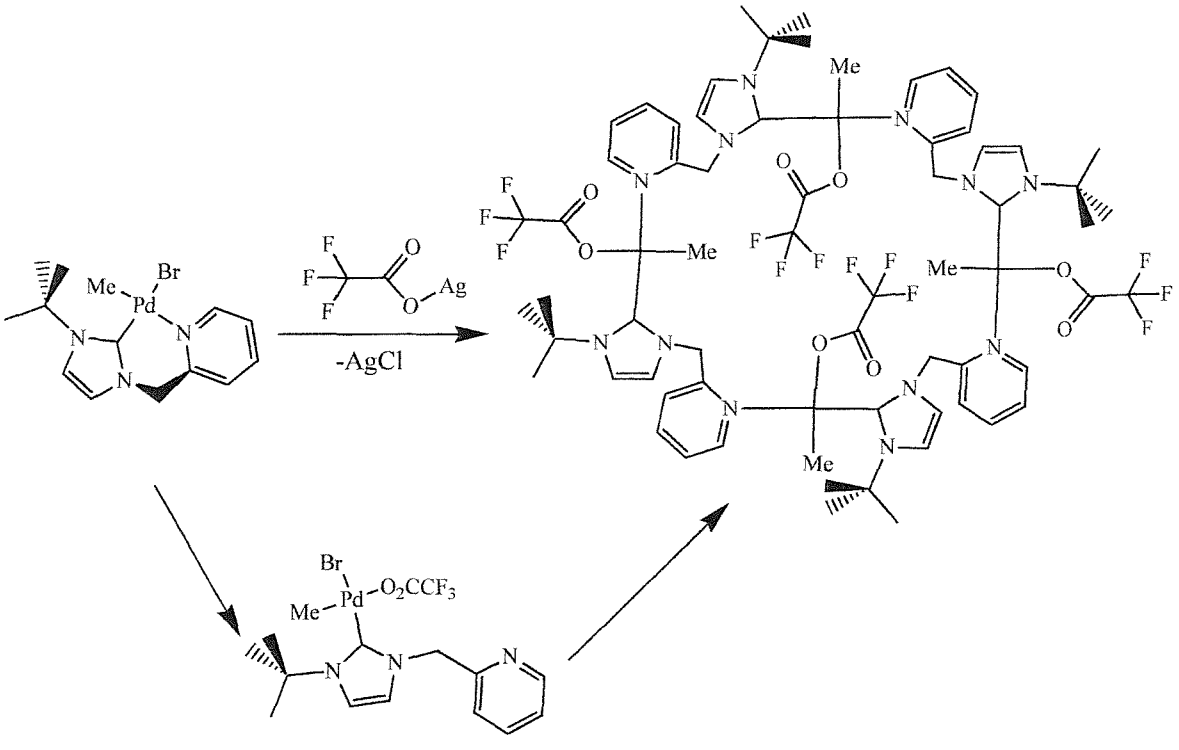

Scheme 6.3. lability of the pyridyl shown by the formation of the tetrameric structure of compound **(6.3)** from the monomeric structure of **(4.1)**.

Since compound **(4.1)** contains a chelating carbene ligand, we believe that the ligand rearrangement necessary for the formation of compound **(6.3)** is a clear manifestation of the hemilability of this ligand system. The exact mechanism is unknown but probably involves a dissociation of the picolyl group from the palladium centre (*Scheme 6.3*).

The hemilability of the ligands can be supported by the observation that, when compounds **(4.3)** and **(4.4)** are reacted with triethylamine, *cis-trans* isomerisation occurs; and the observation that slower decomposition occurs in *reactions* ***6.5.4*** and ***6.5.6*** (which contain the pyridyl type ligands). *Scheme 6.4* shows a possible decomposition pathway for the *reaction* ***6.5.5***, which as it involves a de-ligation step of the picolyl group could explain the slower decomposition observed for the pyridyl complexes. This type of decomposition has been proposed to take place in palladium complexes that contain monodentate carbene ligands and triphenylphosphine.[9]

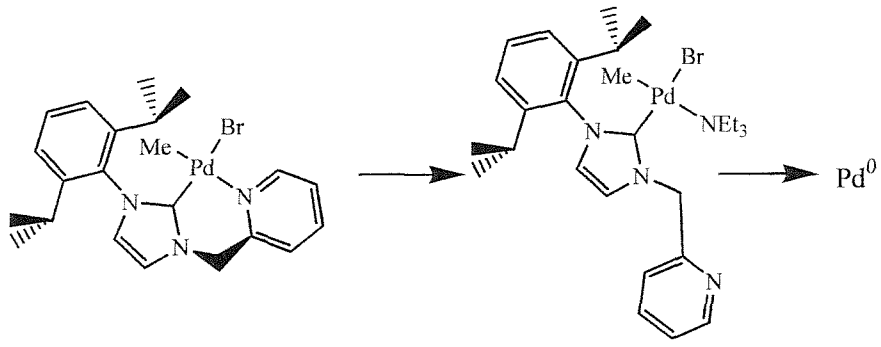

Scheme 6.4. Possible decomposition pathway for *reaction* ***6.5.5***.

EXPERIMENTAL

6.4 Anion exchange reactions of palladium complexes

6.4.1. General method

A dichloromethane or acetonitrile solution of the corresponding silver salt was added drop-wise to a solution of the corresponding palladium carbene complex [either compound **(4.1)**, **(4.2)**, **(4.3)** or **(4.4)**] and stirred at room temperature for 2-12 hours (*Scheme 6.5*). After completion, the reaction mixture was filtered, the volatiles were removed under vacuum and the resulting solid was washed with diethyl ether. Drying under vacuum gave the products as pale yellow solids.

In most cases, the products obtained at this stage were spectroscopically and analytically pure. If not, the solids were purified by recrystallisation from a saturated solution of dichloromethane and diethyl ether or by extraction into hot toluene.

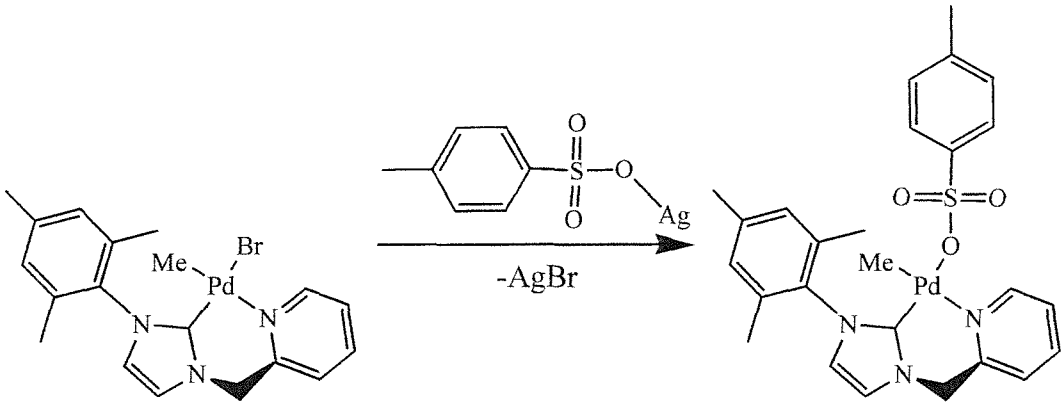

Scheme 6.5. Synthesis of compound **(6.5)**.

(6.1) [3-(*tert*butyl)-1-(α-picolyl) imidazol-2-ylidene] palladium methyl tosylate

This was prepared following the general method from [3-(*tert*butyl)-1-(α-picolyl) imidazol-2-ylidene] palladium methyl bromide **(4.1)** (0.1g, 0.27mmol) and silver tosylate (0.07g, 0.27mmol) in acetonitrile (50ml) by stirring at room temperature for 2 hours. The product was obtained in good yields as a yellow solid. Crystals were obtained by cooling a saturated THF solution (*Figure 6.8*).

MS (ES): *m/z* 377, $[(\text{ligand})\text{PdMe} + \text{MeCN}]^+$.

$\delta_H(CD_3CN)$ 0.4 (3H, s, PdCH_3), 1.6 (9H, s, C(CH_3)$_3$), 2.2 (3H, s, OTs CH_3), 5.4, 5.6 (2H, dd, CH_2), 7.0 (2H, d, OTs *H*), 7.2 (1H, d, 5-imidazol-2-ylidene *H*), 7.3 (1H, m, 5-

picolyl *H*), 7.4 (1H, d, 4-imidazol-2-ylidene *H*), 7.5 (2H, d, OTs *H*), 7.6 (1H, d, 3-picolyl *H*), 7.8 (1H, td, 4-picolyl *H*), 8.5 (1H, d, 6-picolyl *H*).

δ_C(CD_3CN) -9 (Pd*C*H_3), 21 (OTs *C*H_3), 33 [C(*C*H_3)$_3$], 57 (*C*H_2), 60 [*C*(CH$_3$)$_3$)], 119, 140, (OTs *C*), 121 (5-imidazol-2-ylidene *C*), 123 (5-picolyl *C*H), 126 (4-imidazol-2-ylidene *C*), 126 (3-picolyl *C*H), 127, 129 (OTs *C*H), 140 (4-picolyl *C*H), 152 (6-picolyl *C*H), 155 (2-picolyl *C*), 166 (2-imidazol-2-ylidene *C*).

(Found: C, 49.86; H, 4.98; N, 8.02. $C_{21}H_{27}N_3O_3PdS$ calculated: C, 49.66; H, 5.36; N, 8.27%).

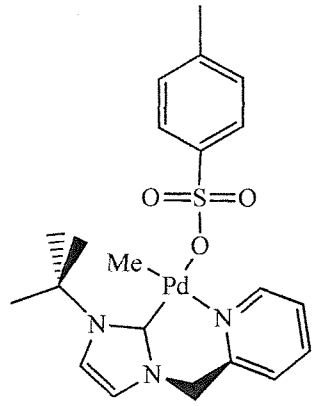

Figure 6.8. Compound **(6.1)**.

(6.2) [3-(*tert*butyl)-1-(α-picolyl) imidazol-2-ylidene] palladium methyl triflate

This was prepared following the general method from [3-(*tert*butyl)-1-(α-picolyl) imidazol-2-ylidene] palladium methyl bromide **(4.1)** (0.1g, 0.27mmol) and silver triflate (0.07g, 0.27mmol) in acetonitrile (50ml) by stirring at room temperature for 2 hours. The product was obtained in good yields as a yellow solid.

MS (ES): *m/z* 377, [(ligand)PdMe + MeCN]$^+$.

δ_H(CD_3CN) 0.5 (3H, s, PdC*H*$_3$), 1.7 (9H, s, C(C*H*$_3$)$_3$), 5.3, 5.7 (2H, dd, CH$_2$), 7.2 (1H, d, 5-imidazol-2-ylidene *H*), 7.3 (1H, d, 4-imidazol-2-ylidene *H*), 7.4 (1H, m, 5-picolyl *H*), 7.6 (1H, d, 3-picolyl *H*), 7.9 (1H, td, 4-picolyl *H*), 8.5 (1H, d, 6-picolyl *H*).

δ_C(CD_3CN) -10 (Pd*C*H$_3$), 32 [C(*C*H$_3$)$_3$], 58 (*C*H$_2$), 60 [*C*(CH$_3$)$_3$)], 118 (*C*F$_3$), 121 (5-imidazol-2-ylidene *C*), 123 (5-picolyl *C*H), 126 (4-imidazol-2-ylidene *C*), 126 (3-picolyl *C*H), 140 (4-picolyl *C*H), 152 (6-picolyl *C*H), 155 (2-picolyl *C*), 169 (2-imidazol-2-ylidene *C*).

(Found: C, 36.87; H, 4.77; N, 8.21. $C_{15}H_{21}F_3N_3O_3PdS$ calculated: C, 37.01; H, 4.35; N, 8.63%).

(6.3) [3-(*tert*butyl)-1-(α-picolyl) imidazol-2-ylidene] palladium methyl trifluoroacetate

This was prepared following the general method from [3-(*tert*butyl)-1-(α-picolyl) imidazol-2-ylidene] palladium methyl bromide **(4.1)** (0.1g, 0.27mmol) and silver trifluoroacetate (0.059g, 0.27mmol) in acetonitrile (50ml) by stirring at room temperature for 2 hours. The product was obtained in good yields as a yellow solid. X-ray diffraction quality crystals were obtained by layering a saturated solution of dichloromethane with diethyl ether (*Table 6.1*).

MS (ES): *m/z* 336, $[(ligand)PdMe]^+$; 377, $[(ligand)PdMe + MeCN]^+$.

$\delta_H(CDCl_3)$ 0.5 (3H, br. s, $PdCH_3$), 1.7 (9H, s, $C(CH_3)_3$), 5.3 (2H, s, CH_2), 6.4 (1H, d, 5-imidazol-2-ylidene *H*), 7.0 (1H, d, 4-imidazol-2-ylidene *H*), 7.1 (1H, d, 3-picolyl *H*), 7.2 (1H, t, 5-picolyl *H*), 7.5 (1H, td, 4-picolyl *H*), 8.8 (1H, d, 6-picolyl *H*).

$\delta_C(CDCl_3)$ -8 ($PdCH_3$), 32 [$C(CH_3)_3$], 57 (CH_2), 58 [$C(CH_3)_3$)], 119 (CF_3), 120 (5-picolyl *C*H), 121 (5-imidazol-2-ylidene *C*), 123 (3-picolyl *C*H), 125 (4-imidazol-2-ylidene *C*), 138 (4-picolyl *C*H), 151 (6-picolyl *C*H), 152 (2-picolyl *C*), 159 (2-imidazol-2-ylidene *C*), 174 (CO_2).

(Found: C, 42.42; H, 4.14; N, 9.06. $C_{16}H_{20}F_3N_3O_2Pd$ calculated: C, 42.73; H, 4.48; N, 9.34 %).

Pd(1)-C(4)	1.96(3)	O(1)-C(2)	1.17(3)
Pd(1)-C(1)	2.10(2)	O(2)-C(2)	1.28(3)
Pd(1)-N(4)	2.11(2)	O(3)-C(31)	1.25(2)
Pd(1)-O(1)	2.165(16)	O(4)-C(31)	1.19(2)
Pd(2)-C(25)	1.91(2)	O(5)-C(47)	1.24(2)
Pd(2)-C(30)	1.94(2)	O(6)-C(47)	1.27(2)
Pd(2)-N(7)	2.097(17)	O(7)-C(63)	1.28(2)
Pd(2)-O(4)	2.245(14)	O(8)-C(63)	1.19(2)
Pd(3)-C(41)	1.94(3)	N(1)-C(4)	1.33(3)
Pd(3)-C(46)	2.04(2)	N(2)-C(4)	1.37(3)
Pd(3)-N(10)	2.09(2)	N(5)-C(25)	1.31(2)
Pd(3)-O(5)	2.145(15)	N(6)-C(25)	1.37(2)
Pd(4)-C(57)	1.89(2)	N(8)-C(41)	1.36(2)
Pd(4)-N(3)	1.99(2)	N(9)-C(41)	1.36(2)
Pd(4)-C(62)	2.08(2)	N(11)-C(57)	1.317(19)
Pd(4)-O(7)	2.170(15)	N(12)-C(57)	1.40(2)

C(4)-Pd(1)-C(1)	85.3(10)	C(25)-Pd(2)-N(7)	176.2(7)
C(4)-Pd(1)-N(4)	169.0(8)	C(30)-Pd(2)-N(7)	91.0(7)
C(1)-Pd(1)-N(4)	89.2(8)	C(25)-Pd(2)-O(4)	95.0(6)
C(4)-Pd(1)-O(1)	96.8(8)	C(30)-Pd(2)-O(4)	175.8(8)
C(1)-Pd(1)-O(1)	174.6(10)	N(7)-Pd(2)-O(4)	88.2(6)
N(4)-Pd(1)-O(1)	89.5(6)	C(41)-Pd(3)-C(46)	86.8(11)
C(25)-Pd(2)-C(30)	86.0(10)	C(41)-Pd(3)-N(10)	170.0(6)

C(46)-Pd(3)-N(10)	89.3(7)	C(33)-N(7)-Pd(2)	112.4(10)
C(41)-Pd(3)-O(5)	95.3(8)	C(53)-N(10)-Pd(3)	129.5(13)
C(46)-Pd(3)-O(5)	175.1(8)	C(49)-N(10)-Pd(3)	115.0(12)
N(10)-Pd(3)-O(5)	89.2(6)	O(1)-C(2)-O(2)	133(3)
C(57)-Pd(4)-N(3)	178.3(6)	N(1)-C(4)-N(2)	103(2)
C(57)-Pd(4)-C(62)	89.6(10)	N(1)-C(4)-Pd(1)	133(2)
N(3)-Pd(4)-C(62)	89.8(7)	N(2)-C(4)-Pd(1)	124(2)
C(57)-Pd(4)-O(7)	91.5(7)	N(5)-C(25)-N(6)	97.6(16)
N(3)-Pd(4)-O(7)	89.2(7)	N(5)-C(25)-Pd(2)	126.6(16)
C(62)-Pd(4)-O(7)	177.0(7)	N(6)-C(25)-Pd(2)	135.4(15)
C(2)-O(1)-Pd(1)	112.3(19)	O(4)-C(31)-O(3)	131(2)
C(31)-O(4)-Pd(2)	112.4(12)	N(8)-C(41)-N(9)	102.3(17)
C(47)-O(5)-Pd(3)	113.4(9)	N(8)-C(41)-Pd(3)	124.7(15)
C(63)-O(7)-Pd(4)	114.5(10)	N(9)-C(41)-Pd(3)	132.9(16)
C(16)-N(3)-Pd(4)	119.7(13)	O(5)-C(47)-O(6)	130.3(17)
C(12)-N(3)-Pd(4)	129.8(15)	N(11)-C(57)-N(12)	98.6(14)
C(17)-N(4)-Pd(1)	128.2(13)	N(11)-C(57)-Pd(4)	130.7(13)
C(21)-N(4)-Pd(1)	115.9(13)	N(12)-C(57)-Pd(4)	129.5(12)
C(37)-N(7)-Pd(2)	131.8(10)	O(8)-C(63)-O(7)	127(2)

Table 6.1. Selected bond lengths (Å) and angles (°) for compound **(6.3)**.

(6.4) [3-(*tert*butyl)-1-(α-picolyl) imidazol-2-ylidene] palladium methyl benzoate

This was prepared following the general method from [3-(*tert*butyl)-1-(α-picolyl) imidazol-2-ylidene] palladium methyl bromide **(4.1)** (0.1g, 0.27mmol) and silver benzoate (0.067g, 0.27mmol) in acetonitrile (50ml) by stirring at room temperature for 2 hours. The product was obtained in good yields as a yellow solid. Crystals were obtained by cooling a saturated THF solution.

MS (ES): *m/z* 377, $[(\text{ligand})\text{PdMe} + \text{MeCN}]^+$.

$\delta_H(CDCl_3)$ 0.6 (3H, s, PdC*H*$_3$), 1.7 (9H, s, C(C*H*$_3$)$_3$), 5.5 (2H, v. br, CH_2), 6.9 (1H, d, 5-imidazol-2-ylidene *H*), 7.0-7.3 (6H, m, benzoate *H*, 4-imidazol-2-ylidene *H*, 3,5-picolyl *H*), 7.5 (1H, td, 4-picolyl *H*), 8.0 (2H, d, benzoate *H*), 8.7 (1H, d, 6-picolyl *H*).

$\delta_C(CDCl_3)$ -7 (PdCH$_3$), 32 [C(*C*H$_3$)$_3$], 57 (*C*H$_2$), 60 [*C*(CH$_3$)$_3$)], 119 (5-picolyl *C*H), 120 (5-imidazol-2-ylidene *C*), 123 (3-picolyl *C*H), 124 (4-imidazol-2-ylidene *C*), 118, 128, 129, 130 (benzoate *C*), 138 (4-picolyl *C*H), 152 (6-picolyl *C*H), 153 (2-picolyl *C*), 170 (2-imidazol-2-ylidene *C*), 174 (*C*O$_2$).

(Found: C, 55.20; H, 5.98; N, 8.96. $C_{21}H_{26}N_3O_2Pd$ calculated: C, 54.97; H, 5.71; N, 9.16%).

(6.5) [3-(mesityl)-1-(α-picolyl) imidazol-2-ylidene] palladium methyl tosylate

This was prepared following the general method from [3-(mesityl)-1-(α-picolyl) imidazol-2-ylidene] palladium methyl bromide **(4.2)** (0.1g, 0.23mmol) and silver tosylate (0.060g, 0.23mmol) in acetonitrile (50ml) by stirring at room temperature for 2 hours. The product was obtained in quantitative yields as a yellow solid (*Figure 6.9*).

MS (ES): *m/z* 439, $[(\text{ligand})\text{PdMe} + \text{MeCN}]^+$.

$\delta_H(CD_3CN)$ 0.0 (3H, s, $PdCH_3$), 2.1 (6H, s, mesityl CH_3), 2.4 (3H, s, OTs CH_3), 2.4 (3H, s, mesityl CH_3), 5.7 (2H, s, CH_2), 7.1 (2H, s, mesityl *H*), 7.1 (1H, d, 5-imidazol-2-ylidene *H*),7.3 (2H, d, OTs *H*), 7.6 (1H, m, 5-picolyl *H*), 7.7 (2H,d, OTs *H*), 7.8 (1H, d, 4-imidazol-2-ylidene *H*), 7.9 (1H, d, 3-picolyl *H*), 8.1 (1H, td, 4-picolyl *H*), 8.8 (1H, d, 6-picolyl *H*).

$\delta_C(CD_3CN)$ -5 ($PdCH_3$), 18, 21 (mesityl CH_3), 21 (OTs CH_3), 55 (CH_2), 119, 140, (OTs *C*), 123 (5-imidazol-2-ylidene *C*), 124 (4-imidazol-2-ylidene *C*), 126 (5-picolyl *C*H), 126 (3-picolyl *C*H), 127, 129 (OTs *C*H), 130 (mesityl *C*H), 136, 140, 140 (mesityl *C*),141 (4-picolyl *C*H), 152 (6-picolyl *C*H), 154 (2-picolyl *C*), 168 (2-imidazol-2-ylidene *C*).

(Found: C, 55.10; H, 4.86; N, 7.85. $C_{26}H_{29}N_3O_3PdS$ calculated: C, 54.78; H, 5.13; N, 7.37%).

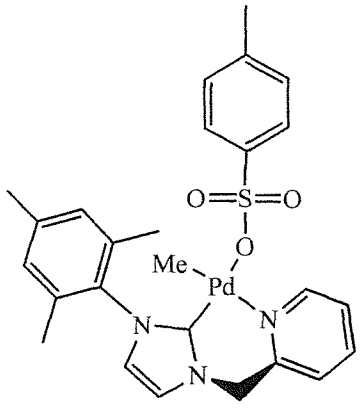

Figure 6.9. Compound **(6.5)**.

(6.6) [3-(mesityl)-1-(α-picolyl) imidazol-2-ylidene] palladium methyl triflate

This was prepared following the general method from [3-(mesityl)-1-(α-picolyl) imidazol-2-ylidene] palladium methyl bromide **(4.2)** (0.1g, 0.23mmol) and silver triflate (0.059g, 0.23mmol) in acetonitrile (50ml) by stirring at room temperature for 2 hours. The product was obtained in quantitative yields as a yellow solid.

MS (ES): *m/z* 439, $[(\text{ligand})\text{PdMe} + \text{MeCN}]^+$.

δ_H(CD_3CN) 0.0 (3H, s, PdCH_3), 2.1 (6H, s, mesityl CH_3), 2.4 (3H, s, mesityl CH_3) 5.6 (2H, s, CH_2), 7.1 (2H, s, mesityl *H*), 7.1 (1H, d, 5-imidazol-2-ylidene *H*), 7.6 (1H, m, 5-picolyl *H*), 7.6 (1H, d, 4-imidazol-2-ylidene *H*), 7.9 (1H, d, 3-picolyl *H*), 8.1 (1H, td, 4-picolyl *H*), 8.8 (1H, d, 6-picolyl *H*).

δ_C(CD_3CN) -9 (PdCH_3), 18, 21 (mesityl CH_3), 56 (CH_2), 119 (CF_3), 123 (5-imidazol-2-ylidene *C*), 124 (4-imidazol-2-ylidene *C*), 126 (5-picolyl *C*H), 126 (3-picolyl *C*H), 130 (mesityl *C*H), 136, 140, 140 (mesityl *C*), 140 (4-picolyl *C*H), 152 (6-picolyl *C*H), 154 (2-picolyl *C*), 168 (2-imidazol-2-ylidene *C*).

(Found: C, 43.98; H, 4.54; N, 7.43. $C_{20}H_{23}F_3N_3O_3PdS$ calculated: C, 43.76; H, 4.22; N, 7.66%).

(6.7) [3-(mesityl)-1-(α-picolyl) imidazol-2-ylidene] palladium methyl trifluoroacetate

This was prepared following the general method from [3-(mesityl)-1-(α-picolyl) imidazol-2-ylidene] palladium methyl bromide **(4.2)** (0.1g, 0.23mmol) and silver trifluoroacetate (0.05g, 0.23mmol) in acetonitrile (50ml) by stirring at room temperature for 2 hours. The product was obtained in quantitative yields as a yellow solid. X-ray diffraction quality crystals were obtained by layering a saturated solution of dichloromethane with diethyl ether (*Table 6.2*).

MS (ES): *m/z* 439, [(ligand)PdMe + MeCN]$^+$.

δ_H($CDCl_3$) 0.1 (3H, s, PdCH_3), 2.0 (6H, s, mesityl CH_3), 2.3 (3H, s, mesityl CH_3) 5.6 (2H, v. br., CH_2), 6.8 (1H, d, 5-imidazol-2-ylidene *H*), 6.9 (2H, s, mesityl *H*), 7.2 (1H, d, 4-imidazol-2-ylidene *H*), 7.4 (1H, br. m, 5-picolyl *H*), 7.5 (1H, br., 3-picolyl *H*), 7.9 (1H, br. t, 4-picolyl *H*), 8.6 (1H, br. d, 6-picolyl *H*).

δ_C($CDCl_3$) -9 (PdCH_3), 18, 21 (mesityl CH_3), 56 (CH_2), 122 (CF_3), 123 (5-imidazol-2-ylidene *C*), 125 (5-picolyl *C*H), 125 (3-picolyl *C*H), 128 (4-imidazol-2-ylidene *C*), 130 (mesityl *C*H), 135, 135, 139 (mesityl *C*), 140 (4-picolyl *C*H), 150 (6-picolyl *C*H), 152 (2-picolyl *C*), 164 (2-imidazol-2-ylidene *C*), 174 (*C*O_2).

(Found: C, 48.98; H, 4.64; N, 7.82. $C_{21}H_{23}F_3N_3O_2Pd$ calculated: C, 49.18; H, 4.52; N, 8.19%).

Ag(1)-O(5)	2.344(16)	Pd(2)-N(6)	2.13(4)
Ag(1)-O(2)	2.44(2)	O(1)-C(20)	1.31(3)
Ag(1)-O(3)	2.437(17)	O(2)-C(20)	1.11(3)
Ag(1)-Pd(1)	2.939(2)	O(3)-C(22)	1.20(3)
Ag(1)-Pd(2)	3.066(3)	O(4)-C(22)	1.23(3)
Pd(1)-C(1)	1.84(3)	O(5)-C(24)	1.27(3)
Pd(1)-C(19)	2.135(19)	O(6)-C(24)	1.11(3)
Pd(1)-O(1)	2.165(17)	N(1)-C(1)	1.24(3)
Pd(1)-N(3)	2.18(2)	N(2)-C(1)	1.50(3)
Pd(2)-C(44)	1.89(3)	N(4)-C(26)	1.55(4)
Pd(2)-C(26)	2.08(3)	N(5)-C(26)	1.30(4)
Pd(2)-O(6)	2.08(2)		

O(5)-Ag(1)-O(2)	106.6(7)	C(44)-Pd(2)-C(26)	92.2(13)
O(5)-Ag(1)-O(3)	135.0(6)	C(44)-Pd(2)-O(6)	87.6(9)
O(2)-Ag(1)-O(3)	112.3(8)	C(26)-Pd(2)-O(6)	171.7(11)
O(5)-Ag(1)-Pd(1)	97.9(4)	C(44)-Pd(2)-N(6)	176.4(11)
O(2)-Ag(1)-Pd(1)	78.4(5)	C(26)-Pd(2)-N(6)	85.9(14)
O(3)-Ag(1)-Pd(1)	111.2(4)	O(6)-Pd(2)-N(6)	94.7(11)
O(5)-Ag(1)-Pd(2)	73.8(4)	C(44)-Pd(2)-Ag(1)	89.9(6)
O(2)-Ag(1)-Pd(2)	89.4(5)	C(26)-Pd(2)-Ag(1)	107.5(9)
O(3)-Ag(1)-Pd(2)	84.6(4)	O(6)-Pd(2)-Ag(1)	80.7(5)
Pd(1)-Ag(1)-Pd(2)	162.75(9)	N(6)-Pd(2)-Ag(1)	87.8(6)
C(1)-Pd(1)-C(19)	96.3(11)	N(1)-C(1)-N(2)	101(2)
C(1)-Pd(1)-O(1)	175.6(8)	N(1)-C(1)-Pd(1)	124(3)
C(19)-Pd(1)-O(1)	84.8(7)	N(2)-C(1)-Pd(1)	134(2)
C(1)-Pd(1)-N(3)	86.2(12)	O(2)-C(20)-O(1)	134(4)
C(19)-Pd(1)-N(3)	177.2(8)	O(3)-C(22)-O(4)	123(4)
O(1)-Pd(1)-N(3)	92.8(8)	O(6)-C(24)-O(5)	135(3)
C(1)-Pd(1)-Ag(1)	101.6(7)	N(5)-C(26)-N(4)	117(3)
C(19)-Pd(1)-Ag(1)	79.8(6)	N(5)-C(26)-Pd(2)	137(3)
O(1)-Pd(1)-Ag(1)	82.8(4)	N(4)-C(26)-Pd(2)	105(3)
N(3)-Pd(1)-Ag(1)	98.4(5)		

Table 6.2. Selected bond lengths (Å) and angles (°) for compound **(6.7)**.

(6.8) [3-(mesityl)-1-(α-picolyl) imidazol-2-ylidene] palladium methyl benzoate

This was prepared following the general method from [3-(mesityl)-1-(α-picolyl) imidazol-2-ylidene] palladium methyl bromide **(4.2)** (0.1g, 0.23mmol) and silver benzoate (0.057g, 0.23mmol) in acetonitrile (50ml) by stirring at room temperature for 2 hours. The product was obtained in quantitative yields as a yellow solid (*Figure 6.10*).

MS (ES): *m/z* 439, $[(\text{ligand})\text{PdMe} + \text{MeCN}]^+$.

$\delta_H(CD_3CN)$ 0.0 (3H, s, PdCH_3), 2.0 (6H, s, mesityl CH_3), 2.4 (3H, s, mesityl CH_3) 5.7 (2H, br., CH_2), 6.9 (1H, d, 5-imidazol-2-ylidene *H*), 7.0 (2H, s, mesityl *H*), 7.2 (1H, d,

4-imidazol-2-ylidene *H*), 7.4 (4H, br., 5-picolyl *H*, benzoate *H*), 7.6 (1H, d, 3-picolyl *H*), 7.9 (1H, t, 4-picolyl *H*), 8.0 (2H, br., benzoate *H*), 8.8 (1H, d, 6-picolyl *H*).

$\delta_C(CD_3CN)$ -10 ($PdCH_3$), 18, 21 (mesityl CH_3), 56 (CH_2), 118 (benzoate *C*), 122 (CF_3), 123 (5-imidazol-2-ylidene *C*), 125 (5-picolyl *C*H), 125 (3-picolyl *C*H), 126 (4-imidazol-2-ylidene *C*), 130 (mesityl *C*H), 130, 130, 131 (benzoate *C*H), 132, 132, 136 (mesityl *C*), 140 (4-picolyl *C*H), 150 (6-picolyl *C*H), 151 (2-picolyl *C*), 169 (2-imidazol-2-ylidene *C*), 170 (CO_2).

(Found: C, 59.72; H, 5.65; N, 8.34. $C_{26}H_{28}N_3O_2Pd$ calculated: C, 59.95; H, 5.42; N, 8.07%).

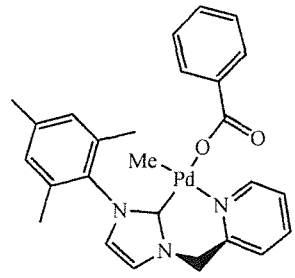

Figure 6.10. Compound **(6.8)**.

(6.9) [3-(2,6-di*iso*propylphenyl)-1-(α-picolyl) imidazol-2-ylidene] palladium methyl tosylate

This was prepared following the general method from [3-(2,6-di*iso*propylphenyl)-1-(α-picolyl) imidazol-2-ylidene] palladium methyl bromide **(4.3)** (0.4g, 0.769mmol) and silver tosylate (0.24g, 0.846mmol) in dichloromethane (50ml) by stirring at room temperature for 12 hours. The product was obtained in quantitative yields as a yellow solid.

MS (ES): *m/z* 469, $[(ligand)PdMe + MeCN]^+$.

$\delta_H(CDCl_3)$ -0.1 (3H, s, $PdCH_3$), 1.0, 1.4 [2 × 6H, br. d, $CH(CH_3)_2$], 2.3 (3H, s, OTs CH_3), 2.4 [2H, septet, $CH(CH_3)_2$], 5.5 (2H, br. s, CH_2), 6.8 (1H, d, 5-imidazol-2-ylidene *H*), 7.1 (2H, d, OTs *H*), 7.2 (1H, d, 4-imidazol-2-ylidene *H*), 7.2 (2H, d, $^iPr_2C_6H_2H$), 7.3 (1H, m, 5-picolyl *H*), 7.4 (1H, t, $^iPr_2C_6H_2H$), 7.5, 7.6 (2H, br., 3,4-picolyl *H*), 7.8 (2H, d, OTs *H*), 8.8 (1H, v. br., 6-picolyl *H*).

$\delta_C(CDCl_3)$ -7 ($PdCH_3$), 21 (OTs CH_3), 24, 26 ($CH(CH_3)_2$), 28 ($CH(CH_3)_2$), 56 (CH_2), 115, 139, (OTs *C*), 122, 135 ($^iPr_2C_6H_3$), 124 (5-picolyl *C*H), 124, 131 ($^iPr_2C_6H_3$), 125 (4-imidazol-2-ylidene *C*), 129 (3-picolyl *C*H), 126, 129 (OTs *C*H), 138 (5-imidazol-2-ylidene *C*), 142 (4-picolyl *C*H), 145 (6-picolyl *C*H), 152 (2-picolyl *C*), 174 (2-imidazol-2-ylidene *C*).

(Found: C, 56.75; H, 5.83; N, 6.55. $C_{29}H_{36}N_3O_3PdS$ calculated: C, 56.81; H, 5.92; N, 6.85%).

(6.10) [3-(2,6-di*iso*propylphenyl)-1-(2-pyridyl) imidazol-2-ylidene] palladium methyl tosylate

This was prepared following the general method from [3-(2,6-di*iso*propylphenyl)-1-(2-pyridyl) imidazol-2-ylidene] palladium methyl bromide **(4.4)** (0.38g, 0.75mmol) and silver tosylate (0.21g, 0.75mmol) in dichloromethane (50ml) by stirring at room temperature for 12 hours. The product was obtained in quantitative yields as a yellow solid. X-ray diffraction quality crystals were obtained by layering a saturated solution of dichloromethane with diethyl ether (*Figure 6.11* and *Table 6.3*).

MS (ES): *m/z* 455, [(ligand)PdMe + MeCN]$^+$.

δ_H($CDCl_3$) 0.0 (3H, s, PdCH_3), 1.1, 1.2 [2 × 6H, d, CH(CH_3)$_2$], 2.3 (3H, s, OTs CH_3), 2.5 [2H, septet, CH(CH_3)$_2$], 6.9 (1H, d, 5-imidazol-2-ylidene *H*), 7.1 (2H, d, OTs *H*), 7.2 (2H, d, ^{i}Pr$_2$C$_6$$H_2$H), 7.4 (1H, m, 5-picolyl *H*), 7.5 (1H, t, ^{i}Pr$_2$C$_6$H$_2$*H*), 7.7 (1H, d, 3-picolyl *H*), 7.8 (2H, d, OTs *H*), 7.9 (1H, d, 4-imidazol-2-ylidene *H*), 8.1 (1H, dt, 4-picolyl *H*), 9.1 (1H, br. d, 6-picolyl *H*).

δ_C($CDCl_3$) -10 (PdCH_3), 21 (OTs CH_3), 23, 25 (CH(CH_3)$_2$), 28 (C H(CH_3)$_2$), 117, 142 (OTs *C*), 122, 135 (^{i}Pr$_2$C$_6$H$_3$), 124 (4-imidazol-2-ylidene *C*), 124 (5-picolyl *C*H), 124, 131 (^{i}Pr$_2$C$_6$H$_3$),126 (3-picolyl *C*H), 127, 129 (OTs *C*H), 140 (5-imidazol-2-ylidene *C*), 143 (4-picolyl *C*H), 145 (6-picolyl *C*H), 150 (2-picolyl *C*), 174 (2-imidazol-2-ylidene *C*).

(Found: C, 55.20; H, 5.42; N, 6.52. $(C_{28}H_{34}N_3O_3PdS)_4CH_2Cl_2$ calculated: C, 54.70; H, 5.61; N, 6.77%).

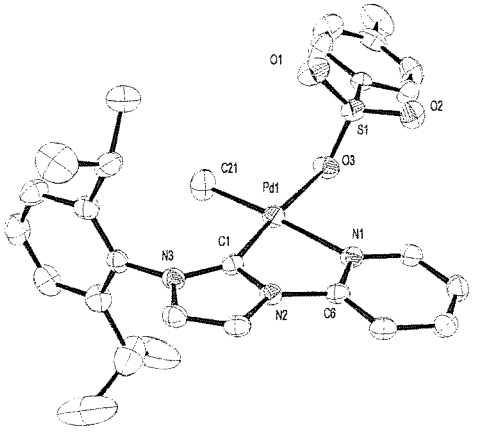

Figure 6.11. X-ray crystal structure of [3-(2,6-di*iso*propylphenyl)-1-(2-pyridyl) imidazol-2-ylidene] palladium methyl tosylate, compound **(6.10)**.

Pd(1)-C(1)	1.947(3)	N(2)-C(6)	1.413(4)
Pd(1)-C(21)	2.017(4)	N(3)-C(1)	1.358(4)
Pd(1)-O(3)	2.124(2)	N(3)-C(8)	1.393(4)
Pd(1)-N(1)	2.142(3)	N(3)-C(9)	1.442(4)
S(1)-O(1)	1.443(2)	C(8)-C(7)	1.328(5)
S(1)-O(2)	1.443(2)	C(5)-C(6)	1.369(5)
S(1)-O(3)	1.480(2)	C(5)-C(4)	1.377(5)
N(2)-C(1)	1.368(4)	N(1)-C(6)	1.339(4)
N(2)-C(7)	1.388(4)		

C(1)-Pd(1)-C(21)	98.36(15)	C(1)-N(2)-C(6)	120.2(2)
C(1)-Pd(1)-O(3)	173.08(11)	C(1)-N(3)-C(8)	110.7(3)
C(21)-Pd(1)-O(3)	88.04(14)	C(1)-N(3)-C(9)	125.7(3)
C(1)-Pd(1)-N(1)	79.49(11)	C(7)-C(8)-N(3)	108.0(3)
C(21)-Pd(1)-N(1)	176.44(17)	C(6)-N(1)-Pd(1)	113.1(2)
O(3)-Pd(1)-N(1)	94.24(9)	N(1)-C(6)-N(2)	112.5(3)
O(1)-S(1)-O(2)	114.64(15)	C(5)-C(6)-N(2)	123.6(3)
O(1)-S(1)-O(3)	112.38(14)	N(3)-C(1)-N(2)	103.4(3)
O(2)-S(1)-O(3)	111.56(14)	N(3)-C(1)-Pd(1)	142.2(2)
S(1)-O(3)-Pd(1)	122.72(13)	N(2)-C(1)-Pd(1)	114.1(2)
C(1)-N(2)-C(7)	112.0(3)		

Table 6.3. Selected bond lengths (Å) and angles (°) for compound **(6.10)**.

Compound	**(6.10)**	**(6.7)**	**(6.3)**
Chemical formula	$C_{28}H_{33}N_3O_3PdS$	$C_{44}H_{38}AgF_9N_6O_6Pd_2$	$C_{68}H_{89}F_{12}N_{12}O_9Pd_4$
Formula weight	598.03	1238.47	1872.11
Crystal system	Monoclinic	Triclinic	Triclinic
Space group	$P\,2_1/c$	P-1	P-1
a/Å	15.0071(2)	13.918(3)	9.852(2)
b/Å	11.7722(2)	15.726(3)	20.026(4)
c/Å	16.2981(2)	15.906(3)	21.056(4)
α/°	90	113.86(3)	89.95(3)
β/°	110.0420(10)	97.85(3)	90.19(3)
γ/°	90	113.49(3)	90.04(3)
V/Å^3	2704.96(7)	2729.8(9)	4154.2(14)
Z	4	2	2
T/K	150(2)	150(2)	150(2)
μ/mm^{-1}	0.797	1.083	0.935
F(000)	1232	1224	1890
No. Data collected	23226	28224	34221
No. Unique data	6178	10149	10208
R_{int}	0.0553	0.2495	0.2498
Final R(|F|) for $F_O > 2\sigma(F_o)$	0.0408	0.1278	0.1095
Final R(F^2) for all data	0.0706	0.3885	0.2650

Table 6.4. Crystallographic parameters for compounds **(6.3)**, **(6.7)** and **(6.10)**.

6.5 Reactions of palladium carbene complexes with phosphines and amines

6.5.1. General method

To a solution of the corresponding palladium carbene complex [either compound **(4.2)**, **(4.3)** or **(4.4)**] in dichloromethane, was added drop-wise a solution of the corresponding phosphine or amine and the mixture stirred at room temperature for 12-48 hours. After completion, the volatiles were removed under vacuum, the resulting solid was washed with diethyl ether, and drying under vacuum gave pale yellow solids.

6.5.2. Reaction between [3-(mesityl)-1-(α-picolyl) imidazol-2-ylidene] palladium methyl bromide (4.2) and triphenylphosphine

This was performed by following the general method from [3-(mesityl)-1-(α-picolyl) imidazol-2-ylidene] palladium methyl bromide **(4.2)** (0.1g, 0.23mmol) and triphenylphosphine (0.055g, 0.23mmol) in dichloromethane (50ml) by stirring at room temperature for 12 hours.

MS (ES): *m/z* 439, $[(\text{ligand})\text{PdMe} + \text{MeCN}]^+$; 662, $[(\text{ligand})\text{PdMe} + \text{PPh}_3]^+$.

$\delta_H(CDCl_3)$ broad peaks.

$\delta_P(CDCl_3)$ -4.

6.5.3. Reaction between [3-(2,6-di*iso*propylphenyl)-1-(α-picolyl) imidazol-2-ylidene] palladium methyl bromide (4.3) and trimethylphosphine

This was performed by following the general method from [3-(2,6-di*iso*propyl-phenyl)-1-(α-picolyl) imidazol-2-ylidene] palladium methyl bromide **(4.3)** (0.05g, 0.02mmol) and trimethylphosphine (0.5ml) in dichloromethane (20ml) by stirring at room temperature for 12 hours.

MS (ES): *m/z* 536, $[(\text{ligand})\text{PdMe} + \text{MeCN}]^+$.

$\delta_H(CDCl_3)$ peaks including 0.2 (3H, br., $PdCH_3$), 1.4, 1.6 [2 × 6H, d, $CH(CH_3)_2$], 1.5 [9H, d, PCH_3], 3.0 [2H, septet, $CH(CH_3)_2$], 5.4, 6.3 (2H, dd, CH_2), 7.2 (1H, d, 5-imidazol-2-ylidene *H*), 7.4 (2H, d, $^iPr_2C_6H_2H$), 7.5 (1H, m, 5-picolyl *H*), 7.6 (1H, t, $^iPr_2C_6H_2H$), 7.9 (1H, d, 4-imidazol-2-ylidene *H*), 8.2 (1H, dt,4-picolyl *H*), 8.5 (2H, d, 3-picolyl *H*), 8.7 (1H, br. d, 6-picolyl *H*).

$\delta_P(CDCl_3)$ 25.

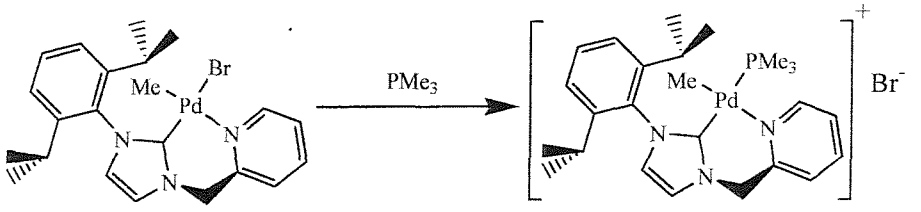

Scheme 6.6. Proposed reaction of compound **(4.3)** with trimethylphosphine.

6.5.4. Reaction between [3-(2,6-di*iso*propylphenyl)-1-(2-pyridyl) imidazol-2-ylidene] palladium methyl bromide (4.4) and trimethylphosphine

This was performed by following the general method from [3-(2,6-di*iso*propyl-phenyl)-1-(2-pyridyl) imidazol-2-ylidene] palladium methyl bromide **(4.4)** (0.05g, 0.02mmol) and trimethylphosphine (0.5ml) in dichloromethane (20ml) by stirring at room temperature for 12 hours.

MS (ES): *m/z* 522, $[(\text{ligand})\text{PdMe} + \text{PMe}_3]^+$.

$\delta_H(CDCl_3)$ 0.2 (3H, s, PdC*H*$_3$), 1.1, 1.2 [2 × 6H, d, CH(C*H*$_3$)$_2$], 1.5 [9H, d, PC*H*$_3$], 2.3 [2H, septet, C*H*(CH$_3$)$_2$], 7.1 (1H, d, 5-imidazol-2-ylidene *H*), 7.3 (2H, d, ^{i}Pr$_2$C$_6$*H*$_2$H), 7.3 (1H, m, 5-pyridyl *H*), 7.5 (1H, t, ^{i}Pr$_2$C$_6$H$_2$*H*), 7.7 (1H, dt, 4-pyridyl *H*), 7.9 (2H, d, 3-pyridyl *H*), 8.2 (1H, d, 4-imidazol-2-ylidene *H*), 8.5 (1H, d, 6-pyridyl *H*).

$\delta_P(CDCl_3)$ 25.

6.5.5. Reaction between [3-(2,6-di*iso*propylphenyl)-1-(α-picolyl) imidazol-2-ylidene] palladium methyl bromide (4.3) and triethylamine

This was performed by following the general method from [3-(2,6-di*iso*propyl-phenyl)-1-(α-picolyl) imidazol-2-ylidene] palladium methyl bromide **(4.3)** (0.05g, 0.02mmol) and trimethyllphosphine (0.5ml) in dichloromethane (20ml) by stirring at room temperature for 48 hours (*Scheme 6.6*).

MS (ES): *m/z* 543, $[(\text{ligand})\text{PdMe} + \text{NEt}_3]^+$.

$\delta_H(CDCl_3)$ 0.1, 0.2 (3H, s, PdC*H*$_3$), 1.0, 1.4 [2 × 6H, br. d, CH(C*H*$_3$)$_2$], 1.1 [6H, t, N(CH$_2$C*H*$_3$)$_3$], 2.4 [2H, septet, C*H*(CH$_3$)$_2$], 2.6 [4H, q, N(C*H*$_2$CH$_3$)$_3$], 5.5 (2H, br., C*H*$_2$), 6.8 (1H, d, 5-imidazol-2-ylidene *H*), 7.2 (2H, d, ^{i}Pr$_2$C$_6$*H*$_2$H), 7.4 (1H, m, 5-picolyl *H*), 7.4 (1H, t, ^{i}Pr$_2$C$_6$H$_2$*H*), 7.4 (1H, d, 4-imidazol-2-ylidene *H*), 7.6 (2H, d, 3-picolyl *H*), 7.8 (1H, dt, 4-picolyl *H*), 9.2, 9.3 (1H, 2 x d, 6-picolyl *H*).

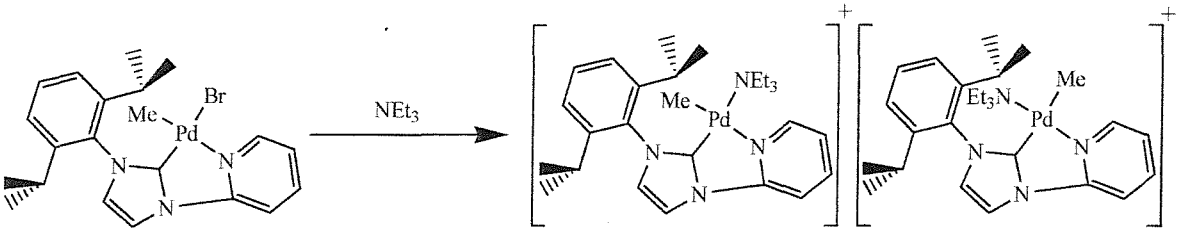

Scheme 6.7. Proposed reaction of compound **(4.4)** with triethylamine.

6.5.6. Reaction between [3-(2,6-di*iso*propylphenyl)-1-(2-pyridyl) imidazol-2-ylidene] palladium methyl bromide (4.4) and triethylamine

This was performed by following the general method from [3-(2,6-di*iso*propyl-phenyl)-1-(2-pyridyl) imidazol-2-ylidene] palladium methyl bromide **(4.4)** (0.05g, 0.02mmol) and trimethyllphosphine (0.5ml) in dichloromethane (20ml) by stirring at room temperature for 48 hours (*Scheme 6.7*).

MS (ES): *m/z* 529, $[(\text{ligand})\text{PdMe} + \text{NEt}_3]^+$.

$\delta_H(CDCl_3)$ 0.3, 0.3 (3H, s, $PdCH_3$), 1.0 [6H, t, $N(CH_2CH_3)_3$], 1.1, 1.3 [2 × 6H, d, $CH(CH_3)_2$], 2.5 [4H, q, $N(CH_2CH_3)_3$], 2.6 [2H, septet, $CH(CH_3)_2$], 7.0 (1H, d, 5-imidazol-2-ylidene *H*), 7.3 (2H, d, $^iPr_2C_6H_2H$), 7.4 (1H, m, 5-pyridyl *H*), 7.5 (1H, t, $^iPr_2C_6H_2H$), 7.6 (2H, d, 3-pyridyl *H*), 7.8 (1H, d, 4-imidazol-2-ylidene *H*), 8.0 (1H, dt, 4-pyridyl *H*), 9.2, 9.4 (1H, 2 x d, 6-pyridyl *H*).

REFERENCES

1 (a) B. Cornils, W.A. Herrmann, *Applied Homogeneous Catalysis with Organometallic Compounds*, Wiley-VCH, Weinheim, **2000**, 725; (b) A.A.D. Tulloch, A.A. Danopoulos, G.J. Tizzard, S.J. Coles, M.B. Hursthouse, R.S. Hay-Motherwell, W.B. Motherwell, *Chem. Commun.*, **2001**, 1270.

2 M.G. Gardiner, W.A. Herrmann, C.-P. Reisinger, J. Schwarz, M. Spiegler, *J. Organomet. Chem.*, **1999**, *572*, 239.

3 M. Scholl, T.M. Trnka, J.P. Morgan, R.H. Grubbs, *Tetrahedron Lett.*, **1999**, *40*, 2247.

4 W.A. Herrmann, L.J. Goossen, C. Køcher, G.R.J. Artus, *Angew. Chem., Int. Ed. Engl.*, 1996, **35**, 2805.

5 J.C.C. Chen, I.J.B. Lin, *Organometallics*, **2000**, *19*, 5113.

6 D.S. McGuinness, N. Saendig, B.F. Yates, K.J. Cavell, *J. Am. Chem. Soc.*, **2000**, *123*, 4029; W.A. Herrmann, V.P.W. Böhm, C.W.K. Gstöttmayr, M. Grosche, C.-P. Reisinger, T. Weskamp, *J. Organomet. Chem.*, **2001**, *617*, 616.

7 P. Braunstein, F. Naud, *Angew. Chem., Int. Ed.*, **2001**, *40*, 680.

8 W.A. Herrmann, L.J. Goossen, M. Spiegler, *Organometallics*, **1998**, *17*, 2162.

9 D.S. McGuinness, N. Saendig, B.F. Yates, K.J. Cavell, *J. Am. Chem. Soc.*, **2001**, *123*, 4029; *Chem. Commun.*, **2001**, 355.

Chapter 7

N-Heterocyclic Carbene Complexes of Nickel (II), Ruthenium (II) and Rhodium (I)

Chapter 7

N-Heterocyclic Carbene Complexes of Nickel (II), Ruthenium (II) and Rhodium (I)

7.1 Introduction

Carbene complexes are now known for all transition metals, except technetium.[1] Most of the published examples are of palladium. However, only very few reports describe transition metal complexes that contain mixed donor *N*-functionalised carbene ligands; only three examples are known of structurally characterised mixed donor *N*-heterocyclic carbene complexes that do not contain palladium. These are:

i) Rhodium coordinated by a carbene-oxazoline ligand.[2]

ii) Molybdenum coordinated by a carbene-allyl ligand.[3]

iii) Iridium coordinated by a carbene-picolyl ligand where the carbene adopts an unusual binding mode.[4]

Described in this chapter are three new mixed donor *N*-heterocyclic carbene complexes of transition metals, two of which are structurally characterised. The nickel complex is the first example of a mixed donor *N*-heterocyclic carbene complex of nickel.

RESULTS AND DISCUSSION

7.2 Synthesis of nickel (II), ruthenium (II) and rhodium (I) complexes

The transition metal complexes described in this chapter were synthesised by the interaction of [3-(mesityl)-1-(α-picolyl) imidazol-2-ylidene] silver bromide **(3.5)**, with nickel dibromide dimethoxyethane, ruthenium dichloride η^6-*p*-cymene dimer or rhodium chloride cyclooctadiene dimer in dichloromethane. The products were isolated as highly coloured solids (*Figure 7.1*).

7.2.1. Elemental analysis and mass spectroscopy

The stoichiometry of compound **(7.2)** was identified by elemental analysis and the electrospray mass spectra obtained confirmed the formation of a ruthenium carbene complex by a peak assigned to the molecular ion made up of the carbene ligand a ruthenium, a chlorine and a *p*-cymene ligand. This molecular ion is consistent with the

formation of a ruthenium complex, which comprises of one carbene ligand, a cymene ligand and two chlorine atoms; similar to the stoichiometry of the complexes described by Nolan.[5] A possible structure for compound **(7.2)** is proposed in *Figure 7.1*.

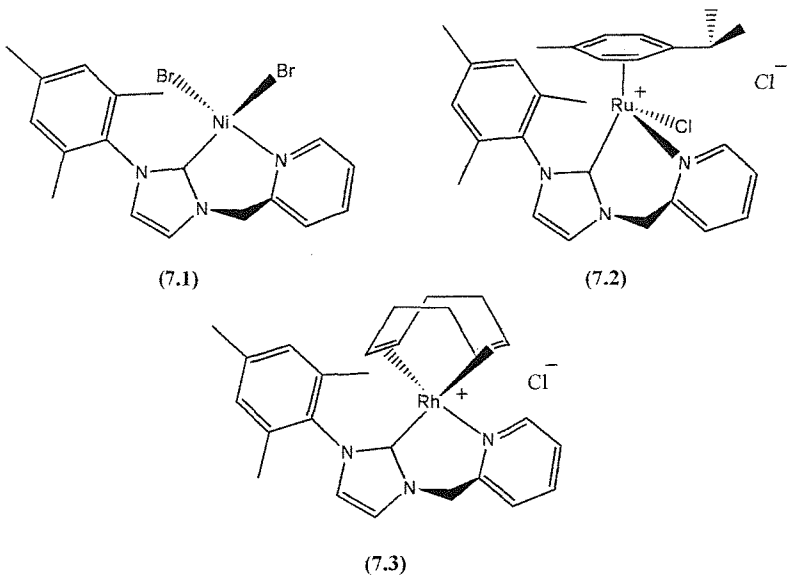

Figure 7.1. Nickel, ruthenium and rhodium compounds synthesised.

The stoichiometry of compounds **(7.1)** and **(7.3)** were identified by elemental analysis, however the silver bromide proved difficult to remove and was only removed after repeated recrystallisations. The crystal structure of **(7.3)** shows that the counter ion is a chloride ion, where as the analysis shows it to be a silver chloride bromide anion. The silver bromide was also difficult to remove from compound **(7.1)** but on recrystallisation was completely removed. The electrospray mass spectrum for compound **(7.1)** was not collected, as the complex was insoluble in suitable solvents for this procedure. However, the electrospray mass spectrum obtained for compound **(7.3)** was consistent with the structure obtained from X-ray diffraction studies (*Figure 7.4*).

7.2.2. X-ray diffraction studies on compound (7.1)

X-ray diffraction quality crystals of [3-(mesityl)-1-(α-picolyl) imidazol-2-ylidene] nickel dibromide **(7.1)** were obtained by layering a saturated dichloromethane solution with petrol. The structure comprises a nickel centre coordinated by two bromine atoms and both the carbene and the picolyl ends of a ligand (*Figure 7.2*). The nickel atom is in a tetrahedral geometry. The unpaired electrons give the complex the intense purple colour as well as its paramagnetism.

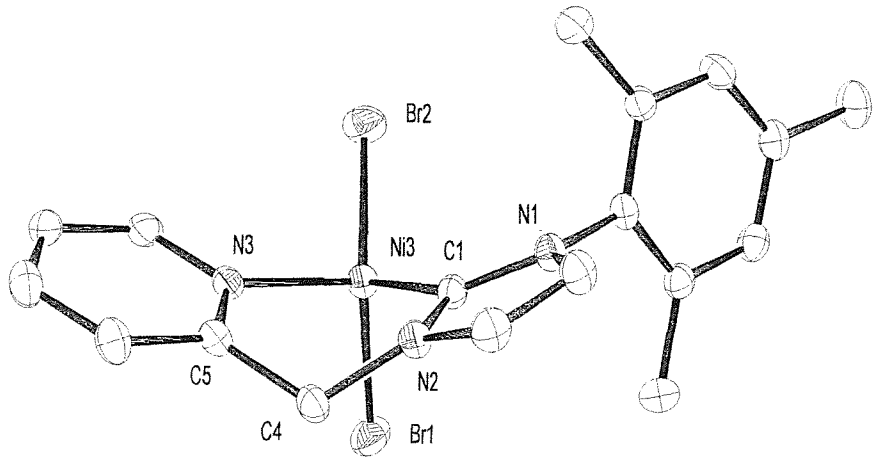

Figure 7.2. X-ray crystal structure of [3-(mesityl)-1-(α-picolyl) imidazol-2-ylidene] nickel dibromide, compound **(7.1)**.

The ligand chelate ring is in a boat type conformation with a bite angle (carbene-nickel-nitrogen) of 92.7°. The ligand can easily accommodate the tetrahedral geometry by reducing the angle created by the methylene bridge (113.1°); in the square planar geometry of compound **(4.2)** this angle is 116.5°. The nickel-carbene and nickel-nitrogen bond lengths are 1.96 and 2.03Å, which are not very different from those of compound **(4.2)**. The rest of the bond angles and bond lengths of the ligand are similar to those of compound **(4.2)**.

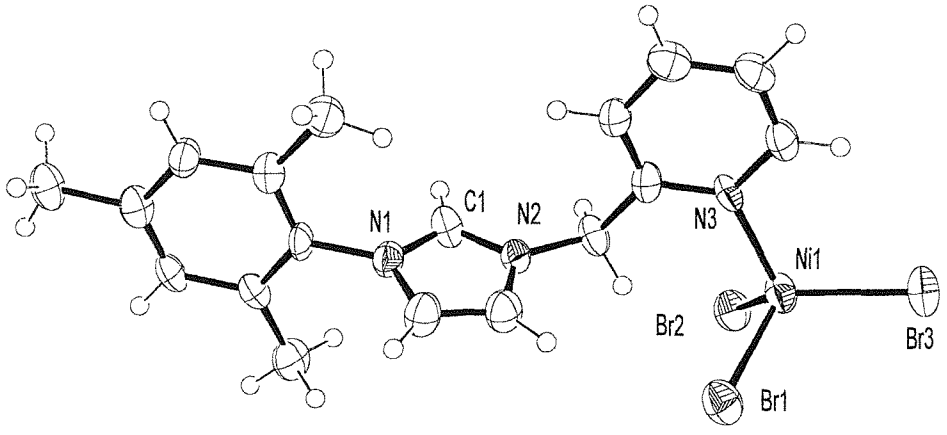

Figure 7.3. X-ray crystal structure of [3-(mesityl)-1-(α-picolyl) imidazolium] nickel tribromide, decomposition product of compound **(7.1)**.

When complex **(7.1)** was recrystallised in air a very small number of blue crystal were also isolated. These blue crystals were also of X-ray diffraction quality and their structure is shown in *Figure 7.3*. The structure comprises a nickel atom coordinated by three bromine atoms and a picolyl moiety. The other end of the ligand is not a carbene but an imidazolium cation. The nickel is in a tetrahedral environment and the nickel-nitrogen bond (2.02Å) is only very slightly shorter than that of compound **(7.1)**. The reason for this decomposition (blue crystals) is unknown but the decomposition does not occur under nitrogen, therefore it is believed that compound **(7.1)** is slightly moisture-sensitive. The purple crystals of **(7.1)** do not dissolve in water and do not show any decomposition over a few hours.

7.2.3. X-ray diffraction studies on compound (7.3)

X-ray diffraction quality crystals of [3-(mesityl)-1-(α-picolyl) imidazol-2-ylidene] rhodium cyclooctadiene chloride **(7.3)** were obtained by layering a saturated dichloromethane solution with diethyl ether. The structure consists of a chloride anion and a cationic rhodium complex. The cationic complex comprises a central rhodium atom coordinated by a η^4-1,5-cyclooctadiene and a chelating carbene ligand in a slightly distorted square-planar geometry (*Figure 7.4*).

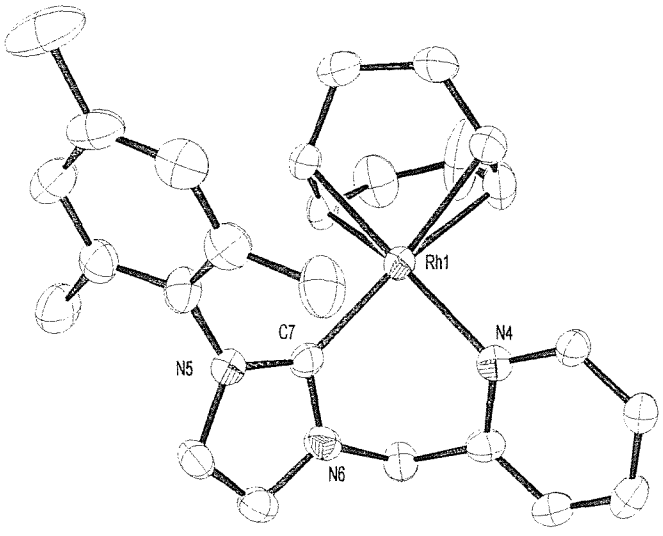

Figure 7.4. Cationic complex from the X-ray crystal structure of [3-(mesityl)-1-(α-picolyl) imidazol-2-ylidene] rhodium cyclooctadiene chloride, compound **(7.3)**.

The carbene-rhodium and the nitrogen-rhodium bond lengths are similar to those reported by Herrmann *et al.*[2]. The distance between the metal centre and the double bonds

of the cyclooctadiene is slightly longer for the atoms *trans* to the carbene end of the ligand. This is in keeping with the carbene being a stronger donor than the picolyl group. The carbene ligand is once again in a boat type conformation but the ligand is even flatter across the methylene bridge (110.1°) than compound **(7.1)**. The bite angle of the ligand (84.6°) is considerably smaller than that of compound **(7.1)** but similar to that of the complex reported by Herrmann *et al.*[2] This tighter bite angle can be accounted for by the longer nitrogen-rhodium bond. The other bond lengths and angles of the ligand are similar to that of compound **(7.1)**.

7.2.4. NMR spectroscopy

The ^{1}H NMR spectrum was not able to be collected for compound **(7.1)** as the complex is paramagnetic due to unpaired *d* electrons (tetrahedral d^8 complex). However, ^{1}H NMR spectroscopy proved to be very useful in identifying the formation of the ruthenium complex **(7.2)**. The spectrum obtained for the reaction contained peaks that showed the formation of a chelating carbene complex by the appearance of a pair of doublets at 5.0 and 5.9 ppm assigned to the protons of the methylene bridge.

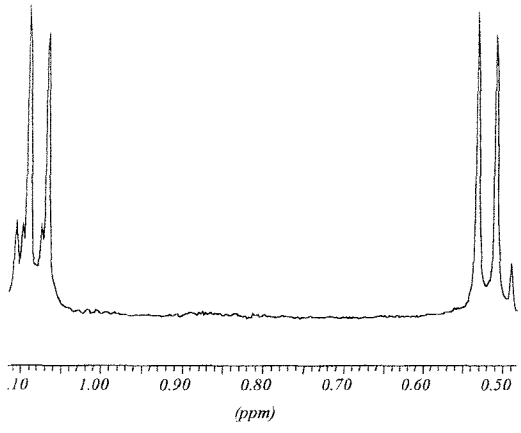

Figure 7.5. ^{1}H NMR spectrum of compound **(7.2)**; isopropyl diastereotopic methyl protons of the η^6-*p*-cymene ligand.

The ruthenium carbene complex was further identified by characteristic peaks at 9.3, 7.9, 7.7 and 7.4 ppm for the protons of the picolyl ring as well as peaks at 7.8 and 7.1 ppm for the protons in the 4- and 5-positions of the imidazol-2-ylidene ring (*Figure 7.6*).

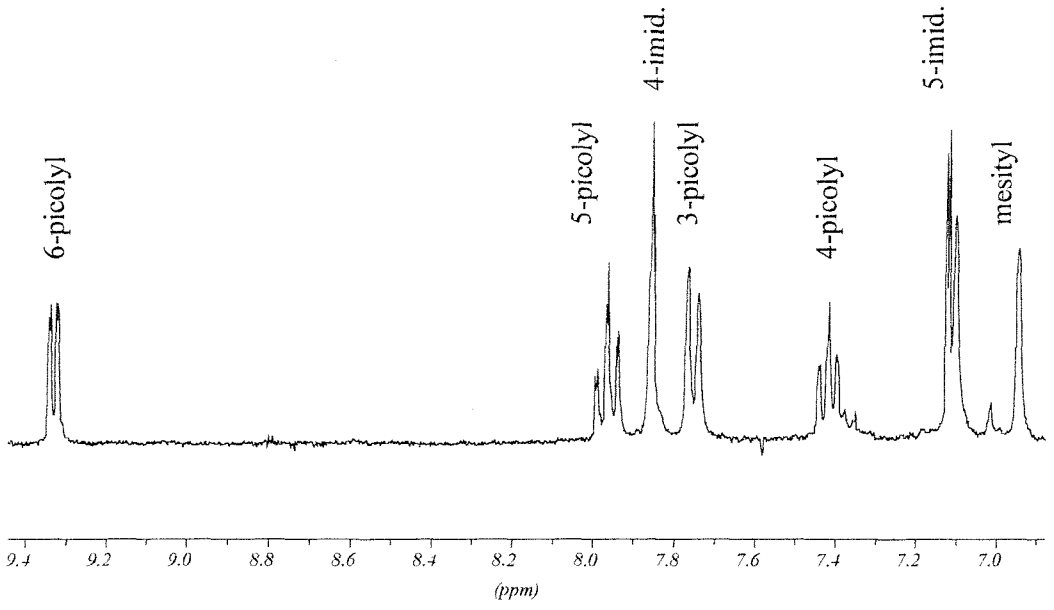

Figure 7.6. ^{1}H NMR spectrum of compound **(7.2)**; between 9.4 and 6.9 ppm.

These peaks in the spectrum of compound **(7.2)** were of very similar shift, and symmetry to those of the palladium complex **(4.2)** with the same chelating ligand. Peaks were also identified in the ^{1}H NMR spectrum for the cymene ligand and the mesityl group of the carbene ligand. The cymene has no plane of symmetry in this complex; this was demonstrated by the spectrum containing two peaks for the isopropyl methyls (*Figure 7.5*) as well as four peaks for the ring protons. The lack of symmetry of the complex supports the suggested structure in *Figure 7.1*.

Compound **(7.3)** was also characterised by ^{1}H NMR spectroscopy. The broad peak assigned to the methylene bridge protons shows that the ring-flipping process (observed for compounds in Chapter Four), happens very rapidly at room temperature. The peaks assigned to the cyclooctadiene ligand were generally broad probably due to the lack of symmetry in the molecule and the rapid ring flipping of the carbene-picolyl chelate. The peak in the ^{1}H NMR spectrum for the proton in the 6-position of the picolyl ring shifted up-field from that of the palladium complex **(4.2)**, giving it a very similar shift to that of the uncoordinated imidazolium salt **(2.2)**. The reason for the chemical shift of this peak is unknown but could be due to a shielding effect of the double bonds of the cyclooctadiene. The peaks for the rest of the ligand are very similar to those observed for compound **(7.2)** and to those of the palladium complex **(4.2)**.

7.3 Conclusions

The synthesis and characterisation of a range of transition metal mixed donor *N*-heterocyclic carbene complexes have been described in this chapter. These include:

i) The first example of a nickel complex that contains a mixed donor *N*-heterocyclic carbene ligand; with the nickel in a tetrahedral environment, chelated by the carbene ligand.

ii) A structurally characterised rhodium complex, the X-ray crystal structure of which shows the cationic rhodium complex to have a distorted square-planar geometry. The carbene and cyclooctadiene ligand are both acting as chelating ligands.

iii) A ruthenium mixed donor carbene complex has been characterised by ^{1}H NMR spectroscopy, mass spectroscopy and chemical analysis. Although no crystal structure was obtained, the complex has been shown to contain a chelating mixed donor carbene ligand. This complex is the first example of a ruthenium complex that contains a mixed donor *N*-heterocyclic carbene ligand, where both donor atoms are coordinated to the metal centre.

These new transition metal carbene complexes are important as there are very few examples with mixed donor carbene ligands. The synthesis and characterisation of these complexes has led to a variety of other transition metal complexes to be synthesised by others.[6]

EXPERIMENTAL

7.4 Synthesis of nickel and rhodium complexes

7.4.1. General method

A dichloromethane solution of [3-(mesityl)-1-(α-picolyl)-imidazol-2-ylidene] silver bromide was added drop wise to a solution of the corresponding metal complex and stirred at room temperature for 4 hours. After completion, the reaction mixture was filtered, the volatiles were removed under vacuum, the resulting solid was washed with diethyl ether, and dried under vacuum. The solids were purified by recrystallisation from a saturated solution of dichloromethane and diethyl ether.

(7.1) [3-(mesityl)-1-(α-picolyl)-imidazol-2-ylidene] nickel dibromide

This was prepared following the general method from [3-(mesityl)-1-(α-picolyl)-imidazol-2-ylidene] silver bromide (0.2g, 0.41mmol) and dimethoxyethane nickel dibromide (0.12g, 0.41mmol) in dichloromethane (40ml) by stirring at room temperature for 4 hours. The product was obtained in quantitative yields as a purple solid. X-ray diffraction quality crystals were obtained by layering a saturated dichloromethane solution with petrol (*Figure 7.7 and Table 7.1*).

(Found: C, 43.60; H, 3.86; N, 8.47. $C_{18}H_{19}N_3NiBr_2$ requires C, 43.68; H, 3.87; N, 8.41%).

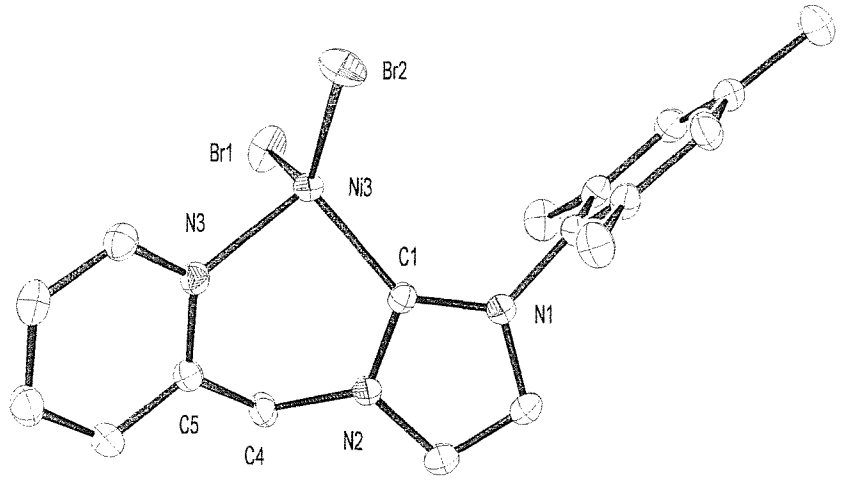

Figure 7.7. X-ray crystal structure of [3-(mesityl)-1-(α-picolyl) imidazol-2-ylidene] nickel dibromide, compound **(7.1)**.

Br(1)-Ni(3)	2.3677(4)	N(1)-C(11)	1.440(3)
Br(2)-Ni(3)	2.3585(4)	N(2)-C(1)	1.349(3)
Ni(3)-C(1)	1.961(2)	N(2)-C(3)	1.384(3)
Ni(3)-N(3)	2.030(2)	N(2)-C(4)	1.462(3)
N(3)-C(5)	1.354(3)	C(2)-C(3)	1.345(4)
N(1)-C(1)	1.348(3)	C(4)-C(5)	1.502(3)
N(1)-C(2)	1.387(3)		
C(1)-Ni(3)-N(3)	92.74(9)	C(1)-N(1)-C(11)	125.97(19)
C(1)-Ni(3)-Br(2)	114.71(7)	C(1)-N(2)-C(3)	111.41(19)
N(3)-Ni(3)-Br(2)	104.15(6)	C(1)-N(2)-C(4)	122.70(19)
C(1)-Ni(3)-Br(1)	106.13(7)	N(1)-C(1)-N(2)	104.64(19)
N(3)-Ni(3)-Br(1)	106.83(6)	N(2)-C(1)-Ni(3)	119.29(16)
Br(2)-Ni(3)-Br(1)	126.556(16)	C(3)-C(2)-N(1)	106.9(2)
C(5)-N(3)-Ni(3)	121.45(16)	N(2)-C(4)-C(5)	113.06(19)
C(1)-N(1)-C(2)	110.85(19)	N(3)-C(5)-C(4)	118.3(2)

Table 7.1. Selected bond lengths (Å) and angles (°) for compound **(7.1)**.

Br(1)-Ni(1)	2.3873(15)	N(1)-C(3)	1.396(11)
Br(2)-Ni(1)	2.3757(15)	N(1)-C(4)	1.458(10)
Br(3)-Ni(1)	2.3783(14)	N(2)-C(1)	1.311(11)
Ni(1)-N(3)	2.024(7)	N(2)-C(2)	1.366(11)
N(3)-C(14)	1.352(10)	N(2)-C(13)	1.470(10)
N(1)-C(1)	1.320(11)	C(3)-C(2)	1.342(12)
N(3)-Ni(1)-Br(2)	110.2(2)	C(1)-N(1)-C(4)	126.0(7)
N(3)-Ni(1)-Br(3)	109.48(18)	C(3)-N(1)-C(4)	124.7(7)
Br(2)-Ni(1)-Br(3)	120.52(6)	C(1)-N(2)-C(2)	109.0(7)
N(3)-Ni(1)-Br(1)	101.51(19)	C(1)-N(2)-C(13)	124.9(7)
Br(2)-Ni(1)-Br(1)	106.50(5)	N(3)-C(14)-C(13)	117.7(8)
Br(3)-Ni(1)-Br(1)	106.79(6)	C(2)-C(3)-N(1)	105.0(8)
C(14)-N(3)-Ni(1)	124.7(6)	N(2)-C(1)-N(1)	108.4(8)
C(1)-N(1)-C(3)	109.2(7)	C(3)-C(2)-N(2)	108.3(8)

Table 7.2. Selected bond lengths (Å) and angles (°) for the decomposition product of compound **(7.1)**.

(7.2) [3-(mesityl)-1-(α-picolyl) imidazol-2-ylidene] ruthenium dichloride η^6-*p*-cymene

This was carried out following the general method by using [3-(mesityl)-1-(α-picolyl)-imidazol-2-ylidene] silver bromide (0.1g, 0.2mmol) and (ruthenium dichloride *p*-cymene)$_2$ (0.09g, 0.1mmol) in dichloromethane (40ml) and stirring at room temperature for 4 hours. The product was obtained in good yields as an orange solid.

MS (ES): *m/z* 548, [(ligand)RuClcymene + MeCN]$^+$.

δ_H($CDCl_3$) 0.5, 1.1 [2 × 3H, d, cym CH(CH_3)$_2$],1.6 (3H, s, cym CH_3), 2.1 (6H, s, mesityl CH_3), 2.3 (3H, s, mesityl CH_3), 3.3 [1H, br., cym CH(CH_3)$_2$], 5.0, 5.9 (2 × 1H, d, CH_2), 5.3, 5.4, 5.7, 5.8 (4 × 1H, d, cym CH), 6.9, 7.1 (2 × 1H, s, mesityl *H*), 7.1 (1H, d, 5-imidazol-2-ylidene *H*), 7.4 (1H, t, 5-picolyl *H*), 7.7 (1H, d, 3-picolyl *H*), 7.8 (1H, d, 4-imidazol-2-ylidene *H*), 7.9 (1H, td, 4-picolyl *H*), 9.3 (1H, d, 6-picolyl *H*).

(Found: C, 44.24; H, 4.74; N, 5.34. $C_{29}H_{37}Cl_2N_3RuAgBr$ requires C, 44.68; H, 4.32; N, 5.80%).

(7.3) [3-(mesityl)-1-(α-picolyl) imidazol-2-ylidene] rhodium cyclooctadiene chloride

This was prepared following the general method from [3-(mesityl)-1-(α-picolyl) imidazol-2-ylidene] silver bromide (0.2g, 0.40mmol) and (rhodium chloride cyclooctadiene)$_2$ (0.1g, 0.20mmol) in dichloromethane (40ml) by stirring at room temperature for 4 hours. The product was obtained in good yields as an orange solid. X-ray diffraction quality crystals were obtained by layering a saturated dichloromethane solution with diethyl ether (*Figure 7.8* and *Table 7.3*).

MS (ES): *m/z* 488, [(ligand)RhCOD + MeCN]$^+$.

δ_H($CDCl_3$) 1.7 (3H, s, mesityl CH_3), 1.9 (2H, br., COD CH_2), 2.1 (3H, s, mesityl CH_3), 2.2 (2H, br., COD CH_2), 2.4 (3H, s, mesityl CH_3), 4.6 (2H, br., CH_2), 6.7 (1H, d, 5-imidazol-2-ylidene *H*), 7.0 (2H, s, mesityl *H*), 7.2 (1H, d, 3-picolyl *H*), 7.3 (1H, d, 4-imidazol-2-ylidene *H*), 7.3 (2H, s, COD CH), 7.4 (1H, m, 5-picolyl *H*), 7.8 (1H, br., 4-picolyl *H*), 7.9, 8.3 (2H, br., COD CH), 8.4 (1H, d, 6-picolyl *H*).

(Found: C, 44.13; H, 4.24; N, 6.29. $C_{26}H_{31}N_3RhAgClBr$ requires C, 43.88; H, 4.39; N, 5.90%).

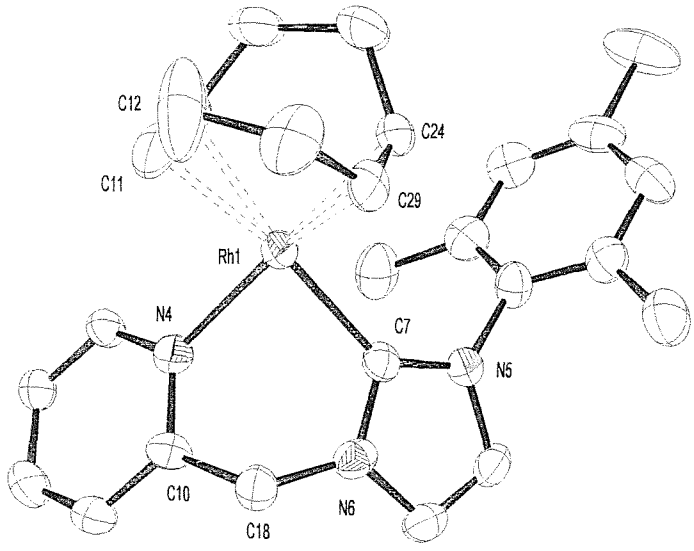

Figure 7.8. X-ray crystal structure of [3-(mesityl)-1-(α-picolyl) imidazol-2-ylidene] rhodium cyclooctadiene chloride, compound **(7.3)**.

Rh(1)-C(7)	2.035(10)
Rh(1)-C(29)	2.119(10)
Rh(1)-N(4)	2.125(9)
Rh(1)-C(24)	2.141(11)
Rh(1)-C(11)	2.190(12)
Rh(1)-C(12)	2.202(12)
N(4)-C(10)	1.357(14)
N(5)-C(7)	1.346(13)
N(5)-C(20)	1.403(15)

N(5)-C(21)	1.442(14)
N(6)-C(7)	1.344(14)
N(6)-C(27)	1.375(14)
N(6)-C(18)	1.467(13)
C(10)-C(18)	1.527(14)
C(11)-C(12)	1.31(2)
C(20)-C(27)	1.327(16)
C(24)-C(29)	1.405(17)

C(7)-Rh(1)-C(29)	92.7(4)
C(7)-Rh(1)-N(4)	84.6(4)
C(7)-Rh(1)-C(24)	94.8(4)
N(4)-Rh(1)-C(11)	91.3(4)
N(4)-Rh(1)-C(12)	97.5(4)
C(10)-N(4)-Rh(1)	119.7(7)
C(7)-N(5)-C(20)	109.4(9)
C(7)-N(5)-C(21)	124.8(9)
C(7)-N(6)-C(27)	110.8(9)
C(7)-N(6)-C(18)	121.8(9)
N(6)-C(7)-N(5)	105.6(9)
N(6)-C(7)-Rh(1)	118.7(7)

N(5)-C(7)-Rh(1)	135.1(8)
N(4)-C(10)-C(18)	116.7(9)
C(12)-C(11)-Rh(1)	73.1(8)
C(11)-C(12)-Rh(1)	72.1(8)
C(39)-C(12)-Rh(1)	109.4(7)
N(6)-C(18)-C(10)	110.1(8)
C(27)-C(20)-N(5)	107.0(10)
C(29)-C(24)-Rh(1)	69.9(6)
C(20)-C(27)-N(6)	107.2(10)
C(24)-C(29)-Rh(1)	71.6(6)

Table 7.3. Selected bond lengths (Å) and angles (°) for compound **(7.3)**.

Compound	(7.3)	(7.1)	(7.1) decomp.
Chemical formula	$C_{26}H_{31}ClN_3O_2Rh$	$C_{18}H_{19}Br_2N_3Ni$	$C_{18}H_{20}Br_3N_3Ni$
Formula weight	555.90	495.89	576.81
Crystal system	Triclinic	Monoclinic	Monoclinic
Space group	*P* -1	*P* 2_1/c	*P* 2_1/c
a/Å	1011.78(4)	1173.110(10)	1125.97(4)
b/Å	1154.86(4)	1056.550(10)	1185.85(4)
c/Å	1434.63(7)	1616.97(2)	1593.24(6)
α/°	73.550(2)	90	90.0000(10)
β/°	73.901(2)	109.9460(10)	104.654(2)
γ/°	81.123(2)	90.0000(10)	90.000(2)
V/Å^3	1539.42(11)	1883.93(3)	2058.14(13)
Z	2	4	4
T/K	150(2)	150(2)	150(2)
μ/mm^{-1}	0.664	5.276	6.773
F(000)	572	984	1128
No. Data collected	11244	22080	12572
No. Unique data	5679	5488	4445
R_{int}	0.0765	0.0478	0.0484
Final R(|F|) for $F_O > 2\sigma(F_o)$	0.1041	0.0345	0.0695
Final R(F^2) for all data	0.1442	0.0461	0.1121

Table 7.4. Crystallographic parameters for compounds **(7.3)**, **(7.1)** and the decomposition product of compound **(7.1)**.

REFERENCES

1 D. Bourissou, O. Guerret, F.P. Gabbaï, G. Bertrand, *Chem. Rev.*, **2000**, *100*, 39.

2 W.A. Herrmann, L. J. Goossen, M. Spiegler, *Organometallics*, **1998**, *17*, 2162.

3 J.A. Chamizo, P.B. Hitchcock, H.A. Jasim, M.F. Lappert, *J. Organomet. Chem.*, **1993**, *451*, 89.

4 S. Gründemann, A. Kovacevic, M. Albrecht, J.W. Faller, R.H. Crabtree, *Chem. Commun.*, **2001**, 2274.

5 L. Jafarpour, J. Huang, E.D. Stevens, S.P. Nolan, *Organometallics*, **1999**, 18, 3760.

6 A.A. Danopoulos, S. Winston, personal communication.

Chapter 8

Palladium (II) *N*-Heterocyclic Carbene Complexes as pre-Catalysts for the Heck Reaction

Chapter 8

Palladium (II) *N*-Heterocyclic Carbene Complexes as Pre-catalysts for the Heck Reaction

8.1 Introduction

The formation of carbon-carbon and carbon-nitrogen bonds plays an important role in the synthesis of organic chemicals. Palladium complexes catalyse a number of transformations leading to the formation of carbon-carbon bonds;[1] one of them is the Heck reaction. The Heck reaction, the palladium catalysed arylation or alkenylation of alkenes, is shown in *Scheme 8.1*.[2]

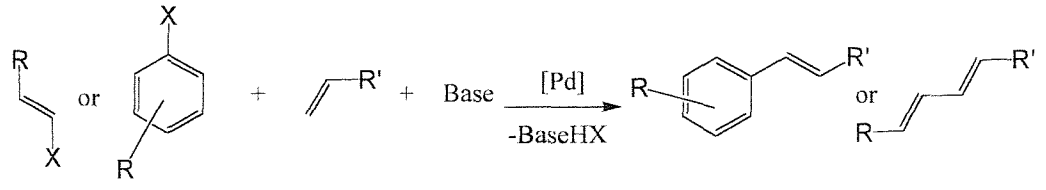

Scheme 8.1. The Heck reaction of aryl or alkenyl halides with alkenes.

The flexibility of the Heck and related reactions (such as Stille, Suzuki, Kumada, Negishi, and amination reactions) has been partly responsible for the huge amount of interest in the area.[3] Although there has been a great deal of research, the full scope and mechanisms of these reactions are not yet fully elucidated.

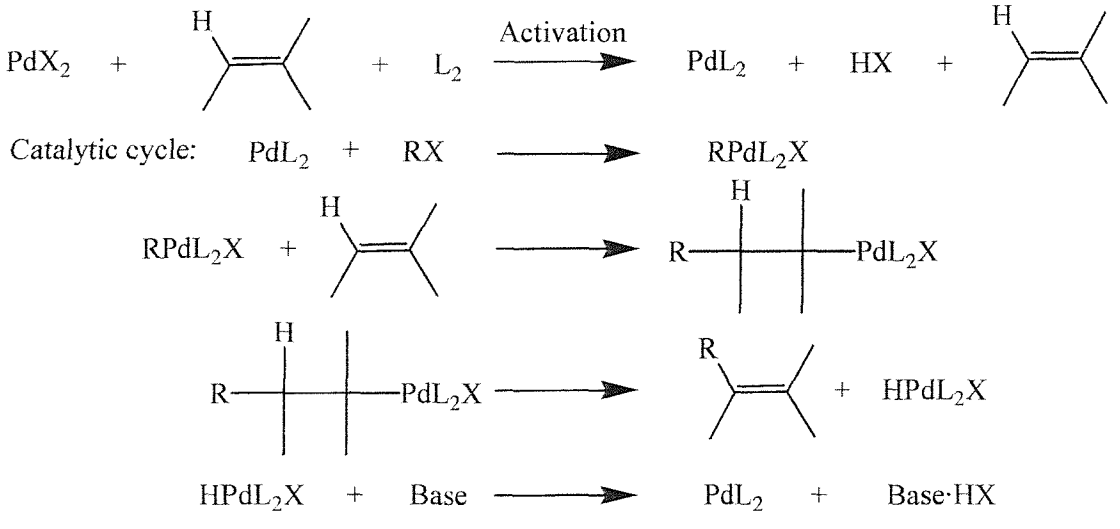

Scheme 8.2. An approximate mechanism for the Heck reaction, as proposed by R.F. Heck.[2]

8.1.1. Mechanisms of the Heck reaction

Probably one of the most debated issues in the Heck reaction is that of the nature and oxidation state of the active palladium species. R.F. Heck proposed the basic mechanism (*Scheme 8.2*), involving an activation step, an oxidative addition step, an insertion step, and a β-hydride elimination followed by the reductive elimination to recycle the palladium complex for the oxidative addition step. This is still generally accepted by most as a suitable general mechanism, but it does not explain a number of observations that have been made. Important questions that are still to be answered originate from the wide variety of different complexes that can act as effective pre-catalysts. For example:

i) Is the reaction taking place in solution (homogeneous) or on the surface of solid particles (heterogeneous) or does it run under both regimes under different conditions?

ii) What is the active catalyst?

iii) What is the operating mechanism?

The answers to these questions are probably not the same for the different types of pre-catalysts as a number of other metals are also known to facilitate the same transformations.[4]

Certain palladium (II) "catalysts" show an induction period (which can be shortened by the use of a reducing agent),[5] implying that the palladium goes through a palladium (0)-palladium (II) cycle, with the palladium (0) species starting the cycle (*Scheme 8.5*). However, this induction period is not observed with all complexes that are active pre-catalysts. In alternative mechanisms, there are no activation steps and the cycle involves palladium (II) and palladium (IV) species; proposed cycles are shown in *Scheme 8.3* and *Scheme 8.4*. The order of the elementary steps in these mechanisms are quite different; the first (*Scheme 8.3*) comprises of (i) the oxidative addition of the olefin to the palladium (II) active complex, (ii) the reductive elimination of HX, and (iii) the oxidative addition of the aryl halide followed by (iv) the reductive elimination of the product. However, the second (*Scheme 8.4*) involves (i) coordination of the olefin, (ii) the attack by a nucleophile on the coordinated olefin, (iii) the oxidative addition of ArX, (iv) the elimination of the nucleophile, (v) the insertion of Ar into the olefin, and (vi) β-hydride elimination and the dissociation of the product (vii) followed by the removal of the hydride by the base.

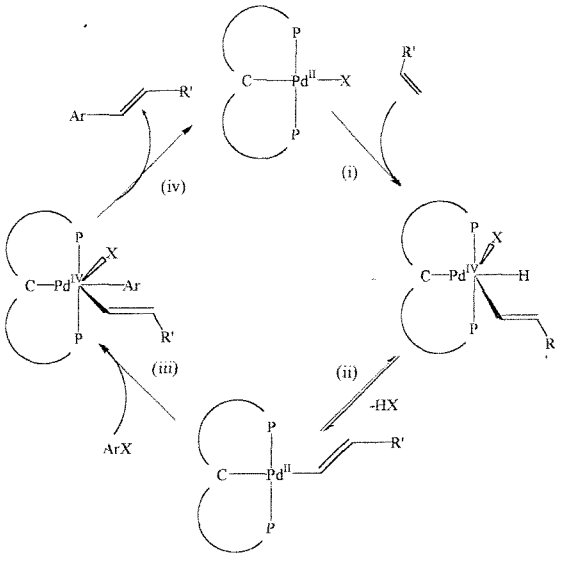

Scheme 8.3. Mechanism proposed by Jensen *et al.*[10] involving an octahedral palladium (IV) species with a pincer type tridentate ligand.

The situation is further complicated by the wide range of ligands that have been used to support homogeneous catalysts as well as a number of heterogeneous systems that are able to perform effectively.[6] Ligands on palladium that have been used in the Heck and similar reactions include a range of pincer tridentate ligands,[7,8,9,10] cyclopalladated phosphines,[11,23,12] cyclopalladated phosphites,[13] cyclopalladated imines,[14] bidentate bis carbenes,[5] mixed donor bidentate carbenes,[15,25] monodentate carbenes,[16,17] monodentate phosphines[18] and bidentate phosphines.[19]

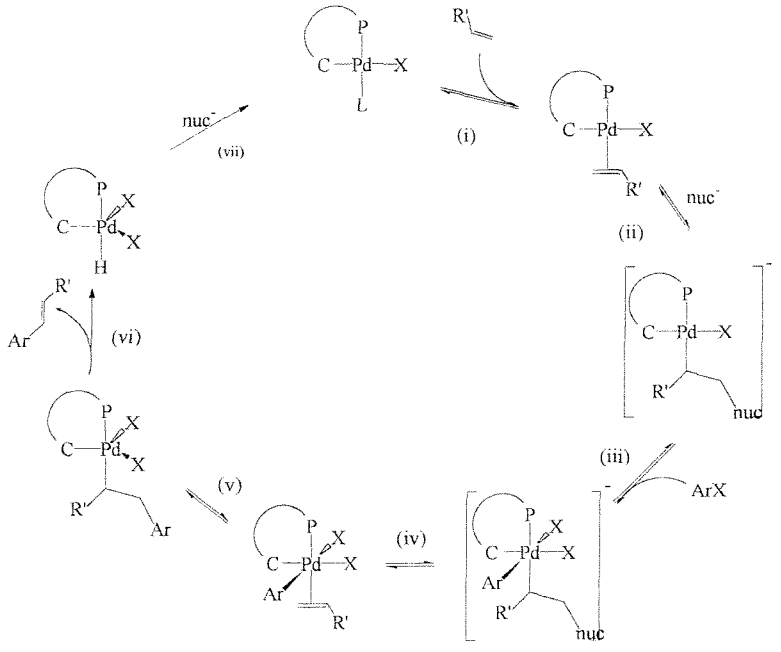

Scheme 8.4. Mechanism proposed by Shaw *et al.* following a palladium (II)-palladium (IV) cycle with a bidentate palladacycle.[20] nuc = nucleophile (Br^-, OH^-)

The use of phosphine ligands in the Heck reaction has been well studied and some conclusions on the mechanism have been drawn.[2,3] It is generally believed that the active catalyst is a 14-electron palladium (0) L_2 species, where L is usually a monodentate or L_2 is a bidentate phosphine.[27] It is believed that the reaction follows a mechanism similar to that shown in *Scheme 8.5*, involving a cycle between palladium (0) and palladium (II) species. The cycle comprises of an oxidative addition of the aryl halide to a 14-electron palladium (0) species followed by a coordination-insertion step, a β-hydride elimination-dissociation step and finally recycling of the palladium (II) to palladium (0) by the action of a base.

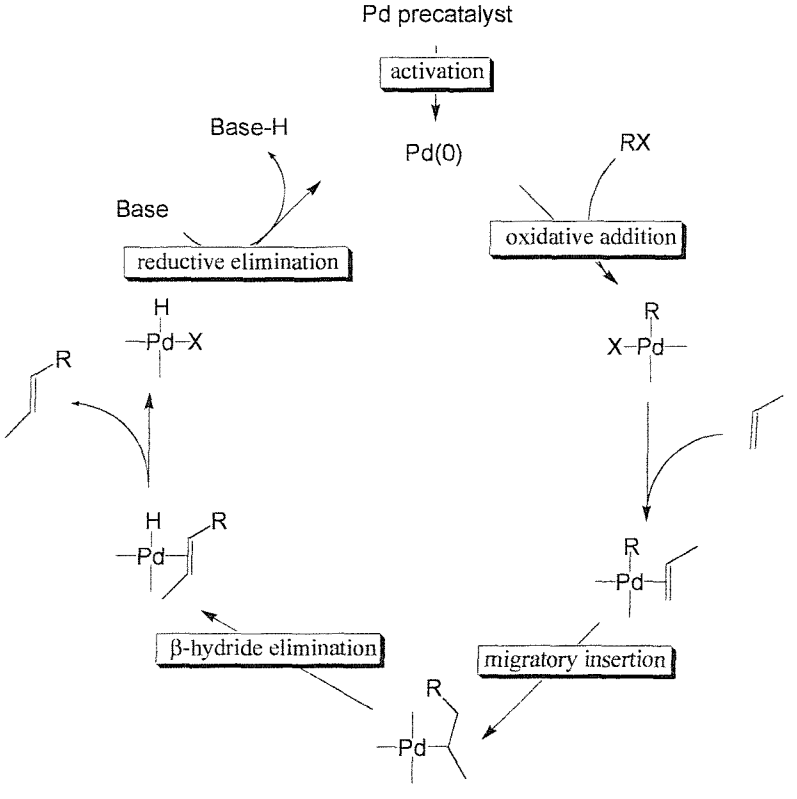

Scheme 8.5. A schematic mechanism for the Heck reaction, which involves a palladium (0)-palladium (II) cycle.[26]

8.1.2. Phosphine free systems for the Heck reaction

Phosphine free systems on the other hand, are less well studied and very few publications exist have shed any light on the nature of the active species or the operating mechanism.[21] From the small number of publications on the mechanism of the Heck reaction catalysed by heterocyclic carbene complexes, the reaction is believed to proceed *via* the oxidative addition of the aryl halide to a palladium(0) species followed by the

abstraction of a halide anion and subsequent coordination and insertion of the olefin into the palladium-aryl bond.

With chelating spectator ligands, the effect of chelate ring size, number and nature of co-donors and the steric influence of *N*-heterocyclic carbene moieties on the activity of the catalyst have been widely ignored. Instead, the focus has been placed on the quest for the most difficult and the most challenging reactions (activation of aryl chlorides) drawing attention away from the difficult mechanistic and comparative studies.

In addition, K. Cavell *et al.*[22] have observed that on interaction of aryl halides with palladium (0) complexes containing sterically unhindered (*N*-methyl derivatised) heterocyclic carbenes, small quantities of eliminated imidazolium salts were formed as well as other decomposition products. They rationalised these products by invoking reductive elimination of the carbene and an alkyl or aryl substituent on the palladium leading to the imidazolium salts. The generality of this observation is now being questioned, as with the more sterically demanding ligand designs reported in this thesis, no similar decompositions were observed under similar conditions. Incorporation of steric bulk above and below the carbene plane possibly prevents interaction of the LUMO of the carbene carbon with the neighbouring substituents on the metal disfavouring reductive elimination and, therefore, increasing the stability of the palladium-carbene bond.

A more detailed mechanism involving a generic chelating ligand (L···L) as well as a palladium (0) catalyst is shown in *Scheme 8.6*. The mechanism comprises:

i) The oxidative addition of an aryl or alkenyl halide to a palladium (0) species;

ii) The coordination of the olefin to the resulting palladium (II) species;

iii) The insertion of the olefin into the metal-aryl or alkenyl bond;

iv) The reductive elimination of the product olefin, either by direct elimination of the olefin or the reduction of the metal centre and then the elimination of the olefin *via* the metal hydride.

In summary, there is not a universal mechanism for the full range of complexes that can catalyse the Heck reaction. As monodentate, bidentate and tridentate ligands have all been shown to be suitable supports of the metal centre, it is plausible that a number of mechanisms could run concurrently.

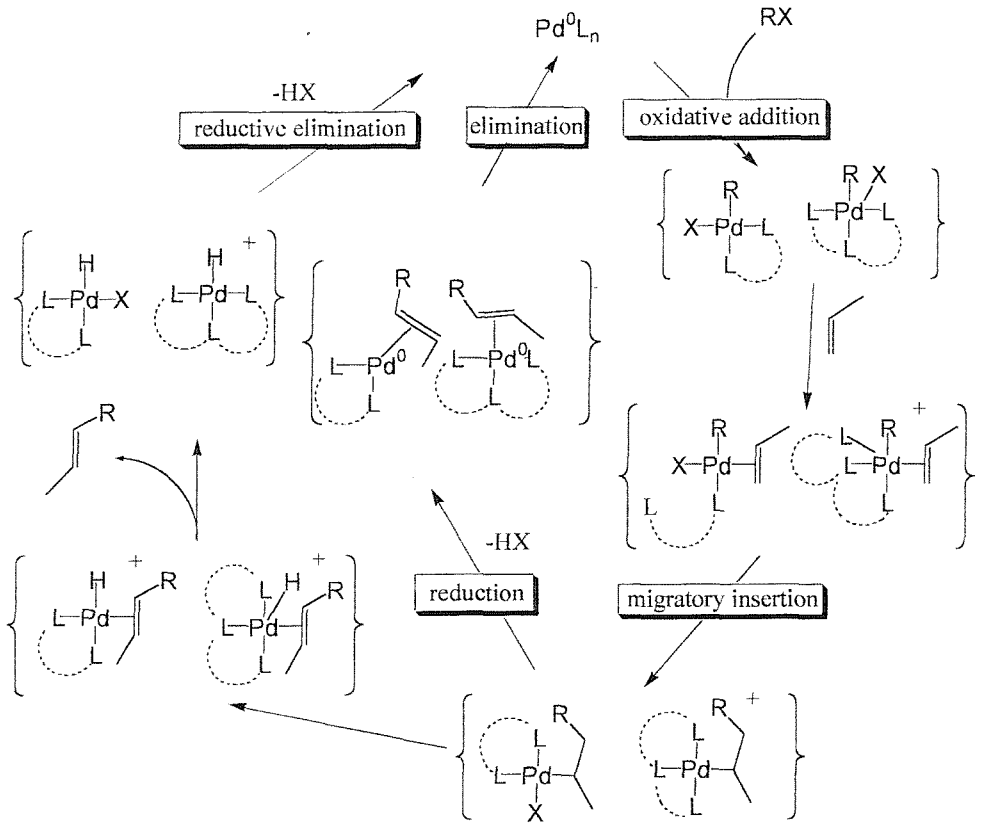

Scheme 8.6. Variations of the mechanism shown in *Scheme 8.5* for the palladium (0)-palladium (II) cycle involving bi- and tri-dentate ligands.

RESULTS AND DISCUSSION

8.2 Heck reactions catalysed by some of the palladium carbene complexes described in Chapters Four and Five

8.2.1. Initial catalytic results

Some of the palladium complexes described in Chapters Four and Five were tested as pre-catalysts for the Heck reaction. The initial results from the catalysis showed that, although the complexes with bidentate ligands are extremely good catalysts for coupling aryl iodides (*Table 8.1*), they are not as effective with aryl bromides and chlorides.[23] However, the activity with aryl iodides was as high as the best-known systems.[24] The initial results showed that the highest turnovers were achieved when triethylamine was used as a base (*entry [3]*); sodium carbonate, sodium acetate and potassium *tert*butoxide were also suitable bases. *N*-methylpyrrolidone was shown to be the best solvent. Complex **(4.1)** was also shown to catalyse amination reactions, see *entries [8]* and *[9]*. The turnover numbers (TON) were calculated from reproducible data obtained by measuring the amount

of product formed in the reaction with reference to an internal standard using gas chromatography and quoted to a reasonable degree of accuracy.

Reaction	Aryl Halide[a]	Alkene[b]/ Amine	Catalyst	Time (h)	Temp (°C)	Catalyst (mmol)	Base	Yield (%)	TON
[1]	PhI	MA	**(4.1)**	5	80	3.5×10^{-4}	NEt_3	5	600
[2]	PhI	MA	**(4.1)**	3	130	3.5×10^{-4}	Na_2CO_3	90	12900
[3]	PhI	MA	**(4.1)**	3	130	3.5×10^{-5}	NEt_3	100	142900
[4]	PhBr	MA	**(4.1)**	152	130	3.5×10^{-4}	NEt_3	20	2900
[5]	4-CH_3O-C_6H_4Br	BA	**(4.1)**	18	140	3.5×10^{-5}	NEt_3	3	4300
[6]	4-NO_2-C_6H_4Br	BA	**(4.1)**	18	140	2.5×10^{-2}	NaOAc	100	200
[7]	4-CH_3CO-C_6H_4Br	BA	**(4.1)**	18	140	2.5×10^{-2}	NaOAc	100	200
[8]	PhBr	PhNHMe[c]	**(4.1)**	24	65	7.0×10^{-4}	KOtBu	10	700
[9]	PhBr	PhNHMe[c]	**(4.1)**	24	65	3.5×10^{-5}	NEt_3	10	14300

[a] Amounts: ArX, 5mmol; alkene/amine, 6 mmol; NEt_3, 7 mmol; NaOAc, 7 mmol; Na_2CO_3, 3.5 mmol; *N*-methyl pyrrolidone was used as solvent. [b] MA = methyl acrylate; BA = *n*butylacrylate. [c] THF was used as solvent. TON determined by GC.

Table 8.1. A range of reactions catalysed by compound **(4.1)**.

8.2.2. High turnover numbers in the Heck coupling of aryl iodides

When complex **(4.1)** was tested to show the lifetime of catalyst's activity with aryl iodides, 1.4 million turnovers were achieved (*entry [14]*). However, on consumption of the substrate, another batch of substrates was added which was completely converted to products within a similar time scale (*entry [15]* in *Table 8.2*). This observation showed that the catalyst was able to lie dormant and then to restart catalysing the coupling reaction. However, this remarkable ability was not observed when using other aryl halides.

Reaction	Aryl Halide[a]	Alkene[b]	Catalyst	Time (h)	Temp (°C)	Catalyst (mmol)	Base	Yield (%)	TON
[10]	PhI	MA	**(4.1)**	1	130	3.5×10^{-5}	NEt_3	85	121400
[11]	PhI	MA	**(4.1)**	2	130	3.5×10^{-5}	NEt_3	95	136000
[12]	PhI	MA	**(4.1)**	3	130	3.5×10^{-5}	NEt_3	100	143000
[13]	PhI	MA	**(4.1)**	6	130	1.75×10^{-5}	NEt_3	100	286000
[14]	PhI	MA	**(4.1)**	18	140	3.5×10^{-6}	NEt_3	98	1400000
[15]	PhI	MA	**(4.1)**	38	140	1.75×10^{-6}	NEt_3	100	2860000

[a] Amounts: ArX, 5mmol; alkene/amine, 6 mmol; NEt_3, 7 mmol; *N*-methyl pyrrolidone was used as solvent. [b] MA = methyl acrylate. TON determined by GC.

Table 8.2. High turnover numbers and turnover frequencies, achieved when coupling phenyl iodide with methylacrylate using compound **(4.1)** as the pre-catalyst.

8.2.3. Heck reaction with aryl chlorides

Compounds **(5.1)** and **(5.3)** were shown to be very effective in catalysing the Heck reaction with aryl chlorides (*Table 8.3*). They showed very good activity even when no activating agent (i.e. NBu_4Br) was used. The palladium complexes with bidentate carbene ligands showed very low activity with the aryl chloride in the absence of any activating agent, similar to those observed by Cavell *et al.*[25] Coupling of aryl bromides could be carried out at relatively low temperatures.

Reaction	Aryl Halide[a]	Alkene[b]	Catalyst	Time (h)	Temp (°C)	Catalyst (mmol)	Base	Yield (%)	TON
[16]	4-CH_3CO-C_6H_4Br	MA	**(5.3)**	18	80	3.5×10^{-3}	NEt_3	60	850
[17]	4-CH_3CO-C_6H_4Br	MA	**(5.1)**	18	80	3.5×10^{-3}	NEt_3	85	1200
[18]	4-CH_3CO-C_6H_4Cl	MA	**(5.3)**	18	140	3.5×10^{-3}	NEt_3	35	500
[19]	4-CH_3CO-C_6H_4Cl	MA	**(5.1)**	18	140	3.5×10^{-3}	NEt_3	45	650

[a] Amounts: ArX, 5mmol; alkene, 6 mmol; NEt_3, 7 mmol; *N*-methyl pyrrolidone was used as solvent. [b] MA = methyl acrylate. TON determined by GC.

Table 8.3. Coupling of aryl chlorides and bromides with methylacrylate.

Aryl chlorides are less reactive than aryl bromides, which are less reactive than aryl iodides; this follows the trend of the bond dissociation energies of the carbon-halogen bond.[26] A major rate-limiting step in the Heck reaction is believed to be the oxidative addition of the aryl halide and so the overall rate is affected by the carbon-halogen bond dissociation energies.[27]

8.2.4. Comparative studies

The focus of the catalytic studies was directed towards detecting and if possible understanding any effects of the structural differences of the palladium complexes to the activity of the catalyst (*Figure 8.1*). This could lead to new catalyst designs and optimisation based on empirical rules that correlate molecular structure with observed activity. The palladium complexes tested were selected with an attempt to draw similarities between the currently fast-developing carbene research and the much more well established phosphine chemistry.[28]

The complexes were chosen to enable the study of the activity of the catalyst against three main features (*Figure 8.1*):

i) The size of the bulky substituents on the carbene moiety;

ii) The bite angle of the resulting chelate;

iii) The nature of the metal coordination sphere as probed by comparing bidentate and tridentate ligands.

8.2.5. Compounds tested for activity in the Heck reaction

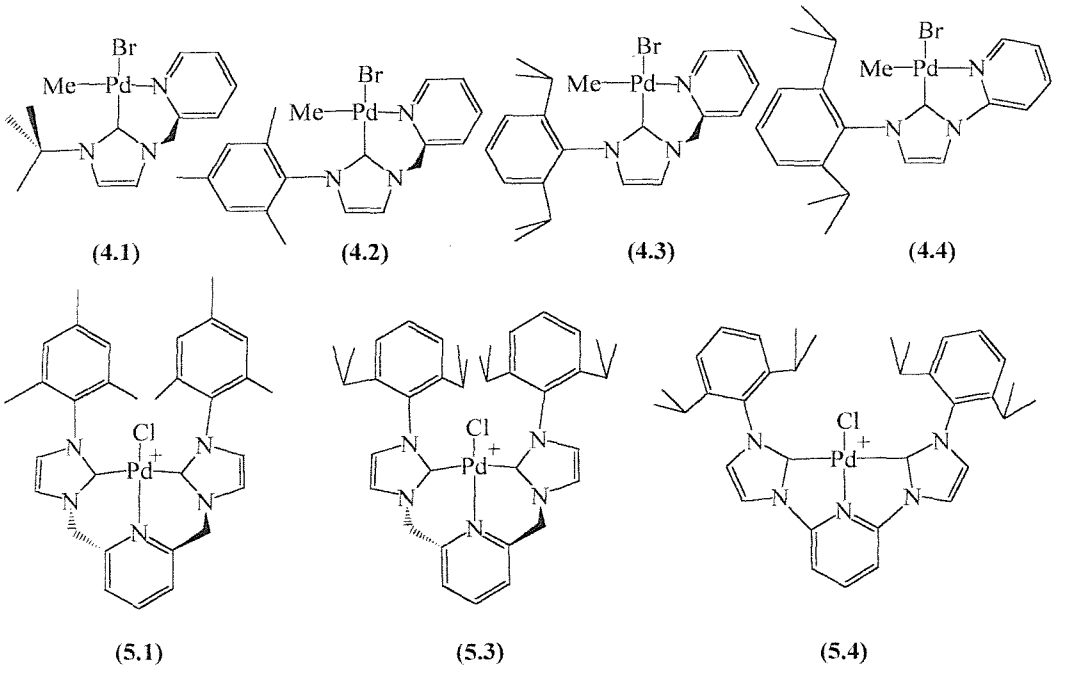

Figure 8.1. Complexes tested as catalysts for the Heck reaction.

The bidentate complexes that were tested are: [3-(*tert*-butyl)-1-(α-picolyl) imidazol-2-ylidene] palladium methyl bromide **(4.1)**, [3-(mesityl)-1-(α-picolyl) imidazol-2-ylidene] palladium methyl bromide **(4.2)**, [3-(2,6-di*iso*propylphenyl)-1-(α-picolyl) imidazol-2-ylidene] palladium methyl bromide **(4.3)** and [3-(2,6-di*iso*propylphenyl)-1-(2-pyridyl) imidazol-2-ylidene] palladium methyl bromide **(4.4)**. The tridentate complexes that were tested are: {α,α'-bis-[3-(mesityl) imidazol-2-ylidene] lutidine} palladium dichloride **(5.1)**, {α,α'-bis-[3-(2,6-di*iso*propylphenyl) imidazol-2-ylidene] lutidine} palladium dichloride **(5.3)** and {2,6-bis-[3-(2,6-di*iso*propylphenyl) imidazol-2-ylidene] pyridine} palladium dichloride **(5.4)**, shown in *Figure 8.1.*

In order to get the clearest results, the design of the experiments was the simplest possible, for example avoiding using any activating materials, quaternary ammonium salts or reducing agents. These are known to affect the reaction in a number of ways, for example making the complexes less prone to decomposition. It was important to be able to identify the effect of the targeted molecular characteristics of the ligand on the true

stability and activity, and because of this, leaving activating agents out was crucial for meaningful comparisons.

8.2.6. Effect of the ligand structure on the activity in the Heck reaction

8.2.6.1. The effect of the size of the R group on the activity of the catalyst

The first observation that became clear when comparing the activity of the complexes with bidentate ligands was that the size of the bulky R group on the imidazol-2-ylidene had little or no effect on turnover number or turnover frequency (*Table 8.4*). Although compound **(4.1)** always slightly under-performed compared to the similar compounds with aryl groups, no significant difference was observed. In addition, no significant difference in turnover number or frequency was observed between compounds **(4.2)** and **(4.3)**. This result can be easily understood if the ligand is considered to be acting as a monodentate during the rate-limiting steps, as the R group would be free to rotate to reduce any steric restrictions. Alternatively, this observation can be accounted for by assuming that there is no steric influence on the rate-limiting steps, either positive or negative.

Reaction	Aryl Halide[a]	Alkene[b]	Catalyst	Time (h)	Temp (°C)	Catalyst (mmol)	Base	Yield (%)	TON
[20]	4-CH_3CO-C_6H_4Br	MA	**(4.1)**	18	140	3.5×10^{-3}	NEt_3	60	850
[21]	4-CH_3CO-C_6H_4Br	MA	**(4.3)**	18	140	3.5×10^{-3}	NEt_3	66	950
[22]	4-CH_3CO-C_6H_4Br	MA	**(4.4)**	18	140	3.5×10^{-3}	NEt_3	74	1050
[23]	4-CH_3CO-C_6H_4Br	MA	**(5.3)**	18	140	3.5×10^{-3}	NEt_3	100	1450
[24]	4-CH_3CO-C_6H_4Br	MA	**(5.4)**	18	140	3.5×10^{-3}	NEt_3	100	1450
[25]	4-CH_3CO-C_6H_4Br	MA	**(5.1)**	18	140	3.5×10^{-3}	NEt_3	100	1450

[a] Amounts: ArX, 5mmol; alkene, 6 mmol; NEt_3, 7 mmol; NaOAc, 7 mmol; Na_2CO_3, 3.5 mmol; *N*-methyl pyrrolidone was used as solvent.
[b] MA = methyl acrylate. TON determined by GC.

Table 8.4. Comparative activity data of palladium complexes in the coupling of bromoacetophenone with methylacrylate, illustrating the effect of the substituent R groups.

The effect of the size of the R group of the tridentate ligands was very pronounced (*Table 8.5*). The complexes involving the ligand containing mesityl groups (compound **(5.1)**) considerably out performed the complexes with the ligand containing the bulkier 2,6-di*iso*propylphenyl groups (compound **(5.3)**). This dramatic difference can be accounted for by the bulk of the ligands restricting the approach of other molecules to the metal

centre. The steric effect of the R group does imply that the ligand arrangement, observed in the solid state of the isolated complexes, must be maintained to a certain degree in the catalytically active species. Therefore, the ligand that restricts the accessibility of the metal centre the least will have the better performance. The difference in their activity is likely to be due to an association process being a rate-limiting step.

Reaction	Aryl Halide[a]	Alkene[b]	Catalyst	Time (h)	Temp (°C)	Catalyst (mmol)	Base	Yield (%)	TON
[26]	4-CH_3CO-C_6H_4Br	MA	**(5.3)**	18	140	3.5×10^{-5}	NEt_3	50	71500
[27]	4-CH_3CO-C_6H_4Br	MA	**(5.4)**	18	140	3.5×10^{-5}	NEt_3	50	71500
[28]	4-CH_3CO-C_6H_4Br	MA	**(5.1)**	18	140	3.5×10^{-5}	NEt_3	100	143000

[a] Amounts: ArX, 5mmol; alkene/amine, 6 mmol; NEt_3, 7 mmol; *N*-methyl pyrrolidone was used as solvent. [b] MA = methyl acrylate. [c] THF was used as solvent. TON determined by GC.

Table 8.5. Comparative activity data on the coupling of bromoacetophenone with methylacrylate for the palladium complexes supported by tridentate ligands, illustrating the effect of the size of the substituent R groups.

Compounds	**C-M** (Å)	**M-N** (Å)	**C-M-C** (°)	**C-M-N** (°)
(4.4)	1.970(4)	2.166(3)	-	79.15(13)
(4.3)	1.969(4)	2.168(3)	-	85.22(13)
(5.4)	2.014(9) 2.033(9)	1.975(7)	158.1(4)	79.2(3) 78.9(3)
(5.3)	2.025(4) 2.029(4)	2.074(3)	175.07(16)	87.41(14) 87.67(14)

Table 8.6. Selected bond lengths and angles for compounds **(4.3)**, **(4.4)**, **(5.4)** and **(5.3)**.

8.2.6.2. The effect of the chelate ring size on activity of the catalyst

Reactions were performed in order to identify the influence on the catalyst activity of the presence of a methylene bridge, which widens the chelate ring size, on the complexes with the *tridentate* ligands. The results did not show any significant difference under a variety of reaction conditions. The reason for this was unclear, since the differences in bite angle, coordination geometry and palladium-nitrogen bond length are pronounced (*Table 8.6*). It is possible however that these structural features affect the activity in a much more subtle way than could be probed with the techniques that were used.

Reaction	Aryl Halide[a]	Alkene[b]	Catalyst	Time (h)	Temp (°C)	Catalyst (mmol)	Base	Yield (%)	TON
[29]	C_6H_5Br	MA	**(4.1)**	75	130	3.5×10^{-4}	NEt_3	35	5000
[30]	C_6H_5Br	MA	**(4.3)**	80	140	3.5×10^{-4}	NEt_3	40	5700
[31]	C_6H_5Br	MA	**(4.4)**	80	140	3.5×10^{-4}	NEt_3	90	12900
[32]	C_6H_5Br	MA	**(5.3)**	18	140	3.5×10^{-5}	NEt_3	15	18600
[33]	C_6H_5Br	MA	**(5.1)**	18	140	3.5×10^{-5}	NEt_3	48	68600

[a] Amounts: ArX, 5mmol; alkene, 6 mmol; NEt_3, 7 mmol; *N*-methyl pyrrolidone was used as solvent. [b] MA = methyl acrylate. TON determined by GC.

Table 8.7. Comparative activity data in the coupling of phenyl bromide with methylacrylate for the palladium bidentate and tridentate complexes, illustrating the effect of the methylene bridge.

In contrast, the influence of the methylene bridge on the activity of the complexes that contain *bidentate* ligands is much more pronounced (*Figure 8.2* and *Table 8.6*). The complex that contained a ligand with a methylene bridge (with larger bite angle and longer palladium-nitrogen bond) proved to have higher turnover frequencies initially but the activity dropped rapidly over time. The complex without the methylene bridge had a much longer lifetime and more consistent activity throughout the reaction period (*Figure 8.2*). There was no induction period observed for any of the reactions studied, however the first samples were taken after five minutes. Compound **(4.3)** was more than three times faster to achieve a fifty percent yield (within around four hours). However, with less reactive substrates compound **(4.4)** achieved much higher turnovers than compound **(4.3)** (*Table 8.7*).

These differences could be related to the pyridyl and picolyl moieties having different degrees of hemilability; the picolyl group dissociating more easily, and frequently, than the pyridyl. In the "picolyl-off" state, the space available for substrate molecules to coordinate to the metal centre could be increased, speeding up associative processes. However, larger bite angles in diphosphine chelate complexes have been shown to favour reductive elimination and dissociation processes. This is considered to be due to the inherently larger angles in the low coordination number intermediates that are formed by these two elementary steps, and this may be the same for analogous carbene ligands.[28]

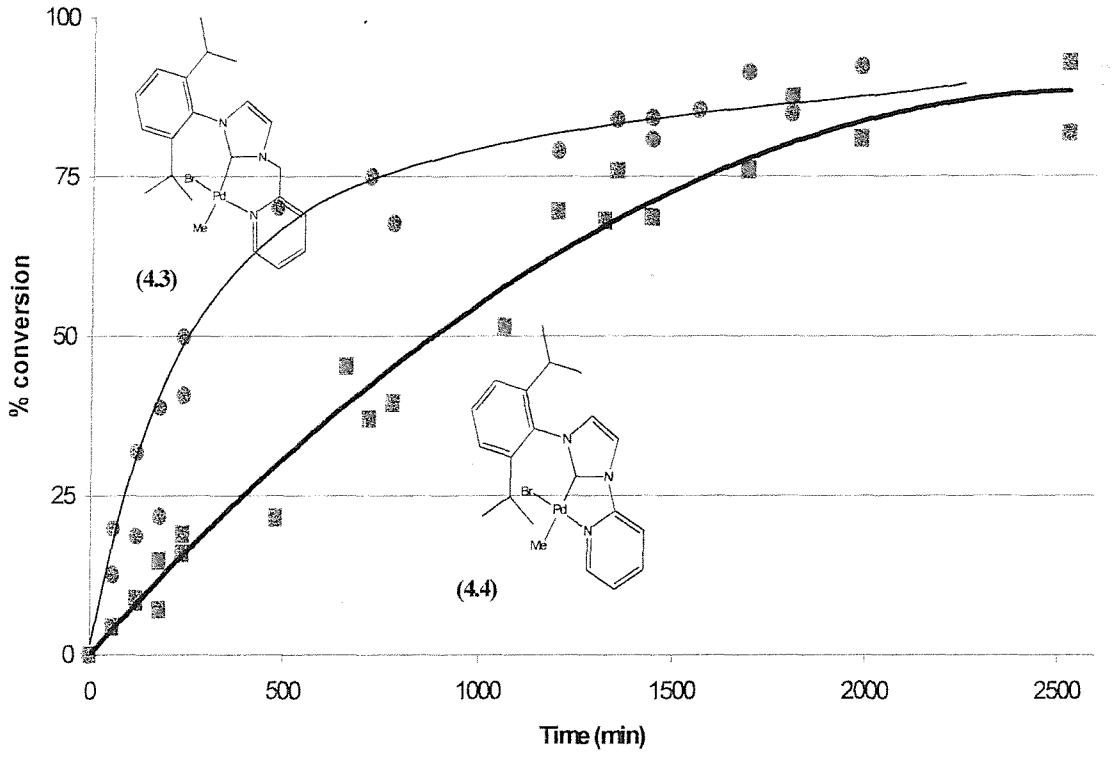

Figure 8.2. Coupling of bromoacetophenone with methylacrylate in the presence of triethylamine and *N*-methyl pyrrolidone, using compounds **(4.3)** and **(4.4)** as pre-catalysts.

It is very difficult to determine which of these possible factors carries more weight; i.e. the ability of the picolyl group to dissociate or the larger bite angle of the ligand topology promoting the coordination geometry changes at the palladium centre. However, further work is being done to identify the species involved in these reactions,[29] as well as to synthesise similar complexes to obtain a fuller picture of the possible effect of hemilability on the catalytic system.[30]

Reaction	Aryl Halide[a]	Alkene[b]	Catalyst	Time (h)	Temp (°C)	Catalyst (mmol)	Base	Yield (%)	TON
[34]	C_6H_5I	MA	**(5.1)**	18	140	3.5×10^{-6}	NEt_3	20	260000
[35]	C_6H_5I	MA	**(4.1)**	18	140	3.5×10^{-6}	NEt_3	98	1400000
[36]	C_6H_5I	MA	**(4.1)**	18	140	1.75×10^{-6}	NEt_3	100	2860000

[a] Amounts: ArX, 5mmol; alkene, 6 mmol; NEt_3, 7 mmol; *N*-methyl pyrrolidone was used as solvent. [b] MA = methyl acrylate. TON determined by GC.

Table 8.8. Comparative "high activity" data in the coupling of phenyl iodide with methylacrylate catalysed by palladium complexes **(5.1)** and **(4.1)**.

8.2.6.3. The effect of ligand denticity (bi- vs. tri-dentate architectures) on the activity of the catalyst

Although the complexes with tridentate ligands, perform better as pre-catalysts than the bidentate analogues, when aryl bromide and chlorides are used as substrates, the latter are considerably more effective as pre-catalysts when aryl iodides are coupled (*Table 8.8*). This is possibly due to different mechanisms being followed by complexes with these two classes of ligands.

The tridentate ligands are quite demanding in coordination space around the metal centre and this could have a restrictive effect on the type of elementary steps that give rise to higher coordination number intermediates. On the other hand, the high coordination power, rigidity and increased order offered by the tridentate ligands may increase the life time of the catalyst by preventing decomposition *via* deligation of the metal centre. This stability could be the reason for the good activity in the coupling of aryl chlorides. It is likely that the carbene ends of the tridentate ligands are still attached during the catalytic cycle, since if one carbene end of the ligand was to become detached, then the catalytic properties would tend to be much more similar to those of the bidentate ligands.

In comparison, the bidentate ligands are less coordinativly saturated and are able to perform extremely high numbers of turnovers when coupling of aryl iodides. This high activity and low coordination could leave the bidentate complexes susceptible to deligation and therefore more prone to decomposition pathways, especially when the reaction cycle is slowed down, i.e. when using aryl chlorides (slower oxidative addition step).

8.3 Conclusions

The complexes tested have been shown to be extremely good pre-catalysts for the Heck reaction. They were also able to catalyse Suzuki and amination reactions although detailed studies were only made for the Heck reaction.

The complexes containing bidentate ligands appear to act as "living" catalysts when coupling aryl iodides. In this case, they achieve very high turnover numbers and are as active as the best-known systems from the literature. Aryl bromides were coupled effectively too, but aryl chlorides were only coupled at very low turnover numbers and frequencies.

Complexes with tridentate ligands demonstrated a much greater activity in coupling the more difficult aryl chloride and bromides. However, aryl iodides were not coupled as rapidly in these systems, compared to the complexes with bidentate ligands.

In comparative tests, it was shown that for the complexes with bidentate ligands, the complexes containing ligands with a methylene bridge could achieve much higher turnover frequencies than those with ligands without a methylene bridge. However, the overall turnover number for the more difficult substrates was higher for the complexes containing the ligands without a methylene bridge.

In addition, it was shown that for complexes with tridentate ligands the steric bulk of the R groups affected the rate and turnover number of the reaction. However, the chelate size of the ligands appeared to have little or no effect on the rate or turnover number. These complexes with *tridentate* ligands were also much more effective at catalysing aryl bromides and chlorides than the similar complexes with bidentate ligands. Nevertheless, they were not able to achieve the extremely high turnover frequencies with aryl iodides that were obtained when using the complexes with bidentate ligands.

The mechanisms that operate are not straightforward, when using the above complexes as catalysts for the Heck reaction. It is possible that the mechanism comprises of a number of diversions or even parallel cycles. The results of the experiments performed suggest that the less the palladium centre's coordination sphere is filled, the higher the possible turnover frequency that can be achieved. The results also showed that the more coordinated the palladium was, the more stable it was towards forming catalytically inactive species. Palladium black was not observed in any of the reactions that were carried out, so the reaction can be assumed to be homogeneous. The differences observed in the catalyst activity for the coupling of particular substrates demonstrate the importance of selecting the appropriate complex (well-ligated or poorly-ligated metal centre) for the specific substrates that are required to be coupled. There appears to be a trade-off between turnover frequency and effectiveness at coupling the more difficult aryl halides.

Compounds **(5.1)** and **(5.3)** are the first examples of chiral complexes that catalyse the coupling of aryl chlorides in phosphine free Heck reactions. The complexes also catalyse the Heck reaction with aryl bromides at temperatures at which the complexes have been proven to remain chiral.

EXPERIMENTAL

8.4 Procedure for Heck reaction

In a typical run, a 50ml Rotaflow ampoule was charged with the corresponding aryl halide (5 mmol), methylacrylate (6 mmol), triethylamine (7 mmol), di(ethylene glycol) dibutylether (500μl) and NMP (5ml). A solution of the catalyst in NMP (1ml) was added to the reaction mixture and rapidly heated to reaction temperature. After the desired time the reaction mixture was rapidly cooled to room temperature and quenched with water (2ml) and dichloromethane (5ml). The organic layer was analysed by gas chromatography.

For example, a 50ml Rotaflow ampoule was charged with 4-CH_3CO-C_6H_4Br (995μl, 5 mmol), methylacrylate (622μl, 6 mmol), triethylamine (1066μl, 7 mmol), di(ethylene glycol) dibutylether (500μl) and NMP (5000μl). A solution of [3-(2,6-di*iso*-propylphenyl)-1-(α-picolyl) imidazol-2-ylidene] palladium methyl bromide **(4.3)** ($3.5x10^{-5}$ mmol) in NMP (1000μl) was added to the reaction mixture and rapidly heated to 140°C. After 18 hours, the reaction mixture was rapidly cooled to room temperature and quenched with water (2ml) and dichloromethane (5ml). The organic layer was analysed by gas chromatography.

REFERENCES

1 B. Cornils, W.A. Herrmann, *Applied Homogemeous Catalysis with Organometallic Compounds*, VCH, Weinheim, **1996**.

2 R.F. Heck, *Org. React.*, **1982**, *72*, 345.

3 A. de Meijere, F.E. Meyer, *Angew. Chem., Int. Ed. Engl.*, **1994**, *33*, 2379; I.P. Beletskaya, A.V. Cheprakov, *Chem. Rev.*, **2000**, *100*, 3009.

4 S Iyer, V.V.Thakur, *J. Mol. Cat.*, **2000**, *157*, 275.

5 W.A. Herrmann, M. Elison, J. Fischer, C. Köcher, G.R.J. Artus, *Angew., Chem. Int. Ed. Engl.*, **1995**, *34*, 2371.

6 A. Biffis, M. Zecca, M. Basato, *J. Mol. Cat.*, **2001**, *173*, 249; C.P. Mehnert, J.Y. Ying, *Chem. Commun.*, **1997**, 2215.

7 A.A.D. Tulloch, A.A. Danopoulos, G.J. Tizzard, S.J. Coles, M.B. Hursthouse, R.S. Hay-Motherwell, W.B. Motherwell, *Chem. Commun.*, **2001**, 1270.

8 M. Ohff, A. Ohff, M.E. van der Boom, D. Milstein, *J. Am. Chem. Soc.*, **1997**, *119*, 11687.

9 E. Peris, J. A. Loch, J. Mata, R. H. Crabtree, *Chem. Commun.*, **2001**, 201.

10 D. Morales-Morales, R. Redón, C. Yung, C.M. Jensen, *Chem. Commun.*, **2000**, 1619.

11 B.L. Shaw, S.D. Perera, E.A. Staley, *Chem. Commun.*, **1998**, 1361.

12 T. Rosner, J. Le Bars, A. Pfaltz, D.G. Blackmond, *J. Am. Chem. Soc.*, **2001**, *123*, 1848.

13 D.A. Albisson, R.B. Bedford, S.E. Lawrence, P.N. Scully, *Chem. Commun.*, **1998**, 2095.

14 M. Nowotny, U. Hanefeld, H. van Koningsveld, T. Maschmeyer, *Chem. Commun.*, **2000**, 1877.

15 A.A.D. Tulloch, A.A. Danopoulos, R.P. Tooze, S.M. Cafferkey, S. Kleinhenz, M.B. Hursthouse, *Chem. Commun.*, **2000**, 1247.

16 D.S. McGuinness, M.J. Green, K.J. Cavell, B.W. Skelton, A.H. White, *J. Organomet. Chem.*, **1998**, *565*, 165.

17 J. Huang, S.P.Nolan, *J. Am. Chem. Soc.*, **1999**, *121*, 9889.

18 R. Stürmer, *Angew. Chem. Int. Ed. Engl.*, **1999**, *38*, 3307; M.G. Andreu, A. Zapf, M. Beller, *Chem. Commun.*, **2000**, 2475; A.F. Littke, C. Dai, G.C. Fu, *J. Am.*

Chem. Soc., **2000**, *122*, 4020; J.P. Wolfe, R.A. Singer, B.H.Yang, S.L. Buchwald, *J. Am. Chem. Soc.*, **1999**, *121*, 9550.

19 B.L. Shaw, S.D. Perera, *Chem. Commun.*, **1998**, 1863.

20 B.L. Shaw, S.D. Perera, E.A. Staley, *Chem. Commun.*, **1998**, 1361.

21 K. Albert, P. Gisdakis, N. Rösch, *Organometallics*, **1998**, *17*, 1608;

22 D.S. McGuinness, K.J. Cavell, B.W. Skelton, A.H. White, *Organometallics*, **1999**, *18*, 1596; D.S. McGuinness, N. Saendig, B.F. Yates, K.J. Cavell, *J. Am. Chem. Soc.*, **2001**, *123*, 4029.

23 W.A. Herrmann, V.P.W. Böhn, C-P. Reisinger, *J. Organomet. Chem.*, **1999**, *576*, 23.

24 M. Ohff, A. Ohff, D. Milstein, *Chem. Commun.*, **1999**, 357.

25 D.S. McGuinness, K.J. Cavell, *Organometallics*, **2000**, *19*, 741.

26 I.P. Beletskaya, A.V. Cheprakov, *Chem. Rev.*, **2000**, *100*, 3009.

27 W. Cabri, I. Candiani, *Acc. Chem. Res.*, **1995**, *28*, 2.

28 P.W.N.M. van Leeuwen, P.C.J. Kamer, J.N.H. Reek, P. Dierkes, *Chem. Rev.*, **2000**, *100*, 2741.

29 J. Evans, S. Fiddy, Personal communication.

30 A.A. Danopoulos, S. Winston, Personal communication.

Chapter 9

Conclusion

Chapter 9
Conclusion

Practical methods to synthesise a large range of unusual imidazolium salts are reported in this thesis. A number of these salts have been used as precursors in the synthesis of new silver, copper, nickel, rhodium, ruthenium and palladium imidazol-2-ylidene complexes. These complexes include:

i) The first structurally characterised examples of silver (I) imidazol-2-ylidene complexes that contain ligands with a second donor group.

ii) The first structurally characterised examples of copper (I) imidazol-2-ylidene complexes; including monomeric, dimeric and polymeric materials.

iii) A range of copper (I) imidazol-2-ylidene complexes with weakly coordinating anions.

iv) The first structurally characterised example of a nickel (II) imidazol-2-ylidene complex that contains a mixed donor *N*-heterocyclic carbene ligand.

v) The first example of a ruthenium (II) imidazol-2-ylidene complex containing a mixed donor ligand with both donor atoms coordinated to the metal centre.

vi) The first structurally characterised examples of chiral imidazol-2-ylidene complexes that contain a stereogenic C_2 axis that did not pre-exist in the ligand (*Figure 9.1*).

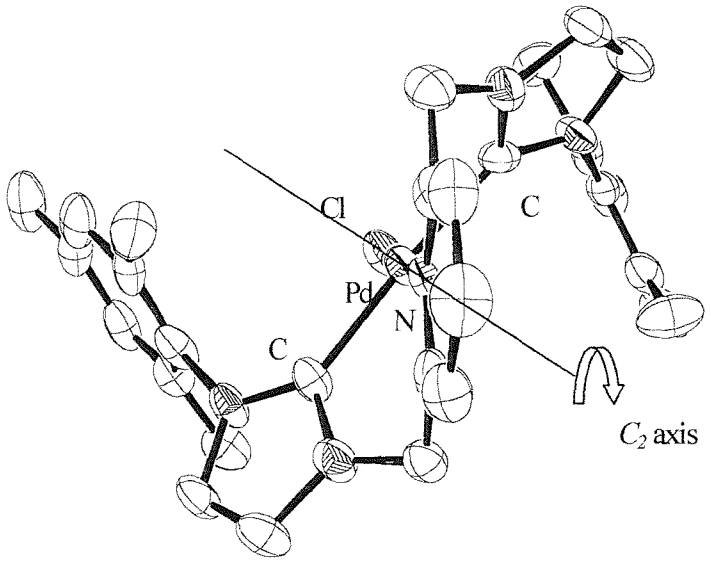

Figure 9.1. Compound **(5.1)**, a chiral palladium imidazol-2-ylidene complex with a C_2 axis.

vii) The first X-ray structure that contains a bidentate imidazol-2-ylidene ligand in both a bridging and a chelating role.

viii) The second structurally characterised example of a rhodium (I) imidazol-2-ylidene complex that contains a mixed donor *N*-heterocyclic carbene ligand.

ix) The second structurally characterised example of a palladium (II) imidazol-2-ylidene complex that contains a bridging mixed donor *N*-heterocyclic carbene ligand.[1]

x) A range of palladium (II) imidazol-2-ylidene complexes with bidentate and tridentate mixed donor carbene ligands and a variety of palladium (II) complexes with weakly coordinating anions.

The imidazolium salts reported in this thesis are functionalised with a variety of other donors, including pyridyl, picolyl, lutidyl, phosphine, phosphine-borane, phosphine oxide, γ-bromopropyl and methoxy moieties as well as substituted with a variety of bulky aryl and alkyl groups. Bis-imidazolium salts have also been prepared with methylene, lutidyl and pyridyl bridges.

Carbene complexes have been prepared from a number of these imidazolium salts. The silver complexes synthesised all contain ligands that are monodentate, with the exception of a structurally-characterised example with a bridging ligand. These silver complexes have been shown to be very useful as ligand transfer agents to late transition metals. The copper complexes synthesised all contain bidentate bridging ligands, with the exception of one complex which has a chelating ligand. Some of the copper complexes are observed to aggregate at higher solution concentrations, which demonstrates the hemilability of the picolyl functionality (*Figure 9.2*).

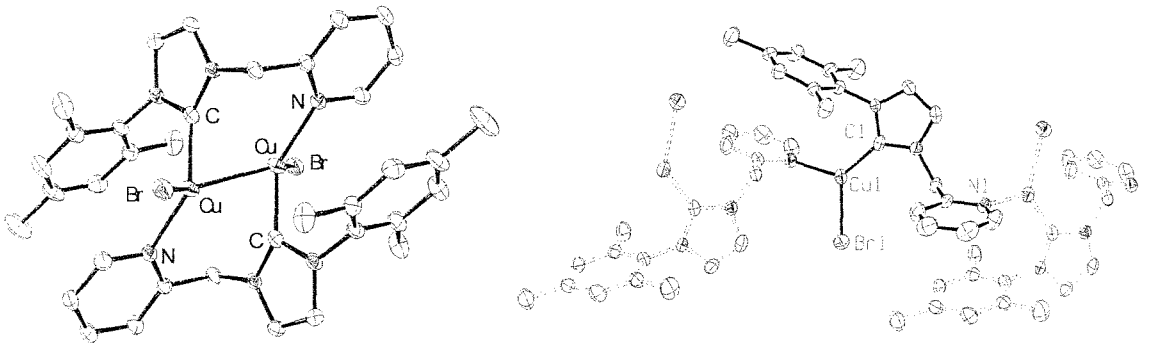

Figure 9.2. Dimeric and polymeric structures of compound **(3.10)**, grown from solutions of different concentration.

The nickel complex **(7.1)** contains a chelating ligand, with the metal in a tetrahedral environment. The rhodium complex **(7.3)** also contains a chelating ligand and the cationic metal complex has a distorted square-planar geometry. The ruthenium complex **(7.2)** was shown by ^{1}H NMR spectroscopy to contain a chelating carbene ligand.

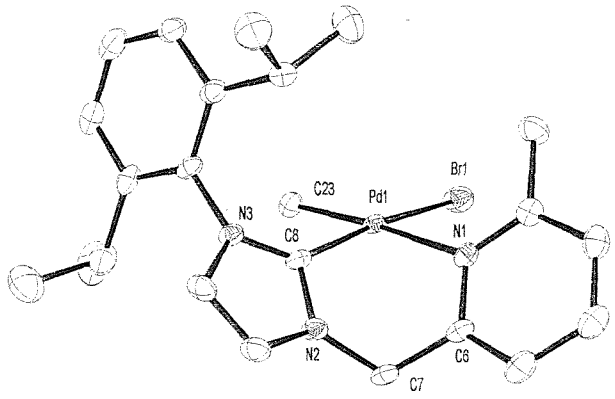

Figure 9.3. X-ray crystal structure of palladium complex **(4.5)**.

The palladium complexes described in Chapter Four include compounds with mixed donor carbene ligands that have different bite angles and varying amounts of steric bulk (*Figure 9.3*). They mostly contain chelating ligands and a number of them have been structurally characterised. Some of these complexes have shown extremely good activity as pre-catalysts for the Heck and amination reactions. In all of the structures obtained, the palladium centre is in a square planar geometry. However, one of the structures comprises of an imidazolium salt coordinated to a palladium centre *via* the picolyl group only. Another example of a complex that does not contain a chelating ligand is compound **(5.7)**, which contains two monodentate functionalised carbene ligands. The palladium complexes described in Chapter Six all contain chelating ligands, except compound **(6.3)**; this comprises four bridging mixed donor carbene ligands that form a tetrameric structure with four palladium centres.

The subtle structural differences between some of the palladium complexes described in Chapter Four have given rise to different catalytic activities for the Heck reaction. A range of the palladium complexes were tested for their activity in the copolymerisation of carbon monoxide and ethylene. However, no activity was observed for the compounds tested and the palladium complexes were reduced to palladium black within only a few minutes. The bite angle of the ligand and the longer palladium-nitrogen bond of the picolyl ligands appear to increase the hemilability of the ligand (as observed for the copper complexes). This has been correlated with the higher turnover frequencies

that have been achieved. However, the larger bite angle complexes are less stable over long periods under catalytic conditions. Hemilability is also supported by reaction of some of these compounds with triethylamine. The reaction causes *cis-trans* isomerisation to occur in the complexes that contain the picolyl-carbene ligand; this is followed by their slow decomposition. Decomposition also occurred when dichloromethane solutions of the palladium complexes were exposed to an atmosphere of carbon monoxide. The decomposition was faster for the complexes bearing a ligand with a methylene bridge; this has been associated with their greater hemilability (*Scheme 9.1*).

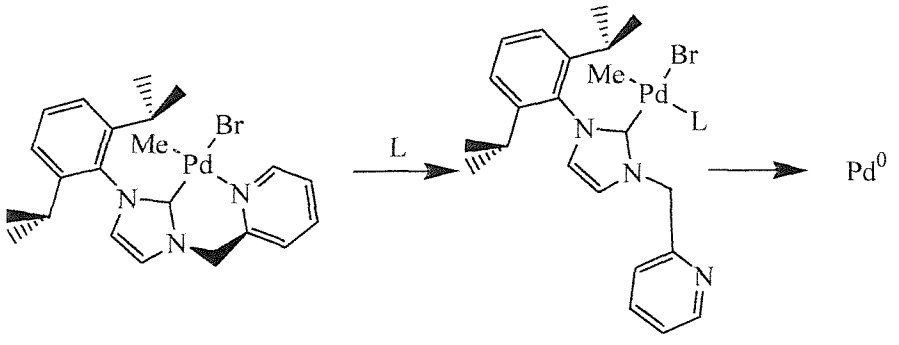

Scheme 9.1. Hemilability demonstrated by the decomposition of compound **(4.3)** where L = triethylamine or carbon monoxide.

The hemilability of the picolyl functionality has been further demonstrated by the conversion of a monomeric complex **(4.1)** (with a chelating carbene ligand), to a tetrameric complex **(6.3)** (with a bridging carbene ligand), by the interaction with silver trifluoroacetate. The exact mechanism of the formation of the tetramer is unknown but it is likely to involve a step in which the picolyl group is detached from the palladium centre. The hemilability of the picolyl functionality may be related to the observation that the complexes, when used as pre-catalysts for the coupling of aryl iodides in the Heck reaction, appear to be "living" catalysts.

The palladium complexes described in Chapter Five include compounds with mixed donor bis-carbene ligands of the "pincer" architecture with different bite angles and variations in the steric bulk. Chapter Five also contains a palladium complex with a bis-carbene ligand bound in two different ways in the same crystal structure (*Figure 9.4*).

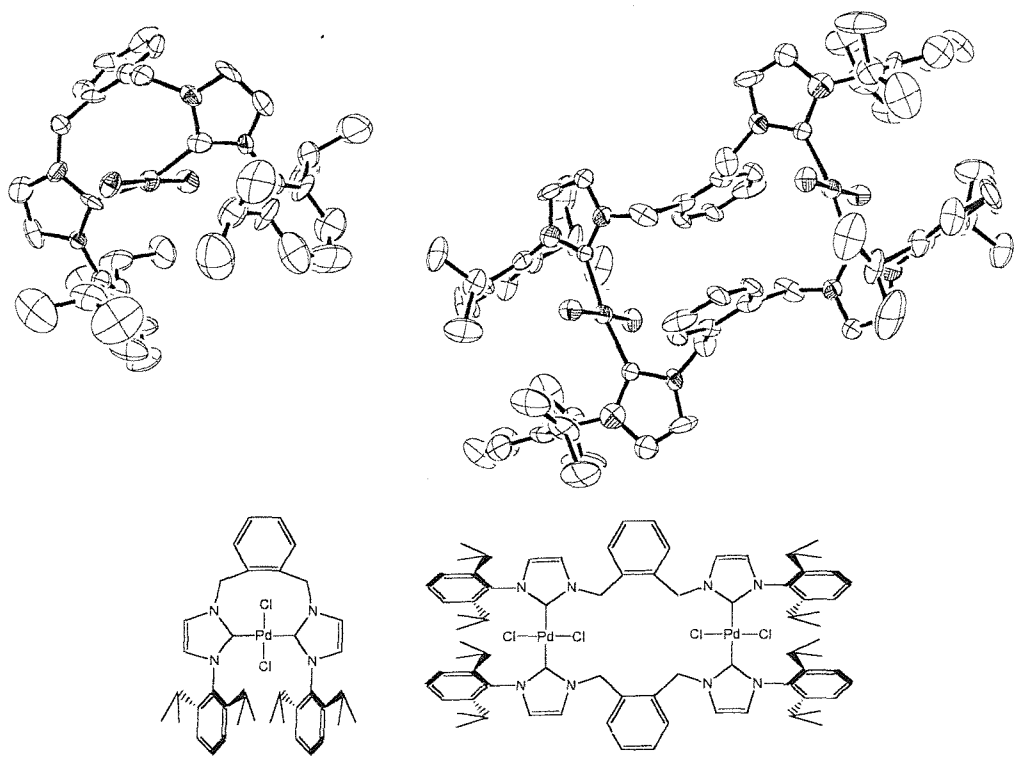

Figure 9.4. Two coordination isomers of compound **(5.5)**.

The palladium complexes that contain tridentate "pincer" ligands with methylene bridges are of considerable interest as they are some of the very few palladium carbene complexes that are chiral. These complexes are particularly interesting as the palladium centre is on the chiral C_2 axis and therefore the chiral information should have a very pronounced influence on the metal centre (i.e. catalytic site). The conformational chirality of these complexes has been shown to persist in solution at temperatures as high as 80°C. At this temperature, the complexes are very active pre-catalysts for the coupling aryl bromides in the Heck reaction. The same complexes are also very effective pre-catalysts for the coupling aryl chlorides in the Heck reaction; they are the first examples of chiral, non-phosphine system that can achieve this.

Important general conclusions from the catalyst testing are:

i) The use of higher denticity ligands enables the complexes to couple more difficult substrates in the heck reaction (aryl chlorides), but also results in lower turnover frequency;

ii) The less ligated palladium centres allow much higher turnover frequencies to be achieved but also result in the faster decomposition of the complexes.

In summary, the catalyst performance appears to be a trade-off between rate, as measured by turnover frequency, and activity.

The large number of complexes and imidazolium salts whose synthesis are reported in this thesis have already generated interest in the scientific and industrial communities by colleagues[2] and others.[3] A range of follow-up studies are underway aiming to clarify some of the questions that have arisen from the synthesis of these new compounds, and to explore the synthesis of similar complexes. In addition, further catalytic studies on these complexes are being explored.[2]

REFERENCES

1 W.A. Herrmann, L.J. Goossen, M. Spiegler, *Organometallics*, **1998**, *17*, 2162.

2 A.A. Danopoulos, S. Winston, R.S. Hay-Motherwell, W.B. Motherwell, J. Evans, S. Fiddy, personal communication.

3 S. Gründemann, A. Kovacevic, M. Albrecht, J.W. Faller, R.H. Crabtree, *Chem. Commun.*, **2001**, 2274; R.E Douthwaite, M.L.H. Green, P.J. Silcock, P.T. Gomes, *Organometallics*, **2001**, *20*, 2611; J.C. Garrison, R.S. Simons, W.G. Kofron, C.A. Tessier, W.J. Youngs, *Chem. Commun.*, **2001**, 1780; P.L. Arnold, A.C. Scarisbrick, A.J. Blake, C. Wilson, *Chem. Commun.*, **2001**, 2340; L.R. Titcomb, S. Caddick, F.G.N. Cloke, D.J. Wilson, D. McKerrecher, *Chem. Commun.*, **2001**, 1388; A. Caballero, E. Diez-Barra, F.A. Jalon, S. Merino, J.Tejeda, *J. Organomet. Chem.*, **2001**, *617*, 395; A.M. Magill, D.S. McGuinness, K.J. Cavell, G.J.P. Britovsek, V.C. Gibson, A.J.P. White, D.J. Williams, A.H. White, B.W. Skelton, *J. Organomet. Chem.*, **2001**, *617*, 546; V. Calo, A. Nacci, L. Lopez, N. Mannarini, *Tetrahedron Lett.*, **2000**, *41*, 8973; J. Pytkowicz, S. Roland, P. Mangeney, *J. Organomet. Chem.*, **2001**, *631*, 157; C.L. Yang, S.P. Nolan, *Synlett*, **2001**, 1539; C.L. Yang, H.M. Lee, S.P. Nolan, *Org. Lett.*, **2001**, *3*, 1511; D.J. Nielsen, K.J Cavell, B.W Skelton, A.H. White, *Organometallics*, **2001**, *20*, 995; D.J. Nielsen, K.J Cavell, B.W Skelton, A.H. White, *Inorganica Chimica Acta*, **2002**, *327*, 116.

Appendix

Experimental Techniques and Instrumentation

Appendix

Experimental techniques

Unless otherwise stated, experiments were performed under dry dinitrogen using standard Schlenk line techniques or in an inert atmosphere dry box (Braun UNILAB) containing dinitrogen, constantly monitoring oxygen levels. Glassware was pre-dried before use. Solvents were dried and then distilled from sodium benzophenone ketyl [light petroleum ether (bp 40-60°C), diethylether and THF], from sodium (toluene and ethanol), or from calcium hydride (dichloromethane and acetonitrile) under a slow continuous stream of dinitrogen. Solvents were thoroughly degassed by the pump fill cycles or by purging with dinitrogen prior to use. Deuterated solvents were dried (d^6-benzene and d^8-toluene over sodium/potassium alloy, d^2-dichloromethane and d^3- acetonitrile over calcium hydride, and d-chloroform over molecular sieves), distilled and degassed by freeze-pump-thaw cycles prior to use. Unless otherwise stated, commercial reagents and solvents were used as received from Acros, Aldrich and Avocado. Compounds synthesised from the literature are: 1-*tert*butyl imidazole,[1] 1-mesityl imidazole,[2] 1-(2,6-diisopropylphenyl) imidazole,[2] 2-bromomethyl-6-methylpyridine hydrogen bromide,[3] 2-bromomethylpyridine hydrogen bromide,[4] 2,6-di(bromomethyl)pyridine hydrogen bromide,[5] $Pd(OAc)_2$,[6] $NiBr_2DME$,[7] $PdBr_2(COD)$, $PdCl_2(COD)$,[8] PdMeBr(COD), PdMeCl(COD),[9] Ph_2PH[10] and AgC_6F_5.[11]

Instrumentation

NMR experiments were performed on Bruker 300, 360 and 400 MHz spectrometers. The spectra were referenced internally using the signal from the residual protio-solvent (^1H) or the signal from the solvent (^{13}C). Chemical shifts are reported as δ values in parts per million down field from trimethylsilane. ^{11}B, ^{31}P NMR, C-H and H-H correlation experiments were recorded by Mrs J.M. Street, Department of Chemistry, University of Southampton.

Mass spectra (electrospray ionisation) were obtained from acetonitrile solutions on a VG Biotec platform. All the calculated isotopic envelopes agree well with the experimentally observed patterns.

Analytical gas chromatography was performed on a Varian 3400 GC equipped with a flame ionization detector and a Hewlett-Packard 3396 series 2 integrator. The yields and turnovers were calculated using di(ethyleneglycol)dibutylether as an internal standard, based on the formation of the product.

Elemental analyses were carried out by the University College London Microanalytical Laboratory.

Single crystal X-ray diffraction data were collected, and structures solved, by S. Winston, S. Kleinhenz, M. E. Light, S. J. Coles, S. Cafferkey and A. Genge, Department of Chemistry, University of Southampton.

REFERENCES

1 R. Scarr, personal communication.

2 A.L. Johnson, U.S. Pat. 3,637,731, 25/01/1972 to E.I. du Pont.

3 M. Newcomb, J.M. Timko, D.M. Walba, D.J. Cram, *J. Am. Chem. Soc.*, **1977**, *63*, 92.

4 B.R. Brown, J. Humphreys, *J. Am. Chem. Soc.*, **1959**, 2040.

5 M.E. Haeg, B.J. Whitlock, H.W. Whitlock, Jr., *J. Am. Chem. Soc.*, **1989**, 692.

6 T.A. Stephenson, (Mrs) S.M. Morehouse, A.R. Powell, J.P. Heffer, G. Wilkinson, *J. Am. Chem. Soc.*, **1965**, 3632.

7 L.G.L. Ward, *Inorg. Synth.*, **1972**, *5*, 156.

8 J. Chatt, (Miss) L.M. Vallarino, L.M. Venanzi, *J. Am. Chem. Soc.*, **1957**, *34*, 13.

9 R.E. Rulke, J.M. Erusting, A.L. Spek, J. Elseveir, P.W.N.M. Van Leeuwen, K. Vrieze, *Inorg. Chem.*, **1993**, *32*, 5769.

10 V.D. Biacho, S. Doronzo, *Inorg. Synth.*, **1976**, *16*, 161.

11 K.K. Sun, W.T. Miller, *J. Am. Chem. Soc.*, **1970**, *72*, 6985.